



UNIVERSITAT DE
BARCELONA

Molecular analysis of MTOC assembly - the role of ninein-like protein

Joel Paz Domínguez

ADVERTIMENT. La consulta d'aquesta tesi queda condicionada a l'acceptació de les següents condicions d'ús: La difusió d'aquesta tesi per mitjà del servei TDX (www.tdx.cat) i a través del Dipòsit Digital de la UB (diposit.ub.edu) ha estat autoritzada pels titulars dels drets de propietat intel·lectual únicament per a usos privats emmarcats en activitats d'investigació i docència. No s'autoritza la seva reproducció amb finalitats de lucre ni la seva difusió i posada a disposició des d'un lloc aliè al servei TDX ni al Dipòsit Digital de la UB. No s'autoritza la presentació del seu contingut en una finestra o marc aliè a TDX o al Dipòsit Digital de la UB (framing). Aquesta reserva de drets afecta tant al resum de presentació de la tesi com als seus continguts. En la utilització o cita de parts de la tesi és obligat indicar el nom de la persona autora.

ADVERTENCIA. La consulta de esta tesis queda condicionada a la aceptación de las siguientes condiciones de uso: La difusión de esta tesis por medio del servicio TDR (www.tdx.cat) y a través del Repositorio Digital de la UB (diposit.ub.edu) ha sido autorizada por los titulares de los derechos de propiedad intelectual únicamente para usos privados enmarcados en actividades de investigación y docencia. No se autoriza su reproducción con finalidades de lucro ni su difusión y puesta a disposición desde un sitio ajeno al servicio TDR o al Repositorio Digital de la UB. No se autoriza la presentación de su contenido en una ventana o marco ajeno a TDR o al Repositorio Digital de la UB (framing). Esta reserva de derechos afecta tanto al resumen de presentación de la tesis como a sus contenidos. En la utilización o cita de partes de la tesis es obligado indicar el nombre de la persona autora.

WARNING. On having consulted this thesis you're accepting the following use conditions: Spreading this thesis by the TDX (www.tdx.cat) service and by the UB Digital Repository (diposit.ub.edu) has been authorized by the titular of the intellectual property rights only for private uses placed in investigation and teaching activities. Reproduction with lucrative aims is not authorized nor its spreading and availability from a site foreign to the TDX service or to the UB Digital Repository. Introducing its content in a window or frame foreign to the TDX service or to the UB Digital Repository is not authorized (framing). Those rights affect to the presentation summary of the thesis as well as to its contents. In the using or citation of parts of the thesis it's obliged to indicate the name of the author.

The background of the slide is a high-magnification electron micrograph of a cell. A large, electron-dense, roughly spherical structure, likely the centrosome or MTOC, is visible in the center. From this structure, numerous microtubules radiate outwards, forming a characteristic aster pattern. The microtubules appear as thin, parallel lines. The surrounding cytoplasm contains various organelles, including what appears to be a nucleus with a nucleolus on the left side. The overall image is in grayscale, typical of electron microscopy.

**Molecular analysis of MTOC assembly
- the role of ninein-like protein**

Joel Paz Domínguez
Universitat de Barcelona
2021



UNIVERSITAT DE BARCELONA

Universitat de Barcelona
Facultat de Biologia
Programa de Doctorat en Biomedicina

Memòria presentada per **Joel Paz Domínguez**
Per optar al títol de Doctor per la Universitat de Barcelona

Director

Dr. Jens Lüders

Doctorando

Joel Paz Domínguez

Tutor

Dr. Eduardo Soriano García

Joel Paz Domínguez

2021

The research described in this thesis was conducted from October 2016 until July 2021 at the Institute for Research in Biomedicine (IRB Barcelona), and supported by a grant of the Ministry of Science, Innovation and Universities (MCIU), reference BFU2015-68354-P. Joel Paz Domínguez was supported by a predoctoral FPI fellowship from the Ministry of Science, Innovation and Universities (MCIU), reference BES-2016-076423.

All rights reserved.

Journey before destination

Acknowledgments

They say that doing a PhD is a life-defining moment, and I could not agree more with that. It has been 5 years already, 5 years of many intense emotions that no one could probably resume in just a few sentences. What it is clear to me is that I would not be here without all the people that have made this journey possible.

First of all, I would like to thank my thesis director **Jens** for the opportunity to become a member of the γ TuRC family. It has been a pleasure to unravel all the mysteries (that are too many) related to how microtubules are nucleated by your side. Thanks for all the constant input on the project and for always being available to meet with any of us, I have never felt lonely or abandoned during this thesis. I would like also to thank you for always bringing inspiration to the project, for always having another hypothesis to propose even when I was already giving up on many things. I feel like I have matured a lot during this thesis both personally and scientifically and it is clear that it would not have been possible without you.

I would also like to say thanks to my former supervisor **Laura**, because she was my main motivation to do a PhD. Thank you for showing me how cool science is and for always been there, motivating me at every step through my early years as a scientist. Your passion for science has always been really inspiring to me!

I am really grateful to all the agencies that have funded my scientific career during these years, mainly MCIU and IRB Barcelona. Without them it would have not been possible for me to do a PhD.

I would like to thanks again to the IRB Barcelona, not only for being an institution that excels at research but also for bringing together a family of scientist and friends.

Starting from the **Lüders' lab**, **Ricardo** was the first person I met and probably one of my best friends nowadays (although Portugal and Spain seem very far away right now). Thanks for always being there, sharing some good laughs and for constantly reminding me that bodyboarding is easier than surfing. To the former members of the lab, **Xico**, thanks for mentoring me when I started and for all those videogames conversations (cool sword you got for your PhD by the way). **Arturito**, “el pangas”, thanks for always

bring a hot topic to the table and for all the desserts you and Ricardo ate when people brought gifts to the lab, you surely saved me from obesity. Congrats on the marriage too! **Nina and Aamir**, probably the best post-docs in town, thanks for including me in your long discussions about science (or Jens for sitting me in the middle of you two). It is a pity that you both left already, I really enjoyed the time we spent outside the lab together. I still have to send you some tortilla to India, Aamir. And Nina, next beer is on me!

Regarding the current members of our lab, **Cristina**, our lab technician, thanks for always been there to help us when we needed, especially during those BioID sessions at 6AM! It is been a pleasure to work with you, I hope one day I can meet your kids! **Fabian**, or Fabianni, thanks for sharing your knowledge with all of us, you have been more a post-doc than a PhD at some points. I am sure that if you continue in Academia, you will be the one that gets the papers before the others. I also enjoyed those times at the playita and those afternoon with you and Ricardo saying stupid things at the lab. **Marta** is perhaps the clear example of leadership without being aware of it. I am really thankful that you joined our lab, you are one of the pillars of the γ TuRC family, always integrating new people and trying to make the lab a place where you want to go to work. Thanks for reminding us that apart from scientist we can be really good friends too. I am also not forgetting about your Salmorejo (ñam ñam!).

To the new ones, **Marcos**, we really do not know much each other but I feel like I have known you for a long time. Thanks for bringing your kindness to the lab and for those desserts you have brought many times, they awesome. Finally, I would like to thank **Chithran** for following my (now ours or his) project to try to give it an end. I think that you only have been at the lab for a few months but I can already see you have improved a lot scientifically (the paper is gonna we awesome). Thanks also for always bringing a smile and a good conversation to the lab.

To the rest of the members of the IRB, **Jurgen**, thanks for everything man, I do not know where to start, but thanks for the surfing sessions and for introducing me to climbing (probably the best thing someone has done for me ever :D). I am really happy that you are having success in Germany and we will share a beer soon! I would like also to thank to **Ernest, Juan, Paloma, Lucia** (although not IRB hehe), **Paloma, Salva, Cris, Helena, Marta, Craig and many others (this list is otherwise endless)** for always having the time to share a beer or a dinner and make me feel that I was not alone during those hard PhD times. I would not like to finish without thanking **Mireia** for her inputs both personally and scientifically, I have really enjoyed working with you on the phase separation experiments!

I would like to thank all the people from the facilities of the UB that have helped me during these years. **Microscopy** (Nikos, Anna y Lidia) I am really thankful for all the expertise and the knowledge you share with me during these years. Also, Nikos, thanks for the nice edit of the image we got selected for the calendar, it was amazing!

Chiquitos Personajes, vaya buen grupito, **Isa** (aka Isita/Osobol), **Sara, Marina, Lorena** (La Lore), **Edu (aka Dudu)** y **Enric (Erquekah)**. Que os voy a decir que no sepáis, gracias por todo, por las risas, por estar en los momentos malos y por todas esas aventuras que hemos vivido, desde estar congelados en Valladolid hasta ese viaje super guapo a Canarias (tenemos que ir sí o sí). Se os quiere amics, y aunque la vida nos mande a cada uno a un lugar sé que siempre nos podremos volver a juntas como en los viejos tiempos. P.D Edu tenemos un viaje pendiente a la west coast papi. P.D.2. Isita muchas gracias por todo el apoyo no sólo emocional sino científico, no sé qué habría hecho sin ti durante estos años <3.

Los del piso, **Adri** (Adriiii), **Dácil** (Dashil) y **Edu** (el fe...guapisimo). Sin vosotros esta tesis no hubiera sido posible. Todas las cosas que hemos compartido en el piso, el sticker de Iris, esos lunes de series, la cuarentena poniéndonos bien en forma y el viaje a Tenerife como colofón. Sin duda ha sido una de las mejores épocas de mi vida, gracias por haber estado ahí, se os quiere.

A todos los bichichis del roco, sin duda esto no hubiera sido lo mismo si la escalada no estuviera en mi vida. En especial agradecer a **Clara y Marcos**, la segunda mejor pareja de escaladores que conozco (adivinen quien podría ser la primera...). En serio muchas gracias a ambos por estar ahí estos años, no hay mejor combinación que un amigo escalador y científico, hay entendimiento en la ciencia y en la roca. Por muchos más viajes juntos (en ese superfurgoché)!

Si cogemos un vuelo a la isla que me vio nacer y crecer, hay mucha gente a la que le tengo que agradecer el siempre haber estado ahí. Para que no se ponga celoso, **Denis** (o Denisuare según el allegado) gracias por siempre haber estado ahí, es increíble cuantas vueltas ha dado la vida desde que estábamos en tercero de la ESO pero aquí seguimos, puede que más unidos que nunca a pesar de la distancia. Saber que siempre estarás ahí me hace más feliz en la vida. **Inma**, gracias por estar siempre ahí, de cualquiera que sea la manera, tenerte en mi vida siempre me hace feliz, estoy muy orgulloso de todo lo que has conseguido y lo que conseguirás. Gracias por escuchar mis cositas de microtubulitos.

A la gente de Biología, los **MAPS**, **Alicia** (Alilanza mi máxima, la primera para que no haya problemas), gracias por haber estado siempre ahí desde las colocadas con el Xilol hasta nuestras charlas por Skype para llorar sobre la tesis, tendría que escribirte dos páginas solo a ti sobre las cosas que te tengo que agradecer (para otra tesis quizás =D). **Sergio** (o Sirgins) gracias por haber estado ahí, eres una de las mejores personas que conozco (aunque tengas que imponer justicia con algunos malhechores, aka yo, de vez en cuando). **Samu** (aka Samuelito/Nopi), muchas gracias por todo Samu, siento que nuestra relación se ha ido afianzando a lo largo de estos años, y siento que puedo contar contigo para lo que sea (hasta para cuando necesito el sticker adecuado). Espero que la gaviota se alce y se venga a Barcelona pronto!. **Samu** (el piratilla), Samu crack, fiero, mastodonte, gracias por haber estado siempre ahí, en nuestro peores días y mejores noches (como picadísimos jugando al Mario Kart en casa de Sergio a las 6 de la morning). **Kevin** (*keveke*), el chico con más estilo de Tenerife Norte, desde que compartimos casi piso en Las Palmas siempre hemos estado unidos, aunque haga mil que no te veo se te echa de menos!. **Manuel** (oOManuOO), que te voy a decir que no sepas, creo que ya hemos sacado todos los debates posibles y nos hemos flameado un poco más que de sobra, pero se que seguiremos así, my man! P.D. Os quiero!

Aunque no sea de la isla, es ya casi isleña, **Marta**, no podía acabar sin agradecerte lo mucho que has hecho por mi como persona. Gracias por enseñarme la capacidad deconstruirme y volver a empezar, de que el amor tiene muchas formas y solo hay que encontrar aquella que nos funcione. Gracias por hacerme evolucionar junto a ti. Y aunque te lo diga poco, te quiero con locura.

Y para acabar quiero darle las gracias por todo a mi familia, a todos los miembros de mi familia por siempre haberme dado el apoyo necesario para continuar con esta tesis. A mis dos abuelas, por preguntarme qué estaba investigando, aunque ellas supieran que no lo iban a entender. Y sobre todo quiero darle las gracias a mi **Madre** y a mi **Padre**, por haber estado siempre ahí, apoyándome desde el día en que nací, y por nunca cortarme las alas sino al contrario, por querer que vuelva lo lejos que haga falta (aunque tenga que ser fuera de la isla). Gracias por todo. Y por último le quiero dar las gracias a mi hermano **Gabriel** (y a **Helena** por su apoyo =D) por enseñarme que el hermano mayor no es siempre es que le tiene que dar lecciones al pequeño, a que no hay que vivir la vida con prisa, y a que a veces, las cosas se arreglan solas. Os quiero mucho a todos.

Table of contents

List of figures, schemes and tables	17
Summary.....	22
List of abbreviations	24
Introduction.....	27
Chapter 1 Basic principles of the microtubule cytoskeleton.....	29
Structure of microtubules.....	31
Microtubule polymerization and dynamic instability	31
Tubulin evolution, tubulin isotypes and post-translational modifications	33
Microtubule associated proteins	36
+TIPs.....	38
Severing enzymes	39
Microtubule motor proteins	41
Chapter 2 Generation of MTOCs	45
Microtubule nucleation (in vitro and in vivo).....	47
Principal components of an MTOC	47
Nucleators	49
γ -tubulin and γ -tubulin complexes.....	49
Recruitment factors	50
Activators	51
Anchoring factors	52
Other regulators	52
Chapter 3 MTOCs, nc-MTOCs and minimal MTOCs.....	55
The centrosome	57
The centrosome as MTOC during interphase	60
Centrosomal and non-centrosomal microtubule organisation during mitosis	64
Non-centrosomal MTOCs	67

Golgi apparatus	67
Nuclear envelope	70
Cell cortex	71
Mitochondria	74
Towards a minimal MTOC.....	74
Aims	78
Materials and Methods	80
Molecular cloning.....	82
Cloning strategy	82
Site-directed mutagenesis.....	82
RT-PCR.....	82
Plasmids	83
Cell culture	84
Stable cell line generation.....	84
GFP-NINL stable cell line.....	84
Cell culture treatments.....	84
Overexpression experiments.....	84
siRNA treatments.....	85
Regrowth experiments.....	86
Immunofluorescence microscopy.....	86
Lysates and Western Blot.....	87
Immunoprecipitation	87
Antibodies	88
BioID experiments.....	89
Biotin-streptavidin affinity purification	89
Digestion on beads.....	90
LCMSMS analysis	90
Data analysis	91
Protein purification	91
Cloning of NINL fragments for bacterial expression.....	91

Purification of bacterially expressed mEGFP-NINL proteins	91
Microscopy analysis for in vitro LLPS	92
NINL mutants	92
NINL-Nt.....	93
NINL-Nt 12P and 16P	93
NINL-Nt 11A and 22A	93
Antibody generation.....	94
Protein purification for antibody generation	94
Rabbit injection and serum extraction	94
Antibody purification	95
Statistical analysis	95
Web resources	95
Results	104
Chapter 1 Molecular characterization of ectopic MTOCs	106
Establishing ectopic MTOC assembly on the outer surface of mitochondria	108
Most POI targeted to mitochondria recruit γ TuRC.....	112
NINL-Nt and CKAP5 induce microtubule nucleation at the ectopic site ...	115
Characterization of components involved in ectopic MTOC formation.....	117
CM1, CEP192-Nt, NINL-Nt and NIN-Nt all recruit NEDD1 to the ectopic site.....	117
PCNT is not required for MTOC formation at the mitochondria.....	119
CDK5RAP2 is not required for MTOC formation at the mitochondria .	119
Mitochondria-targeted CM1, NINL-Nt and NIN-Nt recruit endogenous CKAP5	122
Exploration of the different MTOCs	124
Nucleation at the ectopic site can be activated in trans.....	124
CKAP5 nucleates microtubules possibly through tubulin recruitment ...	125
CM1 and NINL-Nt induce similar nucleation activity when targeted to mitochondria.....	127

Chapter 2 Molecular characterization of MTOC formation by ectopically expressed NINL	130
Identification of minimal NINL region required for MTOC formation.....	132
NINL second coiled coil mediates self-oligomerization	135
NINL 1-287 is the minimal region required to bind γ TuRC.....	137
NINL relationship with other SDA proteins.....	139
NINL interacts with CEP170 through a predicted EF-Hand	140
CEP170 binding is dispensable for MTOC assembly by NINL 1-442	143
CEP170 silencing does not impair ectopic MTOC formation by NINL 1-442.....	144
Search for novel NINL interactors.....	145
BioID reveals candidates involved in ectopic MTOC formation and/or function	145
Requirements for CM1- and NINL fragment-induced ectopic MTOCs	149
NINL fragment- and CM1-induced ectopic MTOC depend on γ TuRC..	149
NEDD1 is required for NINL 1-442-induced but not CM1-induced MTOCs.	150
CKAP5 is required for NINL 1-442-induced but not CM1-induced MTOCs.	152
Chapter 3 NINL and phase separation	155
NINL overexpression generates aberrant structures in cells.....	157
GST-tagged NINL-Nt and NINL 1-287 phase-separate <i>in vitro</i>	158
GFP-tagging induces aggregation of NINL-Nt, whereas NINL 1-442 and NINL 1-287 phase-separate <i>in vitro</i>	160
Disruption of the coiled-coil domains in NINL-Nt impairs droplet formation whereas disruption of aromaticity leads to aggregation in cells	162
Chapter 4 Dissection of the role of NINL at the centrosome	166
NINL localizes to SDAs	168
CEP170 depletion does not remove NINL from SDAs.....	170
NINL localization to SDAs is NIN-independent.....	171
NINL depletion does not remove NIN from SDAs.....	172
NINL localization is CKAP5 dependent.....	172

NINL partially co-localizes with microtubules that seem to be generated from SDAs.....	174
Discussion	176
The mitochondrial targeting system.....	178
Is the ectopic nucleation site an MTOC?.....	180
Targeting to the mitochondrial surface reveals different types of MTOCs..	180
Insight into MTOC formation by NINL.....	184
Does MTOC formation by NINL involve phase separation?	188
Implications of NINL localization at SDAs.....	190
Conclusions	195
References	198

List of figures, schemes and tables

Figure I1. Microtubules are dynamic structures.	32
Figure I2. Principal modification sites of tubulin in a microtubule.	34
Table I1. Main PTMs of tubulin and microtubules.....	35
Figure I3. MAPs carry out many different cellular processes.	37
Figure I4. The diversity of binding mechanisms of +TIPs.....	39
Figure I5. Severing enzymes influence on microtubule dynamics.	41
Figure I6. Microtubule motor proteins “walk” across microtubules to transport its cargo.	43
Figure I7. Components of an MTOC.	48
Figure I8. Main activities and molecular players that could constitute an MTOC. .	49
Figure I9. Centriole duplication cycle.....	58
Figure I10. Microtubule nucleation at the centrosome.....	60
Figure I11. The three microtubule nucleation pathways involved in mitotic spindle assembly.....	66
Figure I12. Main microtubule nucleation pathways of the Golgi as MTOC.....	69
Figure I13. The nuclear envelope acts as an MTOC in myotubes.....	71
Figure I14. Microtubule organization in epithelial cells.....	73
Table M2. List of plasmids used in this thesis.	83
Table M3. siRNAs employed throughout this thesis.	85
Table M4. List of antibodies used for IF and WB.	88
Table M1. Vectors, restriction enzymes and primers employed for molecular cloning.....	96
Table M5. Amino acid sequence of the NINL mutants generated (mutations are indicated in red).	100
Scheme R1. Strategy used to analyse MTOC formation on the outer surface of the mitochondria.	109
Figure R1. Validation of the mitochondrial targeting system.	111
Figure R2. CM1, CEP192-Nt, NINL-Nt and NIN-Nt targeted to mitochondria co-recruit γ -tubulin.	113

Figure R3. CM1, CEP192-Nt, NINL-Nt and NIN-Nt targeted to mitochondria co-recruit GCP8.	114
Figure R4. CM1, NINL-Nt and CKAP5 are capable of inducing microtubule nucleation at the outer surface of the mitochondria.	116
Figure R5. CM1, CEP192-Nt, NINL-Nt and NIN-Nt recruit NEDD1 to the mitochondria.	118
Figure R6. PCNT is not recruited to mitochondria by any of the POI tested.	120
Figure R7. CKD5RAP2 is not recruited to the mitochondria by any of the POI tested.....	121
Figure R8. CM1, NINL-Nt, and NIN-Nt recruit CKAP5 to the mitochondria, even in the absence of microtubules.	123
Table R1. Summary of the ectopic MTOC composition and nucleation capacity after targeting the different POI to the mitochondria.	124
Figure R9. Cytoplasmic expression of CM1 is sufficient to induce nucleation from CEP192 Nt-decorated mitochondria.....	125
Table R2. Summary of CKAP5 domains targeted to mitochondria and their MTOC formation capacity.	126
Figure R10. TOG domains from CKAP5 are required to generate an active MTOC that is γ TuRC-independent.	127
Figure R11. The MTOCs build by CM1 and NINL-Nt when targeted to the mitochondria, share the same microtubule nucleation capacity.	128
Schematic R2. Domain structure of <i>Hs</i> NINL.	132
Table R3. Summary of the results obtained from NINL truncation mutants targeted to mitochondria.	133
Figure R12. NINL 1-442 and NINL 196-584 are sufficient for MTOC formation at the mitochondria.....	134
Figure R13. NINL-Nt and NINL 196-584 targeted to mitochondria are able to recruit cytoplasmic NINL-Nt.	136
Figure R14. NINL 1-287 is the minimal domain necessary for γ TuRC recruitment.	138
Figure R15. NINL-Nt, NINL 1-442 and likely NINL 1-287 co-immunoprecipitate with the γ TuRC.....	139
Figure R16. NINL binds CEP170 through aa 287-383.	140

Figure R17. NINL shares a potential 5 th EF-Hand in the region between aa 301-371.	141
Figure R18. E359K mutation impairs the binding of NINL to CEP170. NIN mainly interacts with NINL-Nt.....	143
Figure R19. E359K mutation does not impair ectopic MTOC formation capacity of NINL 1-442.	143
Figure R20. Depletion of CEP170 does not alter NINL 1-442 MTOC formation capacity.....	144
Figure R21. The interactome of mitochondria targeted NINL fragments contains proteins potentially involved in MTOC formation.	146
Figure R22. GO analyses reveal that NINL interactome is related to microtubules and microtubule-associated processes.....	148
Figure R23. GCP2 depletion dramatically reduces microtubule nucleation capacity of CM1- and NINL 1-442-induced ectopic MTOCs	150
Figure R24. NEDD1 depletion reduces microtubule nucleation capacity of the NINL 1-442-induced MTOC.....	151
Figure R25. CKAP5 depletion impairs microtubule nucleation capacity of the NINL 1-442-induced MTOC.....	152
Figure R26. NINL and NINL-Nt generate aberrant structures that recruit γ -tubulin and nucleate microtubules.....	158
Figure R27. GST-NINL-Nt and GST-NINL 1-287 undergo phase separation <i>in vitro</i>	159
Figure R28. GFP-NINL 1-442 and GFP-NINL 1-287 undergo phase separation <i>in vitro</i> while GFP-NINL-Nt has tendency to protein aggregation.....	161
Figure R29. IDRs prediction of NINL structure.	163
Figure R30. NINL-Nt mutants reveal an important interplay between aromatic residues and coiled-coil domains within NINL.	164
Figure R31. GFP-NINL localizes to SDAs.....	169
Figure R32. NINL localizes to SDAs.....	169
Figure 33. NINL localization to SDAs is CEP170-independent.....	170
Figure R34. NIN depletion does not affect NINL but removes CEP170 from SDAs.	171
Figure R35. NIN localizes to SDAs after NINL depletion.	172

Figure R36. NINL is displaced from SDAs after CKAP5 depletion..... 173

Figure R37. CKAP5 and NINL form spike-like structures that co-localize at SDAs.
..... 173

Figure R38. NINL forms spike-like structures that co-localize with microtubules
early during regrowth. 174

Figure D1. Minimal components required for ectopic MTOC assembly by different
POIs..... 183

Figure D2. Functional characterization of NINL reveals distinct functional regions.
..... 185

Figure D3. NINL localisation and function at SDAs. 192

Summary

Despite decades of work, the molecular requirements underlying microtubule-organizing center (MTOC) formation at the centrosome remain obscure. Progress is hindered by the complexity of this organelle, which is composed of hundreds of proteins that are involved in a range of functions, many unrelated to microtubule organization. To avoid such intricacy, we studied MTOC formation at an ectopic site. Employing a domain previously identified in a splice variant of the centrosome protein Cnn in *Drosophila*, we targeted fusion proteins to the cytoplasmic surface of mitochondria in human U2OS cells. We tested several human candidate proteins based on their described relationship with MTOCs such as CDK5RAP2, CEP192, NIN, NINL and CKAP5. MTOC formation capacity was analysed by probing for recruitment of the nucleator γ TuRC and for microtubule nucleation activity. Interestingly, multiple candidates were able to recruit γ TuRC to the ectopic site. However, only an N-terminal fragment of NINL was able to also induce microtubule nucleation similar to the CM1 region of CDK5RAP2, which served as positive control. Noteworthy, CKAP5 induced microtubule formation at the ectopic site independently of γ TuRC. Testing of NINL truncation mutants allowed mapping of separate regions required for γ TuRC binding and nucleation activation. Biotin-proximity labelling of mitochondrial surface-targeted NINL fragments further identified additional candidate proteins involved in these functions. Using super resolution microscopy, we found endogenous NINL to associate with subdistal appendages (SDAs) of the mother centriole, pointing to a possible role of NINL in MTOC formation at SDAs.

List of abbreviations

γ TuRC	γ -tubulin ring complex
γ TuSC	γ -tubulin small complex
CCPs	Cytosolic carboxypeptidases
CGN	cis-Golgi network
CH	Calponin homology domain
CM1	Centrosomin motif 1
Cnn	Centrosomin
DAs	Distal appendages
DHC	Dynein heavy chain
DIC	Dynein intermediate chain
DIC	Differential interference contrast
DMEM	Dulbecco's Modified Eagle Medium
DP	Desmoplakin
DYNC1H1	Cytoplasmic dynein heavy chain
EB	End-binding protein
EBH	EB homology domain
EM	Electron microscopy
FBS	Fetal bovine serum
GCPs	γ -tubulin complex proteins
IDR	Intrinsically disordered region
IF	Immunofluorescence
LC	Light chain
LIC	Light intermediate chain
LLPS	Liquid-liquid phase separation
MAPs	Microtubule-associated proteins
Mito	Mitochondrial-targeting domain
MTOC	Microtubule-organizing centre
nc-MTOCs	non-centrosomal MTOCs
NINL	Ninein-like protein
NINL	Ninein
NINL-Nt	NINL 1-702
PACT	PCNT-AKAP9 centrosomal targeting
PBS	Phosphate-buffered saline
PCM	Pericentriolar material
PCNT	Pericentrin
PEI	Polyethylenimine
Plp	Pericentrin-like protein

POI	Proteins of interest
PTM	Post-translational modifications
RAN	RAS-related nuclear protein
RCC1	Regulator of chromosome condensation 1
SAFs	Spindle-assembly factors
SDAs	Subdistal appendages
SIM	Structured illumination microscopy
SPM	Spc110/Pcp1 motif
TGN	trans-Golgi network
TPX2	Spindle assembly factor targeting protein for Xklp2
TTL	Tubulin tyrosine ligase
TTLL	tubulin tyrosine ligase-like
WB	Western blot
γ TuRC	γ -tubulin ring complex
γ TuSC	γ -tubulin small complex

Introduction

Chapter 1

Basic principles of the microtubule cytoskeleton

Structure of microtubules

Microtubules along with actin, intermediate filaments and septins are key components of the cytoskeleton. Microtubules are required for various cellular processes such as cell division, intracellular transport of cargos, maintenance of cell morphology or cell migration.

Microtubules are polymeric structures composed of dimers of $\alpha\beta$ -tubulin that assemble in a head-to-tail fashion, as part of so-called protofilaments. Electron microscopy (EM) studies have shown that in most eukaryotic cells microtubules are composed of 13 laterally associated $\alpha\beta$ -tubulin protofilaments (Tilney, 1973). Due to the head-to-tail arrangement of tubulin subunits microtubules have an intrinsic polarity characterised by a relatively dynamic “plus-end” and a more stable “minus-end”. Microtubule plus-end dynamics are affected by three main factors: tubulin isotypes, post-translational modifications (PTMs) of tubulin, and microtubule-interacting proteins. Microtubules are generated in a process called microtubule nucleation.

Microtubule polymerization and dynamic instability

Addition of new $\alpha\beta$ -tubulin dimers to a pre-existing microtubule is termed microtubule polymerization and is a GTP-dependent process. Microtubules are not static structures in live cells. In contrast, microtubules constantly undergo episodes of growing and shrinking at their plus-end. The constant switching between these two states is known as dynamic instability and it is an intrinsic property of microtubules (Mitchison, 1984). Interestingly, dynamic instability is caused by the GTP state of tubulin. Both α - and β -tubulin can bind GTP, but only GTP bound to β -tubulin can be hydrolysed to GDP. GTP hydrolysis occurs with some delay following incorporation of tubulin at the growing plus-end. As a result, most of the microtubule lattice is composed of GDP- β -tubulin whereas the plus-end maintains a so-called “GTP-cap” composed of GTP- β -tubulin. GTP hydrolysis destabilizes the lattice but the GTP-cap prevents depolymerization and allows the growth of the microtubule. Upon loss of the cap the microtubule switches from growth to rapid shrinkage (termed “catastrophe”). The sudden gain of a new cap would switch the microtubule back to normal growth (termed “rescue”) (**Figure 11**) (Seetapun, 2012).

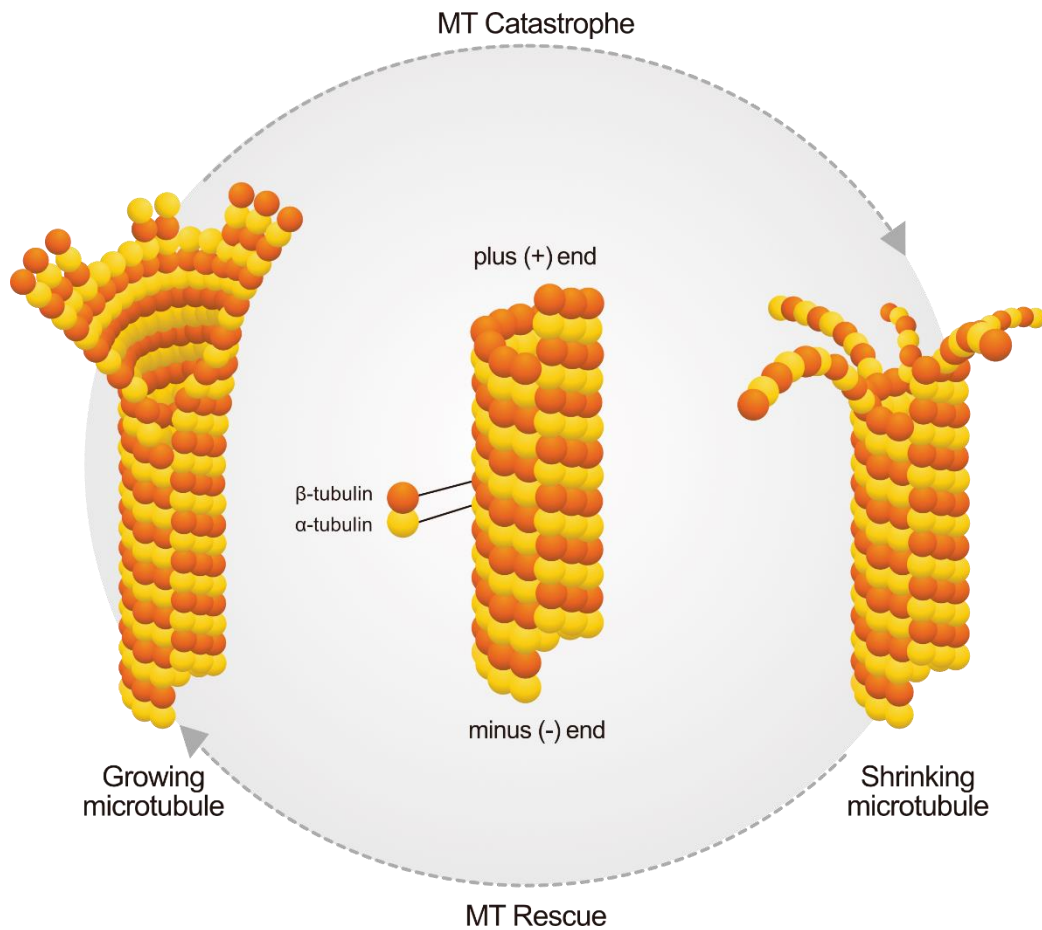


Figure I1. Microtubules are dynamic structures.

Microtubules are formed by the lateral interaction of 13 protofilaments of heterodimers of α - (yellow) and β -tubulin (orange). Due to the arrangement of tubulin dimers in a head-to-tail fashion, microtubules have an intrinsic polarity, with a more stable minus-end and a dynamic plus-end. Microtubules are very dynamic structures that are constantly undergoing episodes of growing and shrinking. The switch from growing to shrinking is known as catastrophe and the opposite process is called rescue. This process is dependent on the state of the GTP-cap.

As described above microtubules are two-state polymers, which undergo sudden transitions between growing and shortening. Interestingly, *in vitro* studies with a purified microtubule motor protein, KIF21B, have proposed that there is an intermediate state where microtubules do not elongate or shrink for longer periods of time, also defined as microtubule pausing (van Riel, 2017). The pausing state can last up to 20 seconds in some microtubules and if proven *in vivo*, it could be relevant for the spatiotemporal regulation of the microtubule network.

Tubulin evolution, tubulin isotypes and post-translational modifications

Tubulins are a highly conserved family of GTPases. In general, tubulins show little structural variation throughout eukaryotic evolution. Notably, tubular structures related to microtubules also exist in prokaryotic cells. FtsZ is a bacterial protein essential for cell division and septation which also belongs to the GTPase family and forms protofilaments (Erickson, 1995; Nogales, 1998). *Bacteria* from the genus *Prostheco bacter* are known to form tubular structures composed of 5 protofilaments of heterodimers of the proteins BtubA and BtubB, that are reminiscent of the 13 protofilament structure of eukaryotic microtubules (Pilhofer, 2011).

In eukaryotic cells, there have been described at least 6 types of tubulins which constitute the tubulin superfamily. It is composed of the well-known α - and β -tubulin and by γ -, δ -, ϵ - and ζ - tubulin (Findeisen, 2014). As microtubules are composed of dimers of $\alpha\beta$ -tubulin, it is not surprising to find that these two types of tubulins have been extensively studied. It has been described that these proteins are encoded by multiple genes in most organisms. In humans, there are 9 genes encoding α -tubulin and 10 genes encoding β -tubulin (<https://www.genenames.org/data/genegroup/#!/group/778>). It has been suggested that the incorporation of these different isotypes of tubulin in the microtubule lattice could have a function in the regulation of microtubule dynamics and mechanical properties, by altering the structure of the lattice or by regulating the interaction with microtubule associated proteins (Gadadhar, 2017). There are some specialized microtubules from particular structures, such as the axoneme (Raff, 2008), or in specific cell types such as neurons (Joshi, 1989), where certain isotypes of β -tubulin are more abundant. It is possible that the homogeneity of isotypes is required for the gain of specialized functions.

Microtubule dynamics and organization are additionally regulated by the PTMs on tubulin. Curiously, tubulin may be modified as a soluble dimer or as part of the microtubule lattice. At a structural level, most PTMs occur on the variable C-terminal tails of α -tubulin and β -tubulin that are exposed on the outer part of the microtubule (**Figure I2**).

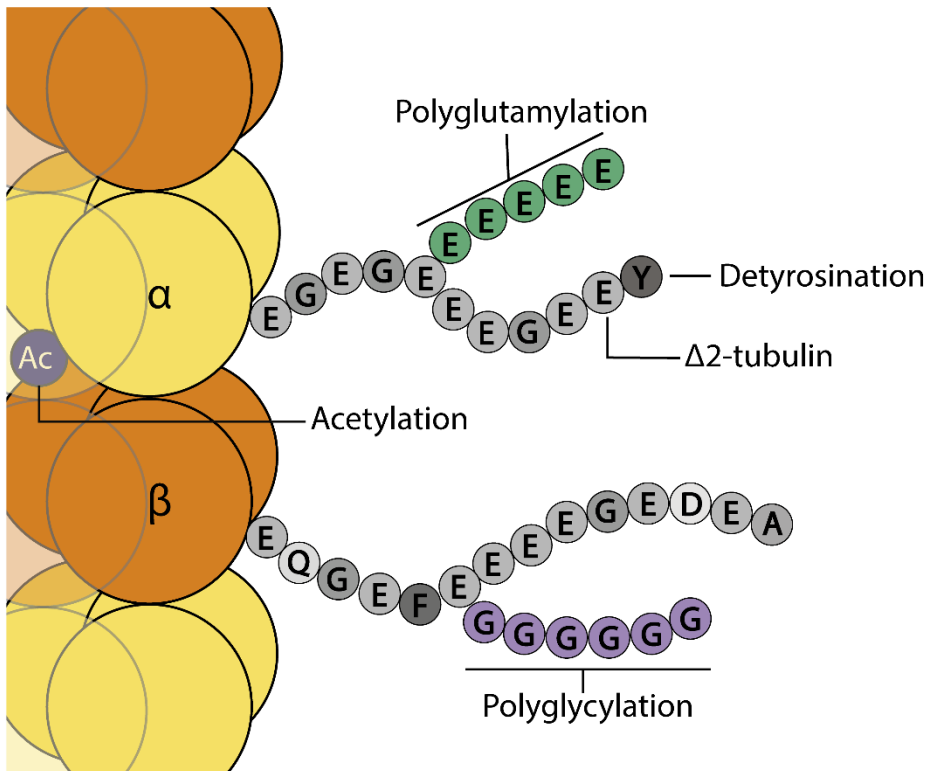


Figure I2. Principal modification sites of tubulin in a microtubule.

Schematic representation of a microtubule with the most common PTMs. The C-tails of both tubulins are represented as aa sequences. Most of the PTMs occur at the C-tail of either α - or β -tubulin. Notice that acetylation is carried out at the lumen of the microtubule. Both tubulins can be modified by adding multiple Gly (G) (polyglycylation) or Glu (E) (polyglutamylation) to the different Glu residues present within the C-tails. The Tyr (Y) present at the end of the tail of α -tubulin can be detyrosinated to make the last Glu available. This Glu can be additionally removed to generate $\Delta 2$ -tubulin, a very common modification in long-lived neurons, cilia and centrosomes.

At the very end of most α -tubulins there is a terminal tyrosine. RNA-independent enzymatic incorporation of this tyrosine was the first modification identified almost 50 years ago (Barra, 1973). Later it was discovered that tubulin tyrosine ligase (TTL) is the protein carrying out that role. Recently, it was discovered that detyrosination of the same residue is carried out by the VASH2/SVBP heterodimer (Zhou, 2019). Cytosolic carboxypeptidases (CCPs) can irreversibly modify detyrosinated tubulin by removing the penultimate glutamate of the C-terminus of α -tubulin giving rise to $\Delta 2$ -tubulin. Both detyrosinated and $\Delta 2$ -tubulin are present in long-lived microtubules, which are commonly found e.g. in neurons, centrioles and cilia (Song, 2015).

Polyglutamylation and polyglycylation are two competing types of PTM that can occur on both α - and β -tubulin. They involve the covalent addition of glutamate or glycine residues to glutamate residues present in the C-terminal tails of tubulins, which serve as a branching point for the formation of a side chain of multiple glutamates/glycines. The TLL (tubulin tyrosine ligase-like) family comprises proteins capable of glutamylation and glycylation of microtubules while the CCP family are the enzymes responsible for deglutamylation. Despite polyglutamylation being one of the major PTMs of the brain and being upregulated upon neuron differentiation, little is known about the specific function of this modification as well as for the role of polyglycylation (Janke, 2011).

Curiously, not all the PTMs take place at the outer surface of the microtubule lattice. Acetylation/Deacetylation has a canonical site at Lys40 of α -tubulin, located at the luminal side of microtubules. Recently it has been shown that the main tubulin acetyltransferase, TAT1, is able to scan the lumen of microtubules in both directions, stochastically acetylating Lys40. Despite tubulin being the major cytoplasmic target for acetylation, its physiological roles are still unclear. Although acetylation is commonly associated with long-lived stable microtubules, it has never been shown a direct effect of acetylation on microtubule stability. Also, double KO mice of the two main tubulin deacetylases, SIRT2 and HDAC6, are viable despite tubulin hyperacetylation (**Table I1**) (Song, 2015).

PTM	Site	Enzyme
Acetylation	At luminal lysine 40 of α -tubulin	TAT1
Deacetylation	On soluble α -tubulin	HDAC6, SIRT2
Tyrosination	Addition to C-terminal of α -tubulin	T [*] TLL
Detyrosination	Removal of C-terminal Tyr	VASH2/SVBP
Glutamylation/ Polyglutamylation	Addition of linear C-terminal Glu (α/β -tub) Addition of various branched Glu to C-terminal Glu	T [*] TLL4, 5, 7 T [*] TLL1, 6, 11, 13
Δ 2 deglutamylation	Removal of C-terminal Glu in detyrosinated microtubules(α -tub)	CCP1-CCP6
Glycylation/ Polyglycylation	Addition of branched Gly to C-terminal Glu (α/β -tub) Addition of various Gly to branched Gly	T [*] TLL3, T [*] TLL8 T [*] TLL10
Deglycylation	Unknown	Unknown

Table I1. Main PTMs of tubulin and microtubules.

Microtubule associated proteins

Regulation of the microtubule network is accomplished by the collective effort of the incorporation of different tubulin isotypes, PTMs of tubulin and several proteins interacting with the microtubule lattice, also known as microtubule-associated proteins (MAPs).

MAPs were defined in this way due to their ability to control the structure of microtubule assemblies by promoting microtubule polymerization, stabilization, or bundling. More recent evidence has shown that they additionally have specific cellular functions, such as linking other cytoskeletal elements, organelles and membranes or monitor the activity of other MAPs (**Figure I3**). Regarding their regulation, it seems that their binding to the microtubules is tightly controlled by PTMs of both MAPs and microtubules (Bodakuntla, 2019).

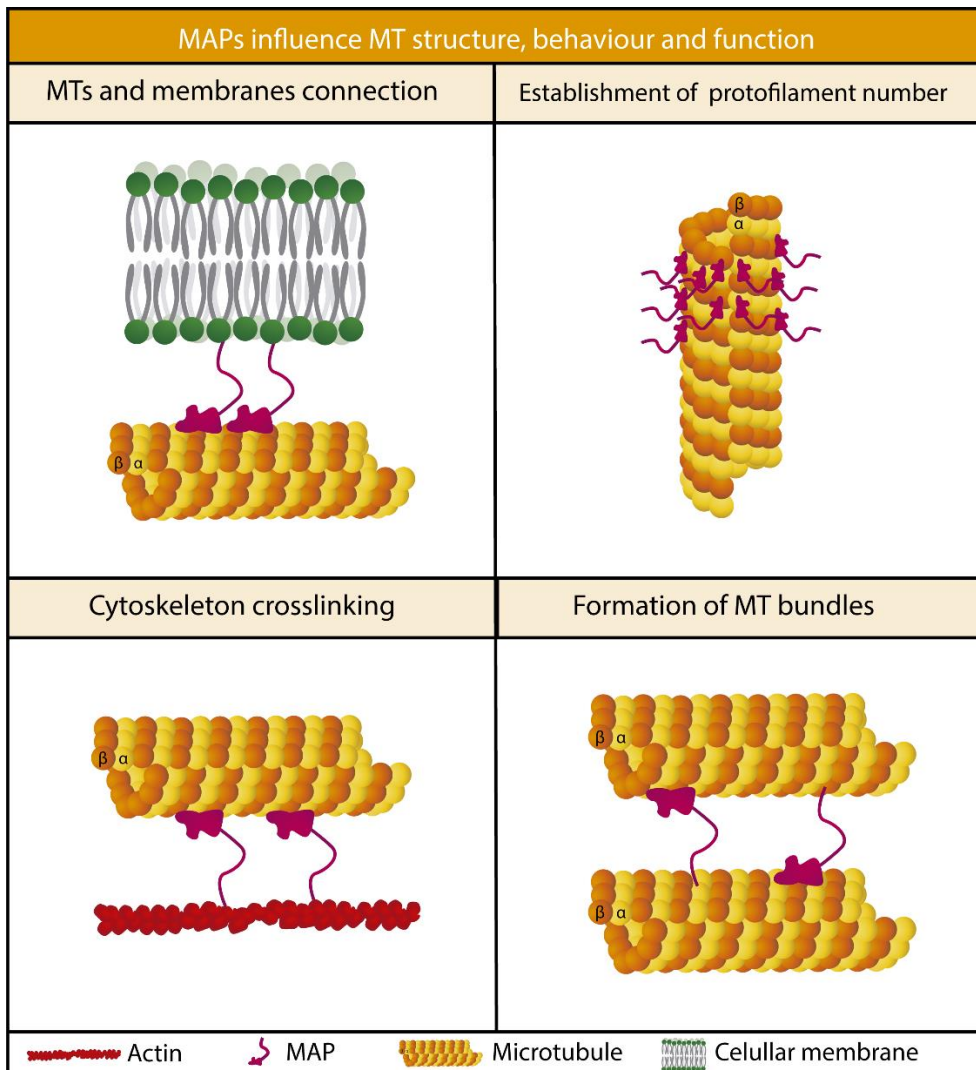


Figure I3. MAPs carry out many different cellular processes.

Scheme depicting some of the functions that MAPs are involved in. They are key for tethering microtubules to the distinct cellular membranes. MAPs such as doublecortin are necessary for the proper establishment of the microtubule protofilament number. They also serve as a bridge between different cytoskeletal elements such as microtubules and actin. In some specific cells, it is common to find microtubule bundles (e.g. neurons) and proteins such as PRC1 or TRIM46 are required to achieve bundling (Bodakuntla, 2019).

In addition, it has been shown that some MAPs can form dense structures along microtubules. Tau protein, one of the most abundant MAPs in brain samples, which is also linked to Alzheimer's disease (Kovacs, 2017), is able to bind to microtubules and reversibly self-associate, which leads to the formation of dynamic tau condensates. Tau condensation promotes the separation of this protein from the

cytosol. *In vitro*, these condensates form liquid-like drops that concentrate tubulin leading to tubulin polymerization and microtubule bundle formation (Hernandez-Vega, 2017). Microtubule polymerization by tau has not been proven *in vivo*, nevertheless, tau forms condensates in particular regions of the microtubule that act as selective barrier, limiting the capacity of microtubule severing-enzymes and regulating the movement of motor proteins (Tan, 2019). These results imply that liquid liquid-phase separation (LLPS) of different MAPs could be another layer of regulation of the microtubule network.

+TIPs

Microtubule plus-end tracking proteins (+TIPs) are a diverse group of proteins with the ability to concentrate on growing microtubule plus-ends. The dynamic plus-end is a region in constant change and therefore its protein network has to be precisely regulated. The master regulators of +TIPs networks are the end-binding proteins (EBs). EBs autonomously bind to microtubules through their calponin homology domain (CH) (Hayashi, 2003) and they regulate the binding of other +TIPs through a carboxy-terminal EEY/F motif and a EB homology domain (EBH). Proteins that contain a cytoskeleton-associated protein Gly-rich domain (CAP-Gly) bind to the EEY/F motif from EBs modulating microtubules dynamics, such as CLIP170 which promotes microtubule rescue (Slep, 2007). Also, the large subunit of the dynactin complex, p150^{Glued} can suppress catastrophes. Another group of proteins that can bind to the CH domain of EBs are proteins containing a SxIP amino acid motif (Honnappa, 2009). CLASPs family of proteins are able to bind through EBs and associate with the microtubule lattice favouring the incorporation of soluble tubulin dimers. The non-motile kinesin MCAK and the motor kinesin Kif18b are also able to bind to EBs via this domain and acts as a complex to induce microtubule depolymerization. The XMAP215 family of polymerases are able to independently associate with tubulin dimers and favour microtubule polymerization (Gard, 1987). Interestingly, there is an intense competition of these proteins to bind to the microtubule plus-end, creating a crowded environment. To ensure continuous delivery of promoting factors to the growing microtubule end, some species have “adhesive” proteins, for example in mammals SLAIN2 (van der Vaart, 2011). This protein is able to interact with CKAP5 (a human XMAP215 family protein) and with CLIP170 at the same time. Moreover, it contains several SxIP domains that enhance its affinity for EBs assuring preferential binding to the microtubule plus-end (**Figure I4**) (Akhmanova, 2015).

Due to their localization, +TIPs are necessary for microtubule guidance, attachment of microtubules plus-ends to different cellular structures and they can even concentrate molecules for signalling purposes. Notably, some +TIPs have also been found to be important at microtubules minus-ends, such as CKAP5 or CLASPs, where they have a further role in the coordination of microtubule nucleation (Popov, 2002; Efimov, 2007; Rivero, 2009; Akhmanova, 2015; Thawani, 2018).

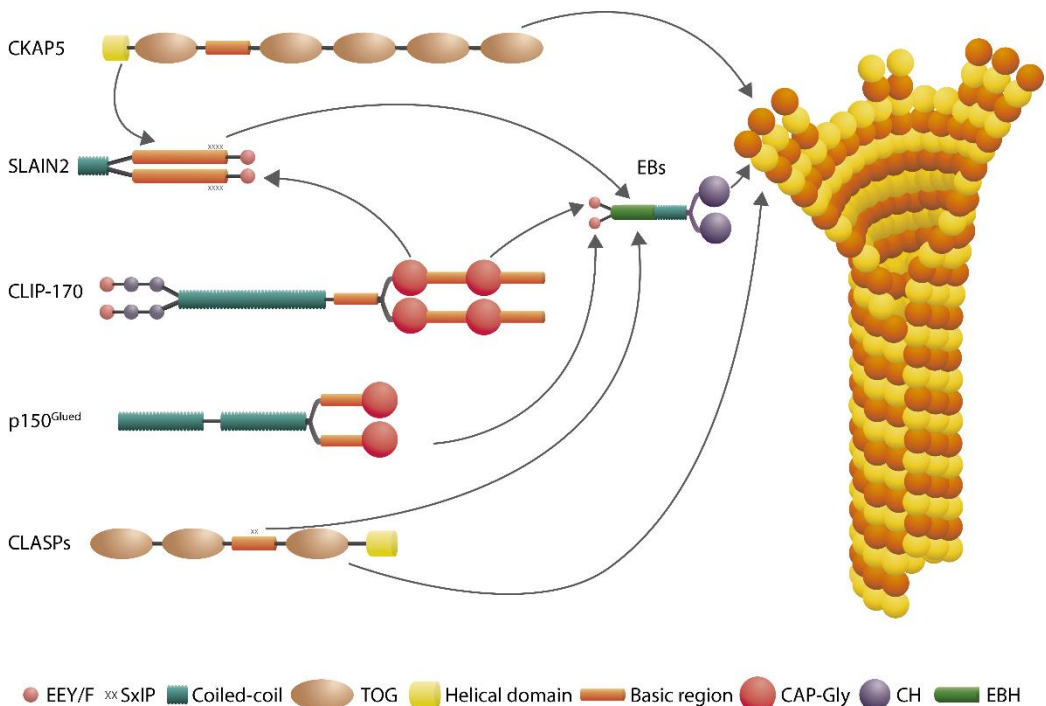


Figure I4. The diversity of binding mechanisms of +TIPs.

Schematic depicting the distinct binding mechanism of several +TIPs to microtubules. Generally, EBs bind first to microtubules through their CH domains and they contain additional domains to incorporate other +TIPs to microtubules. Proteins containing a CAP-Gly domain, such as CLIP170 or p150^{Glued}, bind to the EEY/F domain from EBs. Additionally, proteins that contain a SxIP amino acid motif, such as SLAIN2 and CLASPs, bind to the EBH domain from EBs. Notice that SLAIN2 contains more SxIP motifs than CLASPs, to ensure preferential binding to microtubules. SLAIN2 acts as an adhesive factor and other +TIPs can bind it, normally to promote microtubule polymerization. CKAP5 is a microtubule polymerase that can also bind autonomously to microtubules.

Severing enzymes

While it was generally assumed that microtubule polymerases and depolymerases were in control of the shaping of the microtubule network, another group of proteins defined as microtubule severing enzymes were shown to possess a major role in this

process (Roll-Mecak, 2010; Akhmanova, 2015; McNally, 2018). Microtubule severing enzymes belong to the AAA or ATPases family of proteins. They are associated with diverse cellular activities and are mainly characterised by their ability to remodel protein complexes through ATP hydrolysis. To date, the microtubule severing enzymes family is composed of katanin, spastin and fidgetin (McNally, 1993; Evans, 2005; Roll-Mecak, 2005; Mukherjee, 2012). These enzymes bind along the microtubule lattice and are able to break microtubules by removing tubulin dimers. The extent of the severed region can determine either the amplification or disassembly of the microtubule network (McNally, 2018). Recent *in vitro* studies have shown that both spastin and katanin severing of microtubules, causes a sudden incorporation of GTP-tubulin “islands” at the severed region (Vemu, 2018). This correlates with an increase in the polymerization events and microtubule mass, explaining why in physiological conditions there can be an increase in the number of microtubules in the absence of microtubule nucleation events (**Figure I5**).

Severing enzymes have been described to be fundamental for a variety of cellular processes. Cells rely on severing enzymes for proper cell migration, in the absence of these proteins most of the microtubules bend when they reach the cell cortex impairing proper migration (Zhang, 2011). Cells also required severing enzymes to control the number of microtubules nucleated at the centrosome, katanin breaks the microtubules at their minus ends so that they are not anchored to the centrosome anymore and therefore they are consequentially released (Dong, 2017). Another process that is tightly regulated by microtubule severing enzymes is the microtubule spindle flux during mitosis, as emanating centrosomal microtubules minus-ends have to be detached from the centrosome to ensure a proper flux (Zhang, 2007; McNally, 2018).

Structural work has shed some light into how severing enzymes could remove tubulins from the microtubule lattice. The proposed structure of katanin shows an asymmetric hexamer where the AAA domains from the different subunits are in the inner circle of the hexamer, while the MIT domains (in charge of binding to the microtubules) are linked to that inner circle by flexible arms. In the middle of the inner circle there is a pore that has been hypothesized to bind to the disordered C-tail of α -tubulin and promote the removal of the corresponding tubulin dimer from the microtubule (Zehr, 2017; Nithianantham, 2018). This was model confirmed experimentally very recently with the use of cryoelectron microscopy. Curiously it was observed that katanin binds to the disordered region of β -tubulin, not α -tubulin as predicted (Zehr, 2020).

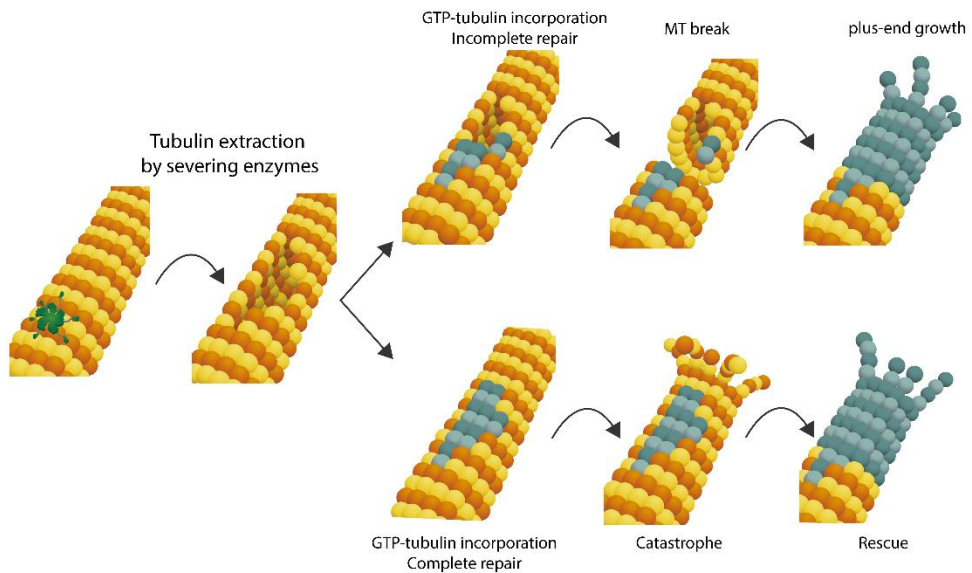


Figure I5. Severing enzymes influence on microtubule dynamics.

Schematic depicting the proposed mechanism of action of katanin and how it affects microtubule dynamics. First, severing enzymes or in this case katanin (green), binds to the C-tails of β -tubulin from microtubules and extracts tubulin dimers generating a gap in the microtubule. This gap can be later repaired by the addition GTP-tubulin. If the repair is incomplete this will induce a microtubule break and as there is GTP-tubulin in that area this will allow for the microtubule plus-end to continue growing. On the other hand, if the repair is complete the stability of the microtubule will not be affected. If at some point the microtubule enters a state of catastrophe, it will be depolymerized until it reaches that GTP enriched area (also known as GTP-island) which will end up in a rescue event. Image based on (Vemu, 2018; Zehr, 2020).

Microtubule motor proteins

The main feature of motor proteins is that they “walk” along cytoskeletal structures. They are divided in actin motor proteins (myosins), and microtubule motor proteins. The latter comprise kinesins and dyneins.

Kinesins are a superfamily of proteins with a total of 45 distinct kinesin-related proteins (Miki, 2001). Although all the members of this family share a common motor domain, only some of them are motor proteins (Sweeney, 2018). Other members of this family have additional roles as direct regulation of microtubule dynamics (e.g. kinesin-13 members as microtubule depolymerases (Desai, 1999; Walczak, 2013)) or microtubule sliding during cell division (e.g. kinesin-5/Eg5 (Goulet, 2013)). Besides the common motor domain, every kinesin has a divergent tail domain, consisting of one or several coiled coil motifs, that allows for

oligomerization of this protein. Kinesins that contain a motor domain generally transport their cargos along microtubules in a plus-end-directed fashion (minus to plus end). Kinesin-1, the first molecular motor described to move cargo along microtubules (Vale, 1985), is able to travel along microtubules by hydrolysis of ATP. The two motor domains of the dimer alternate in the binding to the microtubule, based on ATP/ADP exchange. This process allows the protein to move along microtubules with a high processivity (around 100 steps before detachment) (Block, 1990). Curiously, in a basal state, the two tails from the dimer fold to the motor domains and this protein is inactive (Kaan, 2011)(**Figure I6, Kinesin-1**). Kinesins act as individual motors and its cargo is normally transported by a single kinesin oligomer (Sweeney, 2018).

On the other hand, dyneins belong to the AAA protein family and they are a large family of complex cellular motors involved in axoneme movement and cargo transport. The core protein of the complex is the dynein heavy chain (DHC) or in case of humans the cytoplasmic dynein heavy chain (DYNC1H1). The motor domain (the microtubule binding domain) of the complex comprises DHC, which is connected by a stalk through a hexamer of six AAA domains, resembling the structure of severing enzymes. In the amino-terminal region of the protein there is a tail that mediates the binding to the rest of the components of the dynein complex, namely, dynein intermediate chains (DICs), light intermediate chains (LICs) and light chains (LCs)(Reck-Peterson, 2018; Sweeney, 2018). Altogether, these proteins form a complex of approximately 1.4 MDa. In case of the motor complex, its movement is minus-end-directed (Paschal, 1987) and is dependent on a power stroke that requires the hydrolysis of ATP. This hydrolysis, allows for transitions between strong and weak binding states of the dynein complex to the microtubules (Kon, 2012; Schmidt, 2012; Schmidt, 2015). In contrast to kinesins, it has been found that two or more dynein complexes are bound to the same cargo (Rai, 2013), which enhances the processivity of the motor protein (**Figure I6, Dynein heavy chain**). Moreover, the dynactin complex is generally required for most dynein functions in the cell (Gill, 1991; Schroer, 1991). It is a complex formed by multiple subunits where p150^{Glued} acts as a linker between DIC and the dynactin complex. Other additional effectors such as BICD2, are necessary for the formation of the dynein-dynactin complex (Reck-Peterson, 2018; Sweeney, 2018).

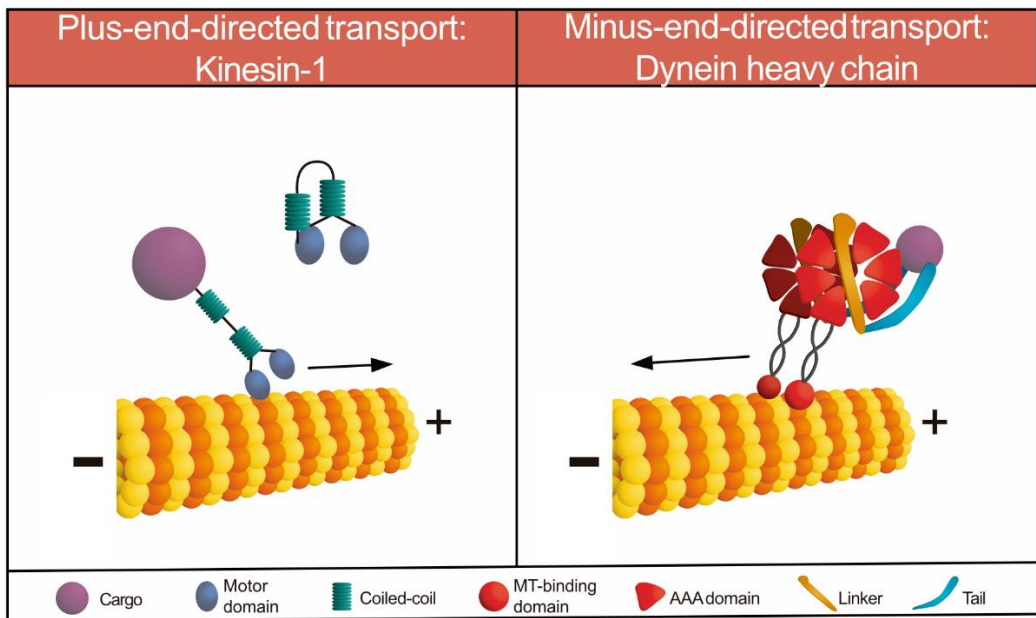


Figure I6. Microtubule motor proteins “walk” across microtubules to transport its cargo.

Schematic showing the different structures and main mechanism of action of the two main families of microtubule motor proteins. Kinesin-1 is a motor protein from the kinesin superfamily, characterised by functioning as individual motors. Therefore, one molecule of kinesin-1 is sufficient to transport its cargo in a plus-end-directed way through microtubules. In a basal state kinesin-1 is folded and inactive. Only when bound to adaptors, kinesin-1 is able to unfold and bind its cargo. The core protein of the dynein complex is the dynein heavy chain (DHC). Normally it binds to microtubules in dimers and this binding is mediated by its microtubule-binding domain. DHC is composed by a hexamer of 6 AAA domains, required to generate the power stroke that induces the movement of the protein through microtubules. It also contains a tail where the rest of the dynein complex proteins and the cargo are bound. This complex moves in a minus-end-directed way along microtubules.

Chapter 2

Generation of MTOCs

Microtubule nucleation (in vitro and in vivo)

In vitro, tubulin dimers can spontaneously polymerize and generate microtubules at a certain concentration (Scheele, 1982). *In vivo*, the generation of new microtubules, termed microtubule nucleation, is spatiotemporally regulated. As many cell functions rely on microtubules, microtubule nucleation cannot be a stochastic process. Therefore, microtubule nucleation is restricted to certain cellular structures, also known as microtubule-organizing centres (MTOCs). A major MTOC in animal cells is the centrosome, composed of two barrel-shaped centrioles and a surrounding proteinaceous scaffold. Generation of an MTOC involves the local enrichment and activation of several factors that promote microtubule nucleation. In this way, microtubule nucleation can be tightly controlled in space and time.

Principal components of an MTOC

Despite the presence of many different types of MTOCs (discussed below), there are several general activities required to generate a fully functional MTOC (**Figure I7**).

If one pictures an MTOC in a canonical way, in theory it is composed by the components shown in **Figure I7**, a recruitment factor, a microtubule nucleator, an activating factor, an anchoring factor and other additional regulators. It is possible that this picture is far from reality. We do not really know if microtubule nucleation and microtubule anchoring happen at the same place (**Figure I8, left side**). One possibility is that there are distinct sites at the same MTOC, one in charge of nucleating microtubules and another site in charge of anchoring the previously nucleated microtubules. It is also unknown if once generated, microtubules preserve their γ TuRC “cap” at their minus-ends or if oppositely its release is necessary for microtubule anchoring (**Figure I8, right side**). It is even possible that there can be MTOC formation in the absence of the prototypical microtubule nucleator. If some proteins are able to undergo LLPS and to interact with soluble tubulin, this could be a potential hotspot for tubulin concentration, which could eventually lead to microtubule nucleation. An interesting debate would be generated then, referring to if this could be considered an MTOC or not.

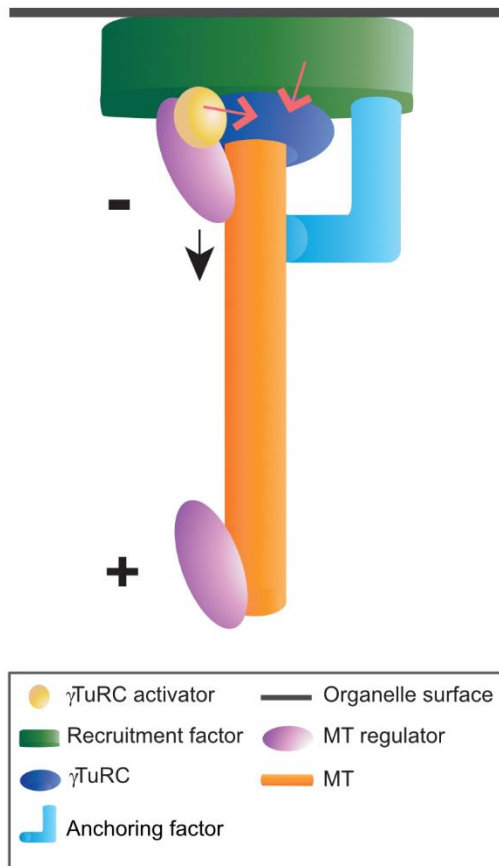


Figure I7. Components of an MTOC.

General overview of the main components required to build a functional MTOC. The nucleator (dark blue) is in charge of the nucleation of microtubules. The main nucleator in eukaryotic cells is the γ TuRC. In most cases, the nucleator has to be targeted to the surface of the MTOC, a function carried out by specific recruitment factors (green). The sole presence of the nucleator is not sufficient to turn microtubule nucleation on, and the presence of an activator (yellow) is required. In some instances, the recruitment factor can act also as an activator (orange arrows = activation of microtubule nucleation). Once microtubules are generated, they need to be attached to the surface of the organelle, a function exerted by anchoring factors (light blue). Additional proteins, microtubule regulators (purple), may be present at the nucleation site to facilitate the microtubule nucleation process by binding and stabilizing early microtubule assembly intermediates or newly formed plus-ends. These regulators may accompany and also be associated with microtubule plus-ends as the microtubules grow. Adapted from (Paz, 2018).

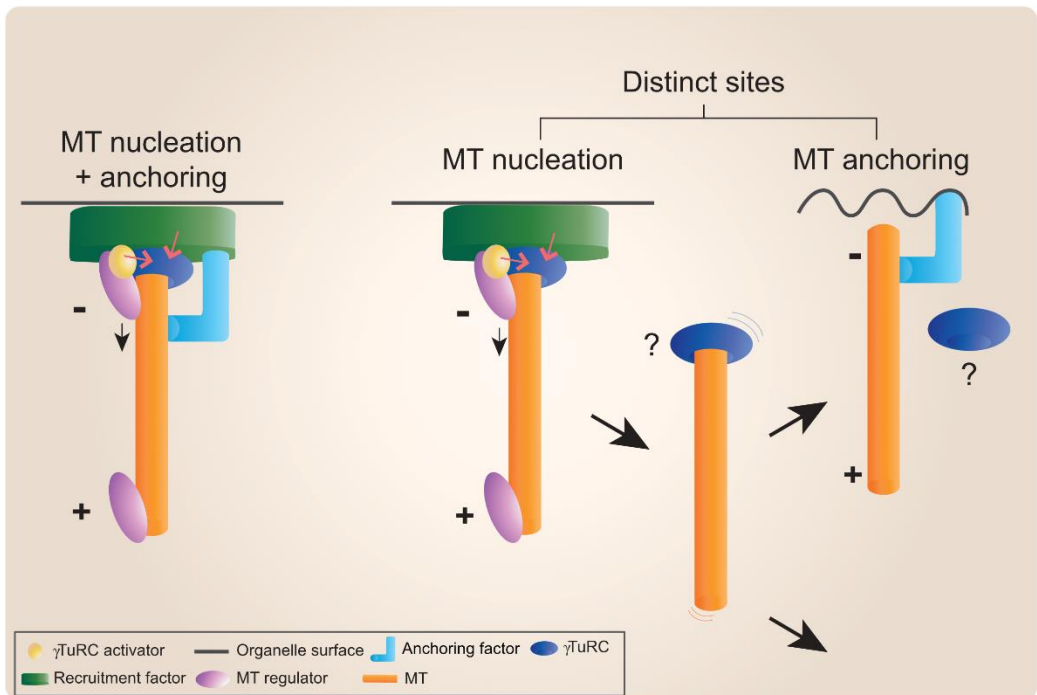


Figure I8. Main activities and molecular players that could constitute an MTOC.

A depiction of two possible scenarios of how microtubules could be organized by an MTOC. On the left side, there is a situation where all the components required (recruitment factor, nucleator, activator, anchoring factor and microtubule regulator) are at the same site. Alternatively, depicted on the right, microtubules are nucleated at one site and then transferred to a different site for anchoring, spatially separating microtubule nucleation from anchoring. It is currently unknown in which cases microtubules preserve the γ TuRC “cap” once nucleated. Adapted from (Paz, 2018).

Nucleators

A core component of MTOCs is the microtubule nucleator. It acts as a catalyst for the microtubule nucleation process. The major nucleator is assumed to be γ -tubulin, which together with γ -tubulin complex proteins (GCPs) forms the γ -tubulin ring complex (γ TuRC) (Moritz, 1995; Zheng, 1995). At a structural level the γ TuRC presents a symmetry that resembles the 13 protofilament symmetry of the microtubule (Tilney, 1973). It is believed that the γ TuRC acts as a template for the generation of new microtubules (Kollman, 2015).

γ -tubulin and γ -tubulin complexes

In many eukaryotes the main nucleator is the γ TuRC. In vertebrates it is composed of the core subunits γ -tubulin, GCPs 2-6, MZT1, MZT2, and an actin-like molecule

(Murphy, 1998; Murphy, 2001; Teixido-Travesa, 2012; Consolati, 2020; Liu, 2020; Wiczorek, 2020; Zimmermann, 2020).

In budding yeast, γ -tubulin forms a complex with the yeast orthologs of GCP2 and GCP3, Spc97 and Spc98 respectively, called γ -tubulin small complex (γ TuSC) (Knop, 1997), but other γ TuRC subunits are absent. Interaction of this complex with Spc110, a yeast homolog of pericentrin (PCNT), is sufficient to induce oligomerization of the complex and generate a γ TuRC-like template for microtubule nucleation (Lin, 2014). Curiously, ring-like oligomers of yeast γ TuSC do not precisely match the 13 protofilament structure of a microtubule. The disposition of γ -tubulin molecules in the γ TuRC suggests that there must be a closing state to match the microtubule symmetry. Yet, experimental correction of this mismatch increased the nucleation activity of the γ TuSC by only twofold, suggesting that there must be another activation mechanism (Kollman, 2015).

In vertebrates including humans, very recent data has shed some light on how the γ TuRC is assembled. Purification and Cryo-EM structure determination of the γ TuRC from *Xenopus laevis* has shown that the γ TuRC ring is formed by 14 γ -tubulin molecules bound to laterally associated γ TuSC and γ TuSC-like complexes, formed by five GCP2-GCP3 pairs, one GCP4-GCP5 pair, and one GCP4-GCP6 pair. Notably, an actin-like molecule of unknown function was found to be present in the luminal region of the ring (Consolati, 2020; Liu, 2020; Wiczorek, 2020; Zimmermann, 2020). Maybe the most striking result from these studies is that the addition of the well-known activator of microtubule nucleation in cells, the CM1 domain of CDK5RAP2, did not cause any structural changes in the γ TuRC and did not increase the microtubule nucleation activity *in vitro* (Liu, 2020). Perhaps, an additional factor is required to achieve activation of the γ TuRC. Work from our laboratory in collaboration with the Llorca group (CNIO, Madrid, Spain) recently demonstrated the reconstitution and Cryo-EM structure of recombinant human γ TuRC, showing that the structure of the recombinant complex matches the structure of the native complex. This is a very powerful tool for the field as now other purified proteins can be added *in vitro* to address how γ TuRC is turned into an active nucleator (Zimmermann, 2020).

Recruitment factors

After the discovery of γ -tubulin/ γ TuRC as the main nucleator at the centrosome, an obvious question was what triggers γ -tubulin localization to the centrosome and

other MTOCs? It was found that both PCNT and AKAP9 contain a centrosomal targeting region, the so-called PACT domain (PCNT-AKAP9 centrosomal targeting) (Gillingham, 2000). Curiously, neither γ -tubulin nor the γ TuRC components contain any similar domain. Later, it was found that both PCNT and AKAP9 have γ TuRC-binding regions. Therefore, these proteins act as a link between the centrosome and the γ TuRC by recruiting the nucleator to the MTOC (Takahashi, 2002).

Notably, there are other proteins capable of recruiting the nucleator to the MTOC. These proteins are able to localize to the different MTOCs most likely by interaction with additional proteins and they have also γ TuRC-binding domains. It is the case of, AKAP9, CDK5RAP2, CEP192, NIN, NINL, or NEDD1. Noteworthy, some of these proteins carry out several functions at MTOCs, as CDK5RAP2, that can act as a recruitment factor and as an activator of microtubule nucleation.

Activators

The sole presence of the nucleator at the MTOC is not sufficient to activate microtubule nucleation. This process requires to be turned on by activators. So far, the only evidence of direct activation of microtubule nucleation stems from experiments with the CM1 (centrosomin motif 1) domain of the centrosomal scaffolding protein CDK5RAP2. It has been shown both *in vitro* and *in vivo* that the presence of a 50aa CM1-containing fragment of CDK5RAP2 is sufficient to potently activate microtubule nucleation (Choi, 2010). Moreover, in live cells there is a massive increase in microtubule nucleation from the cytoplasm, indicating that not all γ TuRCs are localized at specific MTOCs and that there is a population of free γ TuRCs in the cytoplasm that normally is inactive. How γ TuRC is activated by the CM1 domain of CDK5RAP2 is still an open question. Addition of the CM1 domain from CDK5RAP2 did not induce a conformational change of the purified γ TuRC structure (Liu, 2020), previously proposed as the activation mechanism of microtubule nucleation (Kollman, 2015), nor significantly activated microtubule nucleation.

Myomegalin is a CDK5RAP2 paralog that also harbours a CM1 domain, although this protein appears to have a more important role in the activation of microtubule nucleation at the Golgi apparatus (Roubin, 2013).

In budding yeast, Spc110, the budding yeast homolog of PCNT, contains a CM1 domain (that does not seem to be well conserved in human PCNT) and an additional Spc110/Pcp1 motif (SPM). Phosphorylation of Spc110 promotes γ TuSC

oligomerization into γ TuRC-like rings and consequently turns microtubule nucleation on (Lin, 2014). This mechanism of activation of microtubule nucleation seems to be specific for organisms such as budding yeast, which contains only γ TuSC. Whether CM1 binding also triggers changes in the higher-order configuration of γ TuRC is unknown.

Curiously, it has been proposed that in TPX2 (spindle assembly factor targeting protein for Xklp2) there is a CM1 domain composed of two separate stretches of sequences (Alfaro-Aco, 2017). Even though these motifs are important for microtubule nucleation from pre-existing microtubules in mitotic *Xenopus* egg extract, it is unclear if and how they are able to activate γ TuRC.

More recently it has been suggested that the γ TuRC acts as a scaffold for microtubule nucleation by promoting the lateral interaction of $\alpha\beta$ -tubulin dimers (Thawani, 2020; Rice, 2021). At a certain tubulin concentration, the chance to have enough lateral interactions in the γ TuRC could be sufficient to trigger the nucleation of the microtubule. It is possible that these lateral interactions are favoured by the presence of the so called-activators.

Anchoring factors

Most of the microtubules nucleated in the cell are not dispersed around the cytosol. The organization of the microtubule network is achieved thanks to proteins that anchor newly formed microtubules to the distinct MTOCs. These proteins are defined as anchoring factors. In case of the centrosome, the main anchoring protein is NIN (Mogensen, 2000), while this role is fulfilled by CAMSAPs at the Golgi apparatus (Jiang, 2014). γ TuRC has also been proposed to be an anchoring factor, *in vitro* immobilised γ TuRC seems to be sufficient to attach microtubules minus-ends (Consolati, 2020). *In vivo* data is not so robust, although it has been shown that a complex between γ TuRC and its recruitment factor NEDD1, might be sufficient to support microtubule anchoring (Muroyama, 2016). Remarkably, even though it is known that anchoring factors bind to microtubules minus-ends, the mechanism underlying the anchoring of microtubules at MTOCs in cells is still unknown.

Other regulators

Microtubule regulators cooperate with γ TuRC to allow efficient microtubule nucleation and may track and regulate the plus ends of newly formed microtubules

This is the case of proteins from the XMAP215 family and proteins of the TACC family, initially described as microtubule polymerases (Gard, 1987; Gergely, 2000) but later implicated as active members in the MTOC formation process, due to their capacity to bind microtubules minus-ends and cooperate with the γ TuRC (Lee, 2001; Popov, 2002; Singh, 2014; Thawani, 2018).

Chapter 3

MTOCs, nc-MTOCs and minimal MTOCs

The centrosome

The centrosome is one of the essential components many cycling cells. This organelle is composed of two barrel-shaped structures known as centrioles which are surrounded by pericentriolar material (PCM). It is a dynamic organelle which transitions between different states during the cell cycle in what is defined as the centrosome cycle.

After cell division, each cell inherits a centrosome composed of a mature centriole (mother centriole) and non-mature centriole (daughter centriole). The mother centriole contains two distinct structures at the distal region, the distal (DAs) and subdistal appendages (SDAs), both linked to ciliary functions (Uzbekov, 2018; Hall, 2021). During G1, there is disengagement of the pair of centrioles even though they are still tethered. Both centrioles are surrounded by PCM. At the end of G1 and during S phase, a procentriole will form on the proximal, lateral surface of each centriole, which at this point are both called mother centrioles. During S phase the procentrioles elongate but remain engaged to their mothers. During G2 both mother centrioles will recruit additional PCM to have sufficient nucleation capacity to guarantee a proper cell division. At this point, the two centrosomes, each formed by a mother centriole with its daughter, will separate and, prior to mitotic entry, will be positioned at two opposite poles of the cell. After nuclear envelope breakdown each centrosome forms a pole of the forming spindle, ensuring its bipolarity (**Figure I9**) (Nigg, 2011; Conduit, 2015).

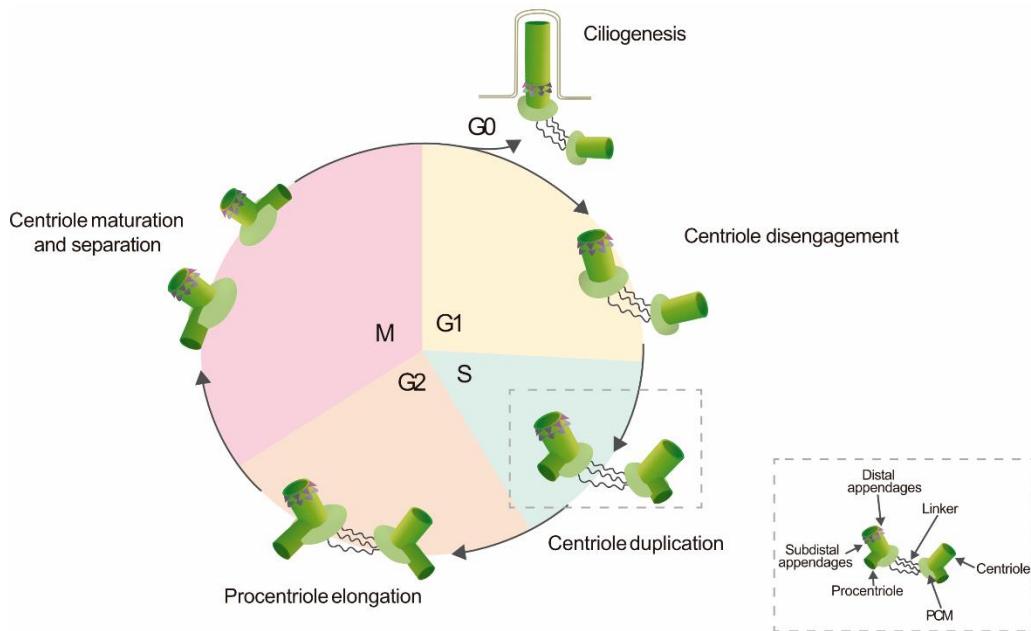


Figure I9. Centriole duplication cycle.

Schematic depicting the centriole duplication cycle. After mitosis the centrosome is composed of a mother centriole (possesses DAs and SDAs) and a “disengaged” daughter centriole, that are tethered by the centrosomal linker. This allows the duplication of each centriole during S phase. Duplication is initiated by the formation of a procentriole on the lateral surface near the proximal end of each centriole. During S phase the newly formed daughters elongate but do not acquire their own PCM until the next cell cycle. During G2, each pair of centrioles will increase their PCM size and both procentrioles will be fully elongated. Between G2 and M, the new mother will mature and acquire DAs and SDAs. To achieve a successful mitosis the centrosomal linker is disrupted between G2 and M and each centrosome is positioned at two opposite poles of the cell. Notice that between M and G1 cells can enter a state of quiescence, also known as G0, where they will exit the cell cycle and can form a structure known as cilium on the mother centriole.

Notably, not all components of centrosomes are involved in generating and organizing microtubules. The PCM is a proteinaceous matrix where microtubule nucleation takes place through concentrating proteins involved in this process. Some examples are γ TuRC, CDK5RAP2 or PCNT. During mitotic centrosome maturation, the amount of PCM at centrosomes increases and the molecular organization of the PCM also changes. This is achieved through phosphorylation of the PCM proteins by mitotic kinases (e.g. PLK1) (Barr, 2004; Haren, 2009). Traditionally, the PCM was described as an amorphous mass that surrounds centrioles (Gould, 1977). In contrast, the gain in microscopy resolution during past decades depicted the PCM as a layered structure formed by different scaffolding

proteins confined to the proximal part of the mother centriole (Fu, 2012; Lawo, 2012; Luders, 2012; Mennella, 2012; Sonnen, 2012; Mennella, 2014; Fu, 2015). More recent studies have challenged the model of concentric layers of the PCM and have proposed that the PCM could be a result of the concentration of different scaffolding proteins that create a liquid-like structure with different properties than the cytosol (e.g. distinct densities), and this process could be mediated by LLPS (Woodruff, 2017; Boeynaems, 2018; Raff, 2019). Studies with *C. elegans* PCM components have shown that the PCM scaffolding protein SPD-5 (no human homolog) is capable to generate condensates *in vitro* that recruit additional PCM proteins. These condensates are able to form microtubule asters that resemble centrosomal asters observed *in vivo* (Woodruff, 2017). How similar are these condensates to the *C. elegans* centrosome is still something to discover.

Noteworthy, is it known from EM studies that there are microtubules anchored at regions where there is no PCM, as the distal part of the mother centriole, specifically at SDAs (Mogensen, 2000; Delgehr, 2005). It remains unclear to date if SDAs have the capacity to also nucleate microtubules or if there is an unknown mechanism that transfers microtubules nucleated in the PCM to the SDAs for anchoring (**Figure I10**) (Paz, 2018).

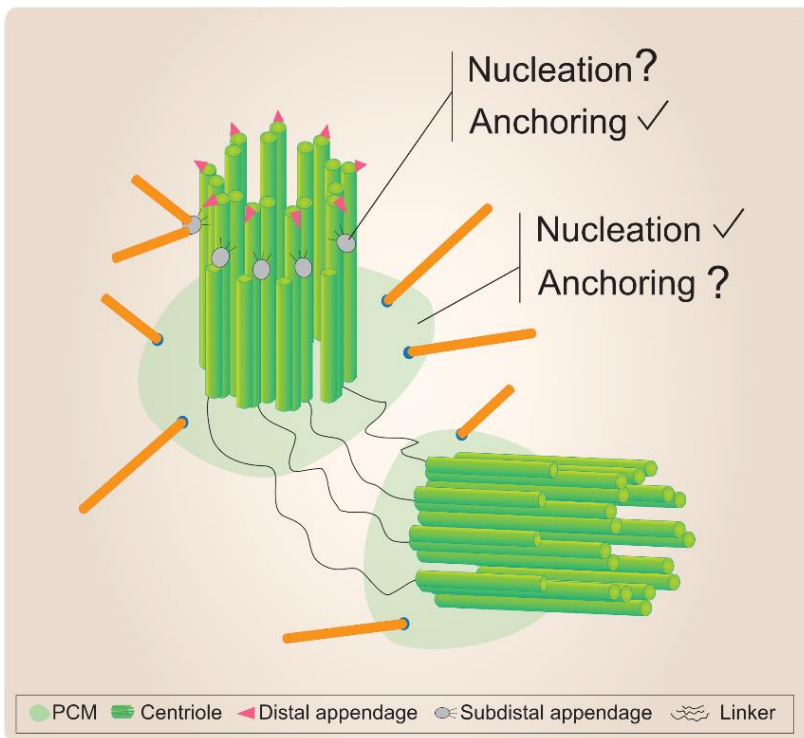


Figure I10. Microtubule nucleation at the centrosome.

Schematic depicting the fate of microtubules nucleated at the centrosome. It is well-known that microtubules are nucleated from the PCM at the centrosome. Curiously, it has not been determined yet whether microtubules that are generated at the PCM are actually anchored there and if so, how this process is carried out. Conversely, it has been shown by EM that there are microtubules anchored at SDAs. It is unclear if they are nucleated there or if microtubules nucleated at the PCM are transported to SDAs by some undescribed mechanism. Adapted from (Paz, 2018).

It is important to mention that the centrosome has several functions besides acting as an MTOC. Centrosomal activity has been linked to various important processes such as controlling the centriole duplication cycle, the formation of cilia, actin network organization, and the regulation of some signalling pathways (Doxsey, 2005; Arquint, 2014; Conduit, 2015; Farina, 2016). Considering this diverse set of functions, there must be an underlying, complex interplay of many different centrosomal proteins. Indeed, according to The Human Protein Atlas around 3% of all human proteins (548 proteins) have been experimentally detected at the centrosome (<https://www.proteinatlas.org/humanproteome/cell/centrosome>). Due to this intricacy and despite many years of study of the centrosome, it is still unclear what are the minimal components required to generate the centrosomal MTOC.

The centrosome as MTOC during interphase

As mentioned before, the PCM is composed of a number of large scaffolding proteins. PCNT is one of those scaffolding proteins that besides its structural role at the centrosome is capable of recruiting the γ TuRC to the PCM (Dictenberg, 1998; Takahashi, 2002). Moreover, it also serves as an activator of microtubule nucleation in yeast, although this function does not seem to be conserved in humans (Lin, 2014). CEP192, another large scaffolding PCM protein, has an interesting relationship with PCNT. During interphase, depletion of CEP192 expands the centrosomal levels of PCNT and conversely, depletion of PCNT increases the centrosomal levels of CEP192 and enhances the levels of microtubule nucleation. These results suggest that PCNT might act as a negative regulator of microtubule nucleation while CEP192 might be an enhancer of this process (O'Rourke, 2014). In line with these results, it was also shown in a different study that silencing of CEP192 caused a 50% reduction of the total microtubule nucleation from the centrosome (Gavilan, 2018). It is tempting to speculate then that this protein has a potential role in the activation of microtubule nucleation. Noteworthy, CEP192 depletion also caused a reduction of the centrosomal γ TuRC fraction, thus it is possible that the reduction in the

centrosomal microtubule nucleation levels shown is caused by the loss of the recruitment factor and subsequently the nucleator. In this last study, it was also described that that in the absence of centrosomes (after treatment with the drug centrinone) and inactivation of the Golgi mediated microtubule nucleation (by depletion of AKAP9), acentriolar structures composed of PCNT, γ TuRC and CDK5RAP2 are assembled in the cytoplasm and they have microtubule nucleation capacity (Gavilan, 2018). Thus, when there is no centrosome or Golgi, PCNT might be able to gather some of the core components to assemble an active MTOC. Together with PCNT and CEP192, CDK5RAP2 is the third major scaffolding protein of the PCM. It is also required to recruit the γ TuRC to the PCM (Fong, 2008) and in this case it has a clear role in the activation of microtubule nucleation through its CM1 domain (Choi, 2010). As shown before, all core PCM scaffolding proteins are capable of acting as recruitment factors and they are somehow linked to the activation of microtubule nucleation.

In addition to these scaffolding proteins there are other proteins that are also involved in the recruitment of the γ TuRC to the centrosome. This is the case of NEDD1, a protein that contains several N-terminal WD repeats that are predicted to form a β -propeller structure and mediate centrosome (and PCM) localization, and a C-terminal γ TuRC-binding region. Depletion of NEDD1 impairs γ TuRC recruitment to the centrosome, but depletion of γ -tubulin does not affect localization of NEDD1 to the centrosome. These properties define NEDD1 as a linker between the centrosome scaffold and γ TuRC (Haren, 2006; Luders, 2006). Interestingly, it was more recently proposed that NEDD1 could have an additional role in attachment of γ TuRCs involved in microtubule anchoring. This is based on the observation that in keratinocytes, depletion of NEDD1 causes a significant reduction of centrosomal γ TuRC and a loss of microtubule anchoring, while microtubule nucleation is only mildly decreased. Contrary, depletion of CDK5RAP2 caused a general decrease in microtubule nucleation activity, but the levels of γ TuRC remained mostly unperturbed (Muroyama, 2016). These results suggest that there might be two different kinds of γ TuRC populations at the centrosome, one involved in microtubule nucleation and one in anchoring. How this is coordinated at a molecular level is still unknown. Another protein that is worth commenting on is MZT1, a conserved subunit of the γ TuRC. First, it was described in fission yeast that it was required for the localization of γ -tubulin complexes to the MTOCs (Masuda, 2013). Later, it was found that in the yeast *Candida albicans* MZT1 is able to interact with the γ TuSC through the N-terminal region of GCP3 and with the CM1-containing proteins Spc72 and Spc110. Moreover, *in vitro*, MZT1 is required for the oligomerization of the γ TuSC by Spc72 and Spc110, which is necessary to turn the

γ TuSC into an active microtubule nucleator (Lin, 2016). In line with these results, in human cells our lab showed that MZT1 is a “priming” factor that recognises γ TuRC integrity by binding not only to GCP3 but also to GCP5 and GCP6. This primes γ TuRC for interaction with the recruitment factor NEDD1 and the CM1 domain of the activator of microtubule nucleation CDK5RAP2 (Cota, 2017). In agreement with the role of MZT1 at the centrosome, tissue specific degradation of MZT1 in *Caenorhabditis elegans* embryonic intestinal epithelial cells causes a loss of the γ TuRC from the centrosome (Sallee, 2018). Another subunit of the γ TuRC that has also been related to the recruitment of the γ TuRC to the centrosome is GCP8/MZT2 (Teixido-Travesa, 2010). Depletion of GCP8 does not disrupt the assembly of the γ TuRC but impairs γ TuRC recruitment to the centrosome and subsequently microtubule nucleation. These defects seem to be specific to interphase centrosomes, as cells do not display any clear mitotic defects.

Referring to how the activation of microtubule nucleation is carried out at the centrosome, CDK5RAP2 has been proposed as nucleation activator, although its depletion does not abolish centrosomal microtubule nucleation (Gavilan, 2018). There are other proteins proposed to contribute to this process. Myomegalin is a large protein that is located at both the Golgi apparatus and the centrosome (Verde, 2001) and it contains a conserved CM1 domain (Lin, 2014), although its major contribution to MTOC formation seems to be at the Golgi (Wu, 2016). Another protein proposed to be a γ TuRC activator is NME7. Mass spectrometry analyses of purified γ TuRC have shown several times that this protein is in close relationship with the γ TuRC (Choi, 2010; Teixido-Travesa, 2010; Wieczorek, 2020). Moreover, it has been shown that its centrosomal localization is dependent on the interaction with the γ TuRC (Liu, 2014). *In vivo*, depletion of NME7 causes a moderate decrease in the microtubule nucleation capacity of the centrosome. *In vitro*, addition of NME7 to purified γ TuRC and tubulin enhances microtubule nucleation levels. Notably, a NME7 kinase deficient mutant reduces microtubule nucleation levels by 40%, linking the kinase activity of this protein with the activation of microtubule nucleation (Liu, 2014). It is yet to be confirmed if this kinase activity regulates microtubule nucleation *in vivo* and if so, what is the molecular mechanism behind this process. Another protein that could possibly carry out an important function at the centrosome is NINL. Almost 20 years ago, a yeast-to-hybrid analysis identified ninein-like protein (NINL) as a PLK1 substrate. NINL is a coiled-coil protein of 156 kDa with an N-terminal region that shares 37% similarity with a corresponding region in ninein (NIN), hence its name. As NIN, NINL also localizes to the centrosome. During interphase NINL is transported along microtubules to the centrosome by interaction with the dynein-dynactin complex. During mitosis PLK1

phosphorylates the NINL molecules that are being transported along microtubules and the ones at the centrosome. This causes dissociation of NINL from its binding partners and dispersion of NINL around the cytoplasm (Casenghi, 2005). Strikingly, overexpression of the full-length protein causes its massive aggregation at the centrosome and amplified microtubule nucleation. Contrary, NIN overexpression does not seem to have this phenotype which indicates that NIN and NINL are two similar proteins with different functions at the centrosome (Casenghi, 2003). While NIN localises to SDAs (Mogensen, 2000), NINL was shown to localize to mother centrioles in *Xenopus* epithelial cells (Rapley, 2005), but its precise centrosomal localization has not been determined.

Unfortunately, data related to how microtubules are anchored at the centrosome is scarce. More than 20 years ago, it was suggested that NIN, a centrosomal protein of 249 kDa, could have a function in microtubule anchoring at the centrosome (Bouckson-Castaing, 1996). However, EM analysis of mouse fibroblasts showed that NIN does not localize to the PCM, the main site of microtubule nucleation, but instead was found at the SDAs of the mother centriole (Mogensen, 2000). Interestingly, the microtubule array is generally focused on the mother centriole, suggesting that is the mother centriole the one in charge of the microtubule anchoring function (Piel, 2000). It was also found that NIN is present at the PCM but its abundance is relatively low (Mogensen, 2000). Curiously, in flies the mother centriole lacks SDAs and NIN localizes to the PCM (Zheng, 2016), so the same function could be shared between different organisms albeit at different regions of the centrosome. Related to the question of how NIN anchors microtubules, it has been described that there is a γ TuRC-binding region in the N-terminal region of NIN. For the proper localization of NIN to SDAs, its C-terminal region is also required (Delgehr, 2005). However, overexpression of a NIN construct with the N- and C-terminus but lacking the middle part was able to displace endogenous NIN from the centrosome and maintain normal microtubule nucleation but not proper anchoring of the microtubules. This suggested that NIN mediates anchoring of microtubules independently of γ TuRC. Apart from NIN, and as already commented, it was recently suggested that in human keratinocytes γ TuRC bound to NEDD1 could provide an anchoring function (Muroyama, 2016), possibly at the PCM. It is also likely that there are additional unidentified proteins in charge of anchoring microtubules at the PCM.

Centrosomal and non-centrosomal microtubule organisation during mitosis

One of the most impressive arrangements of the microtubule network occurs when cells enter mitosis. During mitosis, cells need to ensure the generation of a robust microtubule array, the mitotic spindle, that supports proper segregation of the chromosomes. This is perhaps the reason why spindle assembly is driven by the cooperation of three different microtubule nucleation pathways. Interestingly, there is adaptability between these different pathways and it has been demonstrated that the absence of one is compensated by an increased activity of the others (Hayward, 2014).

As it is generally recognized, the centrosome plays a major role during mitosis. Dynamic microtubules generated from the centrosome ‘search and capture’ the chromosomes and then they attach to the chromosomal kinetochore, forming the so-called K-fibres. Once microtubules are bound to the kinetochore, they become stable and their dynamic instability is lost (**Figure I11**, Centrosomal microtubule nucleation)(Prosser, 2017). Interestingly, mathematical modelling of this mechanism shows that centrosomal microtubule nucleation and ‘search and capture’ alone are not sufficient to explain efficient spindle assembly as well as chromosome capture and congression within the timeframe of mitosis (Wollman, 2005). Therefore, other mechanisms that contribute to spindle microtubule generation are required. In line with this is the finding that the centrosome is not essential for spindle assembly and cell division. Indeed, there are no centrosomes during meiosis I in *Drosophila melanogaster* (Megraw, 2000), removal of centrioles does not affect the early development of *Drosophila melanogaster* embryos (Basto, 2006) and removal of centrosomes in vertebrate cells by laser ablation does not prevent bipolar spindle formation (Khodjakov, 2000).

Apart from centrosomal nucleation, there is also chromatin-mediated microtubule nucleation. The main regulator of chromatin-mediated regulation is the RAS-related nuclear protein (RAN). RAN activity is GTP-dependent. The GTP state of RAN is dependent on the guanine nucleotide exchange factor, regulator of chromosome condensation 1 (RCC1) and the GTPase-activating factor RANGAP1. RCC1 localizes to the periphery of the chromosomes where RAN-GTP is generated. In the vicinity of the chromosomes where the RAN-GTP concentration is high, it binds importin- β to cause release of its cargos (Kaláb, 2006; Clarke, 2008). Importin- β cargos are various spindle-assembly factors (SAFs) including TPX2 (Gruss, 2001). Once TPX2 is released, it is able to recruit Aurora A, which phosphorylates NEDD1

and in turn targets the γ TuRC to the chromosomal region. This cascade of signals eventually causes the activation of microtubule nucleation at the vicinity of the chromosomes (Pinyol, 2013; Prosser, 2017)(**Figure I11**, Chromatin-mediated microtubule nucleation). Additionally, it has been shown that the RAN-GTP pathway controls microtubule nucleation at the kinetochore region. In this scenario, RAN-GTP binds to transportin which releases its inhibitory function over a complex between ELYS and the nucleoporins NUP 107-160, allowing this complex to be targeted to the kinetochore and to recruit the γ TuRC (Mishra, 2010; Bernis, 2014; Yokoyama, 2014; Prosser, 2017). Nucleation of microtubules around chromatin and at the kinetochore does not only provide additional microtubules but, through interaction with centrosomal microtubules, likely also helps centrosomal microtubules to ‘find’ and connect to kinetochores.

Additionally, microtubule nucleation during mitosis also occurs from pre-existing microtubules. The first evidence for this mechanism was obtained when examining γ -tubulin and NEDD1 localization during mitosis. Both proteins are present not only at the centrosome but also along spindle microtubules. Expression of a mutant of NEDD1 that is defective in spindle localization impaired γ TuRC localization along spindle microtubules, reducing microtubule density and delaying spindle assembly (Luders, 2006). Later it was found that spindle localization of γ TuRC depends on another multi-subunit protein complex termed augmin (Goshima, 2008; Lawo, 2009). Phosphorylation of the augmin complex by Aurora A and PLK1 enables its binding to spindle microtubules and the subsequent recruitment of NEDD1 and γ TuRC allows the nucleation of new microtubules from the lattice of pre-existing microtubules, also known as branching microtubule nucleation (**Figure I11**, microtubule-mediated microtubule nucleation) (Petry, 2013; Prosser, 2017).

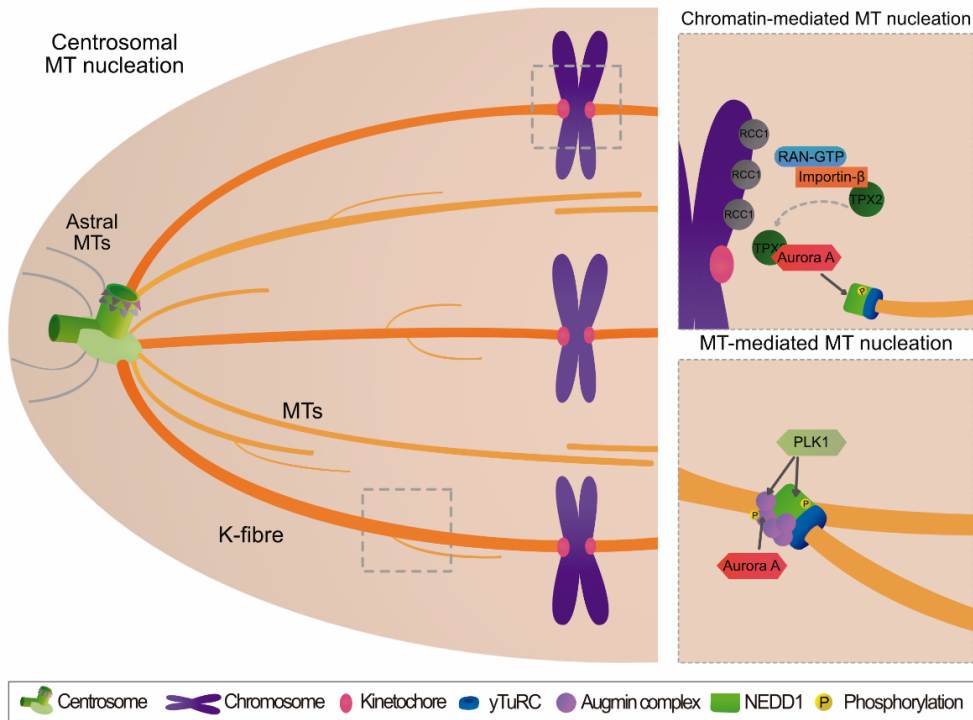


Figure I11. The three microtubule nucleation pathways involved in mitotic spindle assembly

Simplified schematic depicting the three main pathways involved in the generation of microtubules during mitosis. The **centrosomal microtubule nucleation** pathway serves as a basis for the establishment of a proper bipolar spindle, as the two centrosomes duplicated during interphase are now oriented at two opposite poles of the cell. Some of the microtubules generated at the centrosome form bundles that reach the kinetochores of the chromosomes. Those bundles are known as K-fibers and ensure proper pulling of the chromosomes during mitosis. There are also astral microtubules that face the cell cortex needed to maintain the tension and positioning of the bipolar spindle. In the vicinity of the chromosomes there is also **chromatin-mediated microtubule nucleation**. This nucleation pathway is based on the presence of RAN-GTP. RAN-GTP is quickly converted to RAN-GDP around the cytoplasm due to the presence of RANGAP1. Near the chromosomal area, RCC1 transforms RAN-GDP into RAN-GTP, which allows RAN-GTP binding of importin-β. RAN-GTP binding allows for the release of TPX2 from importin-β which is eventually bound to Aurora A that will phosphorylate NEDD1. Phosphorylated NEDD1 will recruit the γTuRC and therefore microtubule nucleation can be activated. The surface of pre-existing microtubules is a platform for **microtubule-mediated microtubule nucleation**. Phosphorylation of the augmin complex and NEDD1 by Aurora A (augmin) and PLK1 (augmin and NEDD1) is sufficient for these two components to form a complex with the γTuRC at the surface of existing microtubules. This process contributes to K-fiber formation as microtubules nucleated as branches are almost parallel to the existing ones.

Non-centrosomal MTOCs

Cell differentiation is a synonym of cell specialization. Many different cell types have adapted the way they build their microtubule network to fulfil more specialized roles. In most of these cells, a common denominator is the loss of the centrosome as the main MTOC and the acquisition of non-centrosomal MTOCs (nc-MTOCs).

Interestingly, there are many ways to assembly nc-MTOCs, and they do not have to be mutually exclusive. One possibility is that once the centrosome becomes inactive, the centrosome components are redirected to other regions of the cell where nc-MTOCs are generated. Another possibility is that nc-MTOCs are formed independently of the centrosome, by incorporating a different subset of proteins. In this scenario, the cell could maintain different MTOCs at the same time. It is also possible that microtubules are generated and afterwards released from the centrosome. Other parts of the cell could have the machinery to capture and anchor these free microtubules. In this case, those structures would not fit in the canonical definition of an MTOC, as microtubule nucleation is absent and possibly the nucleator γ TuRC is not required for the organization of microtubule at such sites.

Golgi apparatus

The Golgi apparatus is a membrane-bound organelle present in eukaryotic cells. Its formation is the result of the coalescence of a set of membrane stacks, which have a major role in vesicle trafficking. Structurally, the Golgi stacks are polarized. Proteins and lipids from the endoplasmic reticulum are transported to the cis-Golgi network (CGN). Afterwards, at the trans-Golgi network (TGN), they are exported as vesicles to other structures of the cell such as endosomes, lysosomes or the plasma membrane. During this transition from CGN to TGN, cargo molecules can be modified and processed (Li, 2019).

Apart from its main function in vesicle trafficking, it was discovered in the early 2000s that the Golgi apparatus has a key role as MTOC (Chabin-Brion, 2001). Curiously, microtubules seem to be exclusively nucleated at the CGN. It is functionally important to generate microtubules at the Golgi for several reasons. Along the cell cycle, the Golgi transitions from a more compact ribbon during interphase to scattered stacks in mitosis. Microtubules nucleated at the Golgi help to assemble the dispersed stacks into the ribbon after mitosis (Miller, 2009). In addition, the Golgi microtubule network has its own intrinsic polarity which allows for

asymmetric vesicle transport and it is required for the acquisition of proper cell polarity. In mesenchymal cells, it has been shown that the Golgi-nucleated microtubules facilitate reorientation of the whole microtubule network in the direction of migration (Wu, 2016). Therefore, the Golgi apparatus has a major role in cell polarization (Wu, 2017). It is also important to note that there is an interplay between the centrosome and the Golgi apparatus in the regulation of the microtubule network, since it has been shown that centrosome removal enhances microtubule nucleation activity from the Golgi (Gavilan, 2018).

At a compositional level the Golgi MTOC is perhaps the best defined, although it is possible that not all proteins involved in Golgi MTOC activity have been identified yet. It is known that the main factor involved in this process is AKAP9 (also known as AKAP450 and AKAP350), a very large scaffolding protein that localises to both the Golgi and the centrosome (Shanks, 2002). AKAP9 binds to the CGN through interaction with the Golgi structural protein GM130 (Rivero, 2009). The nucleator, γ TuRC, is recruited directly by AKAP9, or by association of AKAP9 with the known γ TuRC binders CDK5RAP2 and myomegalin (Wang, 2010; Roubin, 2013; Wang, 2014). Curiously, depletion of myomegalin or CDK5RAP2, the proposed main activators of microtubule nucleation at the Golgi, does not cause a complete reduction on the Golgi microtubule nucleation levels, which might indicate the presence of additional factors undescribed so far (Roubin, 2013; Wu, 2016). Contrary, depletion of AKAP9 abolishes Golgi-microtubule nucleation completely, likely through disruption of the whole MTOC complex (Rivero, 2009). It has been shown that additional MAPs (some of them +TIPs) are required to anchor microtubules to the Golgi apparatus. It was proposed by Wu and collaborators in 2017 that once microtubules are generated at the Golgi, they could lose their γ TuRC cap as their ‘minus end’ is decorated with different proteins such as CAMSAP2, CLASP1, CLASP2 or MTCL1 (Efimov, 2007; Jiang, 2014; Sato, 2014). Noteworthy, most of the CLASPs are located to the TGN by binding to a structural protein named GCC185, allowing for tethering of microtubules also to this area of the Golgi (Efimov, 2007)(**Figure I12**). Besides microtubules nucleated from this organelle, microtubules released from the centrosome can also be attached to the Golgi, either to the CGN or TGN (Wu, 2016). As highlighted before, there is a complex interplay between microtubule plus-end and minus-end binding proteins at the Golgi. In addition, it has been also reported that EBs can also bind to some myomegalin-AKAP9-GM130 complexes allowing for tethering of microtubules to the Golgi apparatus (Yang, 2017).

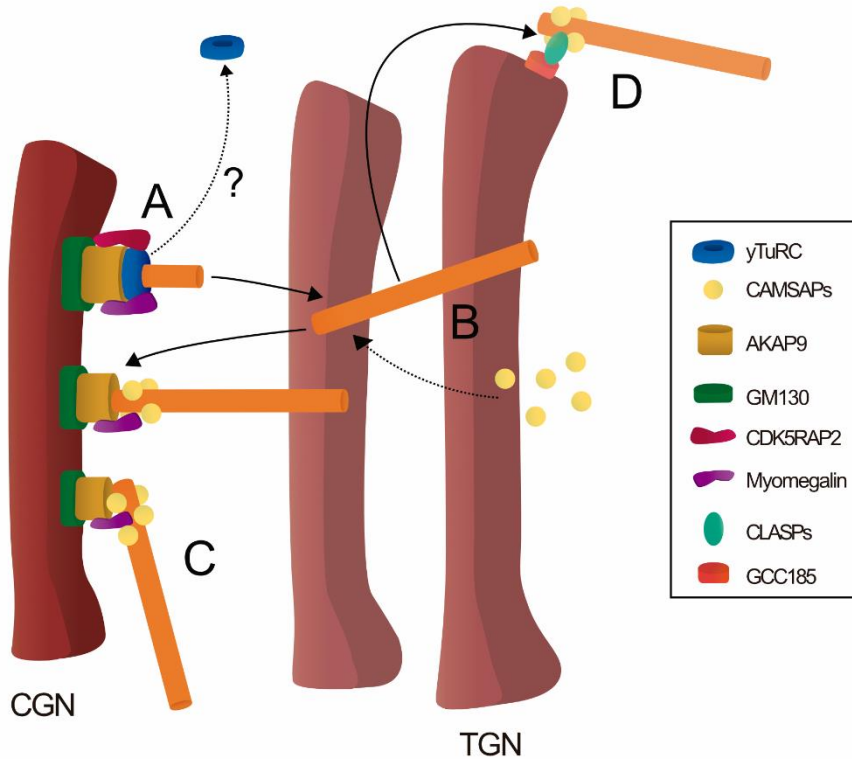


Figure I12. Main microtubule nucleation pathways of the Golgi as MTOC.

Simplified overview of the Golgi apparatus as an MTOC. The Golgi apparatus is composed of a set of membrane stacks. Microtubule nucleation occurs at the CGN. The structural protein GM130 recruits AKAP9, that acts as a γ TuRC recruitment factor. Additional presence of CDK5RAP2 or myomegalin is necessary for activating microtubule nucleation (A). Once microtubules are generated, they are normally detached from this complex and γ TuRC is believed to be released from their minus-ends. Instead, their minus-ends can be decorated with different proteins such as CAMSAPs (B). This allows for the anchoring of the microtubules to the CGN by a complex between myomegalin-AKAP9 and GM130 (C). An additional anchoring complex composed by CLASPs and GCC185 is found at the TGN (D). Additionally, both microtubules nucleated at the Golgi or at the centrosome are susceptible to be anchored either by the CGN or the TGN.

Neurons also seem to use the Golgi apparatus to nucleate microtubules. In *Drosophila* sensory neurons, the somatic CGN has an active role in generating microtubules. This MTOC is γ TuRC-dependent but does not seem to rely on Cnn (Centrosomin, CDK5RAP2 homolog) or Plp (the *Drosophila* homolog of PCNT). Interestingly, microtubules nucleated at the somatic Golgi preferentially grow towards the axon of

the neuron in a kinesin-dependent manner (Mukherjee, 2020). It would be interesting to address whether perturbation of this process has an impact on the overall axon and dendrite polarity as it could serve as a model to explain the differences in between axon and dendrite polarity within flies. Another neuronal structure that has been described in *Drosophila* dendrites are disperse Golgi structures, also known as Golgi outposts, that are able to nucleate microtubules. For this matter it was firstly proposed that microtubule nucleation from Golgi outposts requires γ TuRC and Plp (Ori-McKenney, 2012) but it has been recently shown that these structures are capable of functioning in a γ TuRC-independent manner (Mukherjee, 2020; Yang, 2020). Furthermore, it still needs to be clarified what the relevance of nucleating microtubules from the Golgi outpost is, as experimental removal of the Golgi from dendrites does not affect γ -tubulin localization nor dendrite microtubule polarity (Nguyen, 2014; Yang, 2020). Additionally, it remains to be tested whether the Golgi outpost have a function in mammals.

Nuclear envelope

Skeletal muscle fibres (myotubes) are large multinucleated cells that are the product of the fusion of several individual muscle cells (myoblasts). Upon cell fusion there is a fundamental rearrangement of the microtubule network. The radial centrosomal array is exchanged for a linear non centrosomal array of microtubules that are generated mainly around the nuclear envelope. It is also important to mention that Golgi elements contribute to MTOC formation in these cells (Oddoux, 2013). Both structures are essential for a proper myofibrillogenesis along with the formation of the elongated shape of the cell and correct nuclear positioning (Gimpel, 2017; Muroyama, 2017). The formation of these nc-MTOCs is dependent on the nuclear protein Nesprin-1, which recruits other centrosomal proteins as AKAP9 and PCM1; and subsequently PCNT, CDK5RAP2 and γ -tubulin (and presumably γ TuRC) (Espigat-Georger, 2016; Gimpel, 2017) (**Figure I13**). Very recently it was shown that in cardiomyocytes an additional protein, AKAP6, acts as a bridge between Nesprin-1 and AKAP9, and therefore is necessary for perinuclear MTOC formation. Even more striking was the finding that this complex between AKAP6-AKAP9 tethers the nuclear envelope with the Golgi structures present in these cells, which also acts as an MTOC through a complex between GM130, AKAP9 and possibly NIN and γ TuRC (Vergarajaregui, 2020). These results highlight how tightly interconnected are these two nc-MTOCs in this system.

Although most of the studies related to the role of the nuclear envelope in MTOC formation are linked to mammalian cells, it has been recently found that fat body

cells from *Drosophila melanogaster* organize their microtubules in the same manner. The fly homolog of Nesprin-1, Msp300, seems to have the same role than in myotubes, as it is necessary for nc-MTOC formation. Msp300 targets patronin, the fly homolog of the “minus end” binding protein CAMSAP, and NIN to the nuclear envelope, where they sequentially recruit Msps, a member of the XMAP215 family. This complex is sufficient to generate an MTOC. Notably, even though there is γ TuRC localization to the nuclear envelope, it appears to be dispensable for the nuclear MTOC formation since its depletion does not impair microtubule nucleation at this site (Zheng, 2020).

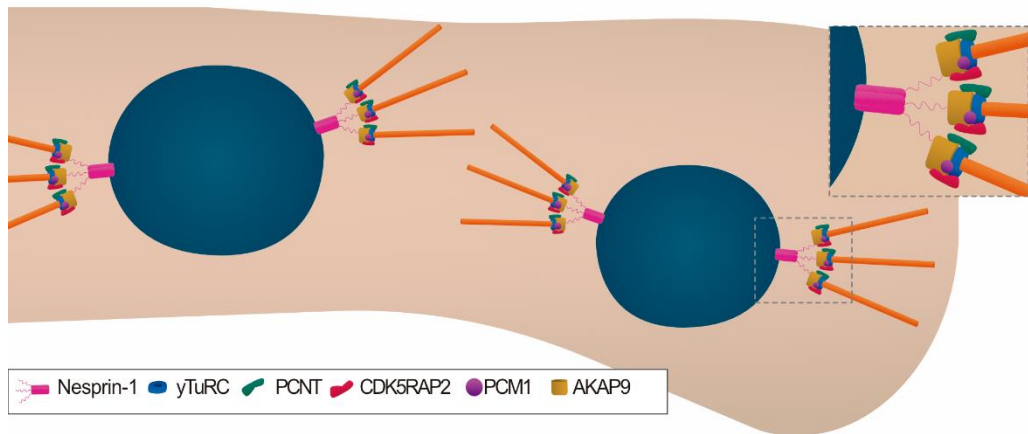


Figure I13. The nuclear envelope acts as an MTOC in myotubes.

Schematic depiction of the composition of the nuclear envelope MTOC present in myotubes. Following myoblasts fusion into myotubes, there is a dramatic rearrangement of the cellular microtubule network. MTOC formation is switched from centrosomes to the periphery of the nuclear envelope. Nesprin-1 is a perinuclear protein that recruits AKAP9 and PCM1, which in return target γ -tubulin (and presumably γ TuRC), CDK5RAP2 and PCNT to the nuclear envelope. This complex is sufficient to make the nuclear envelope a functional MTOC.

Cell cortex

Polarized epithelial cells present a characteristic apico-basal microtubule array, where microtubules plus-ends are facing the basal part of the cell while minus-ends are facing the apical region. In simple epithelial cells, as enterocytes from mice small intestine, γ TuRC is the main nucleating factor present at the apical region of these cells. Notably, γ TuRC localization is dependent on the interaction of one of the ring-complex components, GCP6, with keratin (an intermediate filament protein), present also at the apical region (Ameen, 2001). Moreover, CDK1 phosphorylation

of GCP6 destabilizes the interaction with keratin filaments, suggesting that the general decrease in the CDK1 activity during differentiation can be linked to the assembly of these nc-MTOCs (Oriolo, 2007). Importantly, although microtubule regrowth experiments showed that there is a fraction of microtubules nucleated from these ectopic sites, most of the microtubules located at the apical region were unperturbed upon depolymerization, indicating the presence of a very stable pool of microtubules at this region. It is possible then that some of these stable microtubules are also captured and anchored by this MTOC, a similar function that has also been related to the Golgi apparatus (Wu, 2016). Distinct polarized epithelial cells also contain different types of nc-MTOCs. Polarized epithelia from human colorectal cancer organize their microtubules around the actin enriched region from the apical part of these cells. The spectraplakins ACF7 tethers the actin cytoskeleton with microtubules through CAMSAP3 in a γ TuRC independent manner (Noordstra, 2016). In canine epithelial cells from kidney, NIN is in charge of anchoring microtubules from the apical region of the cell independently of the γ TuRC. CLIP170 is able to target NIN to the adherens junctions at the apical region of the cell, although it is not clear if these two proteins are recruited to the adherens junctions in a microtubule dependent or independent manner. Curiously, NIN depletion seems to not affect the apico-basal microtubule orientation which might be compensated by the presence of other complexes containing p150^{glued} and CAMSAP2 (**Figure I14**, Polarized simple epithelia) (Goldspink, 2017).

In more complex and stratified epithelia such as keratinocytes from human epidermis, microtubules are presented in a cortical array. Curiously, it has been shown that in proliferative keratinocytes the centrosome is active in nucleating microtubules but it has two different populations of γ TuRCs. One bound to NEDD1 which does not nucleate but anchors microtubules and another bound to CDK5RAP2 which is able to activate microtubule nucleation (Muroyama, 2016). Similarly to single epithelial cells, once these cells differentiate, CDK1 downregulation is sufficient to promote NEDD1 and γ TuRC re-localization to the cytoplasm which eventually leads to centrosomal inactivation (Muroyama, 2016). The key factor for establishing this cortical array is the desmosomal linker protein desmoplakin (DP) (Lechler, 2007). DP additionally recruits other fundamental centrosomal proteins such as NIN, Nudel, LIS1 and CLIP170 (**Figure I14**, Stratified epithelia) (Sumigray, 2011).

It is important to comment that with the exception of γ TuRC interaction with intermediate filaments in simple epithelia, none of the forementioned structures

requires the presence of the nucleator to function. Rather than nucleating microtubules they seem to be focused on their anchoring. Therefore, these structures should not be considered as MTOCs, taking into account that microtubule nucleation is absent and as well as the main nucleator. This opens the question of where are the anchored microtubules coming from, as the centrosome loses its activity upon differentiation in epithelial cells.

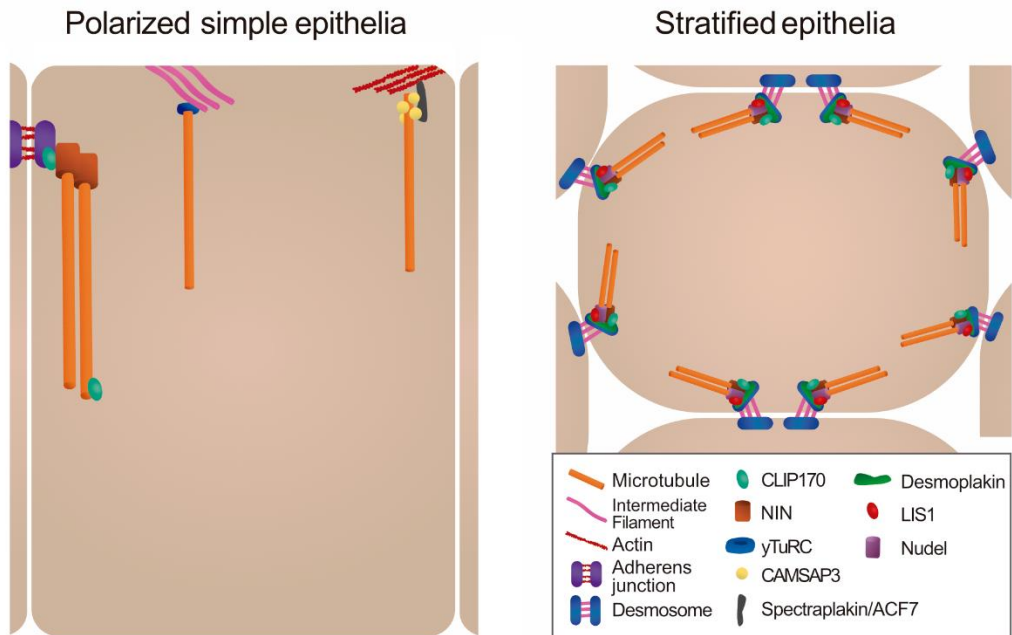


Figure I14. Microtubule organization in epithelial cells.

Schematic with a summary of the different types of microtubule organization present in epithelial cells. **Polarized simple epithelia.** Three different ways to arrange microtubules have been found in epithelial cells. From left to right, the adherens junctions have been shown to serve as a platform to anchor microtubules. CLIP170 is capable of recruiting NIN which is necessary for anchoring microtubules. At the apical part of the cell cortex, keratin (an intermediate filament protein) is able to recruit the γ TuRC, and it is yet to explore if there are other proteins involved. There is presumably microtubule nucleation to some extent but most of the microtubules present at this region seem to be captured and anchored. Additionally, in a similar region, the interaction between actin and the spectraplakins ACF7, anchors microtubules decorated with CAMSAP3. Notice that the first and third structures are mostly focused on microtubule anchoring, and γ TuRC seems not to be present there, therefore they would not be included in the canonical definition of MTOC. **Stratified epithelia.** Once keratinocytes are differentiated, NEDD1 and γ TuRC are relocated from the centrosome to the cytoplasm. At this moment the cell cortex becomes the main microtubule anchoring point in these cells. Desmoplakin (DP) is a desmosomal protein that targets to desmosomes a complex of the centrosomal proteins, NIN, Nudel, LIS1 and

CLIP170, which is necessary for cortical microtubule attachment. Notice again that γ TuRC is not present at the cortical area of the cell, therefore it is likely that these structures serve as a platform for anchoring and stabilizing microtubules. Thus, they could be not considered as MTOC.

Mitochondria

A few years ago, a new type of nc-MTOC was found in *Drosophila melanogaster* testis. It was described that the giant mitochondria from *Drosophila* spermatids are able to function as MTOCs. This organelle is turned into an MTOC thanks to a splicing variant of Cnn, termed CnnT, which is specifically expressed in testis. This splicing variant contains a distinct C-terminus with a mitochondrial-targeting domain. This nc-MTOC seems to be formed by the fly homologs of CDK5RAP2, NEDD1 and γ TuRC. No other major centrosomal components were detected by immunofluorescence (IF). Remarkably, fusion of the CM1 domain of mice CDK5RAP2 with the mitochondrial-targeting domain of CnnT in human cells was sufficient to turn human mitochondria into an MTOC (Chen, 2017).

Towards a minimal MTOC

For many decades the centrosome field has focused on how the centrosome is assembled, how this process is regulated, and, more recently, how centrosome defects are connected to different pathologies. Remarkably, the molecular basis of a core centrosomal function, its role as microtubule-organizing center, are still poorly understood.

Over the years it became clear that the centrosome is a multifunctional organelle, involved not only in microtubule organization but also in centriole duplication, ciliogenesis, cell signalling and actin organization (Doxsey, 2005; Arquint, 2014; Conduit, 2015). Moreover, evolution of proteomics has revealed how complex this organelle is. Proteomic analysis of purified centrosomes and proximity labelling of centrosome proteins have identified the interplay of hundreds of proteins at the centrosome (Andersen, 2003; Jakobsen, 2011; Gupta, 2015; Bauer, 2016). Unfortunately, this insight has not led to a better molecular understanding of centrosomal microtubule organization, but rather added to the complexity of this issue.

Recent *in vitro* studies have provided some molecular insight. TIRF assays with purified human TPX2 and CKAP5 in presence of soluble tubulin, have shown that both proteins can synergistically stimulate γ TuRC-independent microtubule

nucleation (Roostalu, 2015). Therefore, these two proteins could act as a minimal chromatin-dependent microtubule nucleation module during mitosis. Notably, it was recently shown by using *C. elegans* recombinant proteins for *in vitro* assays, that only three proteins are required to assemble a minimal MTOC that recapitulates the properties of the mitotic PCM from *C. elegans* embryos. Two of the proteins commented before, ZYG-9 (CKAP5 homolog) and TPXL-1 (TPX2 homolog) are recruited by condensates of the PCM scaffolding protein SPD-5 (no human homolog). These condensates are able to form microtubule asters that resemble centrosomal asters observed *in vivo*. Curiously, the presence of γ -tubulin enhances but is not required for microtubule aster formation from the condensates (Woodruff, 2017). While this work is a remarkable achievement, it remains unclear how similar these *in vitro* assemblies are to centrosomal MTOCs in cells.

It is evident that the use of *in vitro* assays is a powerful tool to try to elucidate which components are sufficient to generate an MTOC but there are several limitations to this technique. To individually address the role of the proteins of interest, they have to be expressed recombinantly and purified. Unfortunately this is not always possible, especially taking into account the large size and tendency to aggregation of many centrosome proteins. It should also be noted that a live cell is a much more complex system, subject to regulation by different signalling pathways or PTMs, factors that are not easily replicated *in vitro*.

Another interesting approach to study MTOCs is to try to characterise their assembly at ectopic sites in live cells. This can be achieved, for example, by targeting centrosome proteins to these sites through fusion with specific localization domains (Muroyama, 2016; Chen, 2017). This strategy although not very exploited, has revealed some interesting data on how MTOCs are assembled. Targeting of the γ TuRC-binding domains of NEDD1 and CDK5RAP2 to the keratinocyte cortex with a desmosome-targeting domain from desmoplakin (in desmoplakin-null keratinocytes) showed that there might be two different types of γ TuRC populations in these cells (Muroyama, 2016). NEDD1-targeted to the cell cortex was able to recruit γ TuRC but not to activate microtubule nucleation. Contrary, CDK5RAP2 was able to recruit γ TuRC and NEDD1, and activate microtubule-nucleation and microtubule-anchoring from the cell cortex. It is yet to be shown which other proteins are present in this complex. A similar approach was employed by targeting CnnT, a splicing variant from *Drosophila melanogaster* CDK5RAP2 that contains a mitochondrial-targeting domain, to the mitochondria in human cells. Notably, CnnT turned the mitochondria into an MTOC when overexpressed, additionally recruiting

NEDD1 but other centrosomal protein were absent as CEP192, PCNT, CEP152, CPAP or even CDK5RAP2 (Chen, 2017). Similar to the first study, it is left to discover if there are other proteins involved in the generation of this type of MTOC.

After reviewing the existing literature related to microtubule nucleation and generation of MTOCs, it becomes apparent that there are still many questions to solve. One of these key questions is related to what is the minimal set of proteins necessary to assemble an MTOC. As already commented, the inherent complexity of the different MTOCs has hindered answering this question for an important period of time. Simplified scenarios have proven to be a better option to understand MTOC formation. As important *in vitro* tools are still under development and might not always correlate with cellular scenarios, studying MTOC formation at ectopic sites is an appealing approach. Thus, it is the major aim of this thesis to elucidate the minimal requirements for building a functional MTOC by targeting different centrosomal proteins to ectopic sites and revealing their contribution to this process.

Aims

Despite decades of study of the centrosome as MTOC, it is still not clear what the core components required for MTOC assembly are. The complexity inherent to the centrosome and other nc-MTOCs has obscured the interpretation of the data obtained so far. Recently, simpler approaches have been proposed as an alternative to solve this question. *In vitro* studies with minimal components are an interesting option but molecular tools are lacking. Targeting candidate MTOC assembly proteins to ectopic sites that do not have intrinsic microtubule organizing activity is a promising alternative approach to address this question. Based on this, the major objectives of this thesis are:

- Test a subset of candidate proteins for their ability to ectopically generate an active MTOC.
- Characterize the generated ectopic MTOCs for their composition and functional requirements.
- Elucidate the physiological roles of the proteins that promote ectopic MTOC formation.

Materials and Methods

Molecular cloning

Cloning strategy

All the constructs used in this thesis were generated using the same strategy. Vectors were linearized by restriction digestion (list of enzymes used in **Table M1**) for 2 hours at 37°C and then CIP dephosphorylated for 30 minutes. Digested plasmids were then run in a 1% agarose gel for 30 minutes at 120 mV and purified by column purification (Nucleospin® Gel and PCR cleanup). Inserts were generated by PCR amplification (Phusion® high-fidelity DNA polymerase) and then run in a 1% agarose gel for 30 minutes at 120 mV and purified by column purification. Cloning was conducted by homologous recombination with Gibson Assembly®. Following homologous recombination, NEB® 10-beta Competent E. coli (High Efficiency) were used for transformation. Colonies were tested by restriction digestion and positive colonies were confirmed by Sanger sequencing.

All the primers and clones generated are listed in **Table M1** at the end of the **Materials and Methods**.

Site-directed mutagenesis

GFP-NINL 1-442-E359K-Mito mutant was generated using the QuickChange Lightning site-directed mutagenesis kit (Agilent Technologies) on the plasmid GFP-NINL 1-442-Mito following instructions of the manufacturer.

RT-PCR

Genomic DNA was used to generate a plasmid containing CEP192. For the generation of genomic DNA, U2OS cells were seeded in a 10 cm dish. Once confluent, cells were washed once with PBS. Afterwards, TRIzol reagent was added (1 mL per 10 cm dish). Extracts were kept at -80 °C until all samples were collected. TRIzol extracts were thawed and mixed with 1:1 volume of 70 % absolute ethanol. RNA extraction was performed with PureLink RNA Mini Kit (Invitrogen). RNA concentration and purity were measured with a NanoDrop 8000 spectrophotometer (ThermoFisher Scientific). RNA samples were directly processed after extraction. Single-stranded cDNA was synthesized from 1 µg of total RNA in a final volume of 20 µL, using the High-Capacity cDNA Reverse Transcription Kit (Applied Biosystems). cDNA was then used to amplify CEP192 full-length and N-terminus by PCR. Then both fragments were inserted into a GFP-Mito plasmid following the described cloning strategy.

Plasmids

GFP-NINL Fl, GFP-NINL-Nt and GFP-NINL-Ct were a kind gift from Doctor Erich Nigg. GFP-NIN-Nt (*Homo sapiens* isoform 5) was kindly gifted by Doctor Yi-Ren Hong.

A list of all the plasmids used can be found in **Table M2**.

Table M2. List of plasmids used in this thesis.

Plasmid	Tag/s	Selection Marker	Origin
peGFP-C1	GFP	Kan/Neo	AddGene
pCS2-Flag modified (FseI/AscI cassette)	FLAG	Amp	AddGene
pcDNA5 FRT/TO MCS-BirAR118G-FLAG	BirA, FLAG	Amp/Hygro	Gift from Brian Raught
CnnT (pOTB7)		Chlor	Drosophila Genomics Resource Center (AT09084)
GFP-NINL full-length	GFP	Kan/Neo	Gift from the former laboratory of Erich Nigg
GFP-NINL 1–702	GFP	Kan/Neo	Gift from the former laboratory of Erich Nigg
GFP-NINL 694–1382	GFP	Kan/Neo	Gift from the former laboratory of Erich Nigg

mEGFP-3C-His	GFP	Amp	Generated in-house
GFP-NIN-Nt	GFP	Kan/Neo	Gifted by Doctor Yi-Ren Hong

Cell culture

U2OS and HEK293 cells were cultured in Dulbecco's Modified Eagle Medium (DMEM) containing 10% fetal bovine serum (FBS) and penicillin/streptomycin (100 IU/mL and 100 µg/mL, respectively). They were kept at 37°C in a cell culture incubator with a humidified atmosphere containing 5% CO₂.

Stable cell line generation

GFP-NINL stable cell line.

A stable cell line expressing GFP-NINL was generated in U2OS cells by overexpression of a pEGFP-C1 plasmid containing NINL. U2OS cells were plated in a 10 cm dish and transfected with PEI. 24 hours later cells were selected by addition of neomycin.

Cell culture treatments

Overexpression experiments.

U2OS cells were transfected with the described plasmids and linear polyethylenimine (PEI 25K™, Polysciences) diluted in OPTIMEM as described below. 3 µg of plasmid and 15 µl of PEI (1 mg/mL) in 300 µl of OPTIMEM for a 6 well plate, 10 µg of plasmid and 45 µl of PEI (1 mg/mL) in 1 mL of OPTIMEM for a 10 cm dish or 20 µg of plasmid and 90 µl of PEI (1 mg/mL) in 2 mL of OPTIMEM for a 15 cm dish.

For transfection, both reagents were mixed in half volume of OPTIMEM and waited for 15 minutes. Afterwards, the other half volume of OPTIMEM was mixed and the final solution added to cells. Cells were kept at 37°C and cell medium was replaced 4 hours later.

siRNA treatments.

U2OS cells were transfected with the described oligos and Lipofectamine RNAiMAX (Invitrogen) diluted in OPTIMEM as described below. Transfection was conducted in 6 well plates using a siRNA concentration of 50 nM or 100 nM and 7 μ l of siRNA MAX diluted in 300 μ l of OPTIMEM.

For transfection, RNAiMAX was mixed with half of the volume of OPTIMEM and 5 minutes after a mixture of the oligo the other half volume of OPTIMEM was added to it. 10 minutes later the final mixture was added to cells drop wise. Cells were kept at 37°C and cell medium was replaced 4 hours later. Cells were collected between 48 and 72 hours depending on the experiment.

A list of all the siRNAs used can be found in **Table M3**.

Table M3. siRNAs employed throughout this thesis.

siRNA name	Fw oligo 5'->3'	Purchased from
siCEP170	GAAGGAAUCCUCCAAGUCATT	Sigma
siCKAP5	GAGCCCAGAGUGGUCCAAA	Sigma
siGCP2	GGCUUGACUUCAAUGGUUUTT	Sigma
siLuciferase	CGUACGCGGAAUACUUCGA	Sigma
siNEDD1	GCAGACAUGUGUCAAUUUGTT	Sigma
siNIN	GGAAGAAUAUCGUGCACAATT	Sigma
siNINL SmartPool oligo1	GAACUACAAGGAUCAAUUA	Dharmacon
siNINL SmartPool oligo2	CAAAGUGAGUCUUGAGGAA	Dharmacon
siNINL SmartPool oligo3	CUAAAGAAGCUCAGAAUGA	Dharmacon

Regrowth experiments

To evaluate the capacity of U2OS cells of inducing microtubule nucleation under different scenarios regrowth experiments were performed. For regrowth experiments, cells were plated and transfected in 6 well plates containing glass coverslips. To completely depolymerize microtubules from cells, two approaches were used. First method was to depolymerize microtubules by ice-cold treatment during 30 minutes. For the second method, Nocodazole (Sigma-Aldrich) was added to cells at a final concentration of 2.5 mg/mL. Cells were kept at 37°C for 2 hours and then Nocodazole was washed away two times with cold phosphate-buffered saline (PBS) and then PBS was replaced by cold DMEM. Following Nocodazole washout, cells were submitted to an ice-cold treatment for 30 minutes. Right after microtubule depolymerization, to follow microtubule regrowth, coverslips were incubated for several timepoints in DMEM at 37°C and immediately fixed either in cold methanol for 10 minutes at -20°C or with 5% formaldehyde for 10 minutes at room temperature.

Immunofluorescence microscopy

For IF experiments cells were plated in 6 well plates containing glass coverslips. Cells were fixed in cold methanol for 10 minutes at -20°C or with 5% formaldehyde for 10 minutes at room temperature. A PBS-BT buffer (PBS containing 3% BSA, 0.1% TX100, 0.02% sodium azide) was used for blocking cells for 30 minutes. Primary and secondary antibodies were diluted in PBS-BT and incubated for 30 minutes each. DNA was stained with DAPI for 1 minute. Cells were washed 3 times with PBS-BT after primary, secondary and DAPI addition. Coverslips were mounted in microscope glass slides with addition of 5 µl of ProLong® Gold Antifade Reagent mounting media (Thermo Fisher). The same immunofluorescence protocol was followed for both light fluorescent microscopy and structured illumination microscopy (SIM).

Regular images were acquired with an Orca AG camera (Hamamatsu) coupled to Leica DMI6000B microscope with a 100X objective. SIM were obtained with a Zeiss Elyra PS1 microscope with a 63X objective. Images were processed using ImageJ software.

Lysates and Western Blot

To evaluate the levels of protein expression of the different Mito-targeted constructs, cells were plated and transfected in 10 cm dishes. 24 hours after transfection cells were lysed for 20 minutes in lysis buffer (50 mM HEPES, 150 mM NaCl, 5 mM MgCl₂, 1 mM EGTA, 0.5% Triton X-100) supplemented with 1X Protease inhibitor (Complete™, EDTA-free Protease Inhibitor Cocktail). Right after, cells were centrifuged at 13000 rpm at 4 °C for 10 minutes. Pellet was discarded and supernatant was mixed with 6X sample buffer (83 mM Bis-Tris, 50 mM HCl, 3.3% glycerol, 1.3% SDS, 0.3 mM EDTA, 0.01% bromophenol blue, 0.83% β-mercaptoethanol) to a final concentration of 1X.

Samples were separated by SDS-PAGE in Bis-Tris acrylamide gels (4% for stacking and 10% for separating) and run at 120 mV in 1X MOPS buffer (50 mM MOPS, 50 mM Trisbase, 0.1 %SDS, 1 mM EDTA). Proteins were then transferred to nitrocellulose membranes (Milipore) for 60 minutes at 90 V in 1X transfer buffer (25 mM Tris, 192 mM Glycine, 20% methanol, 0.1% SDS). Membranes were blocked in 1X TBS-T (25 mM Tris, 150 mM NaCl, 2 mM KCl and 0.1 % Tween20) + milk (5%) and probed with antibodies diluted in 1X TBST + milk (5%). Primary antibodies were incubated over-night and secondary antibodies were incubated for 30 minutes. Membranes were washed with TBS-T between every incubation step. Membranes were developed with SuperSignal™ West Pico PLUS Chemiluminescent Substrate (Thermo Fisher) in an Odyssey® Fc machine (LICOR Biosciences).

Immunoprecipitation

HEK293 cells were seeded in 15 cm plates and transiently transfected with PEI according to the transfection protocol. 24 hours post-transfection cells were washed once with PBS and harvested by scraping in PBS. Pellets were collected by centrifugation at 1500 rpm for 5 minutes. Cells were lysed on ice for 30 minutes with 500 µL of lysis buffer (see above). Samples were centrifuged for 10 minutes at 4°C at high rpm and supernatants were collected. Protein concentration was measured by Bradford. 10% of the sample volume was collected as input and 6X sample buffer was added. The rest of the lysate was incubated with the desire primary antibody at 4°C for 1 hour on a wheel. 10 µl of magnetic beads (Dynabeads Protein G, Thermo Fisher) were added per sample. Beads were washed 3 times with 500 µl of lysis buffer in an IP magnet device on ice. The mixture of beads plus lysate and primary antibody was incubated for 1 hour on rotation on a wheel for 1 hour at 4°C. Samples were washed with lysis buffer with the help of a magnet on ice. Samples were then eluted by addition of 70 µl of 1X sample buffer to the beads for 5 minutes (lysis buffer was

removed by aspiration). The liquid fraction was collected and samples were incubated for 5 minutes at 95°C. Samples were stored in the freezer or ran in an SDS-PAGE.

Antibodies

A summary of all of the antibodies used for IF and western blot (WB) in this thesis can be found in **Table M4**.

Table M4. List of antibodies used for IF and WB.

Antibody	Species	Concentration IF	Concentration WB	Supplier
α -tubulin	mouse	1:2000		Merck-Sigma
γ -tubulin	mouse	1:500		Exbio
γ -tubulin	mouse		1:5000	Merck-Sigma
γ -tubulin	rabbit	1:500	1:2000	Merck-Sigma
CDK5RAP2	rabbit	1:500		Merck-Sigma
CEP170	rabbit	1:500	1:2000	Bethyl
CEP170	mouse	1:500		Thermo Fisher
CKAP5	rabbit	1:100		Abcam
DAPI		1:50000		Merck-Sigma
FLAG	mouse	1:500	1:5000	Merck-Sigma
GCP2	rabbit		1:2000	In-house
GCP3	rabbit		1:2000	In-house
GCP4	rabbit		1:2000	In-house
GCP8	rabbit		1:5000	In-house

GCP8	rabbit	1:500 (PFA)		In-house
GFP	mouse	1:1000		Thermo Fisher
GFP	rabbit		1:10000	Invitrogen
GFP	rabbit	1:1000		Torrey Pines
NEDD1	rabbit	1:500		In-house
NIN	mouse	1:500		Merck-Sigma
NINL	rabbit	1:500	1:2000	In-house
PCNT	rabbit	1:500		In-house

BioID experiments

Biotin-streptavidin affinity purification

HEK293 cells were seeded in 15 cm plates and transiently transfected the next day following the regular transfection protocol explained before. Medium was changed 4 hours post-transfection. 24 hours post-transfection, 50 μ M of biotin (Bio Basic) was added per plate. For mass spectrometry, 3x 15 cm plates were used per condition. 48 hours post transfection, cells were harvested with Trypsin-EDTA (Sigma-Aldrich). Cell pellets were washed twice in cold PBS and lysed in 10 mL of cold RIPA buffer (50 mM Tris-HCl pH 7.5, 150 mM NaCl, 0.1% SDS, 1% Triton X-100 (Sigma-Aldrich), 1 mM EDTA (Roche), 1 mM EGTA (Sigma-Aldrich), 1:2000 benzonase 25 U/mL (EMD), 1x protease inhibitor cocktail (Roche) and 1x phosphatase inhibitor cocktail (Roche). Lysates were incubated with streptavidin-sepharose beads (GE Healthcare 2-1206-010) during 3 hours in an end-over-end rotator at 4°C in order to isolate the biotinylated proteins. The beads were washed four times in 50 mM ammonium bicarbonate pH 8.3. The beads were then resuspended in 100 μ L of 50 mM ammonium bicarbonate and sent to the Mass Spectrometry & Proteomics Core Facility at IRB Barcelona for further digestion and analysis

Digestion on beads

Tryptic digestion was performed directly on beads by incubating them with 2 μg of trypsin dissolved in 300 μL of 50mM NH_4HCO_3 at 37°C overnight (200 μL were added to the delivered volume). The following morning, and additional 1 μg trypsin was added and incubated for 2 h at 37°C.

Beads were pelleted by centrifugation at 2000 g for 5 min, and the supernatant was transferred to a fresh Eppendorf tube. Beads were washed once with 100 μL of 50 mM ammonium bicarbonate, and these washes were pooled with the first supernatant. Formic acid was added to the eluates to a 1% final concentration. Samples were cleaned up through C18 tips (polyLC C18 tips) and peptides were eluted with 80% acetonitrile, 1% TFA. Take out an aliquot of 10-20% from the sample. Next, samples were diluted to 20% acetonitrile, 0.25% TFA, loaded into strong cation exchange columns and peptides were eluted in 5% NH_4OH , 30% methanol. Finally, samples were evaporated to dry, reconstituted in 50 μL and diluted 1:8 with 3% acetonitrile, 1% formic acid aqueous solution for MS analysis.

LCMSMS analysis

The nano-LC-MS/MS set up was as follows. Digested peptides were diluted in 3% ACN/1% FA. Sample was loaded to a 300 $\mu\text{m} \times 5 \text{ mm}$ PepMap100, 5 μm , 100 \AA , C18 μ -precolumn (Thermo Scientific) at a flow rate of 15 $\mu\text{L}/\text{minute}$ using a Thermo Scientific Dionex Ultimate 3000 chromatographic system (Thermo Scientific). Peptides were separated using a C18 analytical column Acclaim PEPMAP 100 75 $\mu\text{m} \times 50 \text{ cm}$ nanoviper C18 3 μm 100A (Thermo Scientific) with a 90 minutes run, comprising three consecutive steps with linear gradients from 3 to 35% B in 60 minutes, from 35 to 50% B in 5 minutes, and from 50 % to 85 % B in 2 minutes, followed by isocratic elution at 85 % B in 5 minutes and stabilization to initial conditions (A= 0.1% FA in water, B= 0.1% FA in CH_3CN). The column outlet was directly connected to an Advion TriVersa NanoMate (Advion) fitted on an Orbitrap Fusion Lumos™ Tribrid (Thermo Scientific). The mass spectrometer was operated in a data-dependent acquisition mode. Survey MS scans were acquired in the Orbitrap with the resolution (defined at 200 m/z) set to 120,000. The lock mass was user-defined at 445.12 m/z in each Orbitrap scan. The top speed (most intense) ions per scan were fragmented by CID and detected in the linear ion trap. The ion count target value was 400,000 and 10,000 for the survey scan and for the MS/MS scan respectively. Target ions already selected for MS/MS were dynamically excluded for 15 seconds. Spray voltage in the NanoMate source was set to 1.60 kV. RF Lens were tuned to 30%. Minimal signal required to trigger MS to MS/MS switch was set to

5,000. The spectrometer was working in positive polarity mode and singly charge state precursors were rejected for fragmentation.

Data analysis

We performed a twin database search with the software MaxQuant (MQ) (v1.6.14.0 and v.1.6.17.0)(Cox, 2008). The search engine node used was Andromeda (Cox, 2011) for MQ. The database used in the search was SwissProt Human (release 2020_10 and 2021_01) (Consortium, 2020) including contaminants and the user proteins. We run the search against targeted and decoy databases to determine the false discovery rate (FDR). Search parameters included trypsin enzyme specificity, allowing for two missed cleavage sites, oxidation in M and acetylation in protein N-terminus as dynamic modifications. Peptide mass tolerance was 10 ppm and the MS/MS tolerance was 0.6 Da. Peptides with an FDR < 1% were considered as positive identifications with a high confidence level.

For the quantitative analysis, we used a probabilistic scoring algorithm specifically devised for affinity purification essays called SAINTq (Teo, 2016). This algorithm compares control and test samples using the protein-based MS1 intensity for each available bait. We used the protein intensities obtained with the MaxQuant v1.6 software (Cox, 2008) removing contaminant and reverse proteins. In addition, we only considered unique peptides to get protein quantification values. High confidence interactors were defined as those with Bayesian false discovery rate BFDR ≤ 0.02 and fold change FC ≥ 3 according to SAINTq.

Protein purification

Cloning of NINL fragments for bacterial expression

cDNA corresponding to NINL residues 1-287, 1-442, or 1-702 were amplified by PCR and cloned into a modified pOPINE vector to tag NINL with an N-terminal mEGFP-tag (mEGFP-) and a C-terminal 3C protease cleavable hexahistidine tag (-3C-His₆), resulting in pOPINE-mEGFP-NINL(1-x)-3C-His₆. Clones were verified by sequencing.

Purification of bacterially expressed mEGFP-NINL proteins

NINL fragments 1-287, 1-442, or 1-702 were expressed as mEGFP-NINL-3C-His₆ fusion in E.coli Rosetta. Bacteria were grown as 50-100 mL cultures overnight in LB-glucose (LB + 100 μ g/mL ampicillin + 34 μ g/mL chloramphenicol + 1% glucose (w/v)) at 37°C. Cultures were regrown in 1.5-2 L fresh LB-glucose at 37°C

to reach an OD₆₀₀ of 0.6, chilled on ice for 7 minutes, and induced with 0.5 mM IPTG before protein expression was allowed for 21 hours at 18°C.

Cells were harvested by centrifugation and cell pellets were directly used for purification or snap-frozen in liquid nitrogen and stored at -80°C. For mEGFP-NINL-3C-His6 purification, pellets were resuspended on ice in 5 mL HisA (25 mM HEPES pH 7.5, 500 mM NaCl, 10 mM imidazole, 2 mM beta-mercaptoethanol) + 1x complete protease inhibitors EDTA-free + 0.1% IGEPAL CA-630 + 0.25 mg/mL lysozyme + 2 µl DNase (c-Lectra) per gram of cell pellet and lysed using an Emulsiflex homogenizer (Avestin). Lysates were centrifuged for 30 minutes at 15,000 rpm in a JA25.50 rotor at 4°C. Cleared lysates were recovered, filtered through a 0.22 µm syringe filter, and bound to a 1 mL (NINL 1-287, 1-442) or 5 mL (NINL 1-702) HisTrap HP column. Columns were washed with 10 column volumes (CV) HisA and purified by gradient elution against HisB (HisA with 300 mM imidazole). Peak fractions were pooled, supplemented with 50 µg/mL 3C protease to remove His6-tags, and dialyzed overnight at 4°C against 2 L dialysis buffer (HisA without imidazole) using 3.5K MWCO snakeskin dialysis tubing. The next day, digested and dialysed proteins were recovered, centrifuged for 10 minutes at 16,100 g at 4°C, and purified by SEC using a Superdex 200 16/600 column equilibrated in dialysis buffer. Peak fractions were identified by SDS-PAGE, concentrated using Vivaspin 500 centrifugal concentrators of 3,000 MWCO and filtered through 0.22 µm. Final protein concentration was measured through UV absorbance.

Microscopy analysis for in vitro LLPS

Samples were prepared by mixing the determined amount of protein, buffer, and ficoll PM 70 (Sigma). Sealed sample chambers containing protein solutions comprised coverslips sandwiching two layers of 3M™ 300 LSE high-temperature double-sided tape (0.34 mm). Samples were imaged right after with a Zeiss LSM780 confocal microscope. All images within figures were taken with a 60x immersion oil objective and with the same camera settings. Images were further processed with ImageJ software.

NINL mutants

The following plasmids were produced by the IRB Protein Expression Core Facility. The sequences of the synthetic DNA fragments and methods used are summarized as follows.

NINL-Nt

Wild type NINL-Nt was amplified from pEGFP-NINL-Nt-Mito using the indicated primers (Integrated DNA Technologies) with KOD polymerase (Merck Millipore) according to the instructions of the manufacturer. The forward primer deletes the 5' BglII site used for cloning so that an internal BglII site may be used for later mutant cloning steps. After digestion with DpnI (NEB GmbH) to remove the the pEGFP-NINL-Nt-Mito template the 2141 bp insert was purified using Ampure XP (Beckman Coulter) and inserted into the pEGFPC1 plasmid cut with SacII and BglII enzymes (NEB GmbH) by InFusion (Takara Biosciences). The resulting InFusion reactions were then transformed into Omnimax2 cells (ThermoFisher Scientific) and selected on LB agar plates supplemented with 50 µg/mL Kanamycin (Melford Chemicals). Colonies were then inoculated into 5 mL cultures of LB supplemented with 50 µg/mL Kanamycin, grown overnight at 37°C with shaking and the plasmids purified with E.Z.N.A. Plasmid DNA Mini Kit II (Omega Biotek).

NINL-Nt 12P and 16P

To make NINL-Nt 16P and 12P mutations the two fragments with mutations in the region between aa 338-702 of NINL were synthesized by Twist BioSciences. These 1117 bp synthetic fragments were directly inserted into the BglII and SacII-cut pEGFPC1 NINL-Nt plasmid by InFusion (Takara Biosciences) and processed as described for the pEGFPC1-NINL-Nt plasmid.

A list of the specific mutations generated can be found in **Table M5** at the end of the **Materials and Methods**.

NINL-Nt 11A and 22A

To produce these mutants, two fragments for each construct were synthesized (5' aa 1-347, 3' aa 338-702) by Twist BioSciences. The 5' and 3' fragment pairs were designed to overlap by 30 bases so that they may be fused into a single full-length product by PCR. The complete Nt mutant from NINL (5'+3') was obtained by using 25ng of each 5' and 3' fragments as templates and the NINL-Nt forward and reverse primers in a standard KOD polymerase reaction. The resulting 2174 bp fragments were purified from 1% TBE agarose gels using E.Z.N.A. MicroElute Gel Extraction Kit (Omega Biotek) before InFusion into the pEGFPC1 plasmid cut with BglII and SacII enzymes and processing as described for the pEGFPC1-NINL-Nt plasmid.

A list of the specific mutations generated can be found in **Table M5** at the end of the **Materials and Methods**.

Antibody generation

Protein purification for antibody generation

A plasmid containing His-GST-NINL-Nt was first cloned according to the cloning protocol. To increase protein yield, the plasmid was then transformed in BL21 Rosetta (generated in-house) bacteria. Positive colonies were then grown in 2 L of LB at 37°C at an OD600 of 0.1 and 1 mM IPTG was added when OD600 was 0.5. Bacteria were then kept at 18°C overnight. The day after, they were centrifuged and pellets frozen at -80°C. Frozen pellets were thawed and resuspended in 5 mL of Buffer A (30 mM HEPES pH 7.5, 500 mM NaCl, 10 mM imidazole, 1mM β -mercaptoethanol and 0.1% NP-40) plus PMSF (Merck-Sigma) per gram of cell pellet. 0.5 mg/mL of lysozyme (Merck-Sigma) was added and sample was incubated on a tube roller at 4 °C. Samples were lysed with a sonicator and centrifugated at 20000 g for 20 minutes at 4°C. 2ul of DENARASE (c-Lecta) per 10 mL of extract was added to the cleared extract and incubated for 10 minutes on ice. Afterwards, 2 mL of Ni-Sepharose resin (Cytiva) per liter of expression cultured was added to the lysate in a packed column. Columns were then washed with 10 column volumes (CV) of Buffer A, then 5 CV of 5:95 Buffer B-Buffer A (Buffer B is equal to Buffer A but imidazole concentration is 500mM) and 5 CV of 10:90 Buffer B-Buffer A. Protein was eluted in 1 CV fractions using 60:40 Buffer B-Buffer A. The protein was then concentrated using Vivaspin 6 concentrators (Merck-Sigma).

Rabbit injection and serum extraction

To continue with the antibody generation, the “Unitat d'Experimentació Animal de Farmàcia i Unitat d'Experimentació Animal de Psicologia” from the Faculty of Pharmacy (UB) carried out the next part of the process.

In brief, around 1 mg of purified His-GST-NINL-Nt was given to the technicians. Two female New Zealand White rabbits were used for antibody generation. Rabbits were injected with a first dose of 500 μ g of protein diluted in 1 mL Freund's complete adjuvant (FCA). At days 21, 42 and 63, a reinforcement dose was given to the rabbits (250 μ g or protein per rabbit in 1 ml of Freund's incomplete adjuvant (FIA)). At day 73, blood was extracted and its reactivity against the protein was tested (by WB and IF). Once reactivity was confirmed, rabbits were exsanguinated and serum was frozen at -80 °C.

Antibody purification

Purification of the antibody from rabbit serum by WB was conducted following as described in: Fang, L. (2012). Antibody Purification from Western Blotting. *Bio-protocol* 2(6): e133. DOI: [10.21769/BioProtoc.133](https://doi.org/10.21769/BioProtoc.133).

Statistical analysis

Statistical analysis was conducted using the Prism 6 software. Two-tailed unpaired t-tests were performed to compare the experimental groups. More details are described in the figure legends.

Web resources

Resource	Utility	URL	Reference
AlphaFold	Protein structure prediction	https://alphafold.ebi.ac.uk/	(Jumper, 2021)
DISOPRED	Prediction of native disorder within a protein	http://bioinf.cs.ucl.ac.uk/psipred/	(Ward, 2004)
BioGRID	Interactome repository	https://thebiogrid.org/	(Stark, 2006)
ProHits	Analysing and visualizing screens and protein-protein interaction data	https://prohits-viz.org/	(Knight, 2017)
esyN	Build networks from data	http://www.esyn.org/	(Bean, 2014)
ShinyGO	Gene ontology enrichment analysis	http://bioinformatics.sdstate.edu/go/	(Ge, 2020)

Table M1. Vectors, restriction enzymes and primers employed for molecular cloning.

Construct	Vector	Enzymes for digestion	Fw primer 5'->3'	Rv primer 5'->3'
GFP-mito	peGFP-C1	SacII + BamHI	GCAGTCGACGGTACCGC GGAAAACGAGGCCATAG ACTC	TAGATCCGGTGGATCC AATAGAGTACAGAATG CCAG
GFP-CM1-mito	peGFP-C1	EcoRI + Sall	CTCAAGCTTCGAATTCAA CAGTGTCTCCCACCAG	CCGCGGTACCGTCGAC GTAGATATGTTCAAGT GGG
GFP-CM1e-mito	peGFP-C1	EcoRI + Sall	CTCAAGCTTCGAATTCGA AACAGTGTCTCCCACC	CCGCGGTACCGTCGAC AGCTAAGTCTCAACTG CT
GFP-CM1 PCNT-mito	peGFP-C1	EcoRI + Sall	CTCAAGCTTCGAATTCAA CCCTGAAGGAAGATTGG	CCGCGGTACCGTCGAC CTTCTCCAACCTCAGCTC TC
GFP-CM1 PCNT-mito	peGFP-C1	EcoRI + Sall	CTCAAGCTTCGAATTTCAG AGAAAACGCCAGATAG	CCGCGGTACCGTCGAC TTCACGTAACCTCTCAA TGG
GFP-NINL 1-702-mito	peGFP-C1	Sall + SacII	GAATTCTGCAGTCGACAT GGATGAAGAAGAGAACC A	ATGGCCTCGTTTTCCGC GGTGCGGGCTGTGTCC TGCA

GFP- NINL 1-287-mito	peGFP- C1	SalII + SacII	GAATTCTGCAGTCGACAT GGATGAAGAAGAGAACC	ATGGCCTCGTTTTCCGC GGTCTGGTAATGAGAC CAAGCCTTGC
GFP- NINL 1-442-mito	peGFP- C1	SalII + SacII	GAATTCTGCAGTCGACAT GGATGAAGAAGAGAACC	ATGGCCTCGTTTTCCGC GGTCCCCTGCTCCAGA TGCTTG
GFP-NINL 1- 383-mito	peGFP- C1	SalII + SacII	GAATTCTGCAGTCGACAT GGATGAAGAAGAGAACC ACTATG	ATGGCCTCGTTTTCCGC GGTGTGGTAGCAGGCC AGGG
GFP-Nlp 196- 442-mito	peGFP- C1	SalII + SacII	GAATTCTGCAGTCGACAC CCCAGAGAGCCAGATCC	ATGGCCTCGTTTTCCGC GGTCCCCTGCTCCAGA TGCTTG
GFP- NINL 41-287-mito	peGFP- C1	SalII + SacII	GAATTCTGCAGTCGACCT GGAGCAGCAGCTGCC	ATGGCCTCGTTTTCCGC GGTCTGGTAATGAGAC CAAGCCTTGC
GFP- NINL 196-584-mito	peGFP- C1	SalII + SacII	GAATTCTGCAGTCGACAC CCCAGAGAGCCAGATCC	ATGGCCTCGTTTTCCGC GGTGTGCCGTTCTTG GGCA
GFP- NINL 1-195-mito	peGFP- C1	SalII + SacII	GAATTCTGCAGTCGACAT GGATGAAGAAGAGAACC ACTATG	ATGGCCTCGTTTTCCGC GGTGTCAAAGGAGGG GCTGC
GFP-CEP192 iso3-mito	peGFP- C1	EcoRI + SalII	CTCAAGCITCGAATTCAA TGGAAGATTTTCGAGGTA TA	CCGCGGTACCGTCGAC TTAATTTTTTCCAAGAG CTTCA

GFP-CEP192 iso3 Nt-mito	peGFP- C1	EcoRI + Sall	CTCAAGCTTCGAATTCAA TGGAAGATTTTTTCGAGGTA TA	CCGCGGTACCGTCGAC AGAAATTTCACTAGGA GAAGA
GFP-CEP192 iso1 -mito	peGFP- C1	EcoRI + Sall	CTCAAGCTTCGAATTCAA TGAAGACTTCAGATCTGG TTCCA	CCGCGGTACCGTCGAC ATTTTTTCCAAGAGCTT CACCA
GFP-CKAP5- mito	peGFP- C1	EcoRI + Sall	CTCAAGCTTCGAATTCAA TGGGAGATGACAGTGAG TGG	CCGCGGTACCGTCGAC TTTGC GACTGCTCTTTA TTCTCTCC
GFP-CKAP5 1-1428-mito	peGFP- C1	Sall + SacII	GAATTCTGCAGTCGACAT GGGAGATGACAGTGAGT GG	ATGGCCTCGTTTTCCGC GGTAGAGGGTCTCTTT GCTGAC
GFP-CKAP5 1429-2033- mito	peGFP- C1	Sall + SacII	GAATTCTGCAGTCGACGC TGCACCAATAAAACAGGT	ATGGCCTCGTTTTCCGC GGTTTTGCGACTGCTC TTTATTCTCT
GFP-NIN Nt- mito	peGFP- C1	Sall + SacII	GAATTCTGCAGTCGACAT GGATGAGGTGGAGCAGG	ATGGCCTCGTTTTCCGC GGTCTCCTCATGCCTGC AAGTGG
FLAG-NINL- NT	pCS2- Flag modified (FseI/ AscI cassette)	FseI+AscI	TGATGACGACAAAGGCC GGCCAATGGATGAAGAA GAGAACC	AGTTCTAGAGGCGCGC CGCGGGCTGTGTCTTG CAGC
GFP-NINL EF 5 E359K- mito	peGFP- C1	Sall + SacII	GGCCCAGGTCAGCTTCAG AAGGTTACCT	AGGTGAACCTTCTGAA GCTGACCTGGGCC

BirA-Mito	pcDNA5 FLAG- BirAR11 8G	AscI+NotI	CCCGGCGGGCGCGGCC AAACGAGGCCATAGACTC TC	TCGAGTTAGGCGGCCG CAATAGAGTACAGAAT GCCAGCC
BirA-NINL 1- 702-Mito	pcDNA5 FLAG- BirAR11 8G	AscI+NotI	CCCGGCGGGCGCGGCC AATGGATGAAGAAGAGA ACCAC	TCGAGTTAGGCGGCCG CAATAGAGTACAGAAT GCCAGCC
BirA-NINL 1- 442-Mito	pcDNA5 FLAG- BirAR11 8G	AscI+NotI	CCCGGCGGGCGCGGCC AATGGATGAAGAAGAGA ACCAC	TCGAGTTAGGCGGCCG CAATAGAGTACAGAAT GCCAGCC
His-GST- NINL 1-702	peGX- 4T1	Sall+NotI	GAATTCGGGGTCGACAA ATGGATGAAGAAGAGAA CCACT	AGTCACGATGCGGCCG CGCCCGGGGTGTGTC CTG
mEGFP- NINL 1-702	mEGFP- 3C-His	NheI	ATAAAAGCGGTGGTGCT AGCATGGATGAAGAAGA GAACCACTATG	CCCTGAAACAGAACTTC CAGGCCGCGGGCTGTG TCCTG
mEGFP- NINL 1-442	mEGFP- 3C-His	NheI	ATAAAAGCGGTGGTGCT AGCATGGATGAAGAAGA GAACCACTATG	CCCTGAAACAGAACTTC CAGCCCCTGCTCCAGAT GCTTGATTTTC
mEGFP- NINL 1-287	mEGFP- 3C-His	NheI	ATAAAAGCGGTGGTGCT AGCATGGATGAAGAAGA GAACCACTATG	CCCTGAAACAGAACTTC CAGCTGGTAATGAGAC CAAGCCTTG
GFP-NINLNt (for mutants)	peGFP- C1	SacII + BglII (removed afterwards to use BglII site from NINL)	GTCCGACTCAGaTcCGA GCTCAAGCTTCGAATTCT GCAG	GTGGATCCCGGGCCCG CGGTCAGCGGGCTGTG TCCTGCAGCTGC

GFP-NINL- Nt 12P	peGFP- C1	SacII + BglII	Cutted and added synthetic region for the 12P
GFP-NINL- Nt 16P	peGFP- C1	SacII + BglII	Cutted and added synthetic region for the 16P
GFP-NINL- Nt 11A	peGFP- C1	SacII + BglII	Cloned two synthetic regions of the FL 1-702 with the mutations into peGFP-C1
GFP-NINL- Nt 22A	peGFP- C1	SacII + BglII	Cloned two synthetic regions of the FL 1-702 with the mutations into peGFP-C1

Table M5. Amino acid sequence of the NINL mutants generated (mutations are indicated in red).

NINL-Nt	MDEEENHYVSQLREVVYSSCDT* ^T GTGFLDRQELTQLCLKLHLEQQLPVLLQ ^T LLG NDHFARVNFEEFKEGFVAVLSSNAGV ^R PSDEDSSSLESAASSAIPP ^K YVNGSKWYG RRSRPELCAAATEARRVPE ^Q QTQASLKSHLWRSASLESVE ^S PKSDEEAESTKEAQN ELFEAQGQLQ ^T W ^D SEDFGSPQKSCSPSFD ^T PE ^S QIRGVWEELGVGSSGHLSE ^Q EL AVVCQSVGLQGLEKEELEDL ^F NKLDQDGDGKVSLEEFQLGLFSHEPALLLES ^T R VKPSKAWSHYQVPEESGCHITTTSSLVSLCSSLRL ^F SSIDDGSGFAFPDQVLAMW ^T QEGIQNGREILQSLDFSVDEKVN ^L LELTWALDNELMTVDSAVQQAALACYH ^Q EL SYQQGQVEQLARERDKARQDLERA ^E KRNLEFVKEMDDCH ^S TLEQLTEKKIKHL EQGYRERLSLLRSEVEAEREL ^F WEQAHRQRAALEWDVGR ^L QAEEAGLREK ^L TLA LKENSRLQKEIVEVVEKLSDSERLALKLQK ^D LEFVLKDKLEPQSAELLAQEER ^F A AVLKEYELKCRDLQDRNDELQAELEGLWAR ^L PKNRHSPSWSPDGR ^R RRQLPGLGP AGISFLGNSAPVSIETELMMEQVKEHYQDL ^R TQLETKVNY ^Y EREIAALKRNFEKE RKDMEQARRREVSVLEGQKADLEELHEKSQEV ^I WGLQEQLQD ^T AR
---------	---

<p>NINL-Nt 16P</p>	<p>MDEEENHYVSQLREYVSSCDTTGTGFLDRQELTQLCLKLHLEQQLPVLLQTLIG NDHFARVNFEEFKEGFVAVLSSNAGVRPSDEDSSSLESAASSAIPPKYVNGSKWYG RRSRPELCAAATEARRVPEQQTQASLKSHLWRSASLESVESPKSDEEAEESTKEAQN ELFEAQGQLQTWDESEDFGSPQKSCSPSFDTPESQIRGVWHEELGVGSSGHLSEQEL AVVCQSVGLQGLEKEELEDLFNKLDQDGDGKVSLEEFQLGLFSHEPALLLESSTR VKPSKAWSHYQVPEESGCHTTTTSSLVSLCSSLRLFSSIDDGSGFAFPDQVLAMWT QEGIQNGREILQSLDFSVDEKVNLELWALDNELMTVDSAVQPAALACYHQEL SYQPGGQVEQLARERDKARPDLERA EKRNLEFVKEMDDCPSTLEQLTEKKIKHLE QGYPERLSLLRSEVEAERELFWEPAHRQRAALEWDVGRLPAEEAGLREKLTALK ENSPLQKEIVEVVEKLSDSERLALKLPKDLEFVLKDKLEPSAELLAQEERFAAVL KEYPLKCRDLQDRNDELPAELEGLWARLPKNRHSPSPDGRRRQLPGLGPAGIS FLGNSAPVSIETELMMEPVKEHYQDLRTQLETKVNYYPREIAALKRNFEKERKD MEQAPRREVSVLEGGKADLEELHEKSPEVWGLQEQLQDTAR</p>
<p>NINL-Nt 12P</p>	<p>MDEEENHYVSQLREYVSSCDTTGTGFLDRQELTQLCLKLHLEQQLPVLLQTLIG NDHFARVNFEEFKEGFVAVLSSNAGVRPSDEDSSSLESAASSAIPPKYVNGSKWYG RRSRPELCAAATEARRVPEQQTQASLKSHLWRSASLESVESPKSDEEAEESTKEAQN ELFEAQGQLQTWDESEDFGSPQKSCSPSFDTPESQIRGVWHEELGVGSSGHLSEQEL AVVCQSVGLQGLEKEELEDLFNKLDQDGDGKVSLEEFQLGLFSHEPALLLESSTR VKPSKAWSHYQVPEESGCHTTTTSSLVSLCSSLRLFSSIDDGSGFAFPDQVLAMWT QEGIQNGREILQSLDFSVDEKVNLELWALDNELMTVDSAVQQAALACYHQEL SYQQGQVEQLARERDKARQDLERA EKRNLEFVKEMDDCSTLEQLTEKKIKHLE QGYPERLSLLRSEVEAERELFWEPAHRQRAALEWDVGRLPAEEAGLREKLTALK ENSPLQKEIVEVVEKLSDSERLALKLPKDLEFVLKDKLEPSAELLAQEERFAAVL KEYPLKCRDLQDRNDELPAELEGLWARLPKNRHSPSPDGRRRQLPGLGPAGIS FLGNSAPVSIETELMMEPVKEHYQDLRTQLETKVNYYPREIAALKRNFEKERKD MEQAPRREVSVLEGGKADLEELHEKSPEVWGLQEQLQDTAR</p>
<p>NINL-Nt 22A</p>	<p>MDEEENHAVSQLREYVSSCDTTGTGFLDRQELTQLCLKLHLEQQLPVLLQTLIG NDHFARVNAEEFKEGFVAVLSSNAGVRPSDEDSSSLESAASSAIPPKAVNGSKAYG RRSRPELCAAATEARRVPEQQTQASLKSHLARSASLESVESPKSDEEAEESTKEAQN ELFEAQGQLQTWDESEDAGSPQKSCSPSFDTPESQIRGVWHEELGVGSSGHLSEQEL AVVCQSVGLQGLEKEELEDLANKLDQDGDGKVSLEEFQLGLFSHEPALLLESSTR VKPSKAASHAQVPEESGCHTTTTSSLVSLCSSLRLFSSIDDGSGAAFPDQVLAMATQ EGIQNGREILQSLDASVDEKVNLELTAALDNELMTVDSAVQQAALACYHQELS AQQGQVEQLARERDKARQDLERA EKRNLEFVKEMDDCHSTLEQLTEKKIKHLE QGARERLSLLRSEVEAERELAAEQAHRQRAALEWDVGRLQAEEAGLREKLTAL KENSRLQKEIVEVVEKLSDSERLALKLQKDLEAVLKDKLEPSAELLAQEERFAA VLKEYELKCRDLQDRNDELQAELEGLAARLPKNRHSPSAPDGRRRQLPGLGPA GISALGNSAPVSIETELMMEQVKEHYQDLRTQLETKVNAYEREIAALKRNFEKER KDMEQARRREVSVLEGGKADLEELHEKSPEVWGLQEQLQDTAR</p>

NINL-Nt
11A

MDEEENHAVSQLREYVSSCDTTGTGFLDRQELTQLCLKLHLEQQLPVLLQTLIG
NDHFARVNFEEFKEGFVAVLSSNAGVRPSDEDSSSLESAASSAIPPKYVNGSKAYG
RRSRPELCAATEARRVPEQQTQASLKSHLWRSASLESVESPKSDEEAESTKEAQN
ELFEAQGQLQ'TW'DSEDAAGSPQKSCSPSFDTPESQIRGVWEELGVGSSGHLSEQEL
AVVCQSVGLQGLEKEELEDL'FNKLDQDGDGKVSLEEFQLGLFSHEPALLLESSTR
VKPSKAAASHYQVPEESGCHTTTTSSLVSLCSSLRLFSIDDGSGA'AFP'DQV'LAMW'TQ
EGIQNGREILQSLDFSVDEKVNLELT'ALD'NELMTVDSAVQQAALACYHQELSY
QQGQVEQLARERDKARQDLERA'EKRNLEFVKEMDDCHSTLEQLTEKKIKHLEQ
GARERLSLLRSEVEAERELFWEQAHRQRAALEWDVGR'LAQEEAGLREKLTALK
ENSRLQKEIVEVVEKLSDSERLALKLQKDLE'AVLKDKLEPQSAELLAQEERFAAV
LKEYELKCRD'LD'RNDELQAELEGL'ARLPKNRHSPSWSPD'GRRRQLPGLGPAG
ISALGNSAPVSIETELMMEQVKEHYQDLRTQLE'TKVN'AYEREIAALKRNFEKERR
DMEQARRREVSVLEGGKADLEELHEKSQEVIVWGLQEQLQDTAR

Results

Chapter 1

Molecular characterization of ectopic MTOCs

Joel Paz¹, Jens Lüders¹

¹Institute for Research in Biomedicine (IRB Barcelona), The
Barcelona Institute of Science and Technology (BIST), 08028
Barcelona, Spain

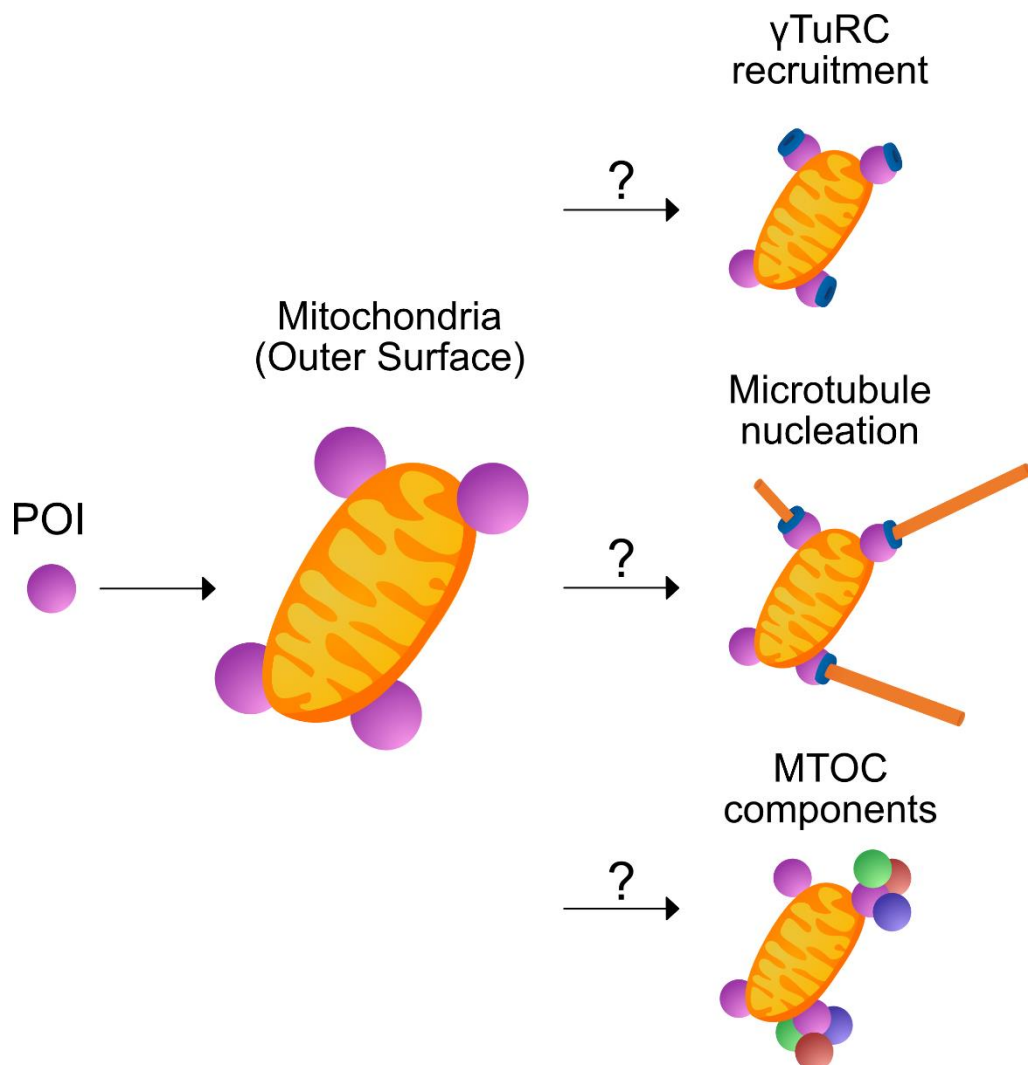
Statement of contribution:

Joel Paz designed, performed and analysed all experiments.

Jens Lüders supervised the project.

Establishing ectopic MTOC assembly on the outer surface of mitochondria

To address the question of what the minimal requirements are for building an MTOC, we decided to move away from the complexity of the centrosome. Our goal was to establish a system where we could induce an MTOC at a cellular site that normally is not involved in microtubule organization. Based on the previous literature, we decided to use the outer surface of mitochondria to assemble an artificial ectopic MTOC. As published before (Chen, 2017), the surface of mitochondria functions as MTOC in the testis of *Drosophila melanogaster*. Here, CnnT a testis-specific splice variant of Cnn, the fly homologue of CDK5RAP2, contains a domain at its C-terminus that targets the protein to the cytoplasmic surface of mitochondria. In human cells, there is no evidence that the mitochondrial surface has any role in the formation or organization of microtubules. Taking advantage of this specific Cnn variant, we subcloned the mitochondrial-targeting domain (Mito) into a human expression plasmid containing an GFP tag. Subsequently, different proteins of interest (POI) were cloned between the GFP and Mito tags for expression and mitochondria targeting in human U2OS cells. We then tested whether the POI were able to generate an MTOC at the outer surface of mitochondria by IF microscopy, by probing for recruitment of the nucleator γ TuRC, by assaying microtubule nucleation and later by detection of additional MTOC components (**Scheme R1**). For the sake of simplicity, we decided to consider these two criteria as sufficient to call these structures MTOCs. Therefore, microtubule-anchoring capacity was not addressed in the following experiments (see **Discussion**).



Scheme R1. Strategy used to analyse MTOC formation on the outer surface of the mitochondria.

The POI chosen were: the CM1 domain (aa 50-135) from CDK5RAP2 (positive control) (Chen, 2017), an N-terminal fragment (aa 1-1000) of CEP192 (the full-length protein has a centrosomal-targeting domain that interfered with the mitochondrial targeting), an N-terminal fragment (aa 1-702) of NINL (a region previously implicated in microtubule nucleation (Casenghi, 2003), an N-terminal fragment (1-699) of NIN (based on its homology with NINL), and full-length CKAP5.

First, we corroborated proper targeting of the POI to mitochondria by IF microscopy using antibodies against GFP and against Tom20. Tom20 is a structural

protein of the outer membrane of mitochondria (Lithgow, 1995) and a commonly used mitochondrial marker. After 24 hours post-transfection, all the POI were efficiently targeted to the mitochondria (**Figure R1**, -Nocodazole), validating the mitochondrial targeting system. Notably, in the cases of NINL and NIN, the distribution of mitochondria seemed to be altered, with the mitochondria being clustered around a specific point of the cell. This region turned out to be the centrosome (data not shown). Clustering of proteins and organelles around the centrosome depends on the minus-end-directed microtubule motor dynein (Burkhardt, 1997) and both NINL and NIN have been described as dynein-binding cargo adapters (Reck-Peterson, 2018). Indeed, by completely removing microtubules with nocodazole treatment, we were able to prevent clustering of mitochondria around the centrosome in both cases (**Figure R1**, +Nocodazole).

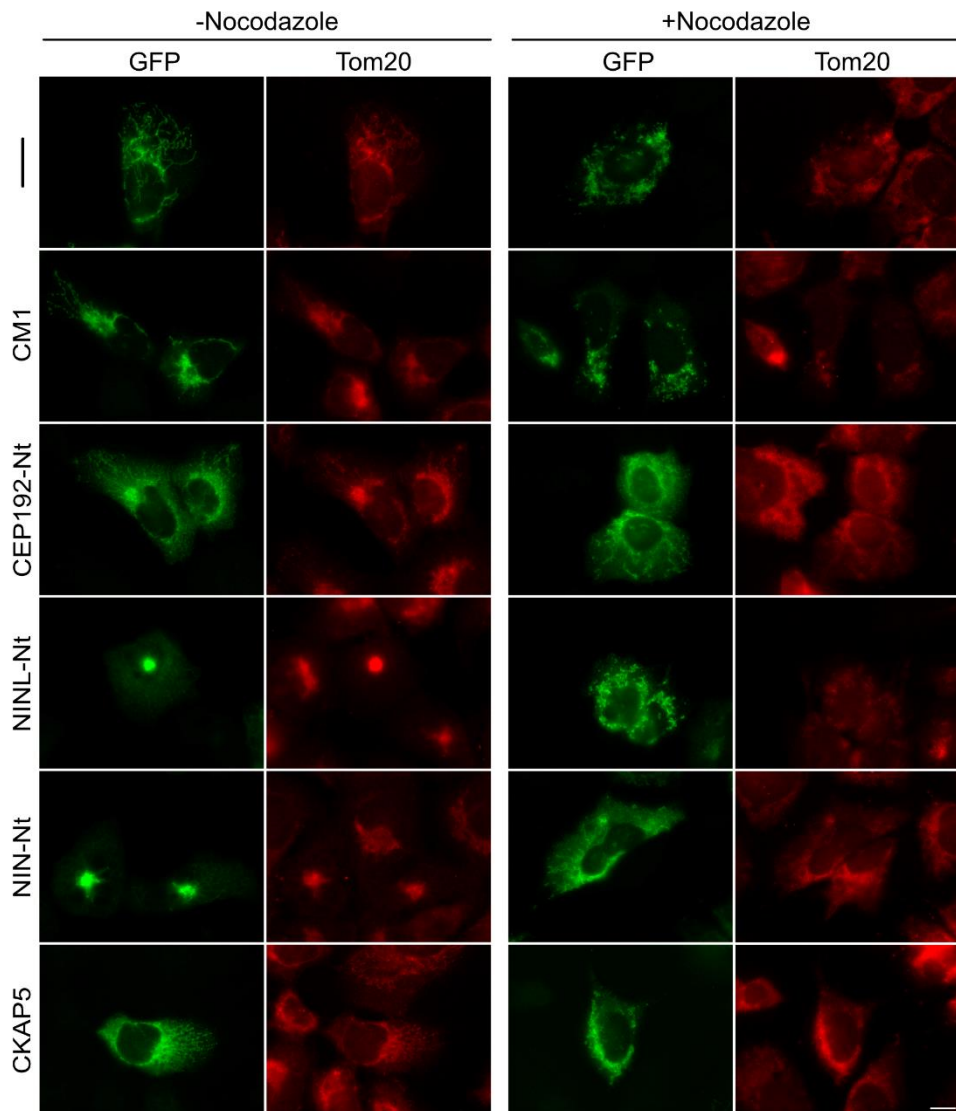
A**B**

Figure R1. Validation of the mitochondrial targeting system.

(A) Schematic of POI fused with GFP and Mito tags. (B) IF images of GFP-POI-Mito constructs expressed in U2OS cells for 24 hours. Tom20 was used as a mitochondrial marker. Clustering of the mitochondria after NINL-Nt and NIN-Nt targeting was observed (-Nocodazole). Addition of Nocodazole for 2 hours was sufficient to prevent clustering (+Nocodazole). Scale bar: 10 μ m.

Based on these results, to ensure consistent mitochondrial distribution when testing different POI, we decided to perform all following targeting experiments in the presence of nocodazole. This also avoided potential interference of the centrosome when assaying microtubule nucleation activity at mitochondria. An additional advantage was that we could monitor which other proteins were recruited to the mitochondria in the absence of microtubules. This would imply that these proteins are recruited to the ectopic site by the POI and not indirectly, through transport along microtubules.

Most POI targeted to mitochondria recruit γ TuRC

As commented in the introduction, in order to generate an MTOC, a microtubule nucleator is generally required. Therefore, to evaluate MTOC assembly at mitochondria in GFP-POI-Mito expressing cells, we first tested whether the main microtubule nucleator, the γ TuRC, was recruited to this site. To do so, we probed for the presence of the γ TuRC core subunit γ -tubulin (**Figure R2**). As described (Chen, 2017), the CM1 region of CDK5RAP2 was able to recruit γ -tubulin to mitochondria, which served as positive control. Likewise, CEP192, NINL and NIN fragments were all able to recruit γ -tubulin to mitochondria. Interestingly, we were not able to observe recruitment of γ -tubulin with the GFP-CKAP5-Mito construct, although it had been published that the C-terminal half of the *Xenopus* version of CKAP5 contains a γ -tubulin-binding region (Thawani, 2018). To further confirm that the whole γ TuRC is targeted to the mitochondria, we explored whether GCP8/MZT2, another γ TuRC subunit (Teixido-Travesa, 2010), was also present at the mitochondria. This was indeed the case (**Figure R3**).

These results suggest that with the exception of CKAP5 all POI targeted to mitochondria induce recruitment of the nucleator γ TuRC to this site.

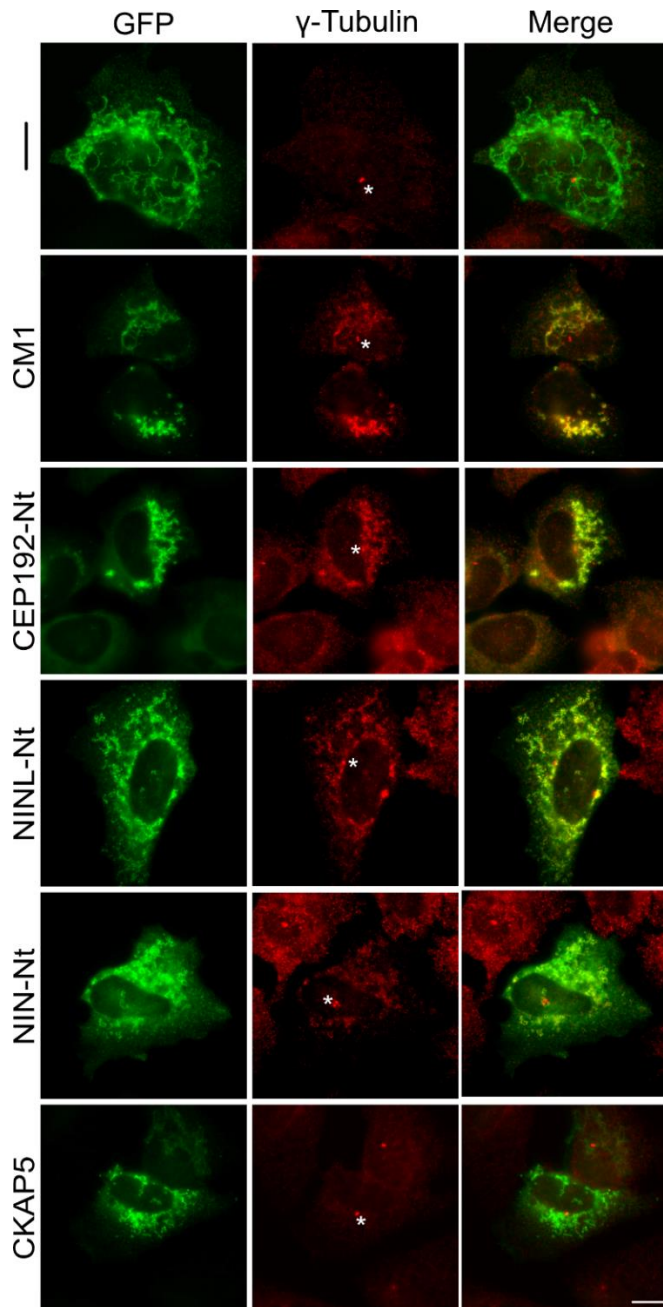


Figure R2. CM1, CEP192-Nt, NINL-Nt and NIN-Nt targeted to mitochondria co-recruit γ -tubulin.

Representative IF images of the POI targeted to the mitochondria in U2OS cells. Nocodazole was added for 2 hours and then cells were put in cold treatment for 30 minutes. Thus, microtubules were completely depolymerized in this experiment. In the case of GFP and CKAP5 targeted to mitochondria, only centrosomal γ -tubulin signal was detected. Asterisks indicate centrosomal signal. Scale bar: 10 μ m.

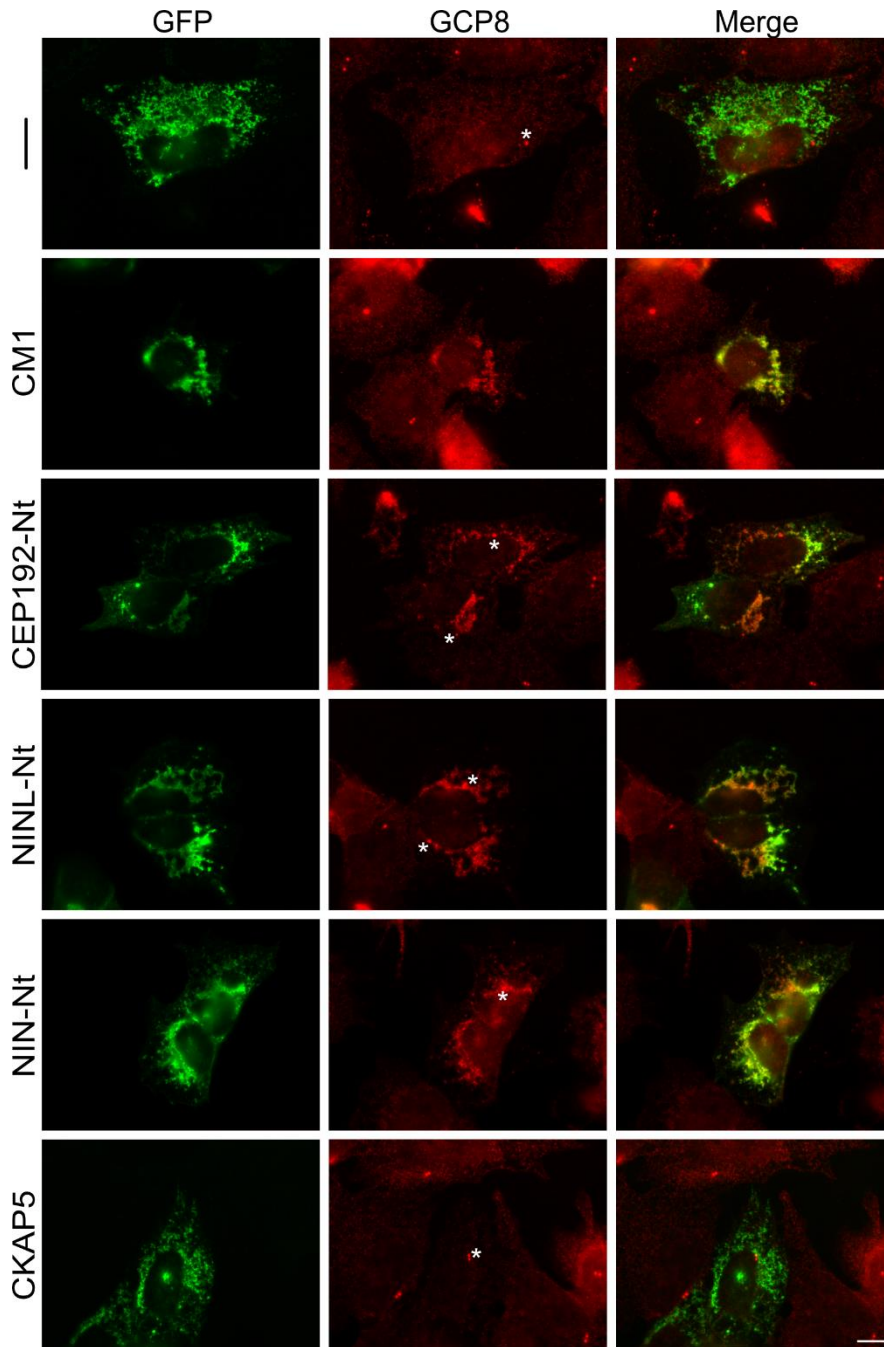


Figure R3. CM1, CEP192-Nt, NINL-Nt and NIN-Nt targeted to mitochondria co-recruit GCP8.

Representative IF images of the POI targeted to the mitochondria in U2OS cells. Nocodazole plus cold treatment was used in this experiment. In the case of GFP alone or GFP-CKAP5 targeted to mitochondria, only centrosomal GCP8 signal was detected. Asterisks indicate centrosomal signal. Scale bar: 10 μ m.

NINL-Nt and CKAP5 induce microtubule nucleation at the ectopic site

Next, we assessed whether POI targeted to the surface of mitochondria were able to induce microtubule nucleation at this site. To test this, a microtubule regrowth assay was performed. Microtubules were completely depolymerized by nocodazole treatment followed by cooling on ice water. To allow microtubule regrowth (nucleation), cells were incubated in culture medium at 37 °C for a certain amount of time before fixation and analysis. As control, we also imaged cells before regrowth (**Figure R4**, 0 s). We found that there was no tubulin signal corresponding to microtubules in regions occupied by mitochondria at time point 0 seconds. However, at 40 seconds of regrowth, we were able to observe microtubule nucleation at the outer surface of the mitochondria for mitochondria-targeted CM1 (positive control), NINL and CKAP5 (**Figure R4**, 40 s, arrowheads). In all cases microtubule asters formed at the centrosome, which served as an internal control that nucleation per se was not disrupted in any of the conditions. These results highlighted two findings. First, the N-terminal region of NINL was sufficient to generate an ectopic MTOC. Second, CKAP5 was also able to generate an MTOC, and in this particular case, it did not seem to require the presence of the γ TuRC (**Figure R2 and Figure R3**).

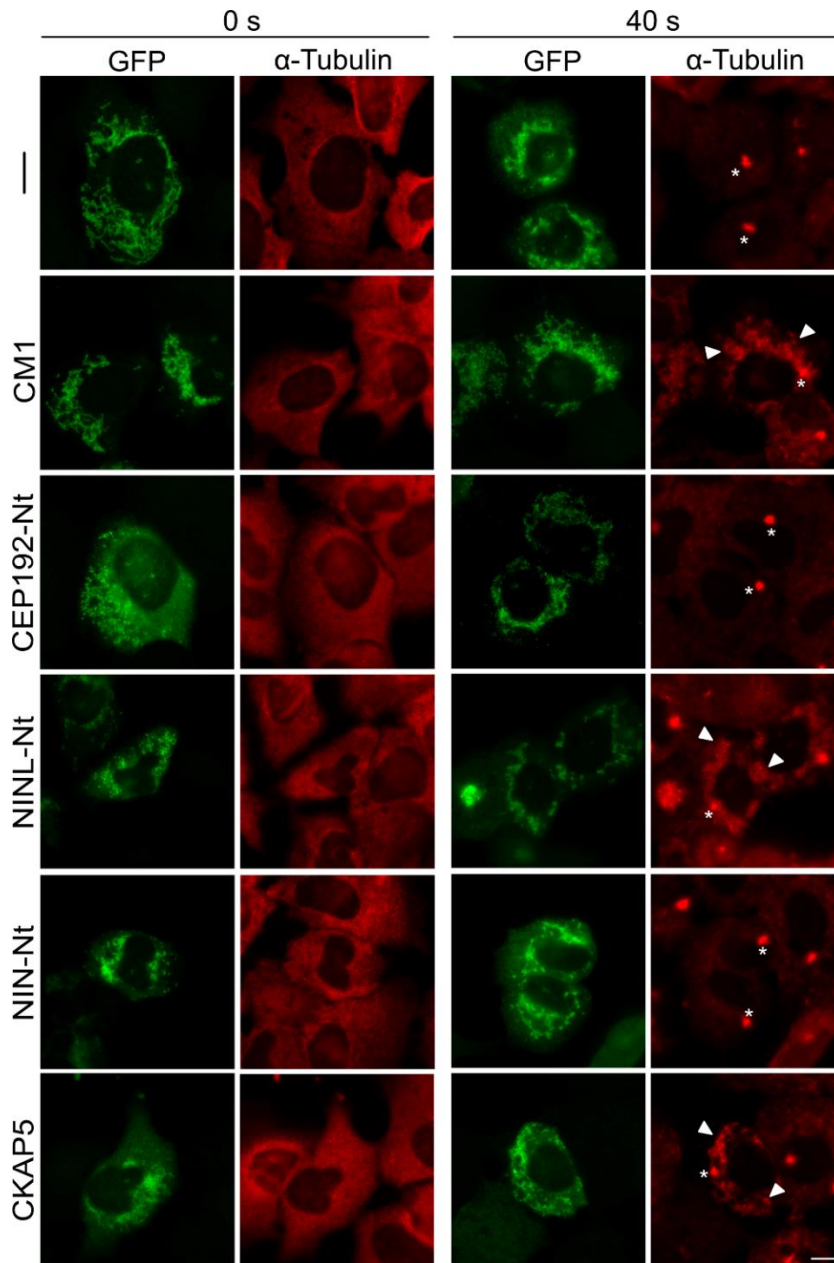


Figure R4. CM1, NINL-Nt and CKAP5 are capable of inducing microtubule nucleation at the outer surface of the mitochondria.

Representative IF images of U2OS cells expressing POI targeted to mitochondria. Nocodazole plus cold treatment was used in this experiment (left panel, 0 s). Additionally, microtubules were allowed to regrow in warm culture medium for 40 seconds to detect microtubule nucleation (right panel, 40s). Microtubule nucleation from the outer surface of the mitochondria was only detected for CM1, NINL-Nt and CKAP5 (right panel, 40s, arrowheads). Asterisks indicate centrosomal signal. Scale bar: 10 μ m.

Characterization of components involved in ectopic MTOC formation

Interestingly, only CM1, NINL-Nt and CKAP5 were able to generate an ectopic MTOC, but not CEP192-Nt and NIN-Nt despite their ability to recruit γ TuRC. This made us hypothesize that recruitment of γ TuRC alone was not sufficient for MTOC formation and that an additional nucleation promoting activity was required. This activity may be provided by some of the POI or by additional factors recruited by these POI. Therefore, we sought to characterize by IF microscopy which other centrosome proteins may be present at the ectopic site.

CM1, CEP192-Nt, NINL-Nt and NIN-Nt all recruit NEDD1 to the ectopic site

As explained in the introduction, NEDD1 is a key factor for targeting γ TuRC to the centrosome to allow centrosomal nucleation (Haren, 2006; Luders, 2006). To test if NEDD1 was also present at the ectopic site, cells were stained with NEDD1 antibody after targeting the different POI to the mitochondria. NEDD1 was present at the mitochondria in all cases except for the negative control and cells expressing mitochondria-targeted CKAP5 (**Figure R5**). As expected for a γ TuRC targeting factor, this result shows that the presence of NEDD1 correlates with the presence of γ TuRC but not with nucleation activity. Of note, although not quantified, it was evident that CEP192-Nt was most efficient in recruiting NEDD1 to mitochondria.

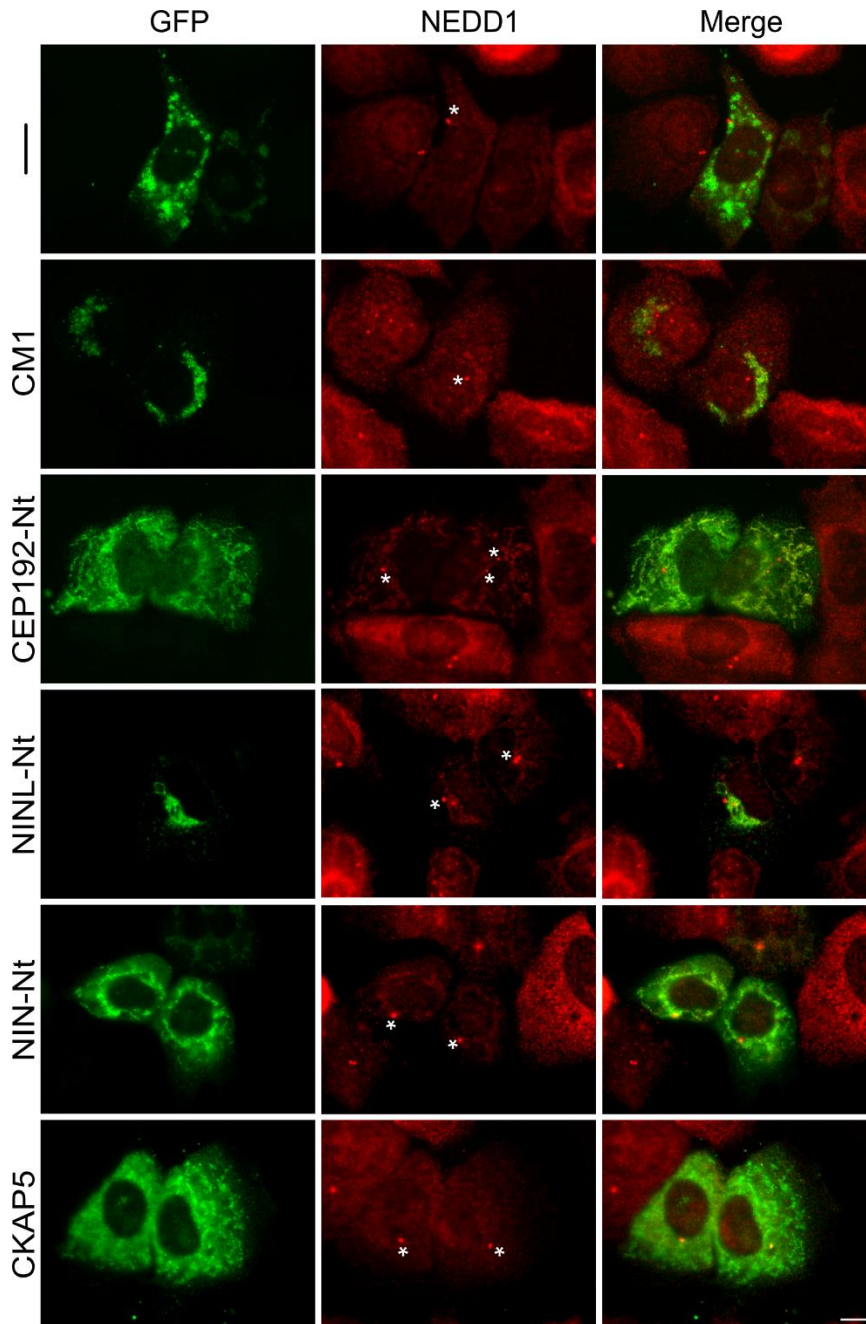


Figure R5. CM1, CEP192-Nt, NINL-Nt and NIN-Nt recruit NEDD1 to the mitochondria.

Representative IF images of the POI targeted to the mitochondria in U2OS cells. Nocodazole plus cold treatment was used in this experiment. In relationship to GFP and CKAP5 targeted to mitochondria, only centrosomal NEDD1 signal was detected. Asterisks indicate centrosomal signal. Scale bar: 10 μ m.

PCNT is not required for MTOC formation at the mitochondria

PCNT is a component of the PCM and has been implicated in contributing to centrosomal γ TuRC recruitment and microtubule nucleation (Dictenberg, 1998; Takahashi, 2002). Recent studies have shown that, after removal of the centrosome and depletion of some centrosomal proteins, PCNT acquires a major role in MTOC formation (Gavilan, 2018). To corroborate if PCNT could be involved in MTOC formation at the mitochondria, we stained cells with PCNT antibodies. In all cases PCNT was readily detected at centrosomes. However, we were never able to detect any PCNT signal at mitochondria in cells expressing any of the mitochondria-targeted POI (**Figure R6**), suggesting that PCNT is not part of the ectopic MTOC.

CDK5RAP2 is not required for MTOC formation at the mitochondria

CDK5RAP2 is a major component of the PCM and has been described as γ TuRC nucleation activator (Choi, 2010). Therefore, it was tempting to speculate that this protein may be present at mitochondria in cases where nucleation activity was observed. Strikingly, we could not detect any CDK5RAP2 signal with any of the constructs used (**Figure R7**). This result indicates that the MTOC generated by mitochondria-targeted NINL-Nt does not involve the nucleation activator CDK5RAP2. It should be noted that the monoclonal anti-CDK5RAP2 antibody that we used for IF does not recognize the CM1 region in the N-terminus of CDK5RAP2. Hence, in cells expressing mitochondria-targeted CM1 there does not seem to be any endogenous full-length CDK5RAP2 at this site.

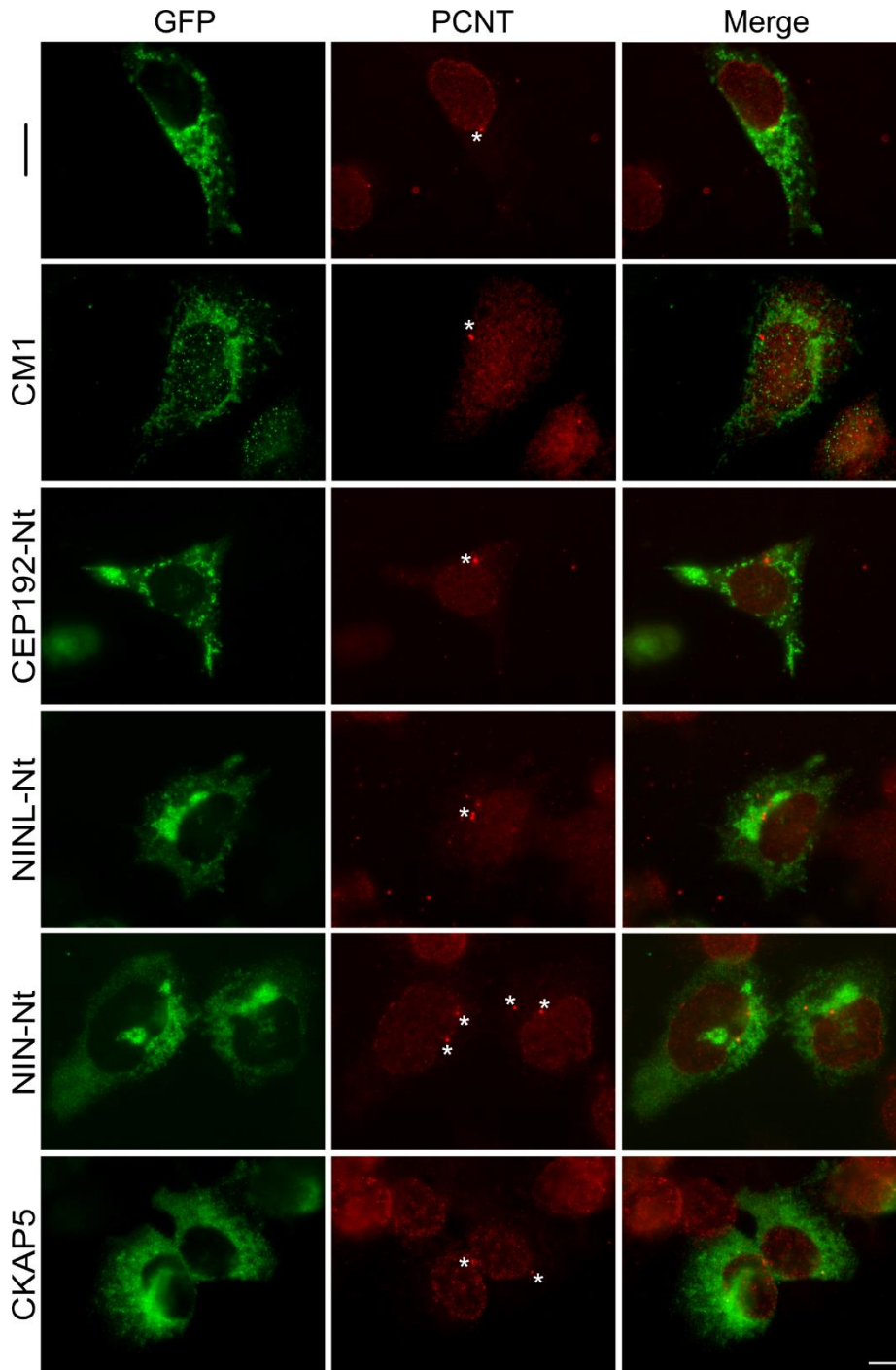


Figure R6. PCNT is not recruited to mitochondria by any of the POI tested.

Representative IF images of U2OS cells expressing POI targeted to mitochondria. Nocodazole plus cold treatment was used in this experiment. In all cases only centrosomal signal of PCNT could be detected. Asterisks indicate centrosomal signal. Scale bar: 10 μ m.

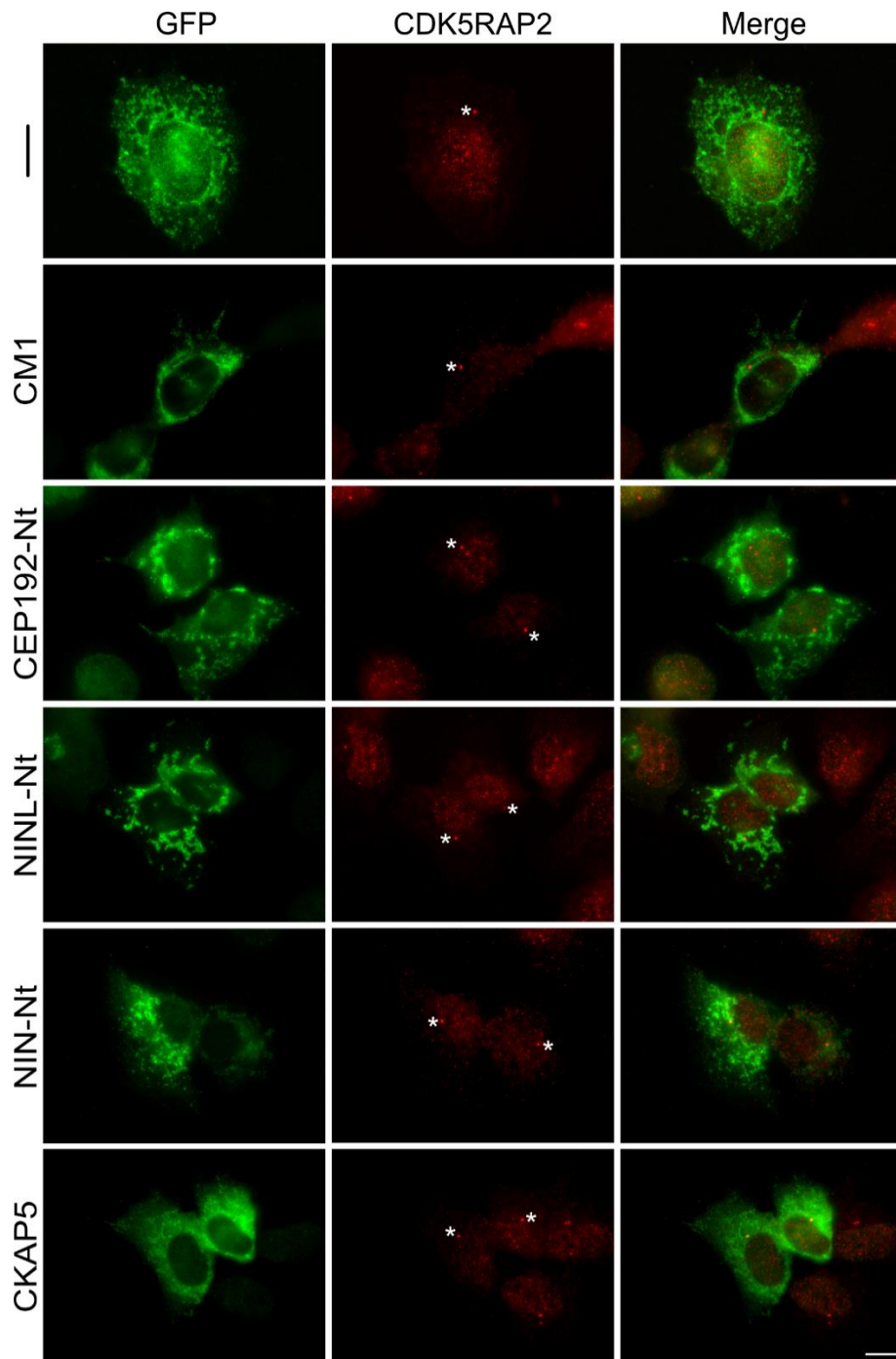


Figure R7. CKD5RAP2 is not recruited to the mitochondria by any of the POI tested.

Representative IF images of U2OS cells expressing POI targeted to mitochondria. Nocodazole plus cold treatment was used in this experiment. In any of the cases only centrosomal signal from CDK5RAP2 could be detected. Asterisks indicate centrosomal signal. Scale bar: 10 μ m.

Mitochondria-targeted CM1, NINL-Nt and NIN-Nt recruit endogenous CKAP5

After excluding the presence of two major PCM components, PCTN and CDK5RAP2, at the ectopic site, we next considered the role of CKAP5. As already described, members of the XMAP215 family such as CKAP5 might have a dual role, not only in promoting microtubule polymerization by binding to the plus-end of microtubules (Tournebise, 2000), but also in microtubule nucleation (Popov, 2002; Wiczonek, 2015; Gunzelmann, 2018; Thawani, 2018). To distinguish between CKAP5 binding to the plus-end of nascent microtubules and binding to the ectopic MTOC, we checked CKAP5 localization by IF in the absence of microtubules (**Figure R8**, 0 s) and after microtubule regrowth (**Figure R8**, 40 s). Interestingly, all the POI that triggered microtubule nucleation (CM1 and NINL-Nt) also recruited endogenous CKAP5, even in the absence of microtubules. As we targeted full-length CKAP5 we cannot rule out whether the antibody was recognising the expressed or the endogenous protein. This result suggests that CKAP5 might be involved in the formation or function of these ectopic MTOCs. However, NIN-Nt, which did not promote microtubule nucleation at the ectopic site, also recruited CKAP5. Thus, the presence of CKAP5 is not necessarily correlated with nucleation activity.

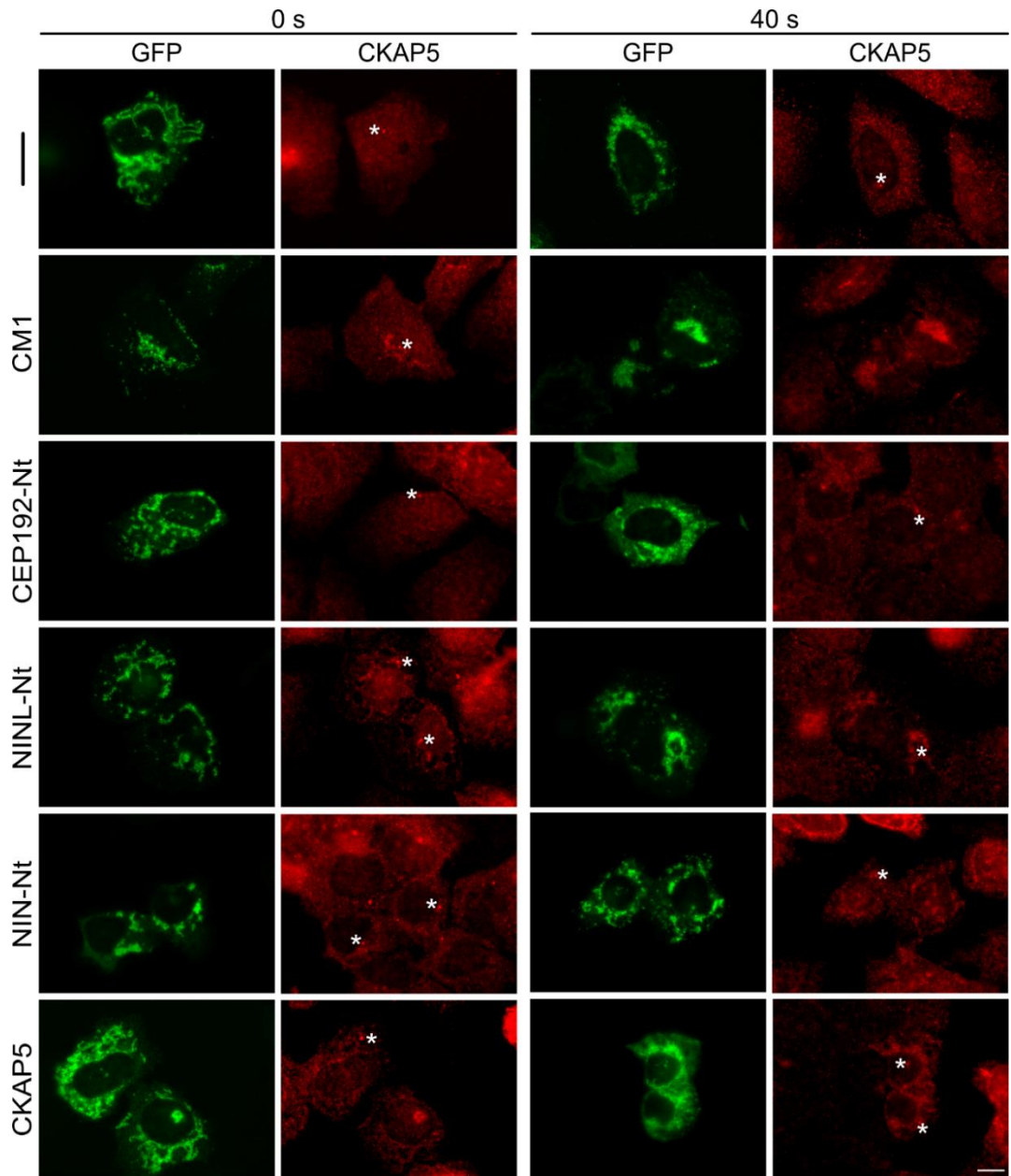


Figure R8. CM1, NINL-Nt, and NIN-Nt recruit CKAP5 to the mitochondria, even in the absence of microtubules.

Representative IF images of U2OS cells expressing POI targeted to mitochondria. Nocodazole plus cold treatment was used in this experiment. CKAP5 signal was analysed in the absence (left panel, 0 s) or in the presence of microtubules (right panel, 40s). CKAP5 signal was detected in both scenarios after targeting CM1, NINL-Nt, NIN-Nt and CKAP5 to the mitochondria. Asterisks indicate centrosomal signal. Scale bar: 10 μ m.

Exploration of the different MTOCs

A summary of the specific region of each POI and the composition of each MTOC formed at the mitochondria can be found in **Table R1**. In brief, we have observed that only three of the constructs targeted were able to generate an active MTOC. Moreover, based on the different endogenous proteins that were co-targeted we could distinguish between two different types of ectopic MTOCs. First, there are those that contain γ TuRC and NEDD1, as is the case for CM1 and NINL-Nt. Second, there is a “non-canonical” MTOC formed by CKAP5 in the absence of γ TuRC.

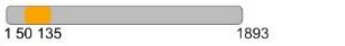




		Nucleation	γ -Tubulin	GCP8	NEDD1	PCNT	CDK5RAP2	CKAP5
GFP		-	-	-	-	-	-	-
<i>Hs</i> CDK5RAP2-CM1		+	+	+	+	-	-	+
<i>Hs</i> CEP192-Nt		-	+	+	+	-	-	-
<i>Hs</i> NINL-Nt		+	+	+	+	-	-	+
<i>Hs</i> NIN-Nt		-	+	+	+	-	-	+
<i>Hs</i> CKAP5		+	-	-	-	-	-	+

Table R1. Summary of the ectopic MTOC composition and nucleation capacity after targeting the different POI to the mitochondria.

These initial results demonstrated the feasibility of our approach to study MTOC formation at a non-centrosomal, ectopic site. Therefore, we decided to use this system for answering additional questions.

Nucleation at the ectopic site can be activated in trans

One curious observation was that mitochondria-targeted CEP192-Nt and NIN-Nt recruited γ TuRC but were unable to induce microtubule nucleation (**Table R1**). A potential explanation may be that these proteins themselves lacked nucleation activating function and were also unable to recruit a suitable activator. To investigate this, we decided to provide an activator of microtubule nucleation in trans by expressing it as diffusible protein in the cytoplasm. A FLAG-tagged version of the known activator CM1 (Choi, 2010) was co-expressed (**Figure R9**, FLAG, second

row) with mitochondria-targeted CEP192-Nt. Strikingly, co-expression of FLAG-CM1 indeed promoted microtubule nucleation from the mitochondria (**Figure R9**, second row). We conclude that γ TuRC recruited by CEP192-Nt can be stimulated to nucleate microtubules by providing an activator in trans.

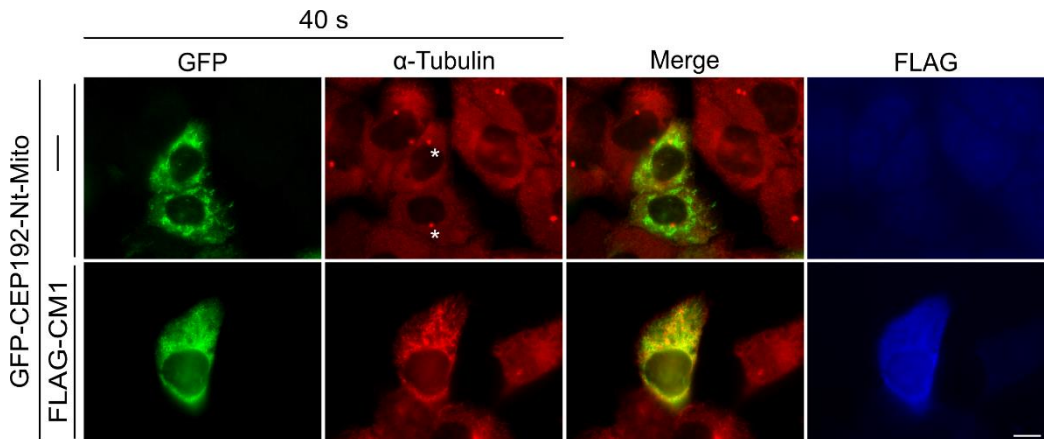


Figure R9. Cytoplasmic expression of CM1 is sufficient to induce nucleation from CEP192 Nt-decorated mitochondria.

Representative IF images of U2OS cells expressing POI targeted to mitochondria. Additionally, FLAG-CM1 was co-expressed to evaluate microtubule nucleation capacity from the mitochondria (second row). Images were taken after 40 seconds (40 s) of microtubule regrowth. Microtubule nucleation was only detected when FLAG-CM1 was co-expressed. Asterisks indicate centrosomal signal. Scale bar: 10 μ m.

CKAP5 nucleates microtubules possibly through tubulin recruitment

Another interesting issue to address was to better understand how CKAP5 may be able to nucleate microtubules in the absence of γ TuRC. Previous work had shown that this protein had the ability to facilitate microtubule nucleation *in vitro* at a certain concentration of free tubulin (Wieczorek, 2015). This function is carried out by the N-terminal part of the protein, which contains several TOG domains that can bind tubulin (Fox, 2014). Depending on the specific TOG domain, soluble or microtubule lattice-incorporated tubulin is preferentially bound (Slep, 2007). It was also suggested that at least *in vitro*, CKAP5 could interact with γ -tubulin through a domain at its C-terminal end (Thawani, 2018). As we were not able to detect any γ -tubulin signal at mitochondria when targeting CKAP5 to this site, we speculated that microtubule nucleation in this case was γ TuRC-independent and dependent on the TOG domains. To verify this idea, we generated truncations of CKAP5 that lacked either

the C-terminal region (CKAP5 1-1428) or the TOG domains (CKAP5 1429-2033) and targeted these to mitochondria (**Table R2**). After performing a regrowth assay, we could observe that only the constructs containing the TOG domains (CKAP5 and CKAP5 1-1428) were effective in generating an active MTOC (**Figure R10**, α -Tubulin). Furthermore, we could not detect recruitment of γ -tubulin at the ectopic site with any of the constructs (**Figure R10**, γ -Tubulin). Remarkably, the levels of general microtubule nucleation (including centrosomal microtubule nucleation) were very reduced in cells where CKAP5 1429-2033 was transfected. It is thus possible that this region has a global dominant-negative effect on microtubule nucleation. In summary, we have shown that CKAP5 is able to build an active MTOC, presumably in a γ TuRC-independent manner through tubulin recruitment via TOG domains.




		Nucleation	γ -Tubulin
Hs CKAP5		+	-
Hs CKAP5 1-1428		+	-
Hs CKAP5 1429-2033		-	-

Table R2. Summary of CKAP5 domains targeted to mitochondria and their MTOC formation capacity.

CKAP5 fragments were subcloned into a vector containing a GFP fluorescent tag and a mitochondrial targeting domain. Proteins were expressed in cells and then microtubule nucleation capacity and γ -tubulin recruitment at the mitochondria were analysed.

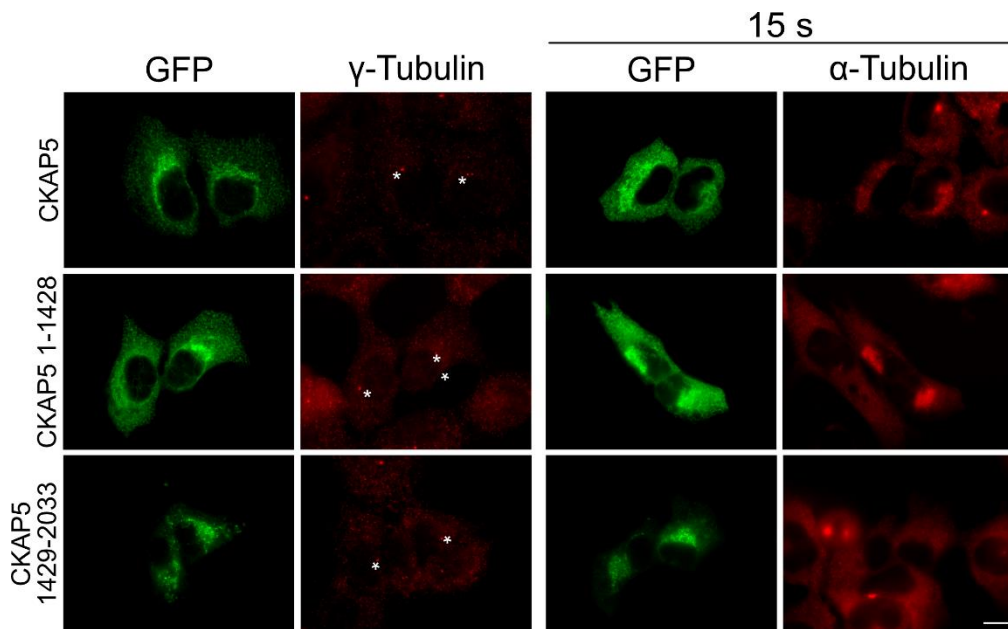


Figure R10. TOG domains from CKAP5 are required to generate an active MTOC that is γ TuRC-independent.

Representative IF images of U2OS cells expressing POI targeted to mitochondria. Ice cold treatment was used in this experiment. Additionally, microtubules were allowed to regrowth in warm culture medium for 15 seconds to detect microtubule nucleation (15 s). Microtubule nucleation/concentration from the outer surface of the mitochondria was detected in CKAP5 and CKAP5 1-1428. No γ -tubulin could be detected with any of the constructs. Asterisks indicate centrosomal signal. Scale bar: 10 μ m.

CM1 and NINL-Nt induce similar nucleation activity when targeted to mitochondria

Next, we focused on the POI that gave rise to the more “canonical” type of MTOC that involved γ TuRC. As both proteins, CM1 and NINL-Nt, appeared to generate an ectopic MTOC, we wondered whether they would have the same microtubule nucleation capacity. For a quantitative analysis, we repeated the regrowth assay but chose a shorter timepoint of microtubule regrowth, aiming to properly distinguish between microtubules being generated from the centrosome, the cytoplasm and the mitochondria. In addition, we took advantage of the increased resolution achievable by Structured Illumination Microscopy (SIM), which allowed visualization of individual short microtubules at the ectopic site. After quantification of the IF images, we could conclude that mitochondria-targeted CM1 and NINL-Nt both induce similar microtubule nucleation activity (**Figure R11**).

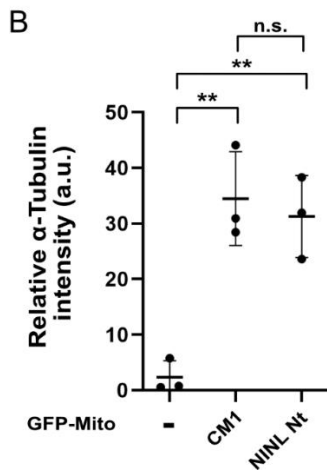
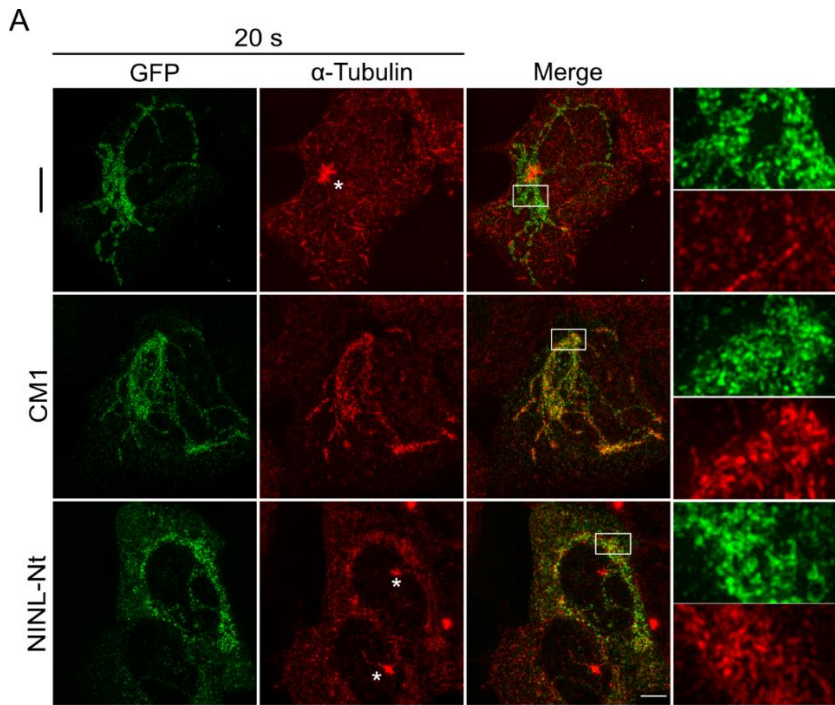


Figure R11. The MTOCs build by CM1 and NINL-Nt when targeted to the mitochondria, share the same microtubule nucleation capacity.

(A) Representative IF images taken with SIM of CM1 and NINL-Nt targeted to mitochondria. Cells were fixed after Nocodazole plus cold treatment, followed by 20 seconds (20 s) of regrowth in warm culture medium. Last column shows insets of ROIs (white rectangle in Merge). Asterisks indicate centrosomal signal. Scale bar: 5 μ m. (B) Quantification of the relative α -tubulin levels from the outer surface of the mitochondria. 15 cells were counted per condition in 3 independent experiments. Statistical significance was determined using an unpaired t-test. ** ($p < 0.005$). n.s. (non-significant). Horizontal bars represent means, error bars SD.

The fact that both CM1 and NINL-Nt are capable of generating an ectopic MTOC and that CM1 is known to directly bind and activate γ TuRC, made us wonder whether NINL may have similar activity. Previous work had implicated the N-terminal region of NINL in γ -tubulin binding (Casenghi, 2003) and we decided to dissect the requirements in more detail.

Chapter 2

Molecular characterization of MTOC formation by ectopically expressed NINL

Joel Paz¹, Cristina Lacasa¹, Gianluca Arauz¹, Marina Gay¹, Ester Sánchez¹, Mar Vilanova¹, Marta Vilaseca¹, Jens Lüders¹

¹Institute for Research in Biomedicine (IRB Barcelona), The Barcelona Institute of Science and Technology (BIST), 08028 Barcelona, Spain

Statement of contribution:

Joel Paz designed, performed and analysed most of the experiments in this chapter.

Cristina Lacasa and Joel Paz co-prepared the BioID-MS samples that led to figure R21.

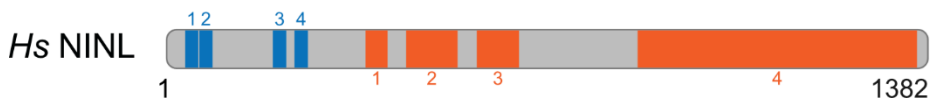
Gianluca Arauz, Marina Gay, Ester Sánchez, Mar Vilanova, and Marta Vilaseca helped with the experimental design and analysed BioID-MS data showed in figure R21.

Jens Lüders supervised the project.

Identification of minimal NINL region required for MTOC formation

We decided to generate several NINL truncations to determine the specific contribution of each region to ectopic MTOC formation. Truncations were based on the described domain structure of NINL in UniProt (Q9Y2I6). NINL contains four EF-Hands near its N-terminus and 4 coiled-coil domains spread along the remaining parts of the protein (**Schematic R2**).

	1	2	3	4
Coiled coil	384-424	484-579	616-699	1046-1375
EF-hand	7-42	41-76	196-231	233-268



Schematic R2. Domain structure of *Hs* NINL.

As described for the experiments carried out in Chapter 1, we analysed γ TuRC-recruitment and microtubule nucleation capacity by IF for each NINL construct targeted to mitochondria. An overview of the main results is presented in **Table R3**. IFs images with the most interesting results can be evaluated in **Figure R12**. It is important to mention that for this chapter, the experiments were not carried out in the presence of nocodazole. Thus, clustering of the mitochondria was detected for some of the constructs, such as NINL-Nt (1-702) (**Figure R12**, NINL-Nt). We noticed that all constructs lacking the third coiled-coil coil domain (aa 616-699) did not cluster the mitochondria around the centrosome (**Figure R12**, NINL 1-442, NINL 1-287). This result would suggest that there is a possible dynein-binding domain in within the third coiled-coil domain of NINL.

		Nucleation	γ -Tubulin	Clustering
NINL Nt (1-702)		+	+	+
NINL 1-442		+	+	-
NINL 1-287		-	+	-
NINL 1-195		-	-	-
NINL 41-287		-	-	-
NINL 196-584		+	+	+
NINL 196-442		-	-	-

Table R3. Summary of the results obtained from NINL truncation mutants targeted to mitochondria.

NINL fragments were subcloned into a vector containing a GFP fluorescent tag and a mitochondrial targeting domain. Afterwards, each mutant was expressed in cells and then microtubule nucleation capacity and γ -tubulin recruitment at the mitochondria were analysed. Clustering of the mitochondria was also annotated.

Focusing on MTOC formation capacity, we first tried to find a minimal region that was still capable of both γ TuRC recruitment and induction of nucleation activity. An interesting finding was that two fragments, NINL 1-442 and NINL 196-584, displayed such properties. Strikingly, a fragment corresponding to the region shared between both, NINL 196-442, was not able to assemble an ectopic MTOC (**Table R3**).

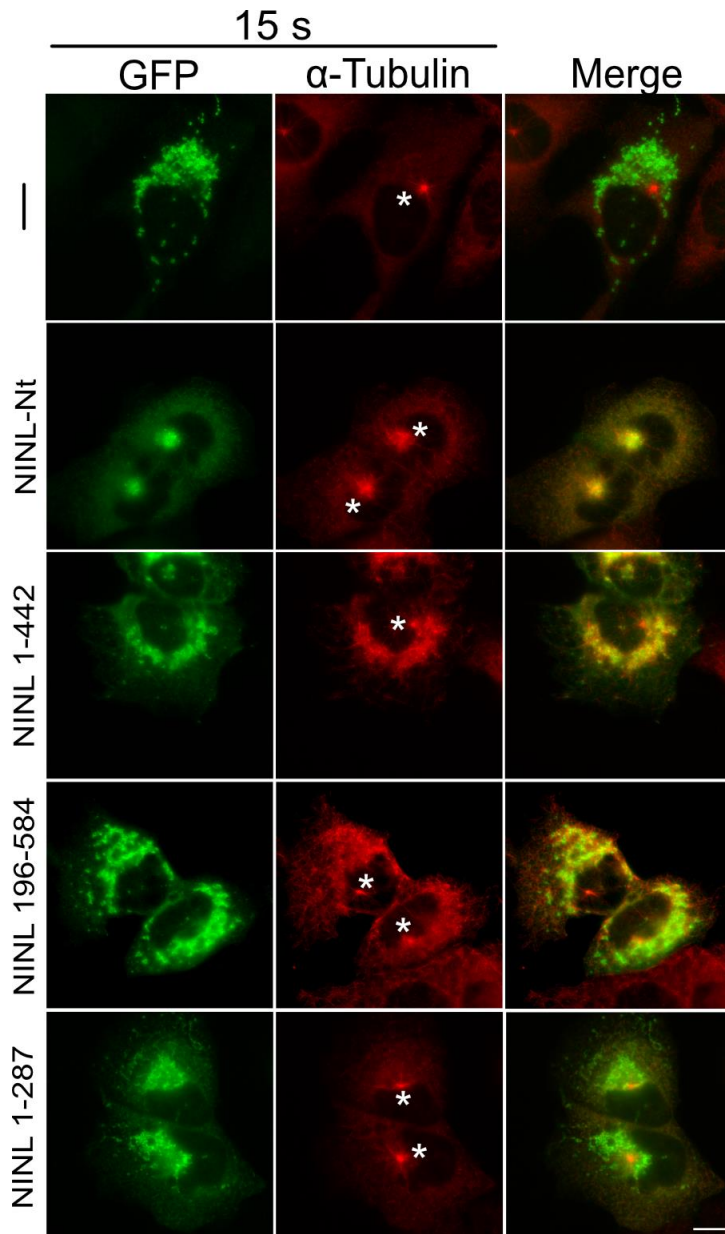


Figure R12. NINL 1-442 and NINL 196-584 are sufficient for MTOC formation at the mitochondria.

Representative IF images of U2OS cells expressing NINL truncations targeted to mitochondria. Ice cold treatment was used in this experiment. Additionally, microtubules were allowed to regrowth in warm culture medium for 15 seconds (15 s) to detect microtubule nucleation. Microtubule nucleation from the outer surface of the mitochondria were detected in cells expressing NINL-Nt, NINL 1-442 and NINL 196-584. Asterisks indicate centrosomal signal. Scale bar: 10 μ m.

NINL second coiled coil mediates self-oligomerization

At that point we were puzzled by the observation that two different parts of NINL seemed to independently allow MTOC assembly. Based on the literature, coiled-coil domains are important for protein-protein interaction and are also involved in protein oligomerization (Burkhard, 2001). Since NINL has several predicted coiled-coil domains, we speculated that one possibility was that one of the two fragments contained a region required for NINL dimerization or oligomerization. If so, this fragment may be able to recruit endogenous full-length NINL for enabling ectopic MTOC assembly. To test this possibility, we designed an experiment where we targeted NINL fragments Nt (1-702), 1-442 and 196-584 to mitochondria, and additionally expressed in the cytoplasm a FLAG-tagged version of NINL-Nt that on its own does not target to mitochondria. Then, we checked whether FLAG-NINL-Nt was recruited to mitochondria in the presence of any of the other constructs (**Figure R13**). Noticeably, only mitochondria-targeted NINL-Nt and NINL 196-584 were able to recruit FLAG-NINL-Nt, suggesting that they were able to interact with FLAG-NINL-Nt. Therefore, the region between 442 and 584, comprising the second coiled-coil region of NINL, may promote dimerization/oligomerization of NINL. This result would be in line with our observation that NINL-Nt had the most robust MTOC assembly activity, which could be potentially explained by recruitment of additional endogenous NINL. The most important outcome from this experiment is that NINL 196-584 may be able to assemble ectopic MTOCs only through recruitment of endogenous NINL and that NINL 1-442, which lacks the second coiled-coil and cannot recruit endogenous NINL, likely contains the minimal region sufficient for generating an ectopic MTOC.

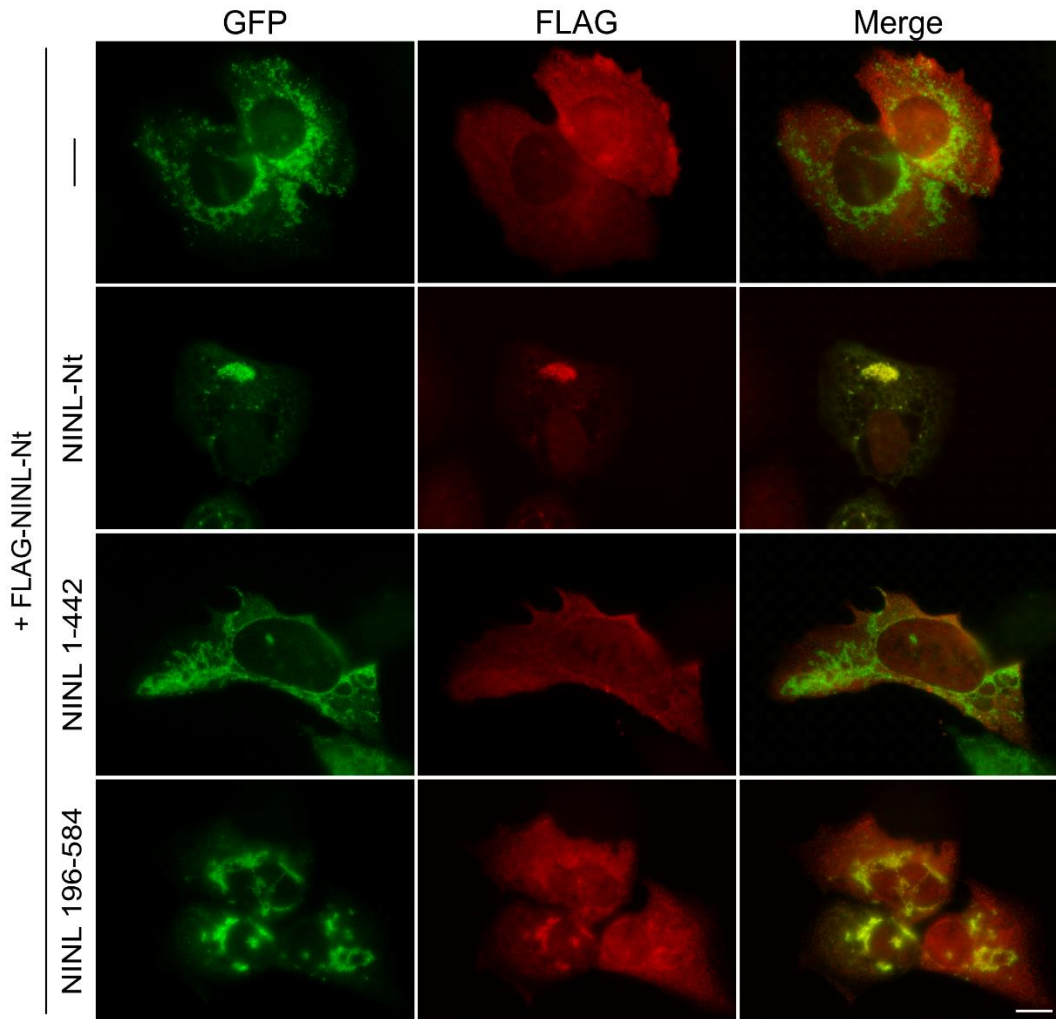
A**B**

Figure R13. NINL-Nt and NINL 196-584 targeted to mitochondria are able to recruit cytoplasmic NINL-Nt.

(A) Schematic of the NINL constructs used. (B) Representative IF images of U2OS cells expressing NINL truncations targeted to mitochondria. Only NINL-Nt and NINL 196-584 recruited additional FLAG-NINL-Nt to the mitochondria. Scale bar: 10 μ m.

NINL 1-287 is the minimal region required to bind γ TuRC

Further dissection of NINL regions revealed that NINL 1-287 was able to recruit γ TuRC, but did not allow microtubule nucleation at the mitochondria (**Figure R14**). It is worth mentioning that γ TuRC recruitment was not observed in every cell, and typically required higher levels of expression of NINL 1-287. Nevertheless, the data suggest that NINL contains a γ TuRC-binding region between aa 1-287. To confirm this result, we performed immunoprecipitation experiments where we pulled-down the different NINL constructs targeted to mitochondria and checked whether γ TuRC subunits were coprecipitated. We could detect interaction of various NINL constructs with γ TuRC but in the case of NINL 1-287, interaction seemed weaker (**Figure R15**).

In summary, we could conclude that NINL 1-442 is the minimal region required to generate an ectopic MTOC. Moreover, it appears that in order to build this MTOC, γ TuRC is recruited by interaction with the region between aa 1-287, whereas nucleation activity additionally requires the region between aa 288-442. It should be noted that we also tried to provide the nucleation activating function of NINL in trans, as described before for mitochondria-targeted CEP192-Nt (**Figure R9**). For this we targeted the γ TuRC-binding NINL 1-287 to mitochondria and co-expressed a FLAG-tagged cytoplasmic version of NINL 288-442 comprising the region require for nucleation activation. The aim was to use NINL 1-287 for recruiting γ TuRC to mitochondria and NINL 288-442 to activate it. However, we were unable to generate an ectopic MTOC in this way (data not shown).

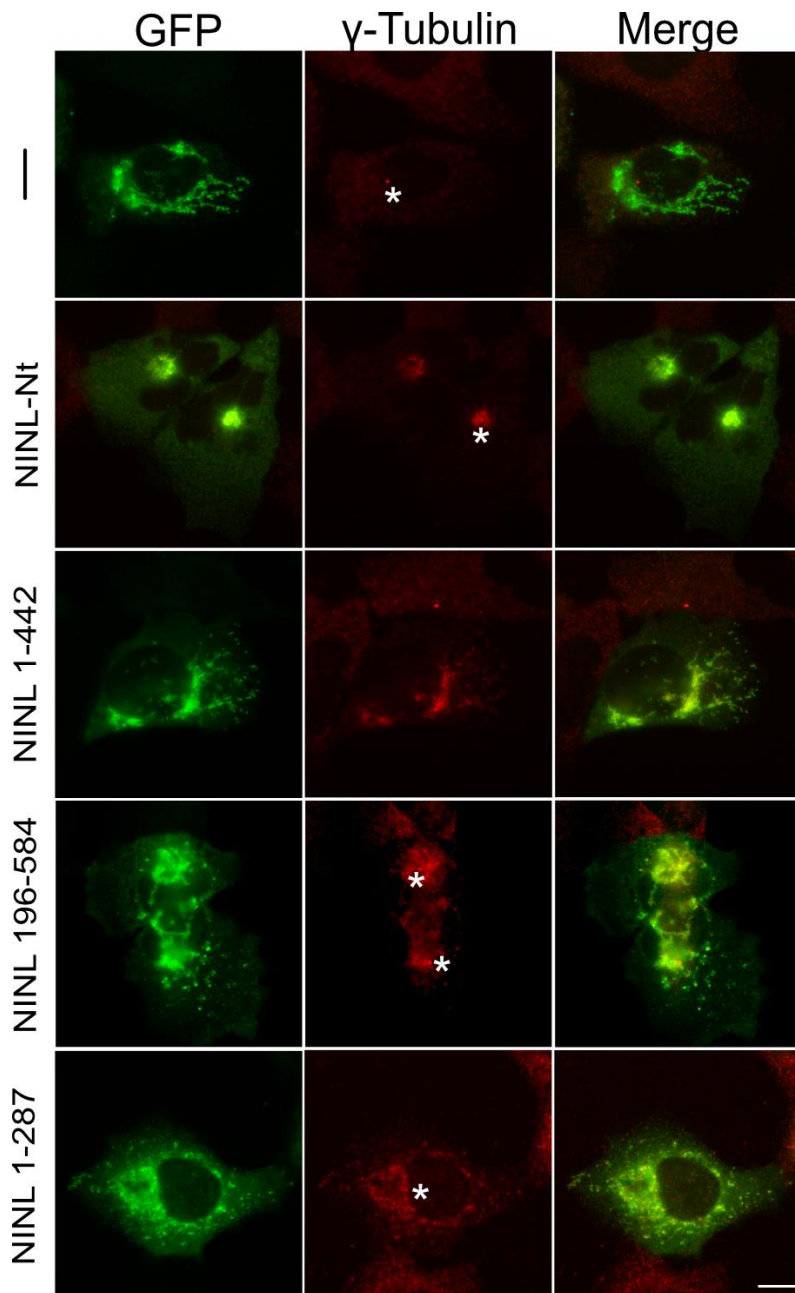


Figure R14. NINL 1-287 is the minimal domain necessary for γ TuRC recruitment.

Representative IF images of U2OS cells expressing NINL truncations targeted to mitochondria. Ice cold treatment was used in this experiment and cells were imaged in the absence of microtubules. γ TuRC recruitment was detected in NINL-Nt, NINL 1-442, NINL 196-584 and NINL 1-287. Asterisks indicate centrosomal signal. Scale bar: 10 μ m.

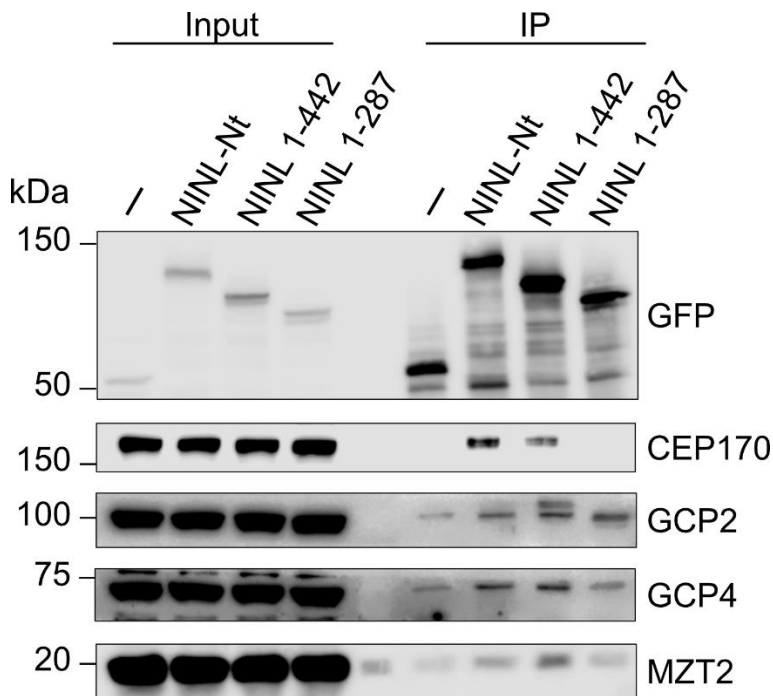


Figure R15. NINL-Nt, NINL 1-442 and likely NINL 1-287 co-immunoprecipitate with the γ TuRC.

Western blot analyses of the indicated proteins after immunoprecipitation with anti-GFP antibodies. Lysates from HEK293 cells were transfected with the indicated GFP-tagged NINL constructs targeted to mitochondria. Input levels are shown on the left side of the WB (Input). Three different γ TuRC components were used as a readout for γ TuRC interaction, GCP2, GCP4 and MZT2. CEP170 was employed as an SDA marker. Representative of 2 independent experiments.

NINL relationship with other SDA proteins

Even after the discovery of NINL 1-442 as a minimal region required to build an MTOC, the underlying mechanism was still elusive. Since we had only found γ TuRC, NEDD1 and CKAP5 present and the mitochondria (**Table R1**), we decided to test whether there might be other proteins required for MTOC formation. It was already described that NINL localizes to the mother centriole at the centrosome and due to its similarity with NIN, it was speculated that it also localizes to the SDAs of the centrosome (Casenghi, 2003; Casenghi, 2005; Rapley, 2005). Therefore, we wondered whether SDA proteins may be involved in ectopic MTOC assembly. Based on the published SDA hierarchy (Chong, 2020) and assuming that NINL and NIN may share a similar localization at SDAs, we tested interaction of NINL with NIN and with the SDA protein CEP170.

NINL interacts with CEP170 through a predicted EF-Hand

While testing γ TuRC interaction with the different NINL constructs by co-immunoprecipitation, we found CEP170 was pulled that down with NINL-Nt and NINL 1-442, but not with NINL 1-287 (**Figure R15**). We decided to repeat this experiment adding NINL 1-383. This additional construct co-immunoprecipitated with CEP170 as well (**Figure R16**). This revealed that there is CEP170-binding region in NINL, located between amino acids 287-383.

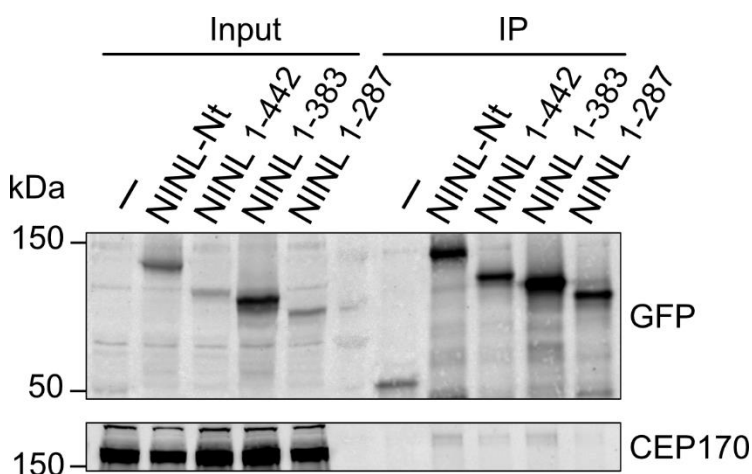
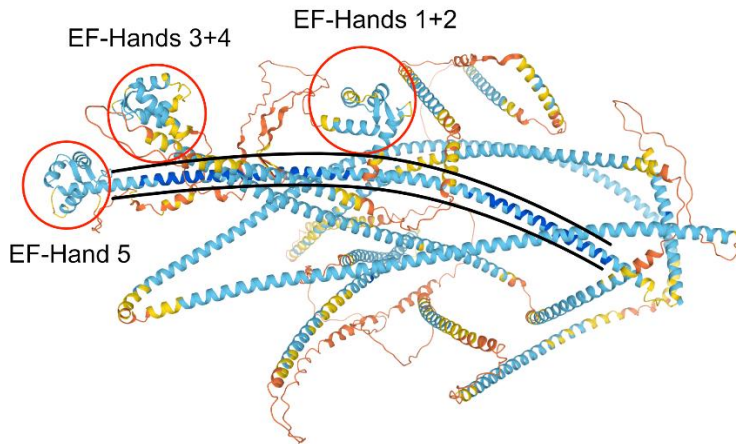


Figure R16. NINL binds CEP170 through aa 287-383.

Western blot analyses of the indicated proteins after immunoprecipitation with anti-GFP antibodies. Lysates from HEK293 cells were transfected with the indicated NINL construct targeted to mitochondria. Input levels are shown on the left side of the WB (Input). CEP170 interacts with NINL-Nt, 1-442 and 1-383. Representative of 2 independent experiments.

Apart from exploring the interaction with CEP170, we also analysed NINL relationship with NIN. According to UniProt (Q8N4C6), NIN contains a fifth EF-Hand between amino acids 317–352 that is not annotated for NINL. However, comparison of the structures of NIN and NINL predicted by the AlphaFold server (Jumper, 2021) suggested that this region is structurally very similar in both proteins. The predictions suggest that both proteins contain a total five EF-Hands (**Figure R17**). Interestingly, the predicted fifth EF-Hand seems to correspond to the region required for CEP170 interaction (**Figure R16**).

NIN (2090aa)



NINL (1382aa)

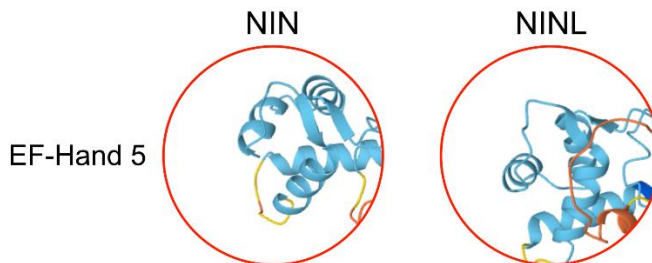
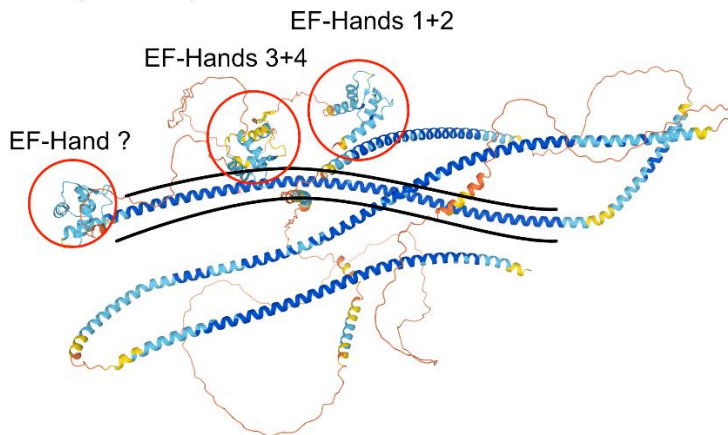


Figure R17. NINL shares a potential 5th EF-Hand in the region between aa 301-371.

Structural prediction with Alphafold server of *Hs* NINL and *Hs* NIN reveals a highly similar N-terminus. EF-Hands 1 to 4 appear to be conserved between both proteins (red circles) and they are surrounded by disordered regions (orange in structure). A 5th EF-Hand is also annotated for NIN in UniProt (NIN, left red circle) and it matches structurally the area between aa 301-370 of NINL, pointing at a possible EF-Hand (highlighted at the bottom). In black is highlighted a highly conserved helix between approximately aa 350-450 (includes the minimal region required to generate an ectopic MTOC).

To directly test if the predicted fifth EF-Hand in NINL was necessary for interaction with CEP170, we decided to introduce specific mutations. As already commented, EF-Hands are calcium binding structures. They are formed by two helices, E and F, and a loop motif that connects both and serves as a pocket where calcium is bound. This loop motif is highly conserved and mutations in it have a strong effect on calcium binding. In particular, mutation of glutamate (E) found in position 12 is commonly used to disrupt the properties of EF-Hands (Pottgiesser, 1994; Gifford, 2007). We generated a corresponding NINL 1-442-E359K mutant targeted to mitochondria and performed immunoprecipitation experiments as before. We found that mutation of the predicted fifth EF-Hand in NINL severely disrupted binding of CEP170 (**Figure R18**). Therefore, we could conclude that NINL interacts with CEP170 through its fifth EF-Hand, presumably through calcium binding.

In this experiment, we also probed the immunoprecipitation of NIN. Indeed, NIN interacted with NINL-Nt (**Figure R18**, NIN), but not with smaller fragments. Considering that NINL 1-442 is the minimal region required for ectopic MTOC assembly but lacks NIN interaction, we concluded that NIN is unlikely involved in this function.

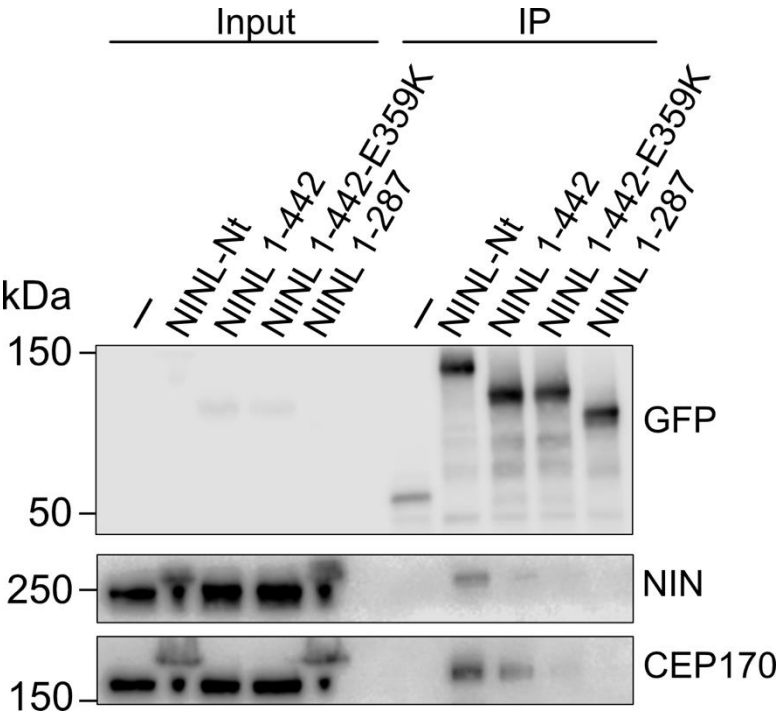


Figure R18. E359K mutation impairs the binding of NINL to CEP170. NINL mainly interacts with NINL-Nt.

Western blot analyses of the indicated proteins after immunoprecipitation with anti-GFP antibodies. Lysates from HEK293 cells were transfected with the indicated NINL construct targeted to mitochondria. Input levels are shown on the left side of the WB (Input). CEP170 interacts with NINL-Nt and 1-442. NINL only interacts with NINL-Nt. Representative of 2 independent experiments.

CEP170 binding is dispensable for MTOC assembly by NINL 1-442

After finding that we could modulate the binding of NINL to CEP170 by a specific point mutation, we decided to test whether this might have an effect on ectopic MTOC formation. Side by side comparison of MTOC formation capacity between NINL 1-442 and NINL 1-442 E359K, revealed that both constructs were equally capable of generating a functional MTOC (**Figure R19**). Hence, we could conclude that this function was independent of CEP170.

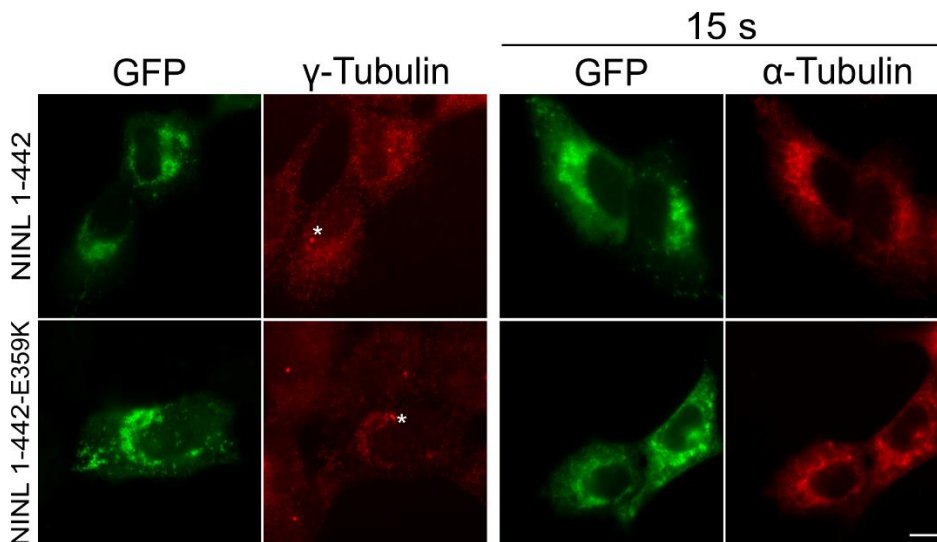


Figure R19. E359K mutation does not impair ectopic MTOC formation capacity of NINL 1-442.

Representative IF images of U2OS cells expressing NINL truncations targeted to mitochondria. Ice cold treatment was used in this experiment and cells were imaged in the absence of microtubules (γ -Tubulin) or after microtubule regrowth (α -Tubulin, 15 s). γ TuRC recruitment as well as microtubule nucleation at the outer surface of the mitochondria were detected in both NINL 1-442 and NINL 1-442 E359K. Asterisks indicate centrosomal signal. Scale bar: 10 μ m.

CEP170 silencing does not impair ectopic MTOC formation by NINL 1-442

To further confirm the previous result, we set up an experiment where we silenced CEP170 while targeting NINL 1-442 to mitochondria and then evaluated its MTOC formation capacity. As predicted, knockdown of CEP170 did not perturb the capacity of NINL 1-442 to generate an ectopic MTOC (**Figure R20**). Therefore, we ruled out that CEP170 was involved in the ability of NINL 1-442 to form an ectopic MTOC.

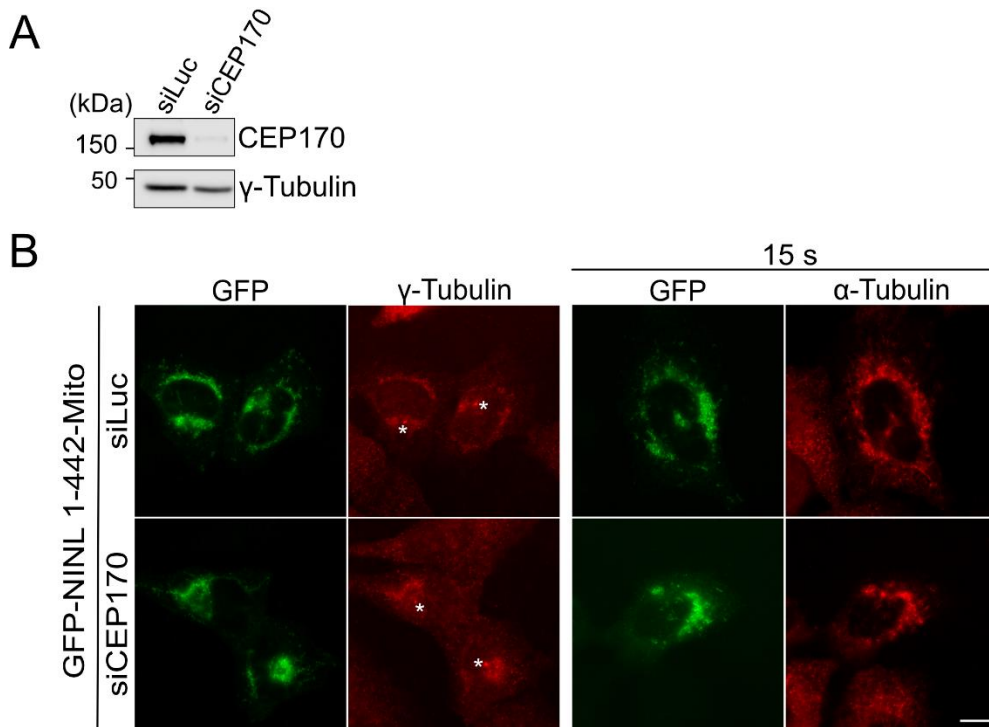


Figure R20. Depletion of CEP170 does not alter NINL 1-442 MTOC formation capacity.

(A) WB analysis of CEP170 siRNA efficiency. Cells were silenced for 72 hours with 100 nM of siCEP170. Luciferase siRNA was used as a control. γ -Tubulin was used as a loading control. (B) Representative IF images of the NINL 1-442 targeted to the mitochondria in U2OS cells. Ice cold treatment was used in this experiment and cells were imaged in the absence of microtubules (γ -Tubulin) or after microtubule regrowth (15 s), after transfection of control or CEP170 siRNA. γ TuRC recruitment as well as microtubule nucleation at the outer surface of the mitochondria were detected independent of CEP170 depletion. Asterisks indicate centrosomal signal. Scale bar: 10 μ m.

Search for novel NINL interactors

So far, we were able to identify several proteins present at ectopic MTOCs induced by NINL 1-442, the main microtubule nucleator γ TuRC and its targeting factor NEDD1, and the stimulator of microtubule nucleation/growth CKAP5 (**Table R1**). However, main components of the centrosomal MTOC such as PCNT and CKD5RAP2 were not present (**Table R1**). The SDA proteins NIN and CEP170 interacted with NINL but were not required for MTOC formation (**Figure R18, R19 and R20**). We wondered whether additional protein that we had not yet tested may participate in NINL-dependent ectopic MTOC assembly. To identify candidates, we set up a biotin proximity ligation assay, termed BioID. This is an assay where a POI is tagged with a promiscuous version of the *E. coli* biotin ligase BirA, which in the presence of biotin will biotinylate proteins that are in close proximity to the POI. This includes direct or indirect interactors and proteins that are only transiently in proximity (Kim, 2016; Roux, 2018).

It is worth to mention that two different groups have conducted BioID experiments with NINL as part of high-throughput studies, but both were done using full-length NINL as bait, which localizes to the centrosome (Gupta, 2015; Redwine, 2017). For our particular purpose, we performed the BioID analysis with mitochondria-targeted NINL-Nt and NINL 1-442.

BioID reveals candidates involved in ectopic MTOC formation and/or function

We performed the BioID experiment in two biological replicates for each NINL construct, NINL-Nt (1-702) and NINL 1-442. After biotinylation, biotinylated proteins were affinity purified and identified by mass spectrometry. For a more robust analysis, we decided to only focus on proteins identified in both biological replicates and shared between both baits (**Figure R21**, Dot plot analysis). Therefore, the hits shown have appeared in 2 different experiments with 2 separate NINL constructs. Remarkably, 68% of the hits were already detected in the previous NINL BioID papers and 37% of them appeared in both studies (**Figure R21**, Dot plot analysis, coloured boxes). Thus, we were confident that our results were significant. It was reassuring to observe that after building a protein network of known physical interactions among all the common hits from the BioID, most of the hits were centred around NINL (**Figure R21**, network analysis). Moreover, the identified proteins made biological sense, since the most enriched cellular components after GO analysis were the centrosome, cytoskeleton and MTOCs (**Figure R22**, GO cellular component). Likewise, GO analysis of the biological processes revealed an

enrichment in microtubule-related processes, such as mitosis, cytoskeleton organization and ciliogenesis (**Figure R22**, GO Biological process).

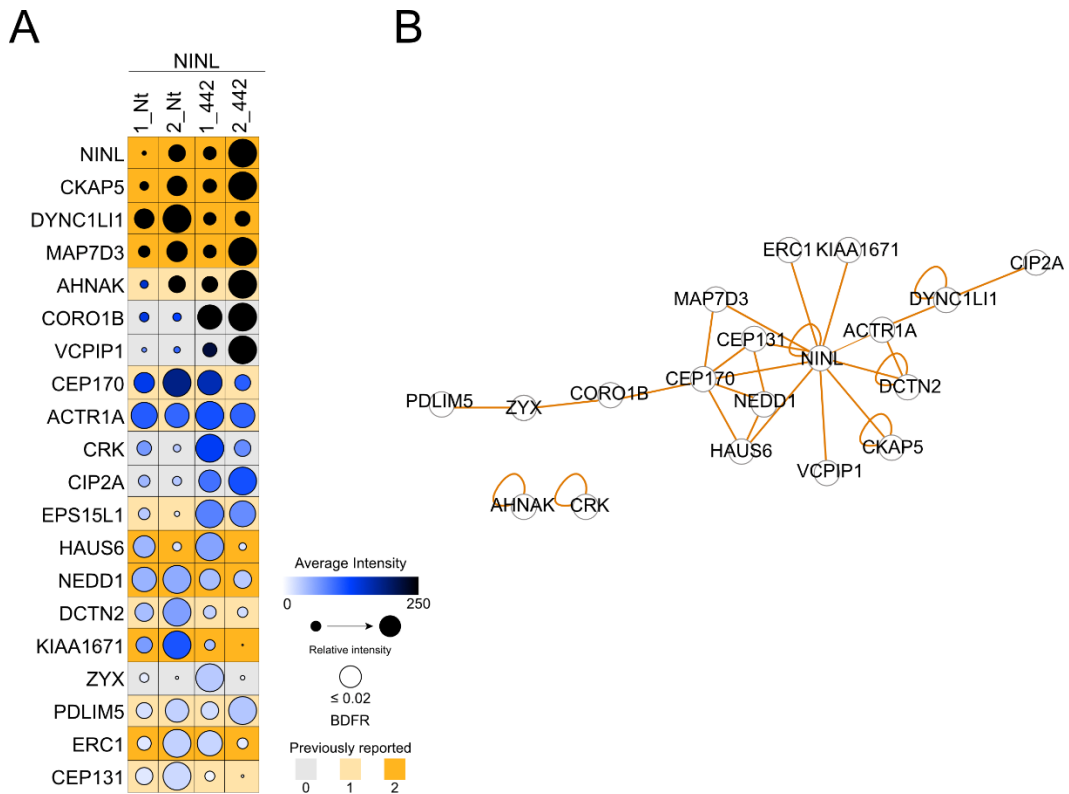


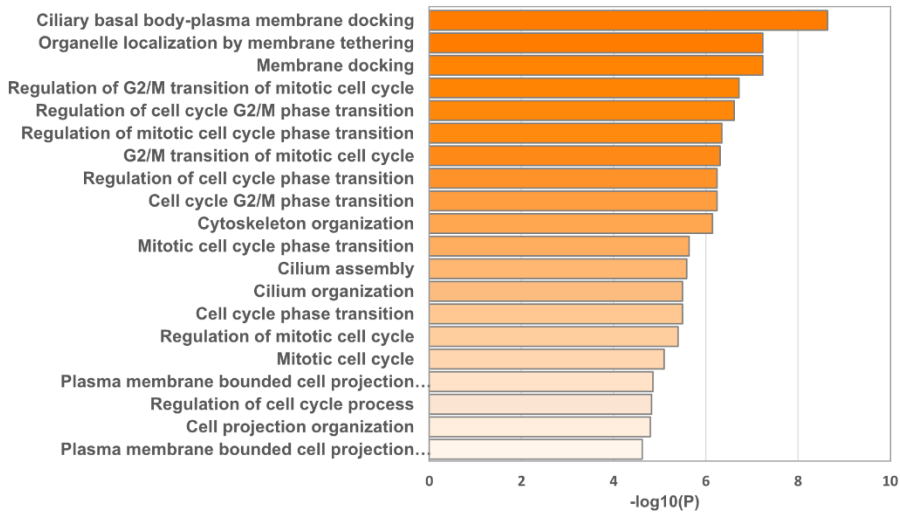
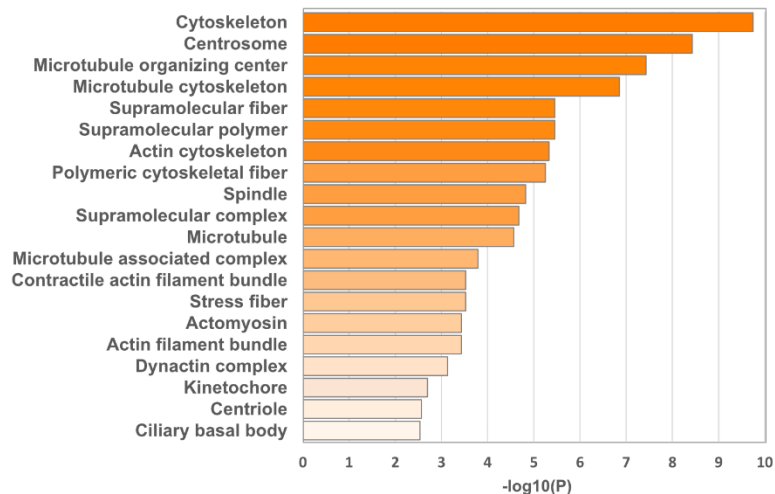
Figure R21. The interactome of mitochondria targeted NINL fragments contains proteins potentially involved in MTOC formation.

(A) Dot Plot analysis of the common hits between NINL-Nt (Nt) and NINL 1-442 (442). Two biological replicates were performed and plotted (1_, 2_) with three technical replicates each. Mass spectrometry data based on intensities was analysed with MaxQuant software (MQq). Hits are ranked based on average intensities. All the hits have an BDFR ≤ 0.02 . Average intensities, relative intensities, BDFR and if the hit was previously reported, are indicated. Dot Plot graph was generated with ProHits. (B) Network clustering of all hits common between NINL-Nt and NINL 1-442. Only physical interactions reported in BioGRID are shown (orange lines). Network clustering was built with esyN software.

After discarding the bait proteins, we were left with 19 candidates. We were excited to find CKAP5 and NEDD1 in this list, which confirmed our previous results, where we had detected these proteins at ectopic MTOCs by IF microscopy. As a matter of fact, CKAP5 was the most enriched hit in our dot plot analysis. We were also aware that we did not detect any of the γ TuRC core subunits in our shared hits analysis

(but detected GCP2 as a hit in one of the replicates of NINL 1-702). An explanation may be that the amount of γ TuRC necessary to induce the formation of an ectopic MTOC is relatively low and thus below our detection limit. However, we robustly identified NEDD1, the main γ TuRC targeting factor. Thus, a more likely explanation may be that NINL fragments interact with γ TuRC through NEDD1 and that the distance between γ TuRC core subunits and the BirA-tagged NINL fragments is beyond the reach of the BirA ligase.

Another hit, CEP170, we had also previously found as an interactor of NINL fragments by immunoprecipitation (**Figure R15 and Figure R16**). Among the remaining candidates were components of the dynein-dynactin complex, such as DYNC1LI1 and DCTN2, that were also previously identified as NINL interactors (Casenghi, 2005; Gupta, 2015; Redwine, 2017). Another interesting protein that was highly enriched in our analysis was MAP7D3, a microtubule-associated protein described to be involved in microtubule assembly and polymerization (Sun, 2011; Yadav, 2014).

A**GO Biological Process****B****GO Cellular component****Figure R22. GO analyses reveal that NINL interactome is related to microtubules and microtubule-associated processes.**

(A) GO Biological Process (BP) analysis of the 20 common hits between NINL-Nt and NINL 1-442. Only the 20 first components are shown based on P-values. P-value cut-off ≤ 0.05 . P-values are displayed as $-\log_{10}(P)$. Most enriched BP is “Cytoskeleton”. Data was generated with ShinyGO software and then plotted in Excel. (B) GO Cellular Component (CC) analysis of the 20 common hits between NINL-Nt and NINL 1-442. Only the 20 first components are shown based on P-values. P-value cut-off ≤ 0.05 . P-values are displayed as $-\log_{10}(P)$. Most enriched CC is “Ciliary basal body-plasma membrane docking”. Data was generated with ShinyGO software and then plotted in Excel.

Requirements for CM1- and NINL fragment-induced ectopic MTOCs

Following the results presented in **Chapter 1** and **Chapter 2**, we hypothesized that in order to generate an ectopic MTOC, NINL 1-442 should require at least two additional components, the nucleator γ TuRC including its targeting factor NEDD1, and the microtubule polymerase CKAP5. To test this, we depleted these proteins by RNAi and analysed whether they had an impact on ectopic MTOC formation. In parallel, we performed this analysis also for CM1-induced ectopic MTOCs, in order to understand whether CM1- and NINL fragment-induced MTOCs differ in their requirements.

NINL fragment- and CM1-induced ectopic MTOC depend on γ TuRC

First, we addressed if ectopic MTOC formation was γ TuRC-dependent. The γ TuRC is the main microtubule nucleator in human cells and in our mitochondrial-targeting assays it was recruited to mitochondria after CM1 and NINL 1-442 targeting (**Figure R2, Figure R3 and Figure R12**). It was described by our laboratory that depletion of the core subunit GCP2 efficiently disrupts γ TuRC (Cota, 2017). Hence, we knocked-down GCP2 by siRNA and analysed microtubule nucleation at mitochondria, as a readout of MTOC formation capacity (**Figure R23**).

Western blotting showed that the depletion of GCP2 was efficient (**Figure R23, WB**) and IF analysis of the negative control cells expressing GFP-Mito (**Figure R23**) revealed reduced microtubule nucleation from the centrosome, confirming efficient inhibition of γ TuRC. Importantly, we could also measure a significant reduction of more than 50% in microtubule nucleation activity at mitochondria after GCP2 depletion in cells expressing GFP-CM1-Mito or GFP-NINL 1-442-Mito. This result indicates that MTOC assembly by CM1 and NINL 1-442 requires γ TuRC.

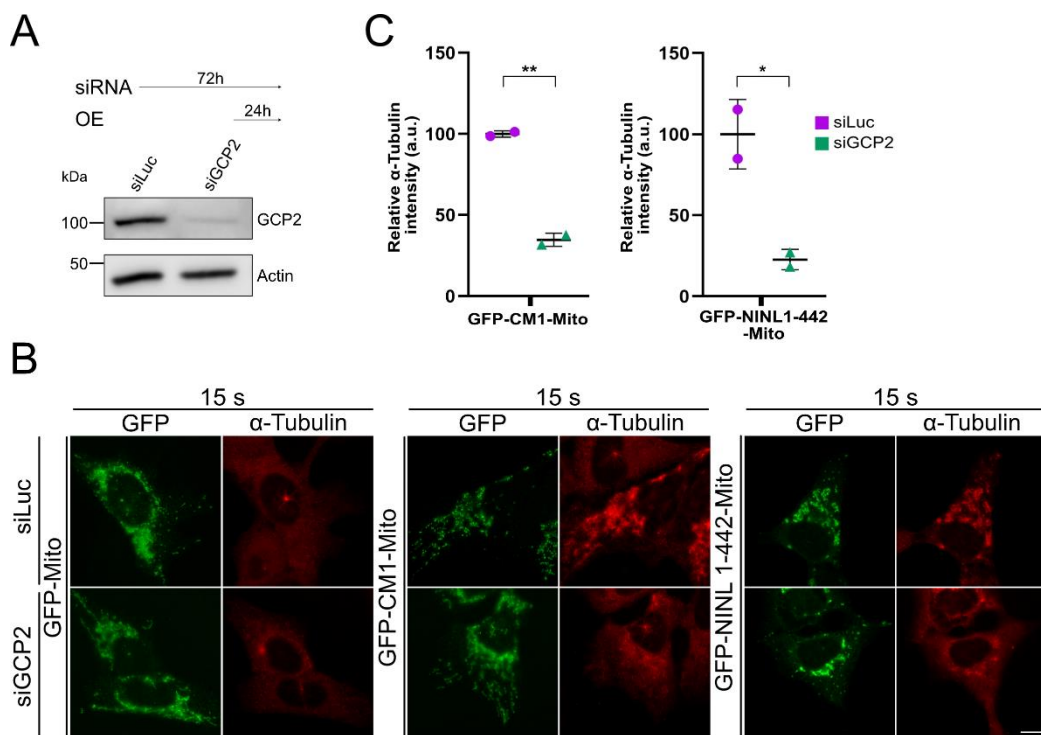


Figure R23. GCP2 depletion dramatically reduces microtubule nucleation capacity of CM1- and NINL 1-442-induced ectopic MTOCs

(A) WB analysis of GCP2 siRNA efficiency. Cells were silenced for 72 hours by transfection with the indicated siRNA and mitochondria-targeted constructs were transfected 48 hours after siRNA transfection. Luciferase siRNA was used as a control. Actin was used as a loading control. (B) Representative IF images of GFP, CM1 and NINL-Nt targeted to mitochondria. Ice cold treatment was used in this experiment and cells were imaged after microtubule regrowth (15 s). Scale bar: 10 μ m. (C) Quantification of the relative α -tubulin intensity at mitochondria after 15 seconds of regrowth. A significant reduction in the microtubule nucleation capacity of more than 50% can be observed after GCP2 depletion in both CM1 and NINL 1-442 expressing cells. 20 cells were counted per condition in 2 independent experiments (40 cells in total). Statistical significance was determined using an unpaired parametric t-test. ** ($p < 0.005$). * ($p < 0.05$).

NEDD1 is required for NINL 1-442-induced but not CM1-induced MTOCs.

If the microtubule nucleator γ TuRC is required to build a functional MTOC, is the targeting factor NEDD1 also required? To answer this question, we depleted NEDD1, which was present when either CM1 or NINL 1-442 were targeted to mitochondria (Figure R5). We were surprised to find that only NINL 1-442 was

dependent on NEDD1 to build a functional MTOC, with a ~50% reduction in its microtubule nucleation capacity, whereas the activity of the CM1-induced MTOC was unaltered (**Figure R24**). Therefore, CM1 and NINL do not seem to employ the same mechanism for γ TuRC recruitment, the former being NEDD1-independent and the latter NEDD1-dependent.

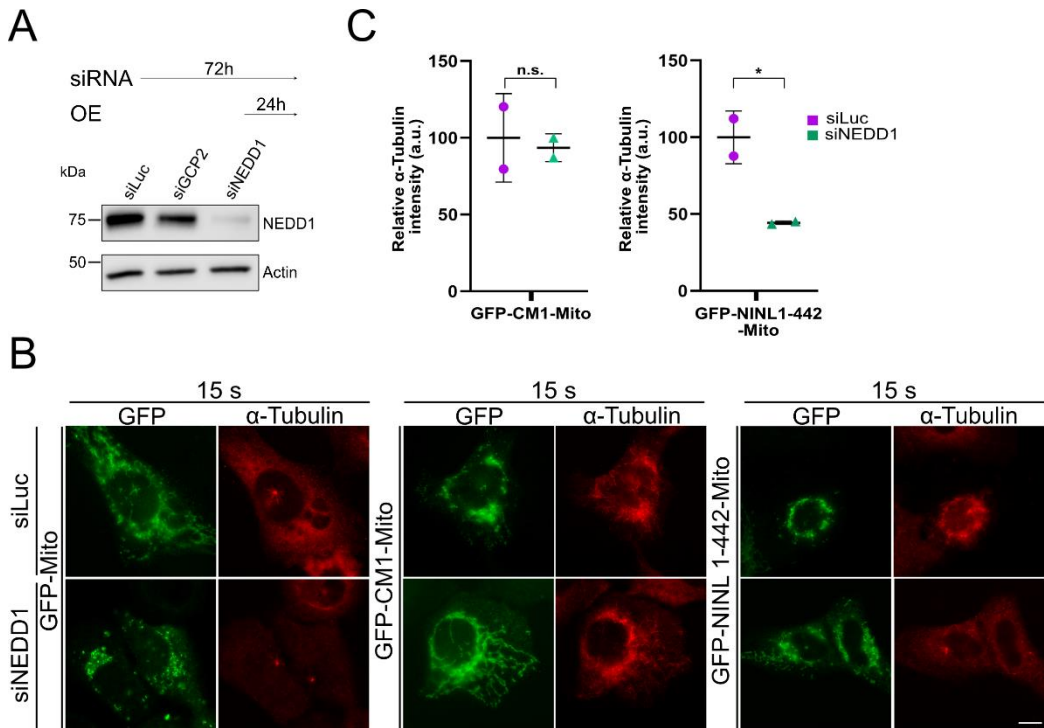


Figure R24. NEDD1 depletion reduces microtubule nucleation capacity of the NINL 1-442-induced MTOC

(A) WB analysis of NEDD1 siRNA efficiency. Cells were silenced for 72 hours by transfection with the indicated siRNA and mitochondria-targeted constructs were transfected 48 hours after siRNA transfection. Luciferase siRNA was used as a control. Actin was used as a loading control. siGCP2 was used as a control of NEDD1 expression levels being independent of GCP2. (B) Representative IF images of GFP, CM1 and NINL-Nt targeted to mitochondria. Ice cold treatment was used in this experiment and cells were imaged after microtubule regrowth (15 s). Scale bar: 10 μ m. (C) Quantification of the relative α -tubulin intensity from the outer surface of the mitochondria after 15" seconds of regrowth. A significant reduction in the microtubule nucleation capacity of more than 50% can be observed after NEDD1 depletion only in NINL 1-442. 20 cells were counted per condition in 2 independent experiments (40 cells in total). Statistical significance was determined using an unpaired parametric t-test. * ($p < 0.05$). n.s. (non-significant).

CKAP5 is required for NINL 1-442-induced but not CM1-induced MTOCs.

As CKAP5 was detected at the mitochondria when targeting either CM1 or NINL 1-442, in the presence or absence of microtubules (**Figure R8**), we also tested the requirement for CKAP5 by siRNA (**Figure R25**). The results were similar to the depletion of NEDD1, NINL 1-442-induced MTOC nucleation capacity was strongly reduced (~75% reduction), while CM1-induced MTOC nucleation capacity was unchanged.

Altogether, this reveals that CM1 and NINL are both able to build functional MTOCs that depend on γ TuRC, but their molecular requirements are different. CM1 seemed to rely only on γ TuRC, whereas NINL 1-442 additionally required the γ TuRC targeting factor NEDD1 and the microtubule growth promoting factor CKAP5.

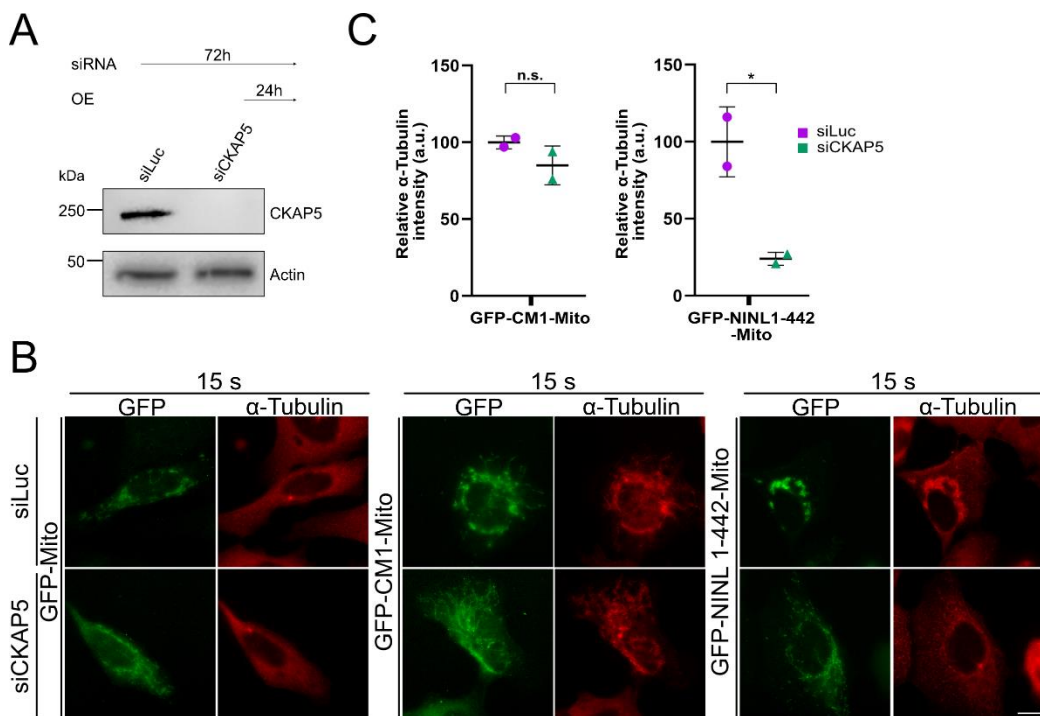


Figure R25. CKAP5 depletion impairs microtubule nucleation capacity of the NINL 1-442-induced MTOC.

(**A**) WB analysis of CKAP5 siRNA efficiency. Cells were silenced for 72 hours by transfection with the indicated siRNA and mitochondria-targeted constructs were transfected 48 hours after siRNA transfection. Luciferase siRNA was used as a control. Actin was used as a loading control. (**B**) Representative IF images of GFP, CM1 and NINL 1-442 targeted to the mitochondria in U2OS cells. Ice cold treatment was used in this experiment

and cells were imaged after microtubule regrowth (15 s). Scale bar: 10 μm . **(C)** Quantification of the relative α -tubulin intensity from the outer surface of the mitochondria after 15'' seconds of regrowth. A significant reduction in the microtubule nucleation capacity up to a 75% can be observed after CKAP5 depletion only in NINL 1-442. 20 cells were counted per condition in 2 independent experiments (40 cells in total). Statistical significance was determined using an unpaired parametric t-test * ($p < 0.05$). n.s. (non-significant).

Chapter 3

NINL and phase separation

Joel Paz¹, Cristina Lacasa¹, Fabian Zimmermann¹, Mireia Pesarrodonà¹, Nick Berrow¹, Xavier Salvatella¹, Jens Lüders¹

¹Institute for Research in Biomedicine (IRB Barcelona), The Barcelona Institute of Science and Technology (BIST), 08028 Barcelona, Spain

Statement of contribution:

Joel Paz designed, performed and analysed all of the experiments in this chapter.

Cristina Lacasa and Fabian Zimmermann purified the NINL constructs used in Figure R27 and R28

Mireia Pesarrodon and Joel Paz performed the experiments shown in Figure R27 and R28.

Nick Berrow generated all the NINL mutants used in Figure R30.

Mireia Pesarrodon and Xavier Salvatella helped with the design and supervision of the experiments related to phase separation.

Jens Lüders supervised the project.

We have shown consistently that NINL 1-442 has the capacity of generating a functional MTOC when targeted to the surface of mitochondria. Moreover, this MTOC seems to further depend on γ TuRC, NEDD1 and CKAP5. We wondered what the precise function of NINL 1-442 in this process was. One possibility was that it merely served as a scaffold for the other factors. Alternatively, NINL 1-442 may have a more active role. In 2017, it was published that recombinant *C. elegans* SPD-5, a centrosomal scaffold protein that is also described as functional homolog of CDK5RAP2, has the ability to generate an MTOC *in vitro*. At a certain concentration SPD-5 undergoes phase separation and SPD-5 condensates recruit other centrosomal proteins that cooperate to induce microtubule nucleation (Woodruff, 2017). Remarkably, early studies of NINL showed that overexpression of this protein in cells induces aggregate-like structures that in some cases resemble intracellular droplets (Casenghi, 2003). We wondered whether the role of NINL in MTOC assembly may also involve phase separation.

NINL overexpression generates aberrant structures in cells.

Our first goal with the following experiments was to reproduce published data related to NINL overexpression in cells (Casenghi, 2003). We tested three different constructs, GFP-tagged full-length NINL, its N-terminal half, NINL-Nt (1-702), and the C-terminal half, NINL-Ct (703-1382) by overexpression in U2OS cells. Afterwards, we analysed cells for the presence of any cytoplasmic assemblies and whether these recruited γ -tubulin and were able to induce microtubule nucleation (similar to the analyses with mitochondria-targeted constructs) (**Figure R26**). Localization was analysed in the absence of microtubules, to prevent microtubule-mediated localization (data not shown). Even without microtubules, full-length NINL was mainly targeted to the centrosome, where is formed a big cluster that recruited additional γ -tubulin and resulted in enhanced microtubule nucleation from the centrosomal area (**Figure R26**). In some cases, additional protein clusters could be detected in the cytoplasm. Interestingly, NINL-Nt and NINL-Ct were not concentrated around the centrosomal area and both formed droplet-like structures throughout the cytoplasm. NINL-Ct structures were generally bigger and less abundant than NINL-Nt structures, which ranged from very small to medium size droplet-like structures. Moreover, NINL-Nt “droplets” also recruited γ -tubulin and were active in the generation of new microtubules, acting as “mini-MTOCs” (**Figure R26**). NINL-Ct did not share these properties (**Figure R26**).

Notably, the NINL-Nt structures were not dispersed in the presence of nocodazole (data not shown), suggesting that in contrast to the clustering of mitochondria

(**Figure R1**), the droplet-like structures observed in this experiment are caused by a dynein-independent mechanism.

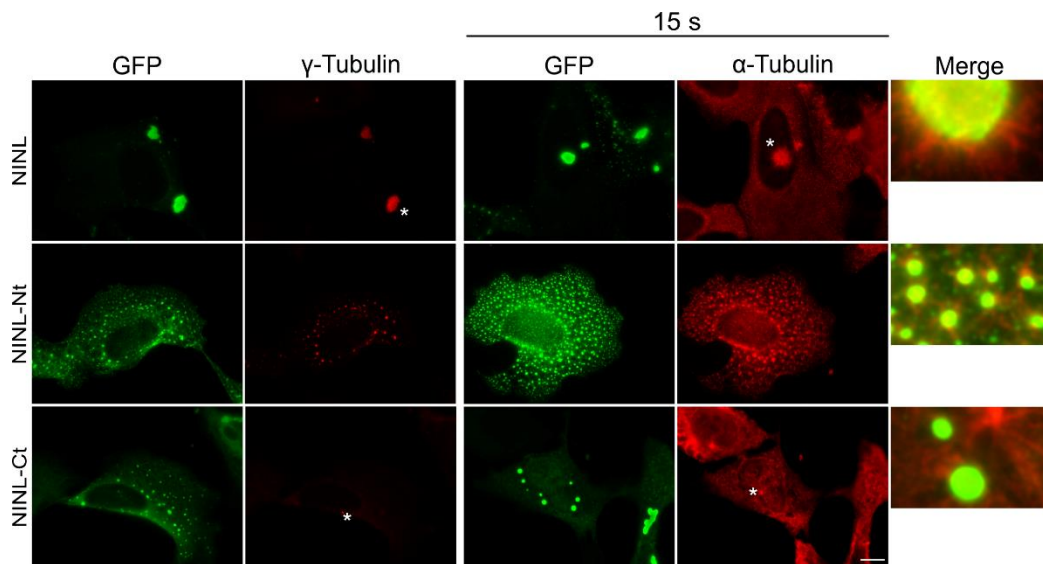


Figure R26. NINL and NINL-Nt generate aberrant structures that recruit γ -tubulin and nucleate microtubules.

Representative IF images of the NINL truncations expressed in U2OS cells. Ice cold treatment was used in this experiment and cells were imaged in the absence of microtubule (γ -Tubulin) or after microtubule regrowth (15 s). Insets of merge images are shown (Merge column). γ TuRC recruitment as well as microtubule nucleation were detected in both NINL and NINL-Nt, from the centrosome and from the “droplets”, respectively. Asterisks indicate centrosomal signal. Scale bar: 10 μ m.

GST-tagged NINL-Nt and NINL 1-287 phase-separate *in vitro*

To determine if the intracellular structures induced by NINL fragments may be a product of LLPS, we tested whether these could also be generated *in vitro* from recombinant proteins. *In vitro* analyses are generally a more straightforward approach to understand if a protein undergoes LLPS, as the protein can be isolated and studied outside the cellular complexity. Since the ability to form an ectopic MTOC seemed to be linked to the N-terminal half, we focused on this part of NINL. Apart from NINL-Nt, we also decided to test NINL 1-287 (minimal fragment able to recruit γ TuRC to mitochondria, **Figure R12**), since it was not able to build a functional MTOC and did not form any type of “droplets” in cells (data not shown). Both NINL fragments were individually expressed in bacteria with a Histidine- and a GST-

tag. The proteins were purified and then mixed in a buffer containing Ficoll, a crowding agent that mimics the cytoplasmic density and is commonly used in phase separation experiments (Zimmerman, 1993; van den Berg, 1999). A drop of this mixture was added to a slide and imaged by differential interference contrast (DIC) microscopy, which allows for visualization without the need of a fluorophore. We used two different concentrations of each protein to test whether the amount of protein could have an effect on LLPS. Indeed, we could observe that both proteins formed condensates *in vitro* (Figure R27). In the case of NINL-Nt this was consistent with our and previously published observations in cells (Casenghi, 2003), but we were surprised to find that at a certain concentration, NINL 1-287 also underwent phase separation.

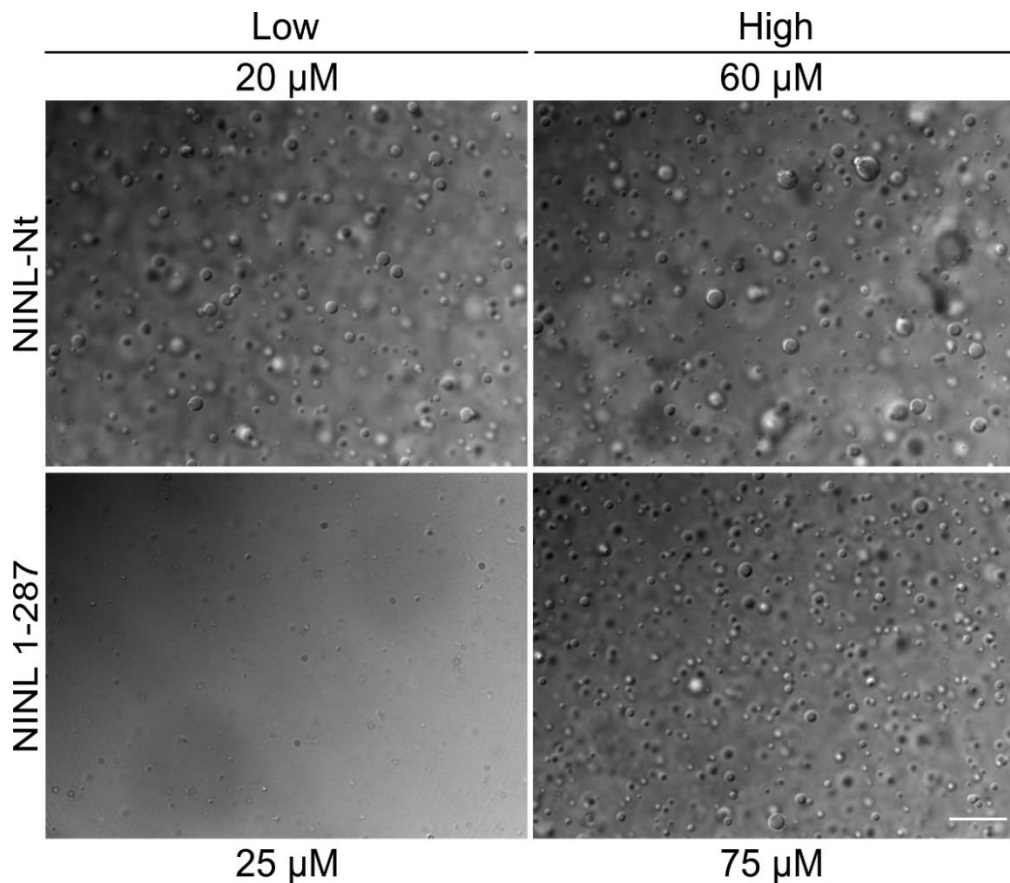


Figure R27. GST-NINL-Nt and GST-NINL 1-287 undergo phase separation *in vitro*.

Representative DIC images of the purified GST-NINL constructs. 10% Ficoll was used for every condition. Two different concentrations of each purified protein were tested, Low and High. At low concentrations, only NINL-Nt phase separates. At higher concentrations, both constructs phase separate. Scale bar: 0.8 μm.

GFP-tagging induces aggregation of NINL-Nt, whereas NINL 1-442 and NINL 1-287 phase-separate *in vitro*

The previous result highlighted the capacity of NINL to undergo phase separation. To explore this further, we generated additional NINL constructs tagged with GFP. The reasoning behind this was that we could also use fluorescence microscopy to observe the condensates. Later on, this would also allow to additionally include fluorescently labelled tubulin, to analyse the ability of NINL fragment condensates to promote microtubule nucleation *in vitro*. We also cloned the minimal NINL fragment that was necessary for MTOC formation in cells, NINL 1-442, to study its phase separation properties. In contrast to NINL-Nt, but similar to NINL 1-287, NINL 1-442 expressed in cells did not form any type of droplet (data not shown). The experiment was conducted in the same way as before, but images were analysed with a confocal fluorescence microscope. In contrast to what we observed with the His-GST tagged protein, GFP-NINL-Nt appeared to generate some sort of aggregates, even at concentrations lower than those previously used (**Figure R28**). We do not have an explanation for this phenomenon, but it is possible that the tag has an influence on the properties of the protein, either on the stability after purification or on the folding. Interestingly, we could appreciate that both NINL 1-442 and NINL 1-287 formed condensates *in vitro* (**Figure R28**). Condensates formed by NINL 1-287 were bigger in size than the ones produced by NINL 1-442.

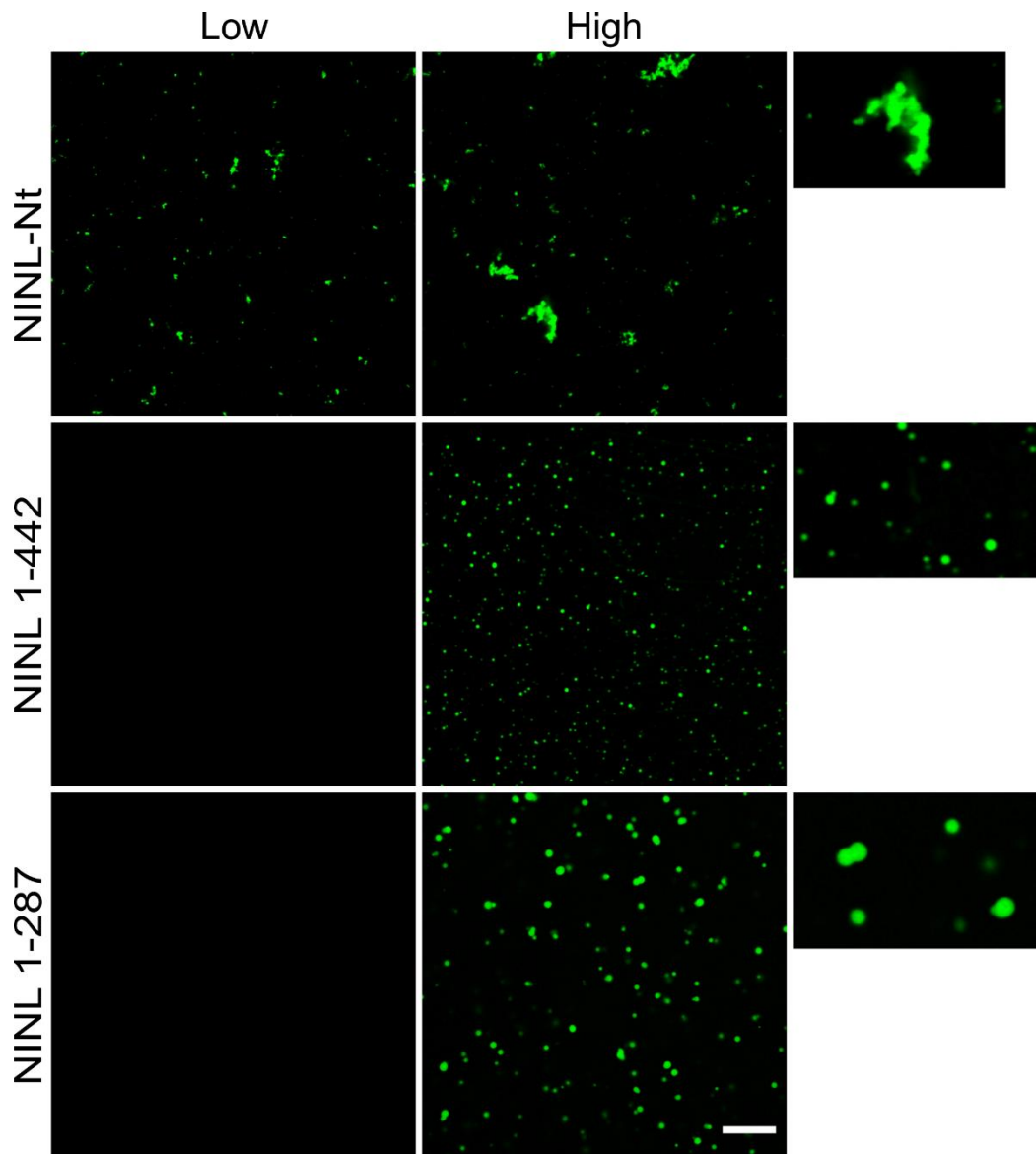


Figure R28. GFP-NINL 1-442 and GFP-NINL 1-287 undergo phase separation *in vitro* while GFP-NINL-Nt has tendency to protein aggregation.

Representative confocal microscopy images of the purified GFP-tagged constructs. 20% Ficoll was used for every condition. Two different concentrations of each purified protein were tested. All constructs, Low concentration = 15 μ M. NINL-Nt, High concentration = 20 μ M. NINL 1-442 and NINL 1-287, High concentration = 50 μ M. Scale bar: 10 μ m.

Disruption of the coiled-coil domains in NINL-Nt impairs droplet formation whereas disruption of aromaticity leads to aggregation in cells

The results of the *in vitro* experiments suggested that NINL fragment behaviour regarding droplet formation and formation of irregular aggregates were closely related. The first 4 EF-Hands of NINL are contained within amino acids 1-287. The region from amino acids 288-702 comprises all three coiled-coil domains, and NINL fragments containing the entire or part of the coiled-coil region showed mixed tendencies between phase separation and aggregation *in vitro* (in particular NINL-Nt). Coiled-coils have been postulated as important regions involved in LLPS (Vega, 2019; Newton, 2021), but in our case, NINL 1-287, which lacks any coiled coil region, also formed condensates, at least *in vitro*. What is the property then that induces phase separation in this region? As NINL was able to induce phase separation on its own, that implied that only discrete oligomerization of NINL was required to achieve condensate formation. This is a typical phenotype of proteins that contain intrinsically disordered regions (IDRs) (Borchers, 2021). Therefore, we speculated that there could be several disordered regions in within NINL. Indeed, computational prediction of the IDRs present in NINL revealed that most of the protein had tendency to be disordered, with exception of the regions where coiled-coil domains were (**Figure R29**). Similar to how two distinct proteins can interact and this can mediate phase separation, the IDRs in within a protein can mediate homotypic interactions (e.g. to induce oligomerization). This can be computationally studied in a model of “stickers” and “spacers” (Harmon, 2017), where “stickers” are the adhesive regions of the protein that mediate the intermolecular interactions, and at the same time the spaces (“spacers”) in between these “stickers” should be taking into account. As IDRs can serve as “stickers”, it is important to maintain this framework of “stickers” and “spacers” in within a protein to preserve its properties (Borchers, 2021). Interestingly, it has been described that this framework can be altered by modulating the aromatic residues within a protein, is this is directly related to its phase separation properties (Holehouse, 2015; Wang, 2018; Martin, 2020). Therefore, we asked whether the coiled-coil domains or the aromaticity were the main drivers of condensate formation of NINL. To achieve this goal, we generated two types of mutants.

- Coiled-coil mutants: we designed mutants where we disrupted the coiled-coils in NINL-Nt. In particular, we designed helix breaking-mutants, that are known to disrupt the coiled-coil domains without altering hydrophobicity. To achieve this, positions “P” in the helices were mutated to prolines (Li, 1996; Truebestein, 2016). This resulted in two mutants, NINL-Nt 12P (12

proline mutations in total) and NINL-Nt 16P (12 proline mutations of 12P mutant plus 4 extra proline mutations). It is important to comment that all the mutations were located in the second and third coiled-coil domain of NINL. We chose to keep the first coiled-coil intact as we had seen that it was important for MTOC formation (it is present in the minimally required fragment, NINL 1-442). Also, as mentioned before, NINL 1-442 did not produce any droplet structures when overexpressed in cells (data not shown).

- Aromaticity mutants: aromatic residues present in NINL-Nt were mutated to alanine, avoiding “a” and “d” positions of the helices to keep coiled-coils unperturbed. Two mutants were designed, NINL-Nt 11A (11 mutations in total) and NINL-Nt 22A (11 alanine mutations of 11A mutant plus 11 extra proline mutations).

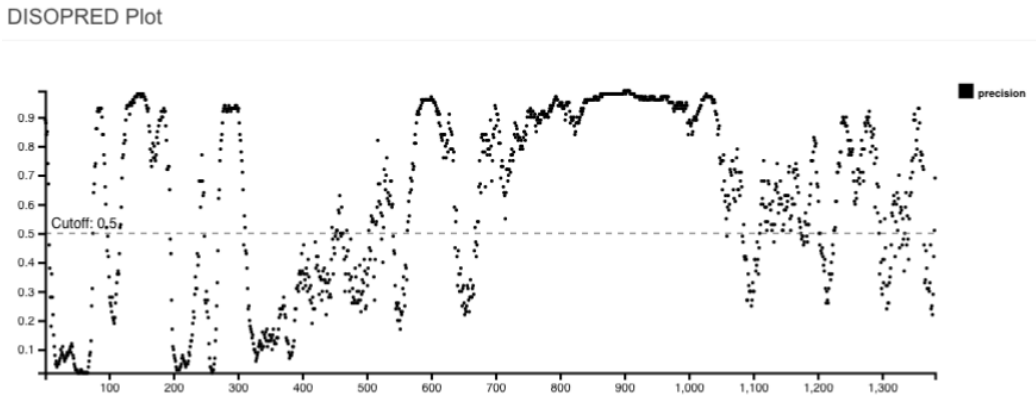


Figure R29. IDRs prediction of NINL structure.

DISOPRED plot showing the predicted IDRs from full-length NINL. x-Axis indicates amino acid position. y-Axis indicates precision of prediction. To consider a region as IDR the cut-off has to exceed 0.5. As it can be observed, most of the protein is predicted to be disordered less the region that comprehend the coiled-coil domains (between aa 350-700).

Once the mutants were synthesized, they were transfected into U2OS cells and the formation of aberrant structures was analysed (**Figure R30**). In contrast to NINL - Nt, both the 12P and 16P mutants with disrupted coiled-coils, did not display any type of droplet formation in cells, instead the signal was diffuse throughout the cytoplasm. This result implies that the coiled-coils in NINL promote droplet formation in cells. Curiously, in some cells we were able to detect signal coming from an area that resembled the centrosome (**Figure R30**, Inset of NINL-Nt 12P). It is possible then that NINL has a centrosomal localization domain in its N-terminal half. A double staining with a centrosomal marker would be needed to test this

hypothesis. The first mutant with reduced aromaticity, NINL-Nt 11A, showed in most of the cells a diffuse distribution all over the cytoplasm, but in some cells we could still appreciate small droplets (**Figure R30**, Inset of NINL-Nt 11A). In contrast, mutant NINL-Nt 22A did not form any droplets. Instead, we observed massive, irregularly shaped structures in most cells, reminiscent of protein aggregation. In summary, it seems that droplet formation in cells involves both coiled-coils and aromaticity. Coiled-coils are required to generate droplets (**Figure R30**, NINL-Nt 12P and 16P). However, if aromaticity is reduced, the coiled-coil domains may drive protein aggregation instead (**Figure R30**, NINL-Nt 22A). Based on these properties, it is tempting to speculate that MTOC formation could be somehow linked to phase separation.

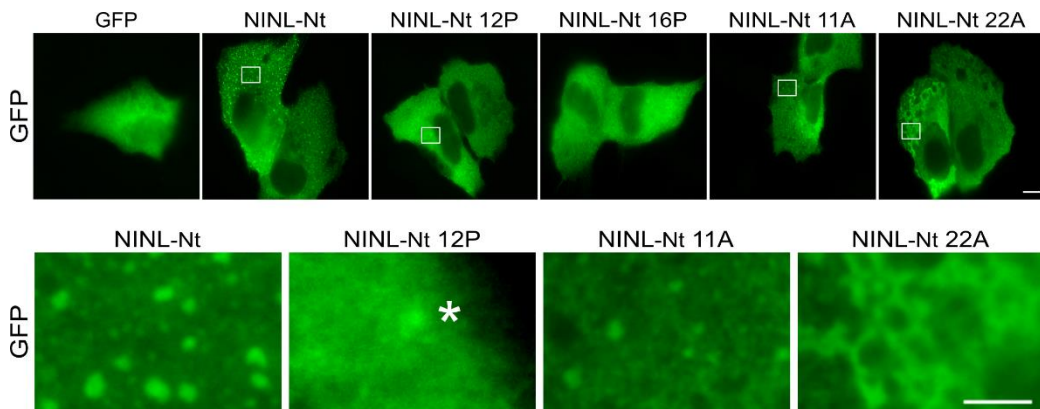


Figure R30. NINL-Nt mutants reveal an important interplay between aromatic residues and coiled-coil domains within NINL.

Representative IF images of the GFP-NINL-Nt mutants expressed in U2OS cells. A GFP antibody was used to analyse the overexpression products. Insets of the most representative mutants are shown (white rectangles). Notice that NINL-Nt 12P seems to have centrosomal localization and NINL-Nt 22A structures resemble aggregates. Asterisks indicate centrosomal signal. Scale bar upper row: 10 μm . Scale bar insets: 2.5 μm .

Chapter 4

Dissection of the role of NINL at the centrosome

Joel Paz¹, Cristina Lacasa¹, Aamir Ali¹, Chithran Vineethakumari¹, Unitat d'Experimentació Animal de Farmàcia², Jens Lüders¹

¹Institute for Research in Biomedicine (IRB Barcelona), The Barcelona Institute of Science and Technology (BIST), 08028 Barcelona, Spain

²Facultat de Farmàcia i Ciències de l'Alimentació, Universitat de Barcelona (UB), 08028 Barcelona, Spain

Statement of contribution:

Joel Paz designed, performed and analysed all of the experiments in this chapter except Figure R36.

Cristina Lacasa and Joel Paz in collaboration with Unitat d'Experimentació Animal de Farmàcia, generated the NINL antibody.

Aamir Ali designed, performed and analysed the experiment shown in Figure R36.

Chithran Vineethakumari reproduced the observations from figures R31, R32, R37 and R38 and is continuing the project.

Jens Lüders supervised the project.

In Chapters 1 and 2 we have shown that targeting of N-terminal NINL fragments to the outer surface of mitochondria allows ectopic MTOC formation and that ectopic MTOC activity requires the γ TuRC, NEDD1, and CKAP5. In addition, in Chapter 3 we have analysed the propensity of N-terminal NINL fragments to phase-separate *in vitro* and form droplets in cells. Since these analyses were all based on assays under non-physiological conditions, in this chapter we tried to address the question of how these findings may relate to the physiological role of NINL at the centrosome.

NINL localizes to SDAs

It was already reported almost 20 years ago that NINL localizes to the centrosome (Casenghi, 2003) and is preferentially associated with one of the centrioles (Casenghi, 2003; Casenghi, 2005; Rapley, 2005). However, the available imaging tools and specific markers at the time were limited and no further characterization of NINL's specific centrosomal localization, for example by electron microscopy, was performed. NIN is a protein that has been studied more extensively and by immunogold electron microscopy was localized to the SDAs of the centrosome (Mogensen, 2000). Due to their similarity, it was hypothesized that NINL should also localize to SDAs. To address this, we generated a stable cell line expressing low levels of GFP-NINL. As shown in Chapter 3, overexpression of NINL generates a large centrosomal cluster of NINL protein without any specific localization (**Figure R26**). We discovered that this aberrant expression of NINL was toxic to cells and only cells that were expressing low levels of GFP-NINL could survive. To study NINL localization in more detail, we used SIM for increased resolution, and included anti-centrin antibodies to mark the distal part of centrioles, and anti-CEP170 antibodies to mark SDAs. IF images showed that GFP-NINL partially co-localized with CEP170 at SDAs (**Figure R31**).

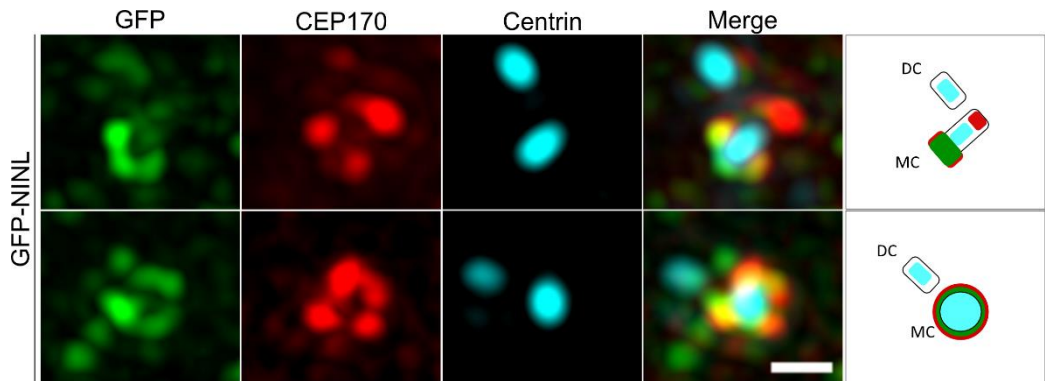


Figure R31. GFP-NINL localizes to SDAs.

Representative SIM images of a stable U2OS cell line expressing low levels of GFP-NINL. Images shown are maximum Z-projections. CEP170 was used as an SDA marker. Centrin was used as a distal-end centriole marker. The schematics depict the interpreted centriole orientation (last column). DC = Daughter centriole. MC = Mother centriole. Scale bar: 0.5 μm .

We then generated rabbit polyclonal antibodies against the N-terminal half of NINL. As we had already observed the localization of the tagged protein to SDAs, we used regular fluorescence microscopy. We were excited to find that endogenous NINL also partially colocalized with CEP170 at SDAs (**Figure R32**, IF panel). We corroborated that our homemade antibody was specific for NINL by WB, after depleting NINL by transfection of siRNA (**Figure R32**, WB).

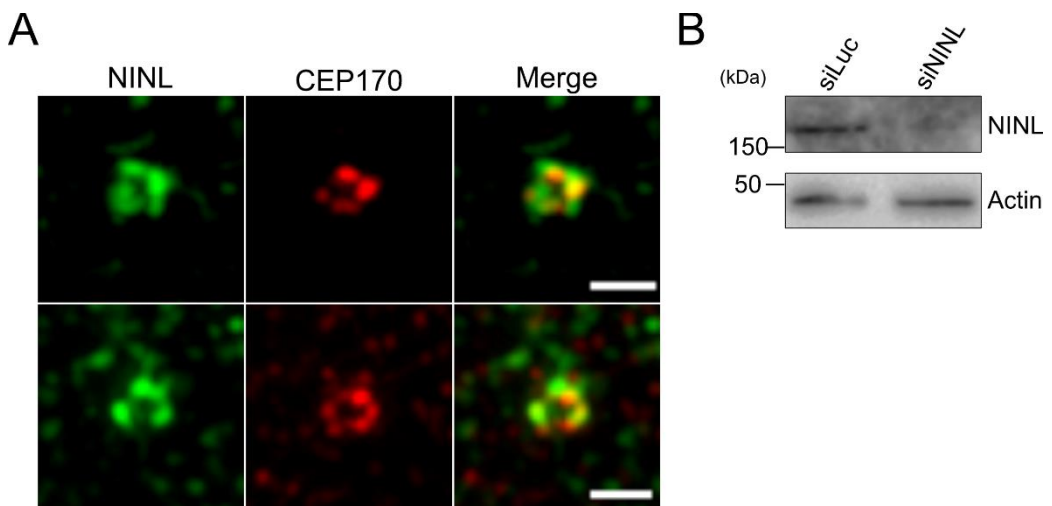


Figure R32. NINL localizes to SDAs.

(A) Representative IF images of U2OS cells expressing endogenous NINL. Images were deconvolved after maximum Z-projection. CEP170 was used as an SDA marker. Scale bar:

1 μm . **(B)** WB analysis of NINL siRNA efficiency. Cells were silenced for 72 hours with siNINL. Luciferase siRNA was used as a control. Actin was used as a loading control.

As a final remark, we have to emphasize on the low effectiveness of all the NINL siRNAs we tested. Even if we could detect many times the protein being reduced by WB (**Figure R32**), NINL levels at SDAs were still high by IF in most of the experiments. Therefore, we decided to focus into understanding NINL localization pattern, its hierarchy in respect to other SDA proteins and its possible functions at SDAs.

CEP170 depletion does not remove NINL from SDAs

Since NINL, NIN, and CEP170 all colocalized at SDAs, we wondered whether their localization is inter-dependent. First, we depleted CEP170 and tested whether NINL levels were reduced at SDAs (**Figure R33**). Although the data was not quantified, it was apparent that removal of CEP170 did not have an effect on NINL localization. This was not unexpected, since in our previous experiments we found that the two proteins only partially colocalized.

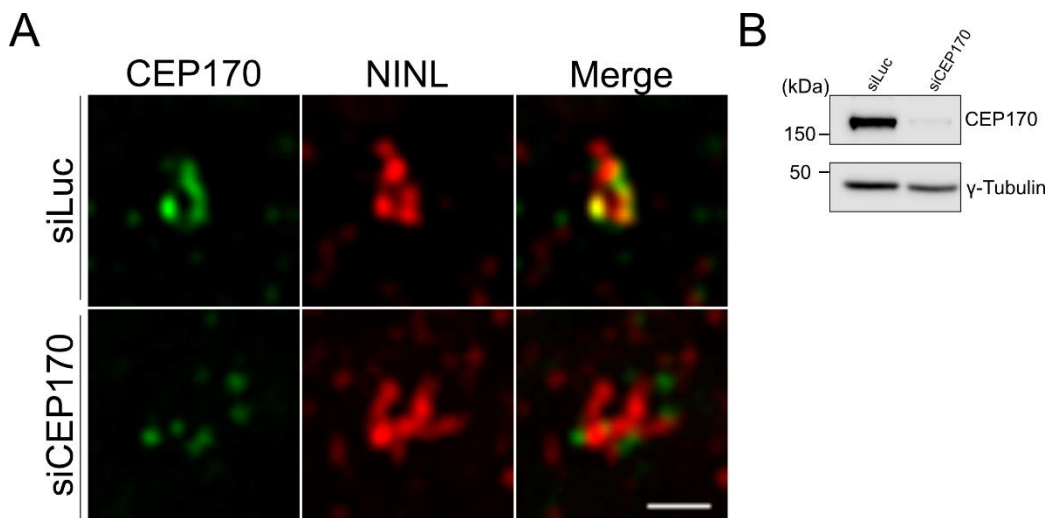


Figure 33. NINL localization to SDAs is CEP170-independent.

(A) Representative IF images of U2OS cells after CEP170 depletion. NINL signal was apparently unperturbed upon CEP170 depletion. Scale bar: 1 μm . **(B)** WB analysis of CEP170 siRNA efficiency. Cells were silenced for 72 hours with siCEP170. Luciferase siRNA was used as a control. γ -Tubulin was used as a loading control.

NINL localization to SDAs is NIN-independent

We next checked if NIN could have an influence on the localization of NINL to SDAs. IF images were taken after depleting NIN by siRNA and the localization of NINL was analysed (**Figure R34, A**). Similar to depletion of CEP170, NIN depletion did not have a clear effect on the localization of NINL to SDAs. At the same time, we also tested the effect of NIN depletion on CEP170, and we could confirm that removal of NIN from SDAs also displaces CEP170 (**Figure R34, B**), as described previously (Mazo, 2016).

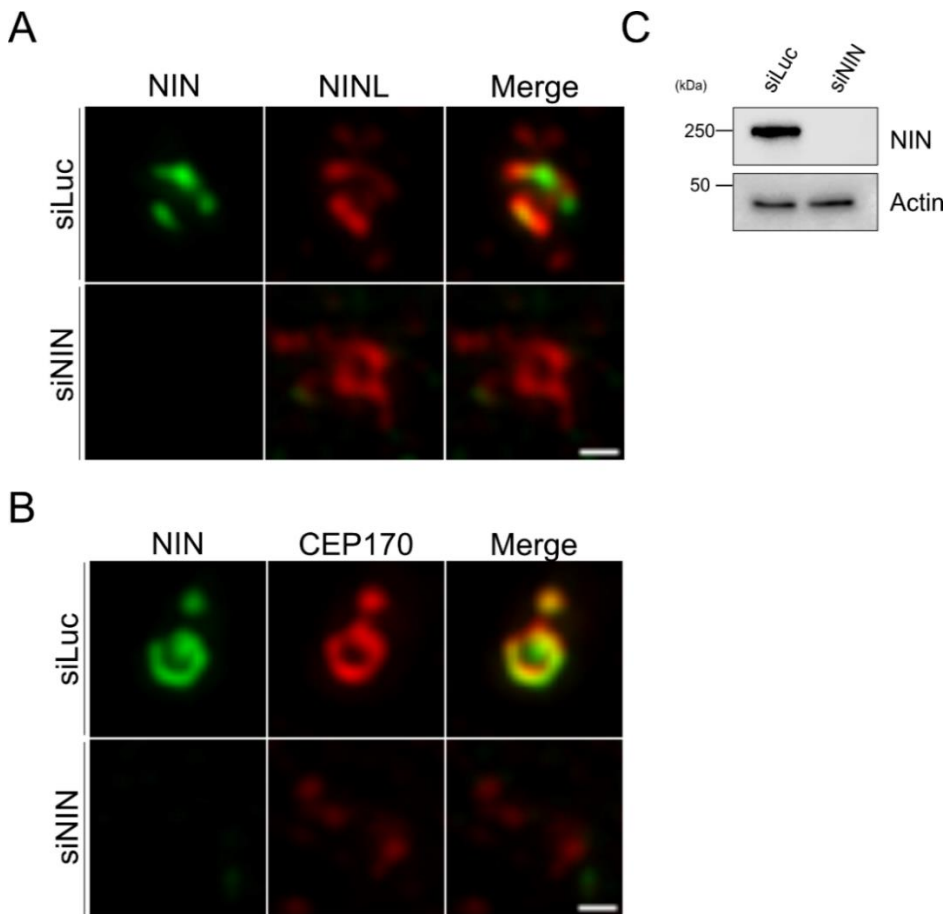


Figure R34. NIN depletion does not affect NINL but removes CEP170 from SDAs.

(A) Representative IF images of U2OS cells after NIN depletion. NINL signal was apparently unperturbed upon NIN depletion. Scale bar: 0.5 μ m. (B) Representative IF images of U2OS cells after NIN depletion. CEP170 signal was strongly reduced after NIN depletion. Scale bar: 0.5 μ m. (C) WB analysis of NIN siRNA efficiency. Cells were silenced for 72 hours with siNIN. Luciferase siRNA was used as a control. Actin was used as a loading control.

NINL depletion does not remove NIN from SDAs

Based on the previous results, NINL localization at SDAs did not require NIN. Therefore, NINL could be upstream of NIN in the SDA recruitment hierarchy or be associated with a different substructure within the SDAs. To distinguish between these possibilities, we next depleted NINL and tested localization of NIN. As shown in **Figure R35**, we could not detect any differences in the NIN levels after depleting NINL by siRNA. This experiment was only quantified once, but NIN localization was clearly unperturbed.

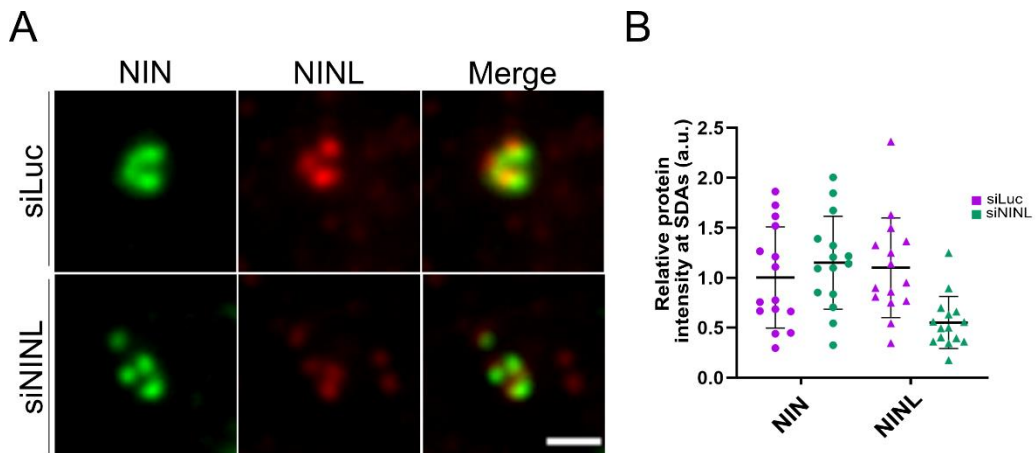


Figure R35. NIN localizes to SDAs after NINL depletion.

(A) Representative IF images of U2OS cells after NINL depletion. Cells were silenced for 72 hours with siNINL. NIN signal was apparently unperturbed upon NINL depletion. Scale bar: 1 μ m. (B) Preliminary quantification of the levels of NIN and NINL after NINL depletion. Relative protein intensity at SDAs was quantified. 15 cells per condition were counted in 1 experiment. NIN does not seem to be altered while NINL is clearly reduced (as seen by IF) after quantification.

NINL localization is CKAP5 dependent

Intriguingly, unpublished results from our laboratory had shown that CKAP5 localizes to both the PCM and SDAs. As described in the previous chapters, CKAP5 is key for NINL 1-442-induced ectopic MTOC formation. Additionally, it was a top hit in our NINL BioID interactome analysis. Thus, we were motivated to further investigate the relationship between these two proteins. Strikingly, we found that CKAP5 depletion had a strong effect on NINL localization to SDAs, where it was strongly reduced or absent (**Figure R36**).

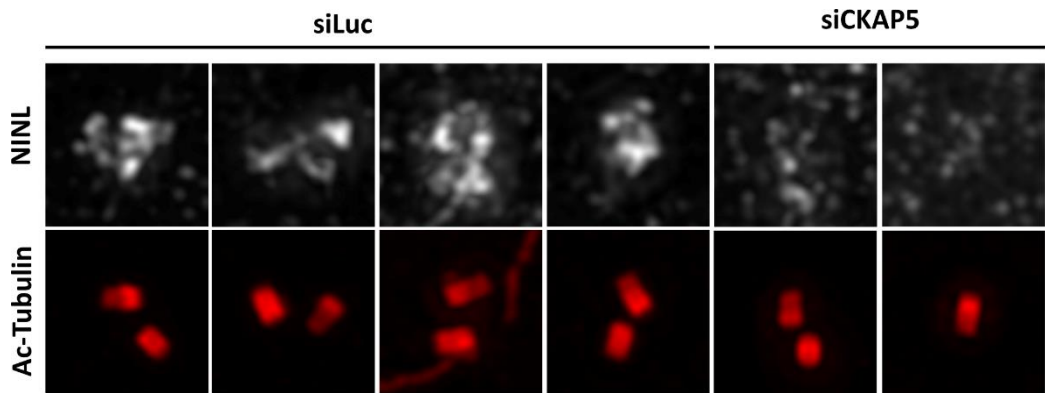


Figure R36. NINL is displaced from SDAs after CKAP5 depletion.

Representative SIM images of U2OS cells after CKAP5 depletion. Images shown are maximum Z-projections. Acetylated-Tubulin (Ac-Tubulin) was used as a centriole marker. NINL is displaced from centrosomes after CKAP5 depletion.

When exploring the localization pattern of NINL and CKAP5 at centrosomes, we noticed that in some cases we could observe spike-like structures extending outwards from SDAs, both in NINL and CKAP5 staining (**Figure R37**). These structures frequently co-localized (**Figure R37**, arrowheads).

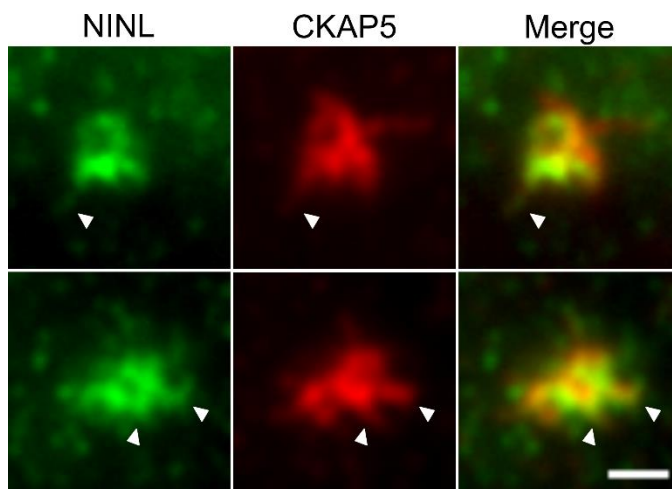


Figure R37. CKAP5 and NINL form spike-like structures that co-localize at SDAs.

Representative IF images of U2OS cells expressing endogenous NINL. Single planes from two different cells are shown. Microtubules were not depolymerized in this experiment. “Spikes” extending out from SDAs can be observed for both NINL and CKAP5 (arrowheads). Scale bar: 0.5 μm .

NINL partially co-localizes with microtubules that seem to be generated from SDAs

After observation of the “spikes” of NINL and CKAP5 emanating from the SDAs (**Figure R37**), we decided to check if these structures colocalized with microtubules. With the use of SIM and after performing a regrowth assay, we could identify that in particular early during regrowth these “spikes” co-localize with microtubules that appear to be nucleated from this area (**Figure 38**).

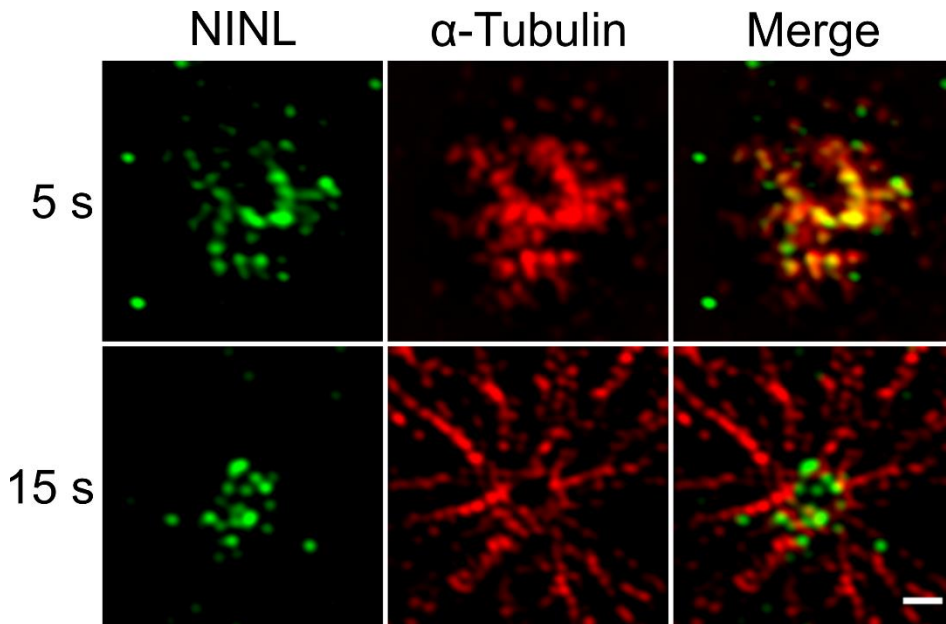


Figure R38. NINL forms spike-like structures that co-localize with microtubules early during regrowth.

Representative SIM images of U2OS cells expressing endogenous NINL. Single planes from two different cells at different microtubule regrowth timepoints (5 s, 15 s) are shown. “Spikes” coming out from SDAs can be observed in NINL case that partially co-localize with newly generated microtubules. Scale bar: 0.5 μ m.

Discussion

The mitochondrial targeting system

One of the first outcomes of this thesis, is the validation that the outer surface of mitochondria can serve as a site for ectopic MTOC assembly and for its functional analysis. While previous work has targeted the CM1 domain to this site (Chen, 2017), we have further explored the capacity of this system by targeting various different POI and testing their MTOC formation capacity (**Table R1**). Using microtubule regrowth assays, we were able to observe microtubule nucleation from the surface of mitochondria for several of the targeted constructs and the recruitment of several other centrosome or microtubule-associated proteins to this site (**Figures R2-R8 and Table R1**). These ectopic MTOCs could be induced not only by CM1 but also by other proteins and differed in composition, indicating that different types of MTOCs could be assembled.

While this system allows relatively rapid screening of candidate MTOC assembly factors, it is likely not suitable for a long-term analysis of ectopic MTOCs. We found that targeting proteins at the outer surface of mitochondria was toxic for cells after a few days of expression. For this reason, we expressed mitochondria-targeted proteins for a maximum of 48 hours.

It is interesting that microtubule nucleation from the ectopic site did not have any obvious inhibitory effect on centrosomal microtubule nucleation in most cases. As can be appreciated in many examples throughout the **Results** section, microtubule nucleation could be detected at the same time at mitochondria and at the centrosome within the same cell (e.g. **Figure R4**). Thus, the system provides an excellent approach to further explore crosstalk between different MTOCs, as recently observed between the centrosome and the Golgi (Wu, 2016; Gavilan, 2018). One case where we did detect a reduction in the centrosomal microtubule nucleation activity was mitochondria-targeted CKAP5-Ct (**Figure R10**). Assuming that not all of the recombinant protein is at mitochondria and since this construct lacks the tubulin and MT lattice-binding TOG domains but may retain γ TuRC or centrosome binding (Popov, 2001; Popov, 2002; Thawani, 2018) it is possible that it has a dominant-negative effect on microtubule nucleation. It is also worth commenting that we did not analyse in detail microtubules in a steady-state scenario, but only after complete microtubule depolymerisation and regrowth. It seemed, however, that at steady-state centrosomal microtubule organization was dominant (data not shown). This may indicate that the ectopic MTOC is not fully functional or that cells regulate microtubule organization to occur predominantly from centrosomes, if present.

As pointed out in the introduction, a multitude of proteins have been described to be involved in MTOC formation (Paz, 2018). In this thesis, we could not test all of these proteins in our system due to time and resource limitations. Proteins that remain to be tested as interesting candidates are, for example, AKAP9, myomegalin, NME7 or TACCs. We also did not test mitotic microtubule assembly factors, such as TPX2 or the augmin complex. Interestingly, a mitochondrial targeting approach was used recently to define the mitotic TACC3-clathrin network. By individually targeting these proteins to the mitochondria while cells were in mitosis, the authors could define TACC3 and clathrin as core proteins of a complex that is additionally composed of CKAP5 and GTSE1 (Ryan, 2021). Thus, targeting to the mitochondrial surface may as well be used to study MTOC assembly and nucleation during mitosis.

Another important centrosomal protein that remains to be further tested is PCNT, a scaffolding protein involved in the formation of the PCM and in γ TuRC recruitment (DICTENBERG, 1998) and, in the case of the yeast homolog Spc110, also characterised as an activator of microtubule nucleation (Lin, 2014). Previous work showed that PCNT assembled cytoplasmic MTOCs after eliminating centrosomes and Golgi MTOC activity (GAVILAN, 2018). Also, it was recently shown that overexpression of the middle region of PCNT induced some sort of condensates in cells that were sufficient to recruit γ TuRC and CKD5RAP2, and nucleate MTs, even though PCNT regions known to be involved in these functions were not present in this construct (JIANG, 2021). Considering these findings, we sought to test whether PCNT could promote ectopic MTOC assembly at mitochondria. We generated a GFP-PCNT-Mito construct lacking the PACT domain (centrosomal-targeting domain) (GILLINGHAM, 2000) but this was not targeted to mitochondria (checked with Tom20 antibody). Notably, the construct clustered around the centrosome and recruited γ TuRC, but we could not detect microtubule nucleation from these clusters (data not shown). This result suggests that PCNT may not be sufficient to generate an MTOC on its own. While we could not target PCNT lacking the PACT domain to mitochondria, we were able to target a smaller PCNT fragment, comprising the proposed CM1 and SPM motifs that were shown to be necessary for activation of microtubule nucleation in yeast (Lin, 2014). However, we detected neither γ TuRC recruitment nor microtubule nucleation at the mitochondria with this construct (data not shown). It is tempting to speculate then that the requirements for specific scaffolding proteins in MTOC formation and regulation may differ between organisms.

Is the ectopic nucleation site an MTOC?

Generally, an MTOC is composed of factors that ensure several important activities, namely, recruitment of γ TuRC, activation of γ TuRC, nucleation of microtubules, and microtubule anchoring (**Figure I7**). In this study, we have referred to the mitochondria-targeted assemblies as MTOCs, to avoid more complex terminology, although we did not demonstrate their anchoring capacity. We can conclude from our results that CM1, NINL-Nt and CKAP5, are capable of assembling microtubule-nucleating centres. This does not exclude that they may function as MTOCs. We did try to elucidate if these nucleation centres could anchor microtubules once they were generated at the outer surface of the mitochondria. We probed for CAMSAP2, a protein known to bind to free microtubule minus-ends after nucleation by γ TuRC and important for anchoring microtubules at the Golgi apparatus (Jiang, 2014; Wu, 2016). We were able to detect recruitment of CAMSAP2 when NINL-Nt was targeted to mitochondria, suggesting that some free minus ends may be present. Curiously, we could only detect this signal when NINL-Nt was clustered around the centrosome (prior to nocodazole treatment) and not after dispersion of the mitochondria (data not shown). Colocalization was not observed with NINL 1-442 (minimal nucleating construct that also did not cluster the mitochondria). We probed also for CAMSAP2 after targeting the CM1 from CDK5RAP2 but we could not detect any signal at the mitochondria (data not shown). It is possible that only in a case where the mitochondria are clustered the signal is strong enough to be detected, as in the case of NINL-Nt. Thus, we could not conclude if microtubule minus ends were bound by CAMSAP2 with this approach. We also tried to do live imaging of microtubules by imaging EB3 comets. EB3 is a +TIP protein (Nakagawa, 2000) commonly used to study growing microtubules (Stepanova, 2003). We generated a stable cell line expressing fluorescently-labelled EB3 and co-expressed GFP-CM1-Mito or GFP-NINL-Nt-Mito. Even though we could detect EB3 comets moving out of the mitochondria, the intensity of the signal and the resolution were not sufficient to conclude if microtubules were anchored at the mitochondria. Optimisation of this technique and careful analysis of EB3 comet orientation would be required in the future to address if microtubules are indeed anchored to the surface of the mitochondria.

Targeting to the mitochondrial surface reveals different types of MTOCs.

Perhaps, the most interesting outcome of this part of the thesis is that we were able to identify three different types of MTOCs. CM1, NINL-Nt and CKAP5 were all efficient in turning the mitochondria into an organelle capable of generating

microtubules. Even more striking was the observation that these proteins rely on different mechanisms to achieve this capacity. At the beginning of our analysis, we already distinguished between γ TuRC-containing (CM1 and NINL-Nt) and γ TuRC-lacking MTOCs (CKAP5) at the outer surface of the mitochondria (**Table R1**). Moreover, it seemed that CM1 and NINL-Nt also involved NEDD1 and CKAP5. To further confirm our findings, depletion of the γ TuRC (by depleting GCP2), NEDD1 and CKAP5 revealed that CM1 and NINL-Nt relied on different factors to exert their functions. CM1 only required γ TuRC (**Figure R23**) while NINL-Nt was dependent on the γ TuRC, NEDD1 and CKAP5 (**Figure R23-25**). The data we provided here extends our knowledge on how the CM1 is capable of inducing MTOC formation. Using the same system, it was previously reported that after targeting CM1 to the mitochondria, γ TuRC and NEDD1 were recruited at the ectopic site (Chen, 2017). We have found that the presence of NEDD1 is dispensable to achieve MTOC formation, and therefore it is possible that CM1 is capable on its own to recruit γ TuRC and activate microtubule nucleation (**Figure D1**). The role of NEDD1 at the ectopic site is unclear. Previous work suggested that there may be two different populations of γ TuRC in cells, one bound to CM1 that is involved in nucleation and one bound to NEDD1 involved in anchoring (Muroyama, 2016). However, more work is required to determine how NEDD1 is recruited to CM1-induced MTOCs and what its role is. Interestingly, it was shown very recently that CDK5RAP2 contains an autoinhibitory domain that serves to control microtubule nucleation in space and time. The region proposed to have this function in humans is located between aa 51-210 of CDK5RAP2 (Tovey, 2021). We should mention that we tried to target to the mitochondria a smaller CM1 containing fragment (aa 50-100) (Choi, 2010) but this did not allow ectopic MTOC formation. For this reason we used a larger fragment (aa 50-135)(Chen, 2017). It would be interesting to test whether including the region between aa 136-210 would have any inhibitory effect on MTOC formation at mitochondria. We also probed for the presence of MZT1 at the mitochondria after CM1 targeting, but we could not detect any signal (data not shown). MZT1 has been proposed as a priming factor to promote γ TuRC interaction with CM1 and its depletion in human cells interferes with cytoplasmic nucleation after overexpression of the CM1 (Lin, 2016; Cota, 2017). It is possible that our inability to detect mitochondrial MZT1 was due to technical issues with our antibody or due to poor fixation of this small protein. Indeed, detection of MZT1 at centrosomes is also more difficult compared to other subunits. Thus, siRNAs experiments would be needed in order to address whether MZT1 is implicated in CM1-mediated MTOC formation. In the future one could also perform a BioID experiment with CM1 targeted to the mitochondria, which could potentially identify additional factors involved in CM1-dependent MTOC assembly.

In the case of NINL-Nt, it was remarkable to find principal differences in ectopic MTOC composition compared with CM1, despite yielding similar microtubule nucleation capacity (**Figure R11**). Three factors, γ TuRC, NEDD1 and CKAP5, were detected at the mitochondria and were necessary for MTOC formation (**Figure D1**). The detection of NEDD1 and CKAP5 as proximity interactors of NINL-Nt by BioID added robustness to these findings (**Figure R21**). As we have explored the role of NINL in ectopic MTOC assembly in more detail, we will discuss this in more detail in a separate section below.

Targeting of CKAP5 to mitochondria corroborated that this protein is not only a microtubule polymerase (Tournebize, 2000; Fox, 2014) and promotes nucleation by γ TuRC (Thawani, 2018), but may also be able to induce microtubule assembly on its own. While, CKAP5 did not seem to recruit any of the proteins that we probed for to mitochondria, the CKAP5-induced structures may be considered “non-canonical”. Due to the absence of γ TuRC it seems that CKAP5 may act as a microtubule nucleator on its own (**Figure D1**). Notably, we found that a fragment of CKAP5 that only contained the TOG domains was sufficient to carry out this function and that a fragment lacking the TOG domain lacked this activity (**Figure R10**). As TOG domains were previously shown to be necessary for tubulin interaction (Fox, 2014; Thawani, 2018), we hypothesise that CKAP5 could generate an MTOC through tubulin concentration, similar to what has been shown for *C. elegans* ZYG-9 (CKAP5 homolog) *in vitro* in the context of MTOCs additionally composed of SPD-5 and TPXL-1 (TPX2 homolog) (Woodruff, 2017). In addition, another study has found that TPX2 and CKAP5 can form a minimal nucleation module *in vitro*, in the absence of γ TuRC (Roostalu, 2015). Since proteins of the TACC family interact with CKAP5 and regulate its activity in cells (Lee, 2001; Ryan, 2021), it would be interesting to explore whether they may also participate in CKAP5-induced ectopic MTOC assembly or function.

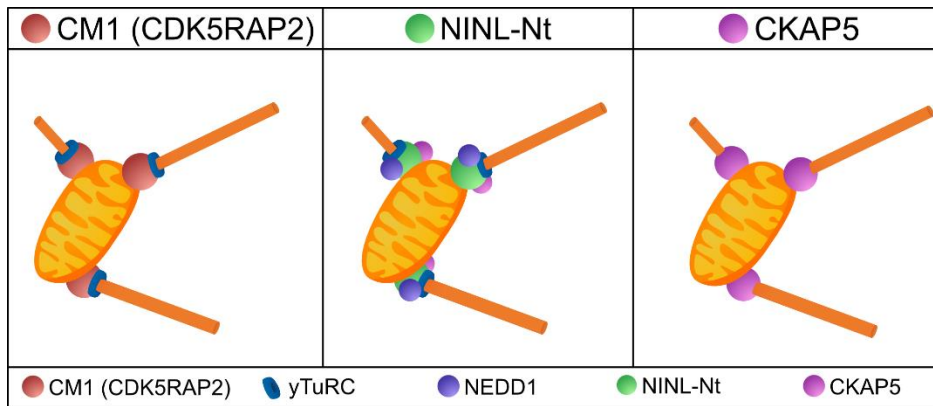


Figure D1. Minimal components required for ectopic MTOC assembly by different POIs

Schematic depicting the minimal set of proteins involved in MTOC assembly by the different POI. It is possible that other untested proteins may participate.

Importantly, some POI did not assemble an MTOC at the mitochondria, namely CEP192-Nt and NIN-Nt. Despite the fact that both recruited NEDD1 and γ TuRC to the ectopic site, they were not able to promote microtubule formation (**Table R1**). This result suggests that CEP192 and NIN may be core components of the centrosome, but are not sufficient to induce MTOC formation. For CEP192 this is particularly interesting, since it has been shown to be crucial for microtubule nucleation at the centrosome (Gomez-Ferreria, 2007; Zhu, 2008; Gavilan, 2018). It is also possible that CEP192 has a more pronounced role during mitosis, as already described (Gomez-Ferreria, 2007), but this was not addressed during this thesis. Although not shown, we also targeted the full-length CEP192 to the mitochondria with very similar results. We decided to only use its N-terminal half because the full-length protein was additionally targeted to the centrosome. Interestingly, we could convert mitochondria-targeted CEP192-Nt into an MTOC by additionally expressing a non-targeted version of CM1 in the cytoplasm (**Figure R9**). This means that this structure was lacking an activator of microtubule nucleation, highlighting the importance of activators of microtubule nucleation in the MTOC formation process. We did not have time to repeat the same experiment with NIN-Nt but it is an appealing future experiment. As NIN is an SDA protein with an established role in microtubule anchoring, we did not expect it to have MTOC forming capacity (Delgehr, 2005). It would have also been interesting to address if the lack of additional anchoring factors, as CAMSAPs or CLIP170 (Wu, 2016; Goldspink, 2017), could be the reason behind NIN not anchoring microtubules at the mitochondria. Unexpectedly, we also observed CKAP5 recruitment to the mitochondria after targeting NIN-Nt, even in the absence of microtubules (**Figure R8**). As there was

no microtubule nucleation from the outer surface of mitochondria in this case, the role of CKAP5 at this site remains unclear. It is possible that CKAP5 recruitment may indicate a functional link with NIN, possibly related to microtubule anchoring. Future work will have to address this.

Insight into MTOC formation by NINL

How does NINL-Nt mediate MTOC formation? The MTOC induced by NINL-Nt at the mitochondria contained a nucleator (γ TuRC), a recruitment factor (NEDD1) and a regulator/activator of microtubule nucleation (CKAP5). Notably, the same proteins were also recruited to the mitochondria in the case of NIN-Nt, but in this case did not provide microtubule nucleation capacity. Therefore, we speculated that NINL-Nt may also contribute to this activity, perhaps in synergy with CKAP5. To address this, we decided to generate several truncation mutants of NINL-Nt, hoping that we might identify a region with CM1-like activity (**Table R3**). This allowed us to define a minimal region that could still assemble an MTOC at the surface of the mitochondria, NINL 1-442. We should mention that, although not quantified, microtubule nucleation from the mitochondria after targeting NINL-Nt (1-702) seemed more robust than nucleation observed for NINL 1-442. As we also showed, the region between aa 443-584(**Figure R13**) that contains the second coiled-coil domain, is involved in oligomerization of NINL. Hence, it is plausible that the reason why NINL 1-442 showed reduced levels of microtubule nucleation was due to the absence of interaction with the endogenous NINL. Interestingly, after removal of the region containing the third coiled-coil domain of NINL we did not observe clustering of the mitochondria around the centrosome anymore, a phenomenon generally mediated by the dynein complex (Burkhardt, 1997). We speculate that the third coiled-coil region of NINL might mediate binding to dynein. Whereas previous work described that NINL binds to dynein through its N-terminus (Casenghi, 2005), we have narrowed down the dynein-binding region to the third coiled-coil domain of NINL. Moreover, a smaller version of NINL, 1-287, was still able to recruit γ TuRC to the mitochondria, but failed to trigger microtubule nucleation (**Figure R14 and Figure R12**). Consistently, a similar γ TuRC binding region was described to be present also in NIN between aa 1-246 (Delgehr, 2005). Thus, we could separate the γ TuRC binding and nucleation activating functions of NINL.

While exploring the relationship of NINL with other proteins we could map the NIN and CEP170 interacting regions. NIN seemed to bind to the region between aa 443-702 (**Figure R18**), while the CEP170 binding region was located in between aa 287-383 (**Figure R16 and R18**). Disruption of a fifth EF-Hand within NINL that

is shared with NIN (**Figure R17**), perturbed CEP170-binding to NINL (**Figure R18**), suggesting that calcium binding may be important for this interaction. However, this mutation did not have any effect on NINL MTOC formation capacity (**Figure R19 and Figure R20**). Thus, the interaction of NINL with CEP170 may be relevant for the endogenous function of these proteins, but was not important for MTOC assembly in our system. All of these interactions are summarised in **Figure D2**.

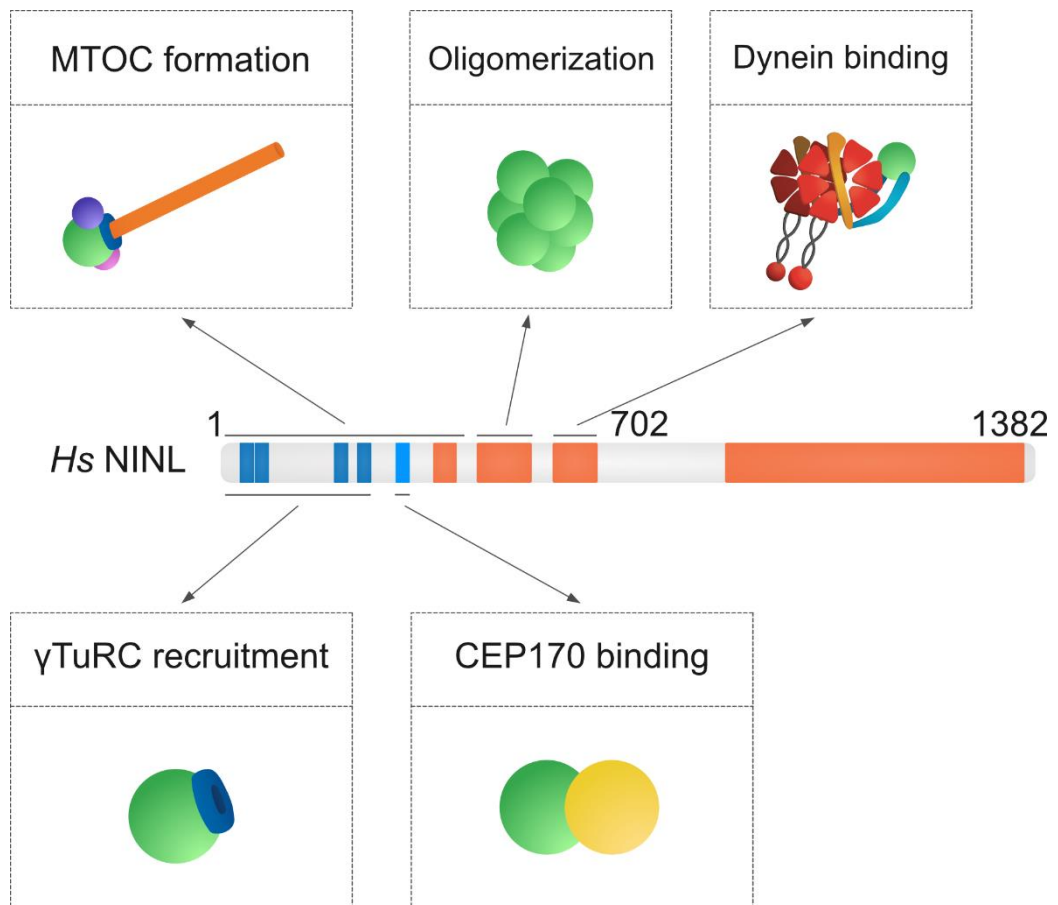


Figure D2. Functional characterization of NINL reveals distinct functional regions.

Schematic depiction of functional regions in the NINL N-terminal half. Two distinct regions in the extreme N-terminal part are involved in γ TuRC binding and nucleation activation, respectively. The position of 4 EF-Hands (dark blue rectangles) and coiled-coil regions (orange rectangles) are shown. We have found that an additional EF-Hand (light blue) is required for binding to CEP170. The second coiled-coiled domain of NINL mediates its oligomerization and the third coiled-coil domain its interaction with dynein.

NINL contains 4 EF-Hands in within the region that is necessary for γ TuRC binding (**Schematic D2**). Thus, we speculated that calcium binding could be important for this function. However, mutation of these EF-Hands did not change the γ TuRC-binding capacity or the microtubule nucleation levels from the mitochondria (data not shown). This was also tried before with some of these EF-Hands (Casenghi, 2004), so we conclude that calcium-binding is not related to γ TuRC recruitment.

To gain more insight into how NINL promotes ectopic MTOC formation, we took advantage of the similarities and differences in the properties of NINL-Nt and NIN-Nt. Despite the sequence similarity in their N-terminal region (aa 1-702) (~37%) (Casenghi, 2003), only NINL-Nt is capable of assembling an MTOC at the mitochondria, while both recruit γ TuRC, NEDD1 and CKAP5 (**Table R1**). Furthermore, both proteins are interactors of dynein (Casenghi, 2005; Redwine, 2017) and cluster mitochondria around the centrosome when targeted (**Figure R1**). Thus, the ability to interact with any of the above proteins is shared by NINL and NIN and therefore cannot explain the difference in their MTOC-inducing capacity. We speculated that the region between aa 288-442 in NINL may be key to this difference by providing activation of microtubule nucleation. We then generated a hybrid protein containing the γ TuRC-binding region from NIN (1-287) and the region 288-442 from NINL, and targeted this construct to mitochondria. The hybrid construct was able to recruit γ TuRC but failed to induce nucleation (data not shown). In addition, we attempted activation by providing NINL 288-442 in *trans*. The γ TuRC binding region NINL 1-287 was targeted to the mitochondria and FLAG-tagged NINL 288-442 was expressed in the cytoplasm, but this also failed to induce an ectopic MTOC. Together these results suggest that γ TuRC recruitment and activation of nucleation, while encoded in different region of NINL, may not be physically separated to promote MTOC assembly.

We also considered the possibility that region 288-442 may invoke additional factors. BioID of both NINL constructs, Nt and 1-442, targeted to mitochondria, revealed 19 hits shared between the two constructs in two separate biological replicates (**Figure R21**). Moreover, 68% of these hits were already described in previous BioID studies with the full-length NINL (Gupta, 2015; Redwine, 2017), validating our results. Interestingly, three of the hits, CKAP5, CEP170 and NEDD1 had been already identified by different approaches during the thesis. Another interesting top hit was MAP7D3, a protein not very well characterised but described to be involved in microtubule assembly and polymerization (Sun, 2011; Yadav, 2014). This is reminiscent of the function initially described for CKAP5 (Gard, 1987; Lee, 2001).

It is tempting to speculate then that MAP7D3 perhaps in cooperation with CKAP5 may contribute to NINL-Nt -dependent MTOC formation. We have the tools now to address this question and we are currently exploring this possibility.

We were surprised to find that a subunit of the augmin complex, HAUS6, was also identified as NINL proximity interactor. At very early stages of the project, we checked whether the augmin complex might play a role in MTOC formation at the mitochondria, but we did not observe any recruitment after targeting the different POI (data not shown). In the light of the BioID data and taking in account the importance of the augmin complex for microtubule nucleation both in mitotic and non-mitotic cells (Goshima, 2008; Sanchez-Huertas, 2016; Cunha-Ferreira, 2018), a careful re-evaluation seems necessary.

Among other interesting hits that we had no time yet to validate and further explore is ERC1 (also known as ELKS), a protein known to attach CLASPs to the cellular cortex. This cluster of CLASPs and ERC1 is used by cells to attach distal microtubule ends (plus-ends) (Lansbergen, 2006). Since CLASPs also tether microtubules minus-ends at the Golgi MTOC (Jiang, 2014), one could speculate that ERC1-CLASP complexes might have a similar function at ectopic MTOCs induced by NINL.

Three components of the dynein-dynactin complex also appear as hits in our BioID dataset, DYNC1LI1, ACRT1A (also known as ARP1) and DCTN2. In general, these proteins appear to be more enriched in the NINL-Nt dataset, which might be explained by the presence of the third coiled-coil domain that we identified as dynein-binding region (**Figure D2**). However, the BioID result suggests that the shorter NINL 1-442 may also interact with dynein, albeit less strongly. As commented before, as both NIN and NINL are interactors of these complex and both cluster the mitochondria, we do not think that dynein interaction is related to MTOC formation.

Another potentially interesting hit from our BioID list is CEP131, a centriolar satellite and centrosomal protein that has been described to be located at the transition zone of primary cilia, a region between the centriole cylinder (basal body) and the cilium shaft. Its depletion is linked to ciliary defects (Hall, 2013). As we have shown that NINL localizes to the distal part of centrioles and SDAs (**Figure 31 and Figure 32**), it may functionally interact with CEP131 in ciliated cells. In addition, it was previously reported that the centrosomal aberrations caused by overexpression of full-length NINL (**Figure R26**) make cancer cells more invasive. Interestingly,

this is also described in the same study to be caused by aberrant structures after overexpression of CEP131 (Ganier, Schnerch, & Nigg, 2018). Thus, there is a chance that these aberrant structures are formed by a complex between NINL and CEP131. However, at this point we have no indication that CEP131 may be involved in NINL MTOC function.

Before exploring the relevance of any of the above protein interactions further, it will be important to first validate the BioID hits by different techniques, such as co-immunoprecipitation or colocalization by IF microscopy of the candidate interactors with endogenous NINL or mitochondria-targeted NINL fragments.

Does MTOC formation by NINL involve phase separation?

Very recently it was described in RPE-1 cells that during centrosome maturation, before mitotic entry, PCNT increases its expression and forms liquid-like droplets that surround the centrosomal area and eventually coalesce at the centrosome. These droplets recruit motor proteins as other PCM components required for microtubule nucleation. The authors proposed that these PCNT condensates might facilitate centrosomal recruitment of PCNT and other centrosomal proteins. Noticeably, the PCNT that is located at the centrosome does not seem to share this property, suggesting that PCNT may be present in two different states (Jiang, 2021). This work may have been inspired by a previous provocative paper claiming that, at least in *C. elegans*, the centrosomal PCM achieves compartmentalization through phase separation from the surrounding cytoplasm. This was based on *in vitro* reconstitution experiments, in which MTOCs could be assembled from purified SPD-5, and *C. elegans* TPX2 and CKAP5 proteins (Woodruff, 2017). These liquid-like spherical assemblies resembled structures that had been described previously in cells overexpressing NINL-Nt (Casenghi, 2003) and that we could reproduce in this thesis (**Figure R26**, NINL). Both NINL-Nt and -Ct overexpression resulted in droplet-like structures in the cytoplasm (**Figure R26**, NINL-Nt and NINL-Ct). Remarkably, only the structures generated by NINL-Nt were capable of recruiting γ -tubulin and nucleating microtubules, similar to the observations with mitochondria-targeted NINL constructs.

We speculate that NINL fragments targeted to mitochondria may undergo some type of phase transition and that this is important for MTOC function. This is prompted not only by the observation of droplets formed by NINL fragments in cells and *in vitro*, but also by the observation that the minimal MTOC-inducing fragment, NINL (1-442), did not promote microtubule nucleation when expressed

as a non-targeted version in the cytoplasm. This was surprising and a fundamental difference to CM1, which promotes MT assembly in both cases, when freely diffusible in the cytoplasm and when targeted to mitochondria. Our current hypothesis is that by targeting NINL 1-442 to the mitochondrial surface we may mimic crowding conditions that could promote phase separation.

Importantly, we could observe droplet-like structures also in *in vitro* using purified recombinant NINL fragments incubated in buffers with crowding agent (**Figure R27 and Figure R28**). Interestingly, even the smallest fragment that we tested, NINL 1-287, was able to form droplets at a certain concentration (**Figure R27 and Figure R28**, NINL 1-287). As this protein is predicted to be mostly disordered, it is possible that the IDRs contained within this fragment may drive phase separation (**Figure R29**). We should comment that the propensity to form these droplet-like structures was influenced by the tag and the presence of additional C-terminal sequences (**Figure R28**, NINL-Nt), which seemed to produce a gradual transition to more irregular aggregates. Now that we have these tools developed, some appealing experiments can be performed in this system. One such experiment would be incubating additional factors such as γ TuRC, CKAP5, or tubulin with NINL droplets *in vitro* and observe if they get incorporated into these structures and if microtubule assembly occurs under any of these conditions. Further characterization of the droplets *in vitro* will also be required, including by live imaging, since their potential liquid-like properties have not yet been properly demonstrated.

To learn more about the potential link between phase separation and NINL, we decided to generate mutant versions of the protein that could disrupt these properties. Based on the predicted IDRs and coiled-coil regions (Vega, 2019; Newton, 2021) as well as the existing aromatic residues (Holehouse, 2015; Wang, 2018; Martin, 2020), which might all be important for phase separation, we designed several NINL mutants. Strikingly, disruption of the second and third coiled-coil in NINL had a profound effect on the formation of droplets in cells. As these coiled-coils mediate dynein-binding and oligomerization, it is possible that these interactions contribute to droplet formation. On the other hand, one of the aromatic mutants, NINL-Nt 11A, had a similar effect, with a more diffuse localization pattern, although we could still detect some condensates in a few cells. Interestingly, in the case of NINL-Nt 22A we could not detect any condensates in most of the cells, but instead large aggregates were detected (**Figure 30**). These results imply that both aromatic residues and coiled-coil domains may be important for droplet formation. If coiled-coils are removed, droplets do not form, while mutation of the aromatic

residues makes NINL-Nt more prone to aggregation. As a next step, we plan to target these mutants to the mitochondrial surface, to test if their inability to form droplets may prevent them from supporting ectopic MTOC formation. Further, it will be important to characterize phase separation properties of these mutants also *in vitro* and in the context of full-length NINL expressed in cells. Important questions to address would be whether mutant NINL localizes similar to endogenous NINL and whether it can rescue any phenotypes observed in cells that lack or are depleted of endogenous NINL.

Implications of NINL localization at SDAs.

What is the role of the endogenous NINL and how does it relate to the findings presented in this thesis? Initial work by the laboratory of Erich Nigg described NINL as a centrosomal protein involved in the regulation of microtubule nucleation (Casenghi, 2003). It was additionally shown in the same article that this protein is regulated by PLK1 phosphorylation, which serves to remove NINL from the centrosome during mitosis. Two years later, it was described that this protein is transported in a dynein-dependent manner to the centrosome, a process also regulated by PLK1 (Casenghi, 2005). Other studies have implicated NINL in cancer development and metastasis (Shao, 2010; Li, 2011; Zhao, 2012) (Ganier, Schnerch, & Nigg, 2018; Ganier, Schnerch, Oertle, , 2018), in autophagy (Xiao, 2021) and, an isoform of NINL, in ciliopathy (van Wijk, 2009), but how these implications may be linked to the molecular and cellular roles of NINL has remained unclear.

As a first step towards addressing this issue, we generated a new antibody against NINL, which showed a clear localization of NINL to centrosomes and in particular to the SDAs of the mother centriole and the proximal ends of both centrioles (**Figure R32**). This staining pattern is consistent with other SDA proteins described (Mazo, 2016; Chong, 2020). Similar localization was also observed in a cell line stably expressing very low levels of GFP-NINL (**Figure R31**) and the staining was reduced after NINL RNAi, suggesting that it is specific. So far, it had only been observed that NINL localized preferentially to the mother centriole (Casenghi, 2003; Casenghi, 2005; Rapley, 2005). Based on the published localization of NIN (Mogensen, 2000), the recently described architecture of the SDAs (Chong, 2020), and that we had detected interaction of NINL with the outer SDA proteins NIN and CEP170 (**Figure R15**, **Figure R16** and **Figure R18**), we speculated that NINL should be located at the outer region of the SDAs. To understand the interdependency between these proteins we depleted CEP170 (**Figure R33**) and NIN (**Figure R34**). Interestingly, depletion of these proteins did not seem to have an effect on NINL

localization, suggesting that it occurred independently of these proteins. Our results with NINL depletion are still preliminary, but suggest that there is also no effect of NINL depletion on NIN localization (**Figure R35**). Together, the data suggest that interaction between these proteins does not determine their SDA localization. Interestingly, NINL is displaced from SDAs after CKAP5 depletion (**Figure R36**). Unpublished data from our laboratory has shown that CKAP5 also localizes at SDAs. Considering that work from our lab recently showed nucleation from distal centriole regions (Schweizer, 2020) and that γ TuRC subunits were found to be associated with SDAs in some cell types (Schweizer, 2020; Schweizer, 2021), it is tempting to speculate that a module of CKAP5-NINL-NEDD1- γ TuRC may be present at SDAs to promote microtubule nucleation from this site. To further characterise how NINL is located, depletion of the inner SDA protein as CEP128 or Centriolin could be used, which may function upstream of NINL. CEP128 was described to interact with ODF2 (even more upstream in the SDA hierarchy) and linked to ciliary function (Monnich, 2018; Kashihara, 2019; Chong, 2020). Moreover, further imaging by SIM and expansion microscopy in combination with additional markers could be used to establish more precisely NINL spatial distribution at SDAs. Another issue that needs to be addressed is the relatively inefficient depletion of NINL at centrosomes by any of the tested siRNAs. In many cases we could observe robust reduction by western blot, as can be observed in **Figure R32**, but centrosomal levels of NINL were depleted less efficiently. This has also prevented us from conducting a thorough phenotypic analysis of NINL-loss-of-function. To overcome this, a CRISPR/Cas9 mediated knockout of NINL would be useful.

Apart from localizing at SDAs, NINL also presented additional centrosome staining that differed from the staining pattern of the canonical SDA proteins NIN and CEP170. In many cells we could detect spike-like staining that seemed to extend away from centrioles. Strikingly, similar “spikes” were also observed for staining of CKAP5, which partially colocalized with NINL (**Figure R37**). Furthermore, NINL also seemed to co-localize with α -tubulin signal at early timepoints during microtubule regrowth. In this case, NINL “spikes” seemed to co-localize with very short microtubules (**Figure R38**). One could speculate that these structures indicate involvement of NINL in microtubule nucleation events, potentially at SDAs (**Figure D3**). Since colocalization with newly formed microtubules is rapidly lost as these elongate, centrosomal NINL distribution may be dynamic. Additional work is required to further elucidate these observations, ideally using NINL KO cells expressing full-length NINL or NINL mutants. This approach could also be used for live imaging to study the dynamics of NINL at the centrosome.

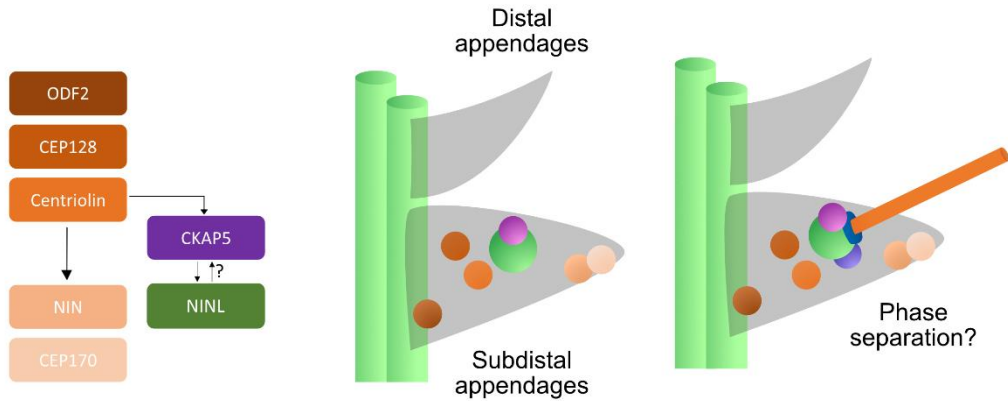


Figure D3. NINL localisation and function at SDAs.

Schematic depicting our suggested NINL localisation to SDAs and its possible role in MTOC formation. Taking into account the already established SDA hierarchy (Chong, 2020) and our findings, we hypothesize that CKAP and NINL might form a complex at SDAs that should be positioned in the hierarchy at the same level or above NIN. NINL localisation seems to be dependent on CKAP5 but it is yet to probe if the reverse is also true. It is possible that a module composed of CKAP5, NINL and potentially γ TuRC could have an important role in MTOC formation at SDAs, an unreported function so far. Moreover, we hypothesize that phase separation could help in the generation of this MTOC, by locally increasing the concentration of the proteins required for its activity.

The observed, potentially dynamic distribution of centrosomal NINL may also be compatible with liquid-like properties, assuming that NINL would form a condensate at the centrosome. Testing this possibility will be challenging due to the relatively small amount of NINL that could be present at centrosomes taking into account the proposed bulk of NIN (if we assume similar populations) (Bauer, 2016) and the small size of the area occupied by NINL.

Many cellular compartments including the centrosomal PCM have been proposed to involve condensate formation (Woodruff, 2017; Boeynaems, 2018). However, a growing number of researchers consider the supporting data in many cases insufficient and have emphasized the need to perform certain key experiments and include additional controls (Alberti, 2019; McSwiggen, 2019; Raff, 2019). It remains to be seen if such data can be provided also for centrosomal NINL.

An important finding of this work is the implication of NINL in centrosomal microtubule nucleation and that SDAs are potentially involved in this activity. Interestingly, while most researchers consider the PCM as the centrosomal site where microtubules are nucleated, very early EM studies already proposed that SDAs may be sites of microtubule nucleation (Vorobjev, 1982; Alieva, 1995). Indeed, this is an attractive hypothesis since nucleation from SDAs would solve the conundrum that exclusive nucleation in the PCM would pose: the physical separation of nucleation (PCM) and anchoring (SDAs), which would require release and transfer of microtubule minus ends over a significant distance.

Another important question is, what is the role of SDA-associated microtubules? One might assume that these microtubules simply increase the total number of microtubules emanating from the centrosomes. However, during mitotic spindle assembly, when centrosomal microtubule nucleation is particularly robust, SDAs do not seem to be required since they are at least partially disassembled at mitotic entry (Vorobjev, 1982). This is in line with the displacement of NINL from the centrosomes during mitosis through PLK1 phosphorylation (Casenghi, 2003; Casenghi, 2005). Another process that involves SDA-associated microtubules is the formation and positioning of cilia. Indeed, depletion of SDA proteins such as ODF2 or CEP128 has shown that these proteins are required for proper ciliogenesis (Ishikawa, 2005; Monnich, 2018). Even more interesting is that depletion of some of the SDA proteins and the cohesion factor CEP250 (protein name: C-Nap1) can alter the ciliary position within the cell by disrupting association between the Golgi apparatus and the cilia (Mazo, 2016). It is tempting to speculate then that the microtubules generated and anchored at SDAs could mediate this function. In addition, these microtubules may also mediate trafficking to and from the cilium, which is important not only for cilium formation, but also homeostasis, and ciliary signalling (Hehnly, 2012; Hall, 2021; Ho, 2021). For these reasons, future NINL loss-of-function studies should also include analysis of ciliogenesis and ciliary signalling.

Conclusions

- The outer surface of mitochondria can serve as a site for ectopic MTOC assembly by various centrosome proteins and facilitates compositional and functional analysis.
- PCNT and CEP192-Nt are capable of recruiting proteins important for MTOC function but fail at ectopic MTOC assembly.
- CEP192-Nt can build an MTOC with the additional presence of an activator of microtubule nucleation.
- The CM1 of CDK5RAP2, NINL-Nt and CKAP5 can induce ectopic MTOC assembly at the outer surface of mitochondria.
- CM1 and NINL-Nt induce similar microtubule nucleation activity when targeted to mitochondria.
- The ectopic MTOC assembled by CM1 requires γ TuRC.
- CKAP5 can induce an ectopic MTOC in the absence of γ TuRC.
- NINL 1-287 is sufficient to recruit γ TuRC at the ectopic site and NINL 1-442 is the minimal region required for assembling an ectopic MTOC.
- The minimal ectopic MTOC assembled by NINL 1-442 requires γ TuRC, NEDD1 and CKAP5.
- The second coiled-coil of NINL mediates its dynein-binding.
- The third coiled-coil of NINL mediates its oligomerization.
- NINL binds to NIN through its second and third coiled-coil domains.

- NINL contains a 5th EF-Hand that is shared with NIN and is necessary for CEP170-binding.
- NIN and CEP170 do not seem to be required for NINL 1-442-induced ectopic MTOC formation.
- The proximity interactome of NINL-Nt and NINL 1-442 targeted to mitochondria includes potential candidates involved in ectopic MTOC formation.
- NINL overexpression generates droplet-like structures that have MTOC activity.
- GST- and GFP- tagged NINL constructs show phase separation properties *in vitro*.
- NINL 1-287 is sufficient to generate condensates *in vitro* and additional C-terminal sequences seem to produce a gradual transition to more irregular aggregates.
- Disruption of the coiled-coil domains of NINL-Nt impairs condensate formation in cells.
- Disruption of the aromatic residues of NINL-Nt leads to aggregation in cells.
- NINL localizes to the SDAs of the mother centriole in cells.
- NINL localization to SDAs is independent of NIN and CEP170.
- NINL localization to SDAs is CKAP5 dependent.
- NINL and CKAP5 form “spikes” that colocalize at SDAs.
- NINL partially co-localizes with microtubules that seem to be generated at SDAs, suggesting that NINL and CKAP5 may have a role in nucleation at SDAs.

References

- Akhmanova, A., & Steinmetz, M. O. (2015). Control of microtubule organization and dynamics: two ends in the limelight. *Nat Rev Mol Cell Biol*, 16(12), 711-726. <https://doi.org/10.1038/nrm4084>
- Alberti, S., Gladfelter, A., & Mittag, T. (2019). Considerations and Challenges in Studying Liquid-Liquid Phase Separation and Biomolecular Condensates. *Cell*, 176(3), 419-434. <https://doi.org/10.1016/j.cell.2018.12.035>
- Alfaro-Aco, R., Thawani, A., & Petry, S. (2017). Structural analysis of the role of TPX2 in branching microtubule nucleation. *J Cell Biol*, 216(4), 983-997. <https://doi.org/10.1083/jcb.201607060>
- Alieva, I. B., & Vorobjev, I. A. (1995). Centrosome behaviour and orientation of centrioles under the action of energy transfer inhibitors. *Cell Biol Int*, 19(2), 103-112. <https://doi.org/10.1006/cbir.1995.1050>
- Ameen, N. A., Figueroa, Y., & Salas, P. J. (2001). Anomalous apical plasma membrane phenotype in CK8-deficient mice indicates a novel role for intermediate filaments in the polarization of simple epithelia. *J Cell Sci*, 114(Pt 3), 563-575.
- Andersen, J. S., Wilkinson, C. J., Mayor, T., Mortensen, P., Nigg, E. A., & Mann, M. (2003). Proteomic characterization of the human centrosome by protein correlation profiling. *Nature*, 426(6966), 570-574. <https://doi.org/10.1038/nature02166>
- Arquint, C., Gabryjonczyk, A. M., & Nigg, E. A. (2014). Centrosomes as signalling centres. *Philos Trans R Soc Lond B Biol Sci*, 369(1650). <https://doi.org/10.1098/rstb.2013.0464>
- Barr, F. A., Sillje, H. H., & Nigg, E. A. (2004). Polo-like kinases and the orchestration of cell division. *Nat Rev Mol Cell Biol*, 5(6), 429-440. <https://doi.org/10.1038/nrm1401>
- Barra, H. S., Rodriguez, J. A., Arce, C. A., & Caputto, R. (1973). A soluble preparation from rat brain that incorporates into its own proteins (14 C)arginine by a ribonuclease-sensitive system and (14 C)tyrosine by a ribonuclease-insensitive system. *J Neurochem*, 20(1), 97-108. <https://doi.org/10.1111/j.1471-4159.1973.tb12108.x>
- Basto, R., Lau, J., Vinogradova, T., Gardiol, A., Woods, C. G., Khodjakov, A., & Raff, J. W. (2006). Flies without centrioles. *Cell*, 125(7), 1375-1386. <https://doi.org/10.1016/j.cell.2006.05.025>
- Bauer, M., Cubizolles, F., Schmidt, A., & Nigg, E. A. (2016). Quantitative analysis of human centrosome architecture by targeted proteomics and fluorescence imaging. *EMBO J*, 35(19), 2152-2166. <https://doi.org/10.15252/embj.201694462>
- Bean, D. M., Heimbach, J., Ficorella, L., Micklem, G., Oliver, S. G., & Favrin, G. (2014). esyN: network building, sharing and publishing. *PLoS One*, 9(9), e106035. <https://doi.org/10.1371/journal.pone.0106035>
- Bernis, C., Swift-Taylor, B., Nord, M., Carmona, S., Chook, Y. M., & Forbes, D. J. (2014). Transportin acts to regulate mitotic assembly events by target binding rather than Ran sequestration. *Mol Biol Cell*, 25(7), 992-1009. <https://doi.org/10.1091/mbc.E13-08-0506>

- Block, S. M., Goldstein, L. S., & Schnapp, B. J. (1990). Bead movement by single kinesin molecules studied with optical tweezers. *Nature*, *348*(6299), 348-352. <https://doi.org/10.1038/348348a0>
- Bodakuntla, S., Jijumon, A. S., Villablanca, C., Gonzalez-Billault, C., & Janke, C. (2019). Microtubule-Associated Proteins: Structuring the Cytoskeleton. *Trends Cell Biol*, *29*(10), 804-819. <https://doi.org/10.1016/j.tcb.2019.07.004>
- Boeynaems, S., Alberti, S., Fawzi, N. L., Mittag, T., Polymenidou, M., Rousseau, F., Schymkowitz, J., Shorter, J., Wolozin, B., Van Den Bosch, L., Tompa, P., & Fuxreiter, M. (2018). Protein Phase Separation: A New Phase in Cell Biology. *Trends Cell Biol*, *28*(6), 420-435. <https://doi.org/10.1016/j.tcb.2018.02.004>
- Borcherds, W., Bremer, A., Borgia, M. B., & Mittag, T. (2021). How do intrinsically disordered protein regions encode a driving force for liquid-liquid phase separation? *Curr Opin Struct Biol*, *67*, 41-50. <https://doi.org/10.1016/j.sbi.2020.09.004>
- Bouckson-Castaing, V., Moudjou, M., Ferguson, D. J., Mucklow, S., Belkaid, Y., Milon, G., & Crocker, P. R. (1996). Molecular characterisation of ninein, a new coiled-coil protein of the centrosome. *J Cell Sci*, *109* (Pt 1), 179-190.
- Burkhard, P., Stetefeld, J., & Strelkov, S. V. (2001). Coiled coils: a highly versatile protein folding motif. *Trends Cell Biol*, *11*(2), 82-88. [https://doi.org/10.1016/s0962-8924\(00\)01898-5](https://doi.org/10.1016/s0962-8924(00)01898-5)
- Burkhardt, J. K., Echeverri, C. J., Nilsson, T., & Vallee, R. B. (1997). Overexpression of the dynamitin (p50) subunit of the dynactin complex disrupts dynein-dependent maintenance of membrane organelle distribution. *J Cell Biol*, *139*(2), 469-484. <https://doi.org/10.1083/jcb.139.2.469>
- Casenghi, M. (2004). *Functional characterization of the novel centrosomal protein Nlp (ninein-like protein)* [Dissertation, LMU Munich, <http://nbn-resolving.de/urn:nbn:de:bvb:19-19622>]
- Casenghi, M., Barr, F. A., & Nigg, E. A. (2005). Phosphorylation of Nlp by Plk1 negatively regulates its dynein-dynactin-dependent targeting to the centrosome. *J Cell Sci*, *118*(Pt 21), 5101-5108. <https://doi.org/10.1242/jcs.02622>
- Casenghi, M., Meraldi, P., Weinhart, U., Duncan, P. I., Körner, R., & Nigg, E. A. (2003). Polo-like Kinase 1 Regulates Nlp, a Centrosome Protein Involved in Microtubule Nucleation. *Developmental Cell*, *5*(1), 113-125. [https://doi.org/10.1016/s1534-5807\(03\)00193-x](https://doi.org/10.1016/s1534-5807(03)00193-x)
- Chabin-Brion, K., Marceiller, J., Perez, F., Settegrana, C., Drechou, A., Durand, G., & Poüs, C. (2001). The Golgi complex is a microtubule-organizing organelle. *Mol Biol Cell*, *12*(7), 2047-2060. <https://doi.org/10.1091/mbc.12.7.2047>
- Chen, J. V., Buchwalter, R. A., Kao, L. R., & Megraw, T. L. (2017). A Splice Variant of Centrosomin Converts Mitochondria to Microtubule-Organizing Centers. *Curr Biol*, *27*(13), 1928-1940 e1926. <https://doi.org/10.1016/j.cub.2017.05.090>

- Choi, Y. K., Liu, P., Sze, S. K., Dai, C., & Qi, R. Z. (2010). CDK5RAP2 stimulates microtubule nucleation by the gamma-tubulin ring complex. *J Cell Biol*, *191*(6), 1089-1095. <https://doi.org/10.1083/jcb.201007030>
- Chong, W. M., Wang, W. J., Lo, C. H., Chiu, T. Y., Chang, T. J., Liu, Y. P., Tanos, B., Mazo, G., Tsou, M. B., Jane, W. N., Yang, T. T., & Liao, J. C. (2020). Super-resolution microscopy reveals coupling between mammalian centriole subdistal appendages and distal appendages. *Elife*, *9*. <https://doi.org/10.7554/eLife.53580>
- Clarke, P. R., & Zhang, C. (2008). Spatial and temporal coordination of mitosis by Ran GTPase. *Nat Rev Mol Cell Biol*, *9*(6), 464-477. <https://doi.org/10.1038/nrm2410>
- Conduit, P. T., Wainman, A., & Raff, J. W. (2015). Centrosome function and assembly in animal cells. *Nat Rev Mol Cell Biol*, *16*(10), 611-624. <https://doi.org/10.1038/nrm4062>
- Consolati, T., Locke, J., Roostalu, J., Chen, Z. A., Gannon, J., Asthana, J., Lim, W. M., Martino, F., Cvetkovic, M. A., Rappsilber, J., Costa, A., & Surrey, T. (2020). Microtubule Nucleation Properties of Single Human γ TuRCs Explained by Their Cryo-EM Structure. *Dev Cell*, *53*(5), 603-617.e608. <https://doi.org/10.1016/j.devcel.2020.04.019>
- Consortium, T. U. (2020). UniProt: the universal protein knowledgebase in 2021. *Nucleic Acids Research*, *49*(D1), D480-D489. <https://doi.org/10.1093/nar/gkaa1100>
- Cota, R. R., Teixido-Travesa, N., Ezquerro, A., Eibes, S., Lacasa, C., Roig, J., & Luders, J. (2017). MZT1 regulates microtubule nucleation by linking gammaTuRC assembly to adapter-mediated targeting and activation. *J Cell Sci*, *130*(2), 406-419. <https://doi.org/10.1242/jcs.195321>
- Cox, J., & Mann, M. (2008). MaxQuant enables high peptide identification rates, individualized p.p.b.-range mass accuracies and proteome-wide protein quantification. *Nat Biotechnol*, *26*(12), 1367-1372. <https://doi.org/10.1038/nbt.1511>
- Cox, J., Neuhauser, N., Michalski, A., Scheltema, R. A., Olsen, J. V., & Mann, M. (2011). Andromeda: a peptide search engine integrated into the MaxQuant environment. *J Proteome Res*, *10*(4), 1794-1805. <https://doi.org/10.1021/pr101065j>
- Cunha-Ferreira, I., Chazeau, A., Buijs, R. R., Stucchi, R., Will, L., Pan, X., Adolfs, Y., van der Meer, C., Wolthuis, J. C., Kahn, O. I., Schätzle, P., Altelaar, M., Pasterkamp, R. J., Kapitein, L. C., & Hoogenraad, C. C. (2018). The HAUS Complex Is a Key Regulator of Non-centrosomal Microtubule Organization during Neuronal Development. *Cell Rep*, *24*(4), 791-800. <https://doi.org/10.1016/j.celrep.2018.06.093>
- Delgehyr, N., Sillibourne, J., & Bornens, M. (2005). Microtubule nucleation and anchoring at the centrosome are independent processes linked by ninein function. *J Cell Sci*, *118*(Pt 8), 1565-1575. <https://doi.org/10.1242/jcs.02302>

- Desai, A., Verma, S., Mitchison, T. J., & Walczak, C. E. (1999). Kin I kinesins are microtubule-destabilizing enzymes. *Cell*, *96*(1), 69-78.
[https://doi.org/10.1016/s0092-8674\(00\)80960-5](https://doi.org/10.1016/s0092-8674(00)80960-5)
- Dictenberg, J. B., Zimmerman, W., Sparks, C. A., Young, A., Vidair, C., Zheng, Y., Carrington, W., Fay, F. S., & Doxsey, S. J. (1998). Pericentrin and gamma-tubulin form a protein complex and are organized into a novel lattice at the centrosome. *J Cell Biol*, *141*(1), 163-174.
<https://doi.org/10.1083/jcb.141.1.163>
- Dong, C., Xu, H., Zhang, R., Tanaka, N., Takeichi, M., & Meng, W. (2017). CAMSAP3 accumulates in the pericentrosomal area and accompanies microtubule release from the centrosome via katanin. *J Cell Sci*, *130*(10), 1709-1715. <https://doi.org/10.1242/jcs.198010>
- Doxsey, S., McCollum, D., & Theurkauf, W. (2005). Centrosomes in cellular regulation. *Annu Rev Cell Dev Biol*, *21*, 411-434.
<https://doi.org/10.1146/annurev.cellbio.21.122303.120418>
- Efimov, A., Kharitonov, A., Efimova, N., Loncarek, J., Miller, P. M., Andreyeva, N., Gleeson, P., Galjart, N., Maia, A. R., McLeod, I. X., Yates, J. R., 3rd, Maiato, H., Khodjakov, A., Akhmanova, A., & Kaverina, I. (2007). Asymmetric CLASP-dependent nucleation of noncentrosomal microtubules at the trans-Golgi network. *Dev Cell*, *12*(6), 917-930.
<https://doi.org/10.1016/j.devcel.2007.04.002>
- Erickson, H. P. (1995). FtsZ, a prokaryotic homolog of tubulin? *Cell*, *80*(3), 367-370. [https://doi.org/10.1016/0092-8674\(95\)90486-7](https://doi.org/10.1016/0092-8674(95)90486-7)
- Espigat-Georger, A., Dyachuk, V., Chemin, C., Emorine, L., & Merdes, A. (2016). Nuclear alignment in myotubes requires centrosome proteins recruited by nesprin-1. *J Cell Sci*, *129*(22), 4227-4237.
<https://doi.org/10.1242/jcs.191767>
- Evans, K. J., Gomes, E. R., Reisenweber, S. M., Gundersen, G. G., & Lauring, B. P. (2005). Linking axonal degeneration to microtubule remodeling by Spastin-mediated microtubule severing. *J Cell Biol*, *168*(4), 599-606.
<https://doi.org/10.1083/jcb.200409058>
- Farina, F., Gaillard, J., Guerin, C., Coute, Y., Sillibourne, J., Blanchoin, L., & Thery, M. (2016). The centrosome is an actin-organizing centre. *Nat Cell Biol*, *18*(1), 65-75. <https://doi.org/10.1038/ncb3285>
- Findeisen, P., Mühlhausen, S., Dempewolf, S., Hertzog, J., Zietlow, A., Carlomagno, T., & Kollmar, M. (2014). Six subgroups and extensive recent duplications characterize the evolution of the eukaryotic tubulin protein family. *Genome Biol Evol*, *6*(9), 2274-2288.
<https://doi.org/10.1093/gbe/evu187>
- Fong, K. W., Choi, Y. K., Rattner, J. B., & Qi, R. Z. (2008). CDK5RAP2 is a pericentriolar protein that functions in centrosomal attachment of the gamma-tubulin ring complex. *Mol Biol Cell*, *19*(1), 115-125.
<https://doi.org/10.1091/mbc.e07-04-0371>
- Fox, J. C., Howard, A. E., Currie, J. D., Rogers, S. L., & Slep, K. C. (2014). The XMAP215 family drives microtubule polymerization using a structurally

- diverse TOG array. *Mol Biol Cell*, 25(16), 2375-2392.
<https://doi.org/10.1091/mbc.E13-08-0501>
- Fu, J., & Glover, D. M. (2012). Structured illumination of the interface between centriole and peri-centriolar material. *Open Biol*, 2(8), 120104.
<https://doi.org/10.1098/rsob.120104>
- Fu, J., Hagan, I. M., & Glover, D. M. (2015). The centrosome and its duplication cycle. *Cold Spring Harb Perspect Biol*, 7(2), a015800.
<https://doi.org/10.1101/cshperspect.a015800>
- Gadadhar, S., Bodakuntla, S., Natarajan, K., & Janke, C. (2017). The tubulin code at a glance. *J Cell Sci*, 130(8), 1347-1353.
<https://doi.org/10.1242/jcs.199471>
- Ganier, O., Schnerch, D., & Nigg, E. A. (2018). Structural centrosome aberrations sensitize polarized epithelia to basal cell extrusion. *Open Biol*, 8(6).
<https://doi.org/10.1098/rsob.180044>
- Ganier, O., Schnerch, D., Oertle, P., Lim, R. Y., Plodinec, M., & Nigg, E. A. (2018). Structural centrosome aberrations promote non-cell-autonomous invasiveness. *EMBO J*, 37(9). <https://doi.org/10.15252/emboj.201798576>
- Gard, D. L., & Kirschner, M. W. (1987). A microtubule-associated protein from *Xenopus* eggs that specifically promotes assembly at the plus-end. *J Cell Biol*, 105(5), 2203-2215. <https://doi.org/10.1083/jcb.105.5.2203>
- Gavilan, M. P., Gandolfo, P., Balestra, F. R., Arias, F., Bornens, M., & Rios, R. M. (2018). The dual role of the centrosome in organizing the microtubule network in interphase. *EMBO Rep*, 19(11).
<https://doi.org/10.15252/embr.201845942>
- Ge, S. X., Jung, D., & Yao, R. (2020). ShinyGO: a graphical gene-set enrichment tool for animals and plants. *Bioinformatics*, 36(8), 2628-2629.
<https://doi.org/10.1093/bioinformatics/btz931>
- Gergely, F., Kidd, D., Jeffers, K., Wakefield, J. G., & Raff, J. W. (2000). D-TACC: a novel centrosomal protein required for normal spindle function in the early *Drosophila* embryo. *EMBO J*, 19(2), 241-252.
<https://doi.org/10.1093/emboj/19.2.241>
- Gifford, J. L., Walsh, M. P., & Vogel, H. J. (2007). Structures and metal-ion-binding properties of the Ca²⁺-binding helix-loop-helix EF-hand motifs. *Biochem J*, 405(2), 199-221. <https://doi.org/10.1042/BJ20070255>
- Gill, S. R., Schroer, T. A., Szilak, I., Steuer, E. R., Sheetz, M. P., & Cleveland, D. W. (1991). Dynactin, a conserved, ubiquitously expressed component of an activator of vesicle motility mediated by cytoplasmic dynein. *J Cell Biol*, 115(6), 1639-1650. <https://doi.org/10.1083/jcb.115.6.1639>
- Gillingham, A. K., & Munro, S. (2000). The PACT domain, a conserved centrosomal targeting motif in the coiled-coil proteins AKAP450 and pericentrin. *EMBO Rep*, 1(6), 524-529. <https://doi.org/10.1093/embo-reports/kvd105>
- Gimpel, P., Lee, Y. L., Sobota, R. M., Calvi, A., Koullourou, V., Patel, R., Mamchaoui, K., Nedelec, F., Shackleton, S., Schmoranzler, J., Burke, B., Cadot, B., & Gomes, E. R. (2017). Nesprin-1alpha-Dependent Microtubule

- Nucleation from the Nuclear Envelope via Akap450 Is Necessary for Nuclear Positioning in Muscle Cells. *Curr Biol*, 27(19), 2999-3009 e2999. <https://doi.org/10.1016/j.cub.2017.08.031>
- Goldspink, D. A., Rookyard, C., Tyrrell, B. J., Gadsby, J., Perkins, J., Lund, E. K., Galjart, N., Thomas, P., Wileman, T., & Mogensen, M. M. (2017). Ninein is essential for apico-basal microtubule formation and CLIP-170 facilitates its redeployment to non-centrosomal microtubule organizing centres. *Open Biol*, 7(2). <https://doi.org/10.1098/rsob.160274>
- Gomez-Ferreria, M. A., Rath, U., Buster, D. W., Chanda, S. K., Caldwell, J. S., Rines, D. R., & Sharp, D. J. (2007). Human Cep192 is required for mitotic centrosome and spindle assembly. *Curr Biol*, 17(22), 1960-1966. <https://doi.org/10.1016/j.cub.2007.10.019>
- Goshima, G., Mayer, M., Zhang, N., Stuurman, N., & Vale, R. D. (2008). Augmin: a protein complex required for centrosome-independent microtubule generation within the spindle. *J Cell Biol*, 181(3), 421-429. <https://doi.org/10.1083/jcb.200711053>
- Gould, R. R., & Borisy, G. G. (1977). The pericentriolar material in Chinese hamster ovary cells nucleates microtubule formation. *J Cell Biol*, 73(3), 601-615. <https://doi.org/10.1083/jcb.73.3.601>
- Goulet, A., & Moores, C. (2013). New insights into the mechanism of force generation by kinesin-5 molecular motors. *Int Rev Cell Mol Biol*, 304, 419-466. <https://doi.org/10.1016/b978-0-12-407696-9.00008-7>
- Gruss, O. J., Carazo-Salas, R. E., Schatz, C. A., Guarguaglini, G., Kast, J., Wilm, M., Le Bot, N., Vernos, I., Karsenti, E., & Mattaj, I. W. (2001). Ran induces spindle assembly by reversing the inhibitory effect of importin alpha on TPX2 activity. *Cell*, 104(1), 83-93. [https://doi.org/10.1016/s0092-8674\(01\)00193-3](https://doi.org/10.1016/s0092-8674(01)00193-3)
- Gunzelmann, J., Rütznick, D., Lin, T. C., Zhang, W., Neuner, A., Jäkle, U., & Schiebel, E. (2018). The microtubule polymerase Stu2 promotes oligomerization of the γ -TuSC for cytoplasmic microtubule nucleation. *Elife*, 7. <https://doi.org/10.7554/eLife.39932>
- Gupta, G. D., Coyaud, E., Goncalves, J., Mojarad, B. A., Liu, Y., Wu, Q., Gheiratmand, L., Comartin, D., Tkach, J. M., Cheung, S. W., Bashkurov, M., Hasegan, M., Knight, J. D., Lin, Z. Y., Schueler, M., Hildebrandt, F., Moffat, J., Gingras, A. C., Raught, B., & Pelletier, L. (2015). A Dynamic Protein Interaction Landscape of the Human Centrosome-Cilium Interface. *Cell*, 163(6), 1484-1499. <https://doi.org/10.1016/j.cell.2015.10.065>
- Hall, E. A., Keighren, M., Ford, M. J., Davey, T., Jarman, A. P., Smith, L. B., Jackson, I. J., & Mill, P. (2013). Acute versus chronic loss of mammalian Azi1/Cep131 results in distinct ciliary phenotypes. *PLoS Genet*, 9(12), e1003928. <https://doi.org/10.1371/journal.pgen.1003928>
- Hall, N. A., & Hehnl, H. (2021). A centriole's subdistal appendages: contributions to cell division, ciliogenesis and differentiation. *Open Biol*, 11(2), 200399. <https://doi.org/10.1098/rsob.200399>

- Haren, L., Remy, M. H., Bazin, I., Callebaut, I., Wright, M., & Merdes, A. (2006). NEDD1-dependent recruitment of the gamma-tubulin ring complex to the centrosome is necessary for centriole duplication and spindle assembly. *J Cell Biol*, 172(4), 505-515. <https://doi.org/10.1083/jcb.200510028>
- Haren, L., Stearns, T., & Luders, J. (2009). Plk1-dependent recruitment of gamma-tubulin complexes to mitotic centrosomes involves multiple PCM components. *PLoS One*, 4(6), e5976. <https://doi.org/10.1371/journal.pone.0005976>
- Harmon, T. S., Holehouse, A. S., Rosen, M. K., & Pappu, R. V. (2017). Intrinsically disordered linkers determine the interplay between phase separation and gelation in multivalent proteins. *Elife*, 6. <https://doi.org/10.7554/eLife.30294>
- Hayashi, I., & Ikura, M. (2003). Crystal structure of the amino-terminal microtubule-binding domain of end-binding protein 1 (EB1). *J Biol Chem*, 278(38), 36430-36434. <https://doi.org/10.1074/jbc.M305773200>
- Hayward, D., Metz, J., Pellacani, C., & Wakefield, J. G. (2014). Synergy between multiple microtubule-generating pathways confers robustness to centrosome-driven mitotic spindle formation. *Dev Cell*, 28(1), 81-93. <https://doi.org/10.1016/j.devcel.2013.12.001>
- Hehnl, H., Chen, C. T., Powers, C. M., Liu, H. L., & Doxsey, S. (2012). The centrosome regulates the Rab11- dependent recycling endosome pathway at appendages of the mother centriole. *Curr Biol*, 22(20), 1944-1950. <https://doi.org/10.1016/j.cub.2012.08.022>
- Hernandez-Vega, A., Braun, M., Scharrel, L., Jahnel, M., Wegmann, S., Hyman, B. T., Alberti, S., Diez, S., & Hyman, A. A. (2017). Local Nucleation of Microtubule Bundles through Tubulin Concentration into a Condensed Tau Phase. *Cell Rep*, 20(10), 2304-2312. <https://doi.org/10.1016/j.celrep.2017.08.042>
- Ho, E. K., & Stearns, T. (2021). Hedgehog signaling and the primary cilium: implications for spatial and temporal constraints on signaling. *Development*, 148(9). <https://doi.org/10.1242/dev.195552>
- Holehouse, A. S., & Pappu, R. V. (2015). Protein polymers: Encoding phase transitions. *Nat Mater*, 14(11), 1083-1084. <https://doi.org/10.1038/nmat4459>
- Honnappa, S., Gouveia, S. M., Weisbrich, A., Damberger, F. F., Bhavesh, N. S., Jawhari, H., Grigoriev, I., van Rijssel, F. J., Buey, R. M., Lawera, A., Jelesarov, I., Winkler, F. K., Wüthrich, K., Akhmanova, A., & Steinmetz, M. O. (2009). An EB1-binding motif acts as a microtubule tip localization signal. *Cell*, 138(2), 366-376. <https://doi.org/10.1016/j.cell.2009.04.065>
- Ishikawa, H., Kubo, A., Tsukita, S., & Tsukita, S. (2005). Odf2-deficient mother centrioles lack distal/subdistal appendages and the ability to generate primary cilia. *Nat Cell Biol*, 7(5), 517-524. <https://doi.org/10.1038/ncb1251>
- Jakobsen, L., Vanselow, K., Skogs, M., Toyoda, Y., Lundberg, E., Poser, I., Falkenby, L. G., Bennetzen, M., Westendorf, J., Nigg, E. A., Uhlen, M., Hyman, A. A., & Andersen, J. S. (2011). Novel asymmetrically localizing

- components of human centrosomes identified by complementary proteomics methods. *EMBO J*, 30(8), 1520-1535.
<https://doi.org/10.1038/emboj.2011.63>
- Janke, C., & Bulinski, J. C. (2011). Post-translational regulation of the microtubule cytoskeleton: mechanisms and functions. *Nat Rev Mol Cell Biol*, 12(12), 773-786. <https://doi.org/10.1038/nrm3227>
- Jiang, K., Hua, S., Mohan, R., Grigoriev, I., Yau, K. W., Liu, Q., Katrukha, E. A., Altelaar, A. F., Heck, A. J., Hoogenraad, C. C., & Akhmanova, A. (2014). Microtubule minus-end stabilization by polymerization-driven CAMSAP deposition. *Dev Cell*, 28(3), 295-309.
<https://doi.org/10.1016/j.devcel.2014.01.001>
- Jiang, X., Ho, D. B. T., Mahe, K., Mia, J., Sepulveda, G., Antkowiak, M., Jiang, L., Yamada, S., & Jao, L. E. (2021). Condensation of pericentrin proteins in human cells illuminates phase separation in centrosome assembly. *J Cell Sci*, 134(14). <https://doi.org/10.1242/jcs.258897>
- Joshi, H. C., & Cleveland, D. W. (1989). Differential utilization of beta-tubulin isotypes in differentiating neurites. *J Cell Biol*, 109(2), 663-673.
<https://doi.org/10.1083/jcb.109.2.663>
- Jumper, J., Evans, R., Pritzel, A., Green, T., Figurnov, M., Ronneberger, O., Tunyasuvunakool, K., Bates, R., Žídek, A., Potapenko, A., Bridgland, A., Meyer, C., Kohl, S. A. A., Ballard, A. J., Cowie, A., Romera-Paredes, B., Nikolov, S., Jain, R., Adler, J., Back, T., Petersen, S., Reiman, D., Clancy, E., Zielinski, M., Steinegger, M., Pacholska, M., Berghammer, T., Bodenstein, S., Silver, D., Vinyals, O., Senior, A. W., Kavukcuoglu, K., Kohli, P., & Hassabis, D. (2021). Highly accurate protein structure prediction with AlphaFold. *Nature*, 596(7873), 583-589.
<https://doi.org/10.1038/s41586-021-03819-2>
- Kaan, H. Y., Hackney, D. D., & Kozielski, F. (2011). The structure of the kinesin-1 motor-tail complex reveals the mechanism of autoinhibition. *Science*, 333(6044), 883-885. <https://doi.org/10.1126/science.1204824>
- Kaláb, P., Pralle, A., Isacoff, E. Y., Heald, R., & Weis, K. (2006). Analysis of a RanGTP-regulated gradient in mitotic somatic cells. *Nature*, 440(7084), 697-701. <https://doi.org/10.1038/nature04589>
- Kashihara, H., Chiba, S., Kanno, S. I., Suzuki, K., Yano, T., & Tsukita, S. (2019). Cep128 associates with Odf2 to form the subdistal appendage of the centriole. *Genes Cells*, 24(3), 231-243. <https://doi.org/10.1111/gtc.12668>
- Khodjakov, A., Cole, R. W., Oakley, B. R., & Rieder, C. L. (2000). Centrosome-independent mitotic spindle formation in vertebrates. *Curr Biol*, 10(2), 59-67. [https://doi.org/10.1016/s0960-9822\(99\)00276-6](https://doi.org/10.1016/s0960-9822(99)00276-6)
- Kim, D. I., Jensen, S. C., Noble, K. A., Kc, B., Roux, K. H., Motamedchaboki, K., & Roux, K. J. (2016). An improved smaller biotin ligase for BioID proximity labeling. *Mol Biol Cell*, 27(8), 1188-1196.
<https://doi.org/10.1091/mbc.E15-12-0844>
- Knight, J. D. R., Choi, H., Gupta, G. D., Pelletier, L., Raught, B., Nesvizhskii, A. I., & Gingras, A. C. (2017). ProHits-viz: a suite of web tools for visualizing

- interaction proteomics data. *Nat Methods*, 14(7), 645-646.
<https://doi.org/10.1038/nmeth.4330>
- Knop, M., & Schiebel, E. (1997). Spc98p and Spc97p of the yeast gamma-tubulin complex mediate binding to the spindle pole body via their interaction with Spc110p. *EMBO J*, 16(23), 6985-6995.
<https://doi.org/10.1093/emboj/16.23.6985>
- Kollman, J. M., Greenberg, C. H., Li, S., Moritz, M., Zelter, A., Fong, K. K., Fernandez, J. J., Sali, A., Kilmartin, J., Davis, T. N., & Agard, D. A. (2015). Ring closure activates yeast gammaTuRC for species-specific microtubule nucleation. *Nat Struct Mol Biol*, 22(2), 132-137.
<https://doi.org/10.1038/nsmb.2953>
- Kon, T., Oyama, T., Shimo-Kon, R., Imamula, K., Shima, T., Sutoh, K., & Kurisu, G. (2012). The 2.8 Å crystal structure of the dynein motor domain. *Nature*, 484(7394), 345-350. <https://doi.org/10.1038/nature10955>
- Kovacs, G. G. (2017). Tauopathies. *Handb Clin Neurol*, 145, 355-368.
<https://doi.org/10.1016/B978-0-12-802395-2.00025-0>
- Lansbergen, G., Grigoriev, I., Mimori-Kiyosue, Y., Ohtsuka, T., Higa, S., Kitajima, I., Demmers, J., Galjart, N., Houtsmuller, A. B., Grosveld, F., & Akhmanova, A. (2006). CLASPs attach microtubule plus ends to the cell cortex through a complex with LL5beta. *Dev Cell*, 11(1), 21-32.
<https://doi.org/10.1016/j.devcel.2006.05.012>
- Lawo, S., Bashkurov, M., Mullin, M., Ferreria, M. G., Kittler, R., Habermann, B., Tagliaferro, A., Poser, I., Hutchins, J. R., Hegemann, B., Pinchev, D., Buchholz, F., Peters, J. M., Hyman, A. A., Gingras, A. C., & Pelletier, L. (2009). HAUS, the 8-subunit human Augmin complex, regulates centrosome and spindle integrity. *Curr Biol*, 19(10), 816-826.
<https://doi.org/10.1016/j.cub.2009.04.033>
- Lawo, S., Hasegan, M., Gupta, G. D., & Pelletier, L. (2012). Subdiffraction imaging of centrosomes reveals higher-order organizational features of pericentriolar material. *Nat Cell Biol*, 14(11), 1148-1158.
<https://doi.org/10.1038/ncb2591>
- Lechler, T., & Fuchs, E. (2007). Desmoplakin: an unexpected regulator of microtubule organization in the epidermis. *J Cell Biol*, 176(2), 147-154.
<https://doi.org/10.1083/jcb.200609109>
- Lee, M. J., Gergely, F., Jeffers, K., Peak-Chew, S. Y., & Raff, J. W. (2001). Msps/XMAP215 interacts with the centrosomal protein D-TACC to regulate microtubule behaviour. *Nat Cell Biol*, 3(7), 643-649.
<https://doi.org/10.1038/35083033>
- Li, J., Ahat, E., & Wang, Y. (2019). Golgi Structure and Function in Health, Stress, and Diseases. *Results Probl Cell Differ*, 67, 441-485.
https://doi.org/10.1007/978-3-030-23173-6_19
- Li, J., & Zhan, Q. (2011). The role of centrosomal Nlp in the control of mitotic progression and tumorigenesis. *Br J Cancer*, 104(10), 1523-1528.
<https://doi.org/10.1038/bjc.2011.130>

- Li, S.-C., Goto, N. K., Williams, K. A., & Deber, C. M. (1996). α -Helical, but not β -Sheet, Propensity of Proline is Determined by Peptide Environment. *Proceedings of the National Academy of Sciences of the United States of America*, 93(13), 6676-6681. <http://www.jstor.org/stable/39368>
- Lin, T. C., Neuner, A., Flemming, D., Liu, P., Chinen, T., Jakle, U., Arkowitz, R., & Schiebel, E. (2016). MOZART1 and gamma-tubulin complex receptors are both required to turn gamma-TuSC into an active microtubule nucleation template. *J Cell Biol*, 215(6), 823-840. <https://doi.org/10.1083/jcb.201606092>
- Lin, T. C., Neuner, A., Schlosser, Y. T., Scharf, A. N., Weber, L., & Schiebel, E. (2014). Cell-cycle dependent phosphorylation of yeast pericentrin regulates gamma-TuSC-mediated microtubule nucleation. *Elife*, 3, e02208. <https://doi.org/10.7554/eLife.02208>
- Lithgow, T., Glick, B. S., & Schatz, G. (1995). The protein import receptor of mitochondria. *Trends Biochem Sci*, 20(3), 98-101. [https://doi.org/10.1016/s0968-0004\(00\)88972-0](https://doi.org/10.1016/s0968-0004(00)88972-0)
- Liu, P., Choi, Y. K., & Qi, R. Z. (2014). NME7 is a functional component of the gamma-tubulin ring complex. *Mol Biol Cell*, 25(13), 2017-2025. <https://doi.org/10.1091/mbc.E13-06-0339>
- Liu, P., Zupa, E., Neuner, A., Bohler, A., Loerke, J., Flemming, D., Ruppert, T., Rudack, T., Peter, C., Spahn, C., Gruss, O. J., Pfeffer, S., & Schiebel, E. (2020). Insights into the assembly and activation of the microtubule nucleator gamma-TuRC. *Nature*, 578(7795), 467-471. <https://doi.org/10.1038/s41586-019-1896-6>
- Luders, J. (2012). The amorphous pericentriolar cloud takes shape. *Nat Cell Biol*, 14(11), 1126-1128. <https://doi.org/10.1038/ncb2617>
- Luders, J., Patel, U. K., & Stearns, T. (2006). GCP-WD is a gamma-tubulin targeting factor required for centrosomal and chromatin-mediated microtubule nucleation. *Nat Cell Biol*, 8(2), 137-147. <https://doi.org/10.1038/ncb1349>
- Martin, E. W., Holehouse, A. S., Peran, I., Farag, M., Incicco, J. J., Bremer, A., Grace, C. R., Soranno, A., Pappu, R. V., & Mittag, T. (2020). Valence and patterning of aromatic residues determine the phase behavior of prion-like domains. *Science*, 367(6478), 694-699. <https://doi.org/10.1126/science.aaw8653>
- Masuda, H., Mori, R., Yukawa, M., & Toda, T. (2013). Fission yeast MOZART1/Mzt1 is an essential gamma-tubulin complex component required for complex recruitment to the microtubule organizing center, but not its assembly. *Mol Biol Cell*, 24(18), 2894-2906. <https://doi.org/10.1091/mbc.E13-05-0235>
- Mazo, G., Soplod, N., Wang, W. J., Uryu, K., & Tsou, M. F. (2016). Spatial Control of Primary Ciliogenesis by Subdistal Appendages Alters Sensation-Associated Properties of Cilia. *Dev Cell*, 39(4), 424-437. <https://doi.org/10.1016/j.devcel.2016.10.006>

- McNally, F. J., & Roll-Mecak, A. (2018). Microtubule-severing enzymes: From cellular functions to molecular mechanism. *J Cell Biol*, *217*(12), 4057-4069. <https://doi.org/10.1083/jcb.201612104>
- McNally, F. J., & Vale, R. D. (1993). Identification of katanin, an ATPase that severs and disassembles stable microtubules. *Cell*, *75*(3), 419-429. [https://doi.org/10.1016/0092-8674\(93\)90377-3](https://doi.org/10.1016/0092-8674(93)90377-3)
- McSwiggen, D. T., Mir, M., Darzacq, X., & Tjian, R. (2019). Evaluating phase separation in live cells: diagnosis, caveats, and functional consequences. *Genes Dev*, *33*(23-24), 1619-1634. <https://doi.org/10.1101/gad.331520.119>
- Megraw, T. L., & Kaufman, T. C. (2000). The centrosome in Drosophila oocyte development. *Curr Top Dev Biol*, *49*, 385-407. [https://doi.org/10.1016/s0070-2153\(99\)49019-2](https://doi.org/10.1016/s0070-2153(99)49019-2)
- Mennella, V., Agard, D. A., Huang, B., & Pelletier, L. (2014). Amorphous no more: subdiffraction view of the pericentriolar material architecture. *Trends Cell Biol*, *24*(3), 188-197. <https://doi.org/10.1016/j.tcb.2013.10.001>
- Mennella, V., Keszthelyi, B., McDonald, K. L., Chhun, B., Kan, F., Rogers, G. C., Huang, B., & Agard, D. A. (2012). Subdiffraction-resolution fluorescence microscopy reveals a domain of the centrosome critical for pericentriolar material organization. *Nat Cell Biol*, *14*(11), 1159-1168. <https://doi.org/10.1038/ncb2597>
- Miki, H., Setou, M., Kaneshiro, K., & Hirokawa, N. (2001). All kinesin superfamily protein, KIF, genes in mouse and human. *Proc Natl Acad Sci U S A*, *98*(13), 7004-7011. <https://doi.org/10.1073/pnas.111145398>
- Miller, P. M., Folkmann, A. W., Maia, A. R., Efimova, N., Efimov, A., & Kaverina, I. (2009). Golgi-derived CLASP-dependent microtubules control Golgi organization and polarized trafficking in motile cells. *Nat Cell Biol*, *11*(9), 1069-1080. <https://doi.org/10.1038/ncb1920>
- Mishra, R. K., Chakraborty, P., Arnaoutov, A., Fontoura, B. M., & Dasso, M. (2010). The Nup107-160 complex and gamma-TuRC regulate microtubule polymerization at kinetochores. *Nat Cell Biol*, *12*(2), 164-169. <https://doi.org/10.1038/ncb2016>
- Mitchison, T., & Kirschner, M. (1984). Dynamic instability of microtubule growth. *Nature*, *312*(5991), 237-242. <https://doi.org/10.1038/312237a0>
- Mogensen, M. M., Malik, A., Piel, M., Bouckson-Castaing, V., & Bornens, M. (2000). Microtubule minus-end anchorage at centrosomal and non-centrosomal sites: the role of ninein. *J Cell Sci*, *113* (Pt 17), 3013-3023.
- Monnich, M., Borgeskov, L., Breslin, L., Jakobsen, L., Rogowski, M., Doganli, C., Schroder, J. M., Mogensen, J. B., Blinkenkjaer, L., Harder, L. M., Lundberg, E., Geimer, S., Christensen, S. T., Andersen, J. S., Larsen, L. A., & Pedersen, L. B. (2018). CEP128 Localizes to the Subdistal Appendages of the Mother Centriole and Regulates TGF-beta/BMP Signaling at the Primary Cilium. *Cell Rep*, *22*(10), 2584-2592. <https://doi.org/10.1016/j.celrep.2018.02.043>
- Moritz, M., Braunfeld, M. B., Sedat, J. W., Alberts, B., & Agard, D. A. (1995). Microtubule nucleation by gamma-tubulin-containing rings in the

- centrosome. *Nature*, 378(6557), 638-640.
<https://doi.org/10.1038/378638a0>
- Mukherjee, A., Brooks, P. S., Bernard, F., Guichet, A., & Conduit, P. T. (2020). Microtubules originate asymmetrically at the somatic golgi and are guided via Kinesin2 to maintain polarity within neurons. *Elife*, 9.
<https://doi.org/10.7554/eLife.58943>
- Mukherjee, S., Diaz Valencia, J. D., Stewman, S., Metz, J., Monnier, S., Rath, U., Asenjo, A. B., Charafeddine, R. A., Sosa, H. J., Ross, J. L., Ma, A., & Sharp, D. J. (2012). Human Fidgetin is a microtubule severing the enzyme and minus-end depolymerase that regulates mitosis. *Cell Cycle*, 11(12), 2359-2366. <https://doi.org/10.4161/cc.20849>
- Muroyama, A., & Lechler, T. (2017). Microtubule organization, dynamics and functions in differentiated cells. *Development*, 144(17), 3012-3021.
<https://doi.org/10.1242/dev.153171>
- Muroyama, A., Seldin, L., & Lechler, T. (2016). Divergent regulation of functionally distinct gamma-tubulin complexes during differentiation. *J Cell Biol*, 213(6), 679-692. <https://doi.org/10.1083/jcb.201601099>
- Murphy, S. M., Preble, A. M., Patel, U. K., O'Connell, K. L., Dias, D. P., Moritz, M., Agard, D., Stults, J. T., & Stearns, T. (2001). GCP5 and GCP6: two new members of the human gamma-tubulin complex. *Mol Biol Cell*, 12(11), 3340-3352. <https://doi.org/10.1091/mbc.12.11.3340>
- Murphy, S. M., Urbani, L., & Stearns, T. (1998). The mammalian gamma-tubulin complex contains homologues of the yeast spindle pole body components spc97p and spc98p. *J Cell Biol*, 141(3), 663-674.
<https://doi.org/10.1083/jcb.141.3.663>
- Nakagawa, H., Koyama, K., Murata, Y., Morito, M., Akiyama, T., & Nakamura, Y. (2000). EB3, a novel member of the EB1 family preferentially expressed in the central nervous system, binds to a CNS-specific APC homologue. *Oncogene*, 19(2), 210-216. <https://doi.org/10.1038/sj.onc.1203308>
- Newton, J. C., Naik, M. T., Li, G. Y., Murphy, E. L., Fawzi, N. L., Sedivy, J. M., & Jogle, G. (2021). Phase separation of the LINE-1 ORF1 protein is mediated by the N-terminus and coiled-coil domain. *Biophys J*, 120(11), 2181-2191.
<https://doi.org/10.1016/j.bpj.2021.03.028>
- Nguyen, M. M., McCracken, C. J., Milner, E. S., Goetschius, D. J., Weiner, A. T., Long, M. K., Michael, N. L., Munro, S., & Rolls, M. M. (2014). Gamma-tubulin controls neuronal microtubule polarity independently of Golgi outposts. *Mol Biol Cell*, 25(13), 2039-2050.
<https://doi.org/10.1091/mbc.E13-09-0515>
- Nigg, E. A., & Stearns, T. (2011). The centrosome cycle: Centriole biogenesis, duplication and inherent asymmetries. *Nat Cell Biol*, 13(10), 1154-1160.
<https://doi.org/10.1038/ncb2345>
- Nithianantham, S., McNally, F. J., & Al-Bassam, J. (2018). Structural basis for disassembly of katanin heterododecamers. *J Biol Chem*, 293(27), 10590-10605. <https://doi.org/10.1074/jbc.RA117.001215>

- Nogales, E., Downing, K. H., Amos, L. A., & Löwe, J. (1998). Tubulin and FtsZ form a distinct family of GTPases. *Nat Struct Biol*, 5(6), 451-458. <https://doi.org/10.1038/nsb0698-451>
- Noordstra, I., Liu, Q., Nijenhuis, W., Hua, S., Jiang, K., Baars, M., Remmelzwaal, S., Martin, M., Kapitein, L. C., & Akhmanova, A. (2016). Control of apico-basal epithelial polarity by the microtubule minus-end-binding protein CAMSAP3 and spectraplakins ACF7. *J Cell Sci*, 129(22), 4278-4288. <https://doi.org/10.1242/jcs.194878>
- Oddoux, S., Zaal, K. J., Tate, V., Kenea, A., Nandkeolyar, S. A., Reid, E., Liu, W., & Ralston, E. (2013). Microtubules that form the stationary lattice of muscle fibers are dynamic and nucleated at Golgi elements. *Journal of Cell Biology*, 203(2), 205-213. <https://doi.org/10.1083/jcb.201304063>
- Ori-McKenney, K. M., Jan, L. Y., & Jan, Y. N. (2012). Golgi outposts shape dendrite morphology by functioning as sites of acentrosomal microtubule nucleation in neurons. *Neuron*, 76(5), 921-930. <https://doi.org/10.1016/j.neuron.2012.10.008>
- Oriolo, A. S., Wald, F. A., Canessa, G., & Salas, P. J. (2007). GCP6 binds to intermediate filaments: a novel function of keratins in the organization of microtubules in epithelial cells. *Mol Biol Cell*, 18(3), 781-794. <https://doi.org/10.1091/mbc.e06-03-0201>
- Paschal, B. M., & Vallee, R. B. (1987). Retrograde transport by the microtubule-associated protein MAP 1C. *Nature*, 330(6144), 181-183. <https://doi.org/10.1038/330181a0>
- Paz, J., & Luders, J. (2018). Microtubule-Organizing Centers: Towards a Minimal Parts List. *Trends Cell Biol*, 28(3), 176-187. <https://doi.org/10.1016/j.tcb.2017.10.005>
- Petry, S., Groen, A. C., Ishihara, K., Mitchison, T. J., & Vale, R. D. (2013). Branching microtubule nucleation in *Xenopus* egg extracts mediated by augmin and TPX2. *Cell*, 152(4), 768-777. <https://doi.org/10.1016/j.cell.2012.12.044>
- Piel, M., Meyer, P., Khodjakov, A., Rieder, C. L., & Bornens, M. (2000). The respective contributions of the mother and daughter centrioles to centrosome activity and behavior in vertebrate cells. *J Cell Biol*, 149(2), 317-330. <https://doi.org/10.1083/jcb.149.2.317>
- Pilhofer, M., Ladinsky, M. S., McDowall, A. W., Petroni, G., & Jensen, G. J. (2011). Microtubules in bacteria: Ancient tubulins build a five-protofilament homolog of the eukaryotic cytoskeleton. *PLoS Biol*, 9(12), e1001213. <https://doi.org/10.1371/journal.pbio.1001213>
- Pinyol, R., Scrofani, J., & Vernos, I. (2013). The role of NEDD1 phosphorylation by Aurora A in chromosomal microtubule nucleation and spindle function. *Curr Biol*, 23(2), 143-149. <https://doi.org/10.1016/j.cub.2012.11.046>
- Popov, A. V., Pozniakovskiy, A., Arnal, I., Antony, C., Ashford, A. J., Kinoshita, K., Tournebize, R., Hyman, A. A., & Karsenti, E. (2001). XMAP215 regulates microtubule dynamics through two distinct domains. *EMBO J*, 20(3), 397-410. <https://doi.org/10.1093/emboj/20.3.397>

- Popov, A. V., Severin, F., & Karsenti, E. (2002). XMAP215 is required for the microtubule-nucleating activity of centrosomes. *Curr Biol*, 12(15), 1326-1330. [https://doi.org/10.1016/s0960-9822\(02\)01033-3](https://doi.org/10.1016/s0960-9822(02)01033-3)
- Pottgiesser, J., Maurer, P., Mayer, U., Nischt, R., Mann, K., Timpl, R., Krieg, T., & Engel, J. (1994). Changes in calcium and collagen IV binding caused by mutations in the EF hand and other domains of extracellular matrix protein BM-40 (SPARC, osteonectin). *J Mol Biol*, 238(4), 563-574. <https://doi.org/10.1006/jmbi.1994.1315>
- Prosser, S. L., & Pelletier, L. (2017). Mitotic spindle assembly in animal cells: a fine balancing act. *Nat Rev Mol Cell Biol*, 18(3), 187-201. <https://doi.org/10.1038/nrm.2016.162>
- Raff, E. C., Hoyle, H. D., Popodi, E. M., & Turner, F. R. (2008). Axoneme beta-tubulin sequence determines attachment of outer dynein arms. *Curr Biol*, 18(12), 911-914. <https://doi.org/10.1016/j.cub.2008.05.031>
- Raff, J. W. (2019). Phase Separation and the Centrosome: A Fait Accompli? *Trends Cell Biol*, 29(8), 612-622. <https://doi.org/10.1016/j.tcb.2019.04.001>
- Rai, A. K., Rai, A., Ramaiya, A. J., Jha, R., & Mallik, R. (2013). Molecular adaptations allow dynein to generate large collective forces inside cells. *Cell*, 152(1-2), 172-182. <https://doi.org/10.1016/j.cell.2012.11.044>
- Rapley, J., Baxter, J. E., Blot, J., Wattam, S. L., Casenghi, M., Meraldi, P., Nigg, E. A., & Fry, A. M. (2005). Coordinate regulation of the mother centriole component nlp by nek2 and plk1 protein kinases. *Mol Cell Biol*, 25(4), 1309-1324. <https://doi.org/10.1128/MCB.25.4.1309-1324.2005>
- Reck-Peterson, S. L., Redwine, W. B., Vale, R. D., & Carter, A. P. (2018). The cytoplasmic dynein transport machinery and its many cargoes. *Nat Rev Mol Cell Biol*, 19(6), 382-398. <https://doi.org/10.1038/s41580-018-0004-3>
- Redwine, W. B., DeSantis, M. E., Hollyer, I., Htet, Z. M., Tran, P. T., Swanson, S. K., Florens, L., Washburn, M. P., & Reck-Peterson, S. L. (2017). The human cytoplasmic dynein interactome reveals novel activators of motility. *Elife*, 6. <https://doi.org/10.7554/eLife.28257>
- Rice, L. M., Moritz, M., & Agard, D. A. (2021). Microtubules form by progressively faster tubulin accretion, not by nucleation-elongation. *J Cell Biol*, 220(5). <https://doi.org/10.1083/jcb.202012079>
- Rivero, S., Cardenas, J., Bornens, M., & Rios, R. M. (2009). Microtubule nucleation at the cis-side of the Golgi apparatus requires AKAP450 and GM130. *EMBO J*, 28(8), 1016-1028. <https://doi.org/10.1038/emboj.2009.47>
- Roll-Mecak, A., & McNally, F. J. (2010). Microtubule-severing enzymes. *Curr Opin Cell Biol*, 22(1), 96-103. <https://doi.org/10.1016/j.ccb.2009.11.001>
- Roll-Mecak, A., & Vale, R. D. (2005). The Drosophila homologue of the hereditary spastic paraplegia protein, spastin, severs and disassembles microtubules. *Curr Biol*, 15(7), 650-655. <https://doi.org/10.1016/j.cub.2005.02.029>
- Roostalu, J., Cade, N. I., & Surrey, T. (2015). Complementary activities of TPX2 and chTOG constitute an efficient importin-regulated microtubule nucleation module. *Nat Cell Biol*, 17(11), 1422-1434. <https://doi.org/10.1038/ncb3241>

- Roubin, R., Acquaviva, C., Chevrier, V., Sedjai, F., Zyss, D., Birnbaum, D., & Rosnet, O. (2013). Myomegalin is necessary for the formation of centrosomal and Golgi-derived microtubules. *Biol Open*, 2(2), 238-250. <https://doi.org/10.1242/bio.20123392>
- Roux, K. J., Kim, D. I., Burke, B., & May, D. G. (2018). BioID: A Screen for Protein-Protein Interactions. *Curr Protoc Protein Sci*, 91, 19 23 11-19 23 15. <https://doi.org/10.1002/cpps.51>
- Ryan, E. L., Shelford, J., Massam-Wu, T., Bayliss, R., & Royle, S. J. (2021). Defining endogenous TACC3-chTOG-clathrin-GTSE1 interactions at the mitotic spindle using induced relocalization. *J Cell Sci*, 134(3). <https://doi.org/10.1242/jcs.255794>
- Sallee, M. D., Zonka, J. C., Skokan, T. D., Raftrey, B. C., & Feldman, J. L. (2018). Tissue-specific degradation of essential centrosome components reveals distinct microtubule populations at microtubule organizing centers. *PLoS Biol*, 16(8), e2005189. <https://doi.org/10.1371/journal.pbio.2005189>
- Sanchez-Huertas, C., Freixo, F., Viais, R., Lacasa, C., Soriano, E., & Luders, J. (2016). Non-centrosomal nucleation mediated by augmin organizes microtubules in post-mitotic neurons and controls axonal microtubule polarity. *Nat Commun*, 7, 12187. <https://doi.org/10.1038/ncomms12187>
- Sato, Y., Hayashi, K., Amano, Y., Takahashi, M., Yonemura, S., Hayashi, I., Hirose, H., Ohno, S., & Suzuki, A. (2014). MTCL1 crosslinks and stabilizes non-centrosomal microtubules on the Golgi membrane. *Nat Commun*, 5, 5266. <https://doi.org/10.1038/ncomms6266>
- Scheele, R. B., Bergen, L. G., & Borisy, G. G. (1982). Control of the structural fidelity of microtubules by initiation sites. *J Mol Biol*, 154(3), 485-500. [https://doi.org/10.1016/s0022-2836\(82\)80008-9](https://doi.org/10.1016/s0022-2836(82)80008-9)
- Schmidt, H., Gleave, E. S., & Carter, A. P. (2012). Insights into dynein motor domain function from a 3.3-Å crystal structure. *Nat Struct Mol Biol*, 19(5), 492-497, s491. <https://doi.org/10.1038/nsmb.2272>
- Schmidt, H., Zalyte, R., Urnavicius, L., & Carter, A. P. (2015). Structure of human cytoplasmic dynein-2 primed for its power stroke. *Nature*, 518(7539), 435-438. <https://doi.org/10.1038/nature14023>
- Schroer, T. A., & Sheetz, M. P. (1991). Two activators of microtubule-based vesicle transport. *J Cell Biol*, 115(5), 1309-1318. <https://doi.org/10.1083/jcb.115.5.1309>
- Schweizer, N., Haren, L., Viais, R., Lacasa, C., Dutto, I., Merdes, A., & Lüders, J. (2020). Sub-centrosomal mapping identifies augmin-γTuRC as part of a centriole-stabilizing scaffold. *BioRxiv*, 2020.2011.2018.384156. <https://doi.org/10.1101/2020.11.18.384156>
- Schweizer, N., & Lüders, J. (2021). From tip to toe - dressing centrioles in γTuRC. *J Cell Sci*, 134(14). <https://doi.org/10.1242/jcs.258397>
- Seetapun, D., Castle, B. T., McIntyre, A. J., Tran, P. T., & Odde, D. J. (2012). Estimating the microtubule GTP cap size in vivo. *Curr Biol*, 22(18), 1681-1687. <https://doi.org/10.1016/j.cub.2012.06.068>

- Shanks, R. A., Steadman, B. T., Schmidt, P. H., & Goldenring, J. R. (2002). AKAP350 at the Golgi apparatus. I. Identification of a distinct Golgi apparatus targeting motif in AKAP350. *J Biol Chem*, 277(43), 40967-40972. <https://doi.org/10.1074/jbc.M203307200>
- Shao, S., Liu, R., Wang, Y., Song, Y., Zuo, L., Xue, L., Lu, N., Hou, N., Wang, M., Yang, X., & Zhan, Q. (2010). Centrosomal Nlp is an oncogenic protein that is gene-amplified in human tumors and causes spontaneous tumorigenesis in transgenic mice. *J Clin Invest*, 120(2), 498-507. <https://doi.org/10.1172/JCI39447>
- Singh, P., Thomas, G. E., Gireesh, K. K., & Manna, T. K. (2014). TACC3 protein regulates microtubule nucleation by affecting gamma-tubulin ring complexes. *J Biol Chem*, 289(46), 31719-31735. <https://doi.org/10.1074/jbc.M114.575100>
- Slep, K. C., & Vale, R. D. (2007). Structural basis of microtubule plus end tracking by XMAP215, CLIP-170, and EB1. *Mol Cell*, 27(6), 976-991. <https://doi.org/10.1016/j.molcel.2007.07.023>
- Song, Y., & Brady, S. T. (2015). Post-translational modifications of tubulin: pathways to functional diversity of microtubules. *Trends Cell Biol*, 25(3), 125-136. <https://doi.org/10.1016/j.tcb.2014.10.004>
- Sonnen, K. F., Schermelleh, L., Leonhardt, H., & Nigg, E. A. (2012). 3D-structured illumination microscopy provides novel insight into architecture of human centrosomes. *Biol Open*, 1(10), 965-976. <https://doi.org/10.1242/bio.20122337>
- Stark, C., Breikreutz, B. J., Reguly, T., Boucher, L., Breikreutz, A., & Tyers, M. (2006). BioGRID: a general repository for interaction datasets. *Nucleic Acids Res*, 34(Database issue), D535-539. <https://doi.org/10.1093/nar/gkj109>
- Stepanova, T., Slemmer, J., Hoogenraad, C. C., Lansbergen, G., Dortland, B., De Zeeuw, C. I., Grosveld, F., van Cappellen, G., Akhmanova, A., & Galjart, N. (2003). Visualization of microtubule growth in cultured neurons via the use of EB3-GFP (end-binding protein 3-green fluorescent protein). *J Neurosci*, 23(7), 2655-2664. <https://doi.org/10.1523/jneurosci.23-07-02655.2003>
- Sumigray, K. D., Chen, H., & Lechler, T. (2011). Lis1 is essential for cortical microtubule organization and desmosome stability in the epidermis. *J Cell Biol*, 194(4), 631-642. <https://doi.org/10.1083/jcb.201104009>
- Sun, X., Shi, X., Liu, M., Li, D., Zhang, L., Liu, X., & Zhou, J. (2011). Mdp3 is a novel microtubule-binding protein that regulates microtubule assembly and stability. *Cell Cycle*, 10(22), 3929-3937. <https://doi.org/10.4161/cc.10.22.18106>
- Sweeney, H. L., & Holzbaur, E. L. F. (2018). Motor Proteins. *Cold Spring Harb Perspect Biol*, 10(5). <https://doi.org/10.1101/cshperspect.a021931>
- Takahashi, M., Yamagiwa, A., Nishimura, T., Mukai, H., & Ono, Y. (2002). Centrosomal proteins CG-NAP and kendrin provide microtubule nucleation sites by anchoring gamma-tubulin ring complex. *Mol Biol Cell*, 13(9), 3235-3245. <https://doi.org/10.1091/mbc.e02-02-0112>

- Tan, R., Lam, A. J., Tan, T., Han, J., Nowakowski, D. W., Vershinin, M., Simo, S., Ori-McKenney, K. M., & McKenney, R. J. (2019). Microtubules gate tau condensation to spatially regulate microtubule functions. *Nat Cell Biol*, 21(9), 1078-1085. <https://doi.org/10.1038/s41556-019-0375-5>
- Teixido-Travesa, N., Roig, J., & Luders, J. (2012). The where, when and how of microtubule nucleation - one ring to rule them all. *J Cell Sci*, 125(Pt 19), 4445-4456. <https://doi.org/10.1242/jcs.106971>
- Teixido-Travesa, N., Villen, J., Lacasa, C., Bertran, M. T., Archinti, M., Gygi, S. P., Caelles, C., Roig, J., & Luders, J. (2010). The gammaTuRC revisited: a comparative analysis of interphase and mitotic human gammaTuRC redefines the set of core components and identifies the novel subunit GCP8. *Mol Biol Cell*, 21(22), 3963-3972. <https://doi.org/10.1091/mbc.E10-05-0408>
- Teo, G., Koh, H., Fermin, D., Lambert, J. P., Knight, J. D., Gingras, A. C., & Choi, H. (2016). SAINTq: Scoring protein-protein interactions in affinity purification - mass spectrometry experiments with fragment or peptide intensity data. *Proteomics*, 16(15-16), 2238-2245. <https://doi.org/10.1002/pmic.201500499>
- Thawani, A., Kadzik, R. S., & Petry, S. (2018). XMAP215 is a microtubule nucleation factor that functions synergistically with the gamma-tubulin ring complex. *Nat Cell Biol*, 20(5), 575-585. <https://doi.org/10.1038/s41556-018-0091-6>
- Thawani, A., Rale, M. J., Coudray, N., Bhabha, G., Stone, H. A., Shaevitz, J. W., & Petry, S. (2020). The transition state and regulation of gamma-TuRC-mediated microtubule nucleation revealed by single molecule microscopy. *Elife*, 9. <https://doi.org/10.7554/eLife.54253>
- Tilney, L. G., Bryan, J., Bush, D. J., Fujiwara, K., Mooseker, M. S., Murphy, D. B., & Snyder, D. H. (1973). Microtubules: evidence for 13 protofilaments. *J Cell Biol*, 59(2 Pt 1), 267-275. <https://doi.org/10.1083/jcb.59.2.267>
- Tournebize, R., Popov, A., Kinoshita, K., Ashford, A. J., Rybina, S., Pozniakovsky, A., Mayer, T. U., Walczak, C. E., Karsenti, E., & Hyman, A. A. (2000). Control of microtubule dynamics by the antagonistic activities of XMAP215 and XKCM1 in *Xenopus* egg extracts. *Nat Cell Biol*, 2(1), 13-19. <https://doi.org/10.1038/71330>
- Tovey, C. A., Tsuji, C., Egerton, A., Bernard, F., Guichet, A., de la Roche, M., & Conduit, P. T. (2021). Autoinhibition of Cnn binding to gamma-TuRCs prevents ectopic microtubule nucleation and cell division defects. *J Cell Biol*, 220(8). <https://doi.org/10.1083/jcb.202010020>
- Truebestein, L., & Leonard, T. A. (2016). Coiled-coils: The long and short of it. *Bioessays*, 38(9), 903-916. <https://doi.org/10.1002/bies.201600062>
- Uzbekov, R., & Alieva, I. (2018). Who are you, subdistal appendages of centriole? *Open Biol*, 8(7). <https://doi.org/10.1098/rsob.180062>
- Vale, R. D., Reese, T. S., & Sheetz, M. P. (1985). Identification of a novel force-generating protein, kinesin, involved in microtubule-based motility. *Cell*, 42(1), 39-50. [https://doi.org/10.1016/s0092-8674\(85\)80099-4](https://doi.org/10.1016/s0092-8674(85)80099-4)

- van den Berg, B., Ellis, R. J., & Dobson, C. M. (1999). Effects of macromolecular crowding on protein folding and aggregation. *EMBO J*, *18*(24), 6927-6933. <https://doi.org/10.1093/emboj/18.24.6927>
- van der Vaart, B., Manatschal, C., Grigoriev, I., Olieric, V., Gouveia, S. M., Bjelic, S., Demmers, J., Vorobjev, I., Hoogenraad, C. C., Steinmetz, M. O., & Akhmanova, A. (2011). SLAIN2 links microtubule plus end-tracking proteins and controls microtubule growth in interphase. *J Cell Biol*, *193*(6), 1083-1099. <https://doi.org/10.1083/jcb.201012179>
- van Riel, W. E., Rai, A., Bianchi, S., Katrukha, E. A., Liu, Q., Heck, A. J., Hoogenraad, C. C., Steinmetz, M. O., Kapitein, L. C., & Akhmanova, A. (2017). Kinesin-4 KIF21B is a potent microtubule pausing factor. *Elife*, *6*. <https://doi.org/10.7554/eLife.24746>
- van Wijk, E., Kersten, F. F., Kartono, A., Mans, D. A., Brandwijk, K., Letteboer, S. J., Peters, T. A., Marker, T., Yan, X., Cremers, C. W., Cremers, F. P., Wolfrum, U., Roepman, R., & Kremer, H. (2009). Usher syndrome and Leber congenital amaurosis are molecularly linked via a novel isoform of the centrosomal ninein-like protein. *Hum Mol Genet*, *18*(1), 51-64. <https://doi.org/10.1093/hmg/ddn312>
- Vega, I. E., Umstead, A., & Kanaan, N. M. (2019). EFhd2 Affects Tau Liquid-Liquid Phase Separation. *Front Neurosci*, *13*, 845. <https://doi.org/10.3389/fnins.2019.00845>
- Vemu, A., Szczesna, E., Zehr, E. A., Spector, J. O., Grigorieff, N., Deaconescu, A. M., & Roll-Mecak, A. (2018). Severing enzymes amplify microtubule arrays through lattice GTP-tubulin incorporation. *Science*, *361*(6404). <https://doi.org/10.1126/science.aau1504>
- Verde, I., Pahlke, G., Salanova, M., Zhang, G., Wang, S., Coletti, D., Onuffer, J., Jin, S. L., & Conti, M. (2001). Myomegalin is a novel protein of the golgi/centrosome that interacts with a cyclic nucleotide phosphodiesterase. *J Biol Chem*, *276*(14), 11189-11198. <https://doi.org/10.1074/jbc.M006546200>
- Vergarajauregui, S., Becker, R., Steffen, U., Sharkova, M., Esser, T., Petzold, J., Billing, F., Kapiloff, M. S., Schett, G., Thievensen, I., & Engel, F. B. (2020). AKAP6 orchestrates the nuclear envelope microtubule-organizing center by linking golgi and nucleus via AKAP9. *Elife*, *9*, e61669. <https://doi.org/10.7554/eLife.61669>
- Vorobjev, I. A., & Chentsov Yu, S. (1982). Centrioles in the cell cycle. I. Epithelial cells. *J Cell Biol*, *93*(3), 938-949. <https://doi.org/10.1083/jcb.93.3.938>
- Walczak, C. E., Gayek, S., & Ohi, R. (2013). Microtubule-depolymerizing kinesins. *Annu Rev Cell Dev Biol*, *29*, 417-441. <https://doi.org/10.1146/annurev-cellbio-101512-122345>
- Wang, J., Choi, J. M., Holehouse, A. S., Lee, H. O., Zhang, X., Jahnel, M., Maharana, S., Lemaitre, R., Pozniakovsky, A., Drechsel, D., Poser, I., Pappu, R. V., Alberti, S., & Hyman, A. A. (2018). A Molecular Grammar Governing the Driving Forces for Phase Separation of Prion-like RNA

- Binding Proteins. *Cell*, 174(3), 688-699 e616.
<https://doi.org/10.1016/j.cell.2018.06.006>
- Wang, Z., Wu, T., Shi, L., Zhang, L., Zheng, W., Qu, J. Y., Niu, R., & Qi, R. Z. (2010). Conserved motif of CDK5RAP2 mediates its localization to centrosomes and the Golgi complex. *J Biol Chem*, 285(29), 22658-22665.
<https://doi.org/10.1074/jbc.M110.105965>
- Wang, Z., Zhang, C., & Qi, R. Z. (2014). A newly identified myomegalin isoform functions in Golgi microtubule organization and ER-Golgi transport. *J Cell Sci*, 127(Pt 22), 4904-4917. <https://doi.org/10.1242/jcs.155408>
- Ward, J. J., Sodhi, J. S., McGuffin, L. J., Buxton, B. F., & Jones, D. T. (2004). Prediction and functional analysis of native disorder in proteins from the three kingdoms of life. *J Mol Biol*, 337(3), 635-645.
<https://doi.org/10.1016/j.jmb.2004.02.002>
- Wieczorek, M., Bechstedt, S., Chaaban, S., & Brouhard, G. J. (2015). Microtubule-associated proteins control the kinetics of microtubule nucleation. *Nat Cell Biol*, 17(7), 907-916. <https://doi.org/10.1038/ncb3188>
- Wieczorek, M., Urnavicius, L., Ti, S. C., Molloy, K. R., Chait, B. T., & Kapoor, T. M. (2020). Asymmetric Molecular Architecture of the Human gamma-Tubulin Ring Complex. *Cell*, 180(1), 165-175 e116.
<https://doi.org/10.1016/j.cell.2019.12.007>
- Wollman, R., Cytrynbaum, E. N., Jones, J. T., Meyer, T., Scholey, J. M., & Mogilner, A. (2005). Efficient chromosome capture requires a bias in the 'search-and-capture' process during mitotic-spindle assembly. *Curr Biol*, 15(9), 828-832. <https://doi.org/10.1016/j.cub.2005.03.019>
- Woodruff, J. B., Ferreira Gomes, B., Widlund, P. O., Mahamid, J., Honigsmann, A., & Hyman, A. A. (2017). The Centrosome Is a Selective Condensate that Nucleates Microtubules by Concentrating Tubulin. *Cell*, 169(6), 1066-1077 e1010. <https://doi.org/10.1016/j.cell.2017.05.028>
- Wu, J., & Akhmanova, A. (2017). Microtubule-Organizing Centers. *Annu Rev Cell Dev Biol*, 33, 51-75. <https://doi.org/10.1146/annurev-cellbio-100616-060615>
- Wu, J., de Heus, C., Liu, Q., Bouchet, B. P., Noordstra, I., Jiang, K., Hua, S., Martin, M., Yang, C., Grigoriev, I., Katrukha, E. A., Altelaar, A. F. M., Hoogenraad, C. C., Qi, R. Z., Klumperman, J., & Akhmanova, A. (2016). Molecular Pathway of Microtubule Organization at the Golgi Apparatus. *Dev Cell*, 39(1), 44-60. <https://doi.org/10.1016/j.devcel.2016.08.009>
- Xiao, W., Yeerken, D., Li, J., Li, Z., Jiang, L., Li, D., Fu, M., Ma, L., Song, Y., Zhang, W., & Zhan, Q. (2021). Nlp promotes autophagy through facilitating the interaction of Rab7 and FYCO1. *Signal Transduct Target Ther*, 6(1), 152. <https://doi.org/10.1038/s41392-021-00543-1>
- Yadav, S., Verma, P. J., & Panda, D. (2014). C-terminal region of MAP7 domain containing protein 3 (MAP7D3) promotes microtubule polymerization by binding at the C-terminal tail of tubulin. *PLoS One*, 9(6), e99539.
<https://doi.org/10.1371/journal.pone.0099539>

- Yang, C., Wu, J., de Heus, C., Grigoriev, I., Liv, N., Yao, Y., Smal, I., Meijering, E., Klumperman, J., Qi, R. Z., & Akhmanova, A. (2017). EB1 and EB3 regulate microtubule minus end organization and Golgi morphology. *J Cell Biol*, 216(10), 3179-3198. <https://doi.org/10.1083/jcb.201701024>
- Yang, S. Z., & Wildonger, J. (2020). Golgi Outposts Locally Regulate Microtubule Orientation in Neurons but Are Not Required for the Overall Polarity of the Dendritic Cytoskeleton. *Genetics*, 215(2), 435-447. <https://doi.org/10.1534/genetics.119.302979>
- Yokoyama, H., Koch, B., Walczak, R., Ciray-Duygu, F., González-Sánchez, J. C., Devos, D. P., Mattaj, I. W., & Gruss, O. J. (2014). The nucleoporin MEL-28 promotes RanGTP-dependent γ -tubulin recruitment and microtubule nucleation in mitotic spindle formation. *Nat Commun*, 5, 3270. <https://doi.org/10.1038/ncomms4270>
- Zehr, E., Szyk, A., Piszczek, G., Szczesna, E., Zuo, X., & Roll-Mecak, A. (2017). Katanin spiral and ring structures shed light on power stroke for microtubule severing. *Nat Struct Mol Biol*, 24(9), 717-725. <https://doi.org/10.1038/nsmb.3448>
- Zehr, E. A., Szyk, A., Szczesna, E., & Roll-Mecak, A. (2020). Katanin Grips the β -Tubulin Tail through an Electropositive Double Spiral to Sever Microtubules. *Dev Cell*, 52(1), 118-131.e116. <https://doi.org/10.1016/j.devcel.2019.10.010>
- Zhang, D., Grode, K. D., Stewman, S. F., Diaz-Valencia, J. D., Liebling, E., Rath, U., Riera, T., Currie, J. D., Buster, D. W., Asenjo, A. B., Sosa, H. J., Ross, J. L., Ma, A., Rogers, S. L., & Sharp, D. J. (2011). Drosophila katanin is a microtubule depolymerase that regulates cortical-microtubule plus-end interactions and cell migration. *Nat Cell Biol*, 13(4), 361-370. <https://doi.org/10.1038/ncb2206>
- Zhang, D., Rogers, G. C., Buster, D. W., & Sharp, D. J. (2007). Three microtubule severing enzymes contribute to the "Pacman-flux" machinery that moves chromosomes. *J Cell Biol*, 177(2), 231-242. <https://doi.org/10.1083/jcb.200612011>
- Zhao, W., Song, Y., Xu, B., & Zhan, Q. (2012). Overexpression of centrosomal protein Nlp confers breast carcinoma resistance to paclitaxel. *Cancer Biol Ther*, 13(3), 156-163. <https://doi.org/10.4161/cbt.13.3.18697>
- Zheng, Y., Buchwalter, R. A., Zheng, C., Wight, E. M., Chen, J. V., & Megraw, T. L. (2020). A perinuclear microtubule-organizing centre controls nuclear positioning and basement membrane secretion. *Nat Cell Biol*, 22(3), 297-309. <https://doi.org/10.1038/s41556-020-0470-7>
- Zheng, Y., Mennella, V., Marks, S., Wildonger, J., Elnagdi, E., Agard, D., & Megraw, T. L. (2016). The Seckel syndrome and centrosomal protein Ninein localizes asymmetrically to stem cell centrosomes but is not required for normal development, behavior, or DNA damage response in Drosophila. *Mol Biol Cell*, 27(11), 1740-1752. <https://doi.org/10.1091/mbc.E15-09-0655>

- Zheng, Y., Wong, M. L., Alberts, B., & Mitchison, T. (1995). Nucleation of microtubule assembly by a gamma-tubulin-containing ring complex. *Nature*, 378(6557), 578-583. <https://doi.org/10.1038/378578a0>
- Zhou, C., Yan, L., Zhang, W. H., & Liu, Z. (2019). Structural basis of tubulin detyrosination by VASH2/SVBP heterodimer. *Nat Commun*, 10(1), 3212. <https://doi.org/10.1038/s41467-019-11277-8>
- Zhu, F., Lawo, S., Bird, A., Pinchev, D., Ralph, A., Richter, C., Muller-Reichert, T., Kittler, R., Hyman, A. A., & Pelletier, L. (2008). The mammalian SPD-2 ortholog Cep192 regulates centrosome biogenesis. *Curr Biol*, 18(2), 136-141. <https://doi.org/10.1016/j.cub.2007.12.055>
- Zimmerman, S. B., & Minton, A. P. (1993). Macromolecular crowding: biochemical, biophysical, and physiological consequences. *Annu Rev Biophys Biomol Struct*, 22, 27-65. <https://doi.org/10.1146/annurev.bb.22.060193.000331>
- Zimmermann, F., Serna, M., Ezquerra, A., Fernandez-Leiro, R., Llorca, O., & Luders, J. (2020). Assembly of the asymmetric human γ -tubulin ring complex by RUVBL1-RUVBL2 AAA ATPase. *Sci Adv*, 6(51). <https://doi.org/10.1126/sciadv.abc0894>